

PHENOMENOLOGY OF A
PSEUDOSCALAR GLUEBALL AND
CHARMED MESONS

Dissertation
zur Erlangung des Doktorgrades
der Naturwissenschaften

vorgelegt beim Fachbereich Physik
der Johann Wolfgang Goethe-Universität
in Frankfurt am Main

von
Walaa I. Eshraim

Frankfurt am Main 2015
(D30)

vom Fachbereich Physik (13)
der Johann Wolfgang Goethe-Universität als Dissertation angenommen.

Dekan: Prof. Dr. Rene Reifarth

1. Gutachter: Prof. Dr. Dirk-Hermann Rischke
2. Gutachter: Prof. Dr. Stefan Schramm

Datum der Disputation: 24.07.2015

To
the spirit that gives life to my body
My Mother
Sanaa

To
the blood that lets my heart beat
My Father
Ibrahim

and

To
the world that has to be full of love,
peace, safety, fidelity,
probity, sincerity,
justice, equality
and liberty.

Zusammenfassung

Die Quantenchromodynamik (QCD) ist die Theorie, welche die Wechselwirkung zwischen Quarks und Gluonen beschreibt. Die fundamentale Symmetrie, die der QCD zugrunde liegt, ist die lokale $SU(3)_c$ -Farbsymmetrie. Aufgrund vom Confinement der Quarks und Gluonen werden im niederenergetischen Bereich die physikalischen Freiheitsgrade durch Hadronen (Mesonen und Baryonen) repräsentiert. In den letzten Jahren wurden zahlreiche effektive niederenergetische Modelle für die starke Wechselwirkung entwickelt, denen eine chirale Symmetrie zugrunde liegt. Die chirale Symmetrie ist eine weitere Symmetrie der QCD-Lagrangedichte, die im Limes verschwindender Quarkmassen (dem sogenannten chiralen Limes) realisiert ist. Diese Symmetrie wird durch nichtverschwindende Stromquarkmassen explizit gebrochen. Im QCD-Vakuum ist die chirale Symmetrie spontan gebrochen. Als Konsequenz entstehen pseudoskalare (Quasi-)Goldstone-Bosonen, die für Up- und Down-Quarks (d.h. für $N_f = 2$ Quarkflavors) den Pionen entsprechen. Für $N_f = 3$, d.h. wenn auch das Strange-Quark betrachtet wird, entsprechen die Goldstone-Bosonen den Pionen, Kaonen und dem Eta-Meson. Das η' -Meson ist kein Goldstone-Boson wegen der chiralen Anomalie. Die chirale Symmetrie kann in hadronischen Modellen in sogenannter linearer oder nichtlinearer Repräsentation realisiert werden. Im nichtlinearen Fall werden nur Goldstone-Bosonen betrachtet. In neueren Modellen jedoch werden auch die Vektormesonen dazu addiert. Im linearen Fall enthalten die Modelle auch die chiralen Partner der Goldstone-Bosonen. Wenn man diese Modelle auf den Vektorsektor erweitert, enthalten Sie sowohl Vektor-als auch Axialvektor-Mesonen. In diesem Zusammenhang haben aktuelle Bemühungen zur Entwicklung des sogenannten erweiterten linearen Sigma-Modells (eLSM) für $N_f = 2$ und für $N_f = 3$ geführt. Zusätzlich zur chiralen Symmetrie wird im eLSM die Symmetrie unter Dilatation (Skaleninvarianz) und die anomale Brechung dieser Symmetrie (Spuranomalie) berücksichtigt. Für $N_f = 2$ war es im Rahmen des eLSM zum ersten Mal möglich, (pseudo-)skalare sowie (axial-)vektorielle Mesonen in einem chiralen Modell zu beschreiben: Die Massen und Zerfallsbreiten stimmen gut mit den Resultaten der Particle Data Group (PDG) überein. Als Folge der nicht-abelschen Natur der lokalen $SU(3)$ -Farbsymmetrie tragen die Eichfelder der QCD, die Gluonen, eine Farbladung. Daher wechselwirken sie stark miteinander. Wegen des Confinements erwartet man, dass Gluonen auch farblose, bzw. "weiße", Objekte bilden können. Diese werden als Gluebälle bezeichnet.

Die ersten Berechnungen der Glueball-Massen basierten auf dem Bag-Modell. Später erlaubten numerische Gitterrechnungen die Bestimmung des vollen Glueballspektrums. In voller QCD (d.h. Gluonen plus Quarks) findet eine Mischung zwischen den Gluebällen und Quark-Antiquark-Konfigurationen mit denselben Quantenzahlen statt, was die Identifikation der Resonanzen, die von der PDG gelistet sind, zusätzlich erschwert. Die Suche nach Zuständen, die vorrangig Gluebälle sind, ist ein aktives aktuelles Forschungsgebiet. Dadurch erhofft man sich ein besseres Verständnis für das nichtperturbative Verhalten der QCD. Obwohl zurzeit einige Kandidaten für Gluebälle existieren, wurde noch kein Zustand eindeutig identifiziert, der vorrangig ein Glueball ist. Im Allgemeinen sollten die Glueball-zustände

zwei Eigenschaften im Hinblick auf den Zerfall erfüllen. Erstens ist ein Glueball flavorblind, da die Gluonen an alle Quarkflavors mit derselben Stärke koppeln. Zweitens besitzen Gluebälle eine schmale Zerfallsbreite, die im Large- N_c -Limes wie $1/N_c^2$ skaliert. Im Vergleich dazu skaliert ein Quark-Antiquark-Zustand wie $1/N_c$. Der leichteste Glueballzustand, den die Gitterrechnungen vorhersagen, ist ein skalar-isoskalärer Zustand ($J^{PC} = 0^{++}$) mit einer Masse von etwa 1.7 GeV. Die Zerfallsbreite der Resonanz $f_0(1500)$ ist flavorunabhängig und schmal. Aus diesem Grund ist diese Resonanz ein guter Kandidat für einen Zustand, der vorrangig ein skalarer Glueball ist. Zusätzlich ist die Resonanz $f_0(1700)$ ein Glueball-Kandidat, da ihre Masse in der Nähe der Vorhersagen der Gitterrechnungen liegt, und da sie in den gluonreichen Zerfällen des J/ψ -Mesons produziert wird. Beide Szenarien wurden in vielen Arbeiten untersucht, in denen die Mischung zwischen $f_0(1370)$, $f_0(1500)$ und $f_0(1710)$ betrachtet wird. Der zweitleichteste Glueball, der von den Gitterrechnungen vorhergesagt wird, ist ein Tensor-Zustand mit den Quantenzahlen 2^{++} und einer Masse von etwa 2.2 GeV. Ein guter Kandidat dafür könnte die sehr schmale Resonanz $f_0(2200)$ sein, falls sich ihr Drehimpuls experimentell zu $J = 2$ bestimmen lässt. Der drittleichteste Glueball ist ein pseudoskalärer Zustand ($J^{PC} = 0^{-+}$) mit einer Masse von etwa 2.6 GeV. Open-charm Mesonen bestehen aus einem Charm-Quark und einem Up-, Down- oder Strange-Antiquark. Sie wurden im Jahre 1976, zwei Jahre später als das J/ψ -Meson ($c\bar{c}$ -Zustand), entdeckt. Seit dieser Zeit gab es signifikante experimentelle und theoretische Fortschritte im Bereich der Spektroskopie und bei der Bestimmung der Zerfälle dieser Mesonen. In dieser Arbeit zeigen wir, wie im Rahmen eines chiralen-symmetrischen Modells, welches das Charm-Quark als zusätzlichen Freiheitsgrad enthält, die ursprüngliche $SU(3)$ -Flavor-Symmetrie der Hadronen zu einer $SU(4)$ -Symmetrie erweitert werden kann. Die chirale Symmetrie wird durch die große Strommasse des Charm-Quarks stark explizit verletzt.

Zerfall von pseudoskalaren Gluebällen in skalare und pseudoskalare Mesonen

In dieser Arbeit untersuchen wir die Zerfälle des pseudoskalaren Glueballs, dessen Masse laut Gitterrechnungen zwischen 2 und 3 GeV liegt. Wir konstruieren eine effektive chirale Lagrangedichte, die das pseudoskalare Glueballfeld G an skalare und pseudoskalare Mesonen mit $N_f = 3$ koppelt. Danach berechnen wir die Breiten für die Zerfälle $G \rightarrow PPP$ und $G \rightarrow PS$, wobei P und S pseudoskalare und skalare Quark-Antiquark-Zustände kennzeichnet. Die pseudoskalaren Zustände umfassen das Oktett der pseudo-Goldstone-Bosonen, während sich der skalare Zustand S auf das Quark-Antiquark-Nonet oberhalb von 1 GeV bezieht. Der Grund dafür besteht darin, dass die chiralen Partner der pseudoskalaren Zustände nicht mit Resonanzen unterhalb von 1 GeV identifiziert werden sollten. Die konstruierte chirale Lagrangedichte enthält eine unbekannte Kopplungskonstante, die nur experimentell bestimmt werden kann. Aus diesem Grund präsentieren wir die Resultate in Form von Verzweungsverhältnissen für die Zerfälle des pseudoskalaren Glueballs G in drei pseudoskalare Mesonen oder ein skalares und ein pseudoskalares Meson. Diese Verzweungsverhältnisse hängen von keinen weiteren Parametern ab, sobald die Glueballmasse fixiert wird. Wir betrachten zwei Möglichkeiten: i) In Übereinstimmung mit Gitterrechnungen wählen wir die Masse des pseudoskalaren Glueballs zu etwa 2.6 GeV. Die Existenz und die Zerfallseigenschaften hypothetischer pseudoskalärer Resonanzen können im zukünftigen PANDA-Experiment getestet werden. (Das PANDA-Experiment misst die Proton-Antiproton-Streuung. Daher kann der pseudoskalare Glueball direkt als ein Zwi-

schenzustand produziert werden.) ii) Wir nehmen an, dass die Resonanz $X(2370)$ (gemessen im Experiment BESIII) vorrangig ein pseudoskalärer Glueball-Zustand ist. Daher benutzen wir dafür die Masse 2.37 GeV. Unsere Ergebnisse sagen voraus, dass $KK\pi$ der dominante Zerfallskanal ist, gefolgt von einem beinahe gleich großem $\eta\pi\pi$ - und $\eta'\pi\pi$ -Zerfallskanal. Der Zerfallskanal in drei Pionen verschwindet. Beim BESIII-Experiment wäre es möglich, durch die Messung des Verzweigungsverhältnisses für $\eta'\pi\pi$ und anderer Zerfallskanäle zu bestimmen, ob $X(2370)$ vorrangig ein pseudoskalärer Glueball ist. Für das PANDA-Experiment liefern unsere Resultate nützliche Hinweise für die Suche nach pseudoskalären Gluebällen.

Phänomenologie der Charm-Mesonen

Wir vergrößern die globale Symmetrie des erweiterten linearen Sigma Modells (eLSM) zu einer globalen $SU(4)_R \times SU(4)_L$ Symmetrie, indem wir das Charm-Quark einbauen. Das eLSM enthält zusätzlich zu skalaren und pseudoskalären Mesonen auch Axialvektor- und Vektormesonen. Wir benutzen die Parameter aus dem niederenergetischen Sektor der Mesonen. Die verbleibenden drei freien Parameter (die von der Strommasse des Charm-Quarks abhängen) werden an Massen der Charmed Mesonen angepaßt. Die Resultate für Open-Charm-Mesonen stimmen gut mit den experimentellen Ergebnissen überein (die Abweichung beträgt etwa 150 MeV). Für Charmonia weichen unsere Resultate für die Massen stärker von der experimentellen Daten ab. Unser Modell stellt dennoch ein nützliches Werkzeug dar, um einige Eigenschaften der Charm-Zustände, wie zum Beispiel das chirale Kondensat, zu untersuchen.

Zusammenfassend bedeutet die Tatsache, dass eine (obwohl in diesem Stadium nur grobe) qualitative Beschreibung durch die Verwendung eines chiralen Modells und insbesondere der ermittelten Parameter durch die Untersuchung von $N_f = 3$ Mesonen erzielt wurde, dass auch im Sektor der Charm-Mesonen ein Überrest der chiralen Symmetrie vorhanden ist. Die chirale Symmetrie ist immer noch präsent, da sich die Parameter des eLSM als Funktion der Energieskala kaum verändern. Neben den Massentermen, die den Großteil der gegenwärtigen Charm-Quarkmasse beschreiben, sind alle Wechselwirkungsterme dieselben wie im niederenergetischen effektiven Modell, welches unter der Forderung nach chiraler Symmetrie und Dilatationsinvarianz konstruiert wurde. Als Nebenprodukt unserer Arbeit haben wir das Charm-Kondensat auf die gleiche Größenordnung wie die strange und non-strange Quarkkondensate bestimmt. Dies stimmt ebenfalls mit der auf $U(4)_R \times U(4)_L$ erweiterten chiralen Dynamik überein.

Was die Zuweisung der skalaren und axial-vektoriellen Strange-Charm-Quarkonium-Zustände D_{S0} und D_{S1} betrifft, erhalten wir das folgende: falls ihre Masse über dem jeweiligen Schwellenwert liegt, ist ihre Zerfallsbreite zu groß. Dies wiederum bedeutet, dass sich diese Zustände, auch wenn sie existieren, der Detektion entzogen haben. In diesem Fall kann es sich bei den Resonanzen $D_{S0}^*(2317)$ und $D_{S1}(2460)$ um dynamisch generierte Pole handeln (alternativ hierzu auch um Tetraquarks oder molekulare Zustände). Unsere Ergebnisse implizieren auch, dass die Interpretation der Resonanz $D_{S1}(2536)$ als Mitglied des axial-vektoriellen Multiplets nicht favorisiert ist, da die experimentelle Breite zu schmal im Vergleich zur theoretischen Breite eines Quarkonium-Zustands derselben Masse ist. Die Untersuchung dieser Resonanzen erfordert die Berechnung von Quantenfluktuationen und wird Thema zukünftiger Studien sein.

Zerfälle von Open-Charm-Mesonen

Die Ergebnisse für die Konstanten aus den schwachen Zerfällen von pseudoskalaren Open-Charm- D - und D_s -Mesonen sind in guter Übereinstimmung mit den experimentellen Werten. Wir berechnen die OZI-dominierten Zerfälle der Charmed-Mesonen. Die Resultate für $D_0(2400)^+$, $D_0(2400)^0$, $D_0(2007)$, $D(2010)$, $D(2420)^0$, und $D(2420)^+$ sind vergleichbar mit den Ergebnissen für die Ober- und Untergrenzen der PDG, obwohl die theoretischen Fehler ziemlich groß sind. In unserem Modell ist es dennoch möglich, gleichzeitig die Zerfälle von Open-Charm-Vektormesonen und ihren chiralen Partnern, den Axialvektormesonen, zu beschreiben.

Zerfälle von Charmonium-Mesonen

Wir erweitern unser $U(4)_R \times U(4)_L$ -symmetrisches lineares Sigma Modell mit Axialvektor- und Vektormesonen um ein Dilaton-Feld, welches ein skalarer Glueball ist. Zusätzlich bauen wir Wechselwirkungen eines pseudoskalaren Glueballs mit (pseudo-)skalaren Mesonen ein, um die Eigenschaften der OZI-unterdrückten Charmonia zu untersuchen. Wir berechnen die OZI-unterdrückten Zerfälle der skalaren und pseudoskalaren Charmonium-Zustände, $\chi_{c0}(1P)$ und $\eta_c(1S)$. Wir machen Vorhersagen für einen pseudoskalaren Glueball mit einer Masse von etwa 2.6 GeV, welcher im PANDA-Experiment bei FAIR gemessen werden kann. Zusätzlich geben wir Vorhersagen für einen pseudoskalaren Glueball mit einer Masse von etwa 2.37 GeV an. Dieser Glueball entspricht der im BESIII-Experiment gemessenen Resonanz $X(2370)$, die beim Zerfall vom Charmonium-Zustand η_c gemessen wird. Wir berechnen auch den Mischungswinkel zwischen pseudoskalaren Gluebällen mit einer Masse von 2.6 GeV und dem Hidden-Charm-Meson η_c .

Die Tatsache, dass eine qualitative Beschreibung dieser Zerfälle im Rahmen eines chiralen Modells, dessen Parameter für $N_f = 3$ bestimmt wurden, möglich ist, ist ein Indiz dafür, dass ein Teil der chiralen $SU(3)_R \times SU(3)_L$ -Symmetrie im Charm-Sektor weiterhin erhalten ist. Ein weiterer Hinweis für eine teilweise erhaltene chirale $SU(3)_R \times SU(3)_L$ -Symmetrie besteht darin, dass die Parameter des erweiterten linearen Sigma-Modells keine starke Energieabhängigkeit besitzen. Wir berechnen schließlich das Charm-Kondensat, welches von derselben Größenordnung ist wie das Non-strange- und das Strange-Quarkkondensat. Das ist auch in Übereinstimmung mit der zu $U(4)_R \times U(4)_L$ -vergrößerten chiralen Dynamik.

Darüber hinaus haben wir ein Dilatonfeld, ein skalares Glueballfeld und die Wechselwirkung eines pseudoskalaren Glueballfeldes mit (pseudo-)skalaren Mesonen unter $U(4)_R \times U(4)_L$ -Symmetrie einbezogen. Anschließend haben wir die Breite des Zerfalls des Charmonium-Mesons χ_{c0} in zwei oder drei Strange- oder Non-Strange-Mesonen und in einen skalaren Glueball G berechnet. Letzterer ist eine Mischung der Resonanzen $f_0(1370)$ sowie $f_0(1500)$ und $f_0(1700)$. Der Zerfall des Charmonium-Zustands in Open-Charm-Mesonen ist hingegen innerhalb des eLSM verboten. Ferner haben wir die Breite des Zerfalls des pseudoskalaren Charmonium-Zustands η_C in leichte Mesonen und in einen pseudoskalaren Glueball \tilde{G} über den Kanal $\eta_C \rightarrow \pi\pi\tilde{G}$ bestimmt. Dies wurde mittels des Wechselwirkungsterms des pseudoskalaren Glueballs für zwei Fälle durchgeführt. Zum einen für eine Masse von 2.6 GeV, wie sie von Gitter-QCD-Rechnungen in der Quenched-Näherung vorhergesagt wurde und im bevorstehenden PANDA-Experiment an der FAIR-Anlage gemessen werden kann. Zum an-

deren für eine Glueballmasse von 2.37 GeV, die der Masse der Resonanz $X(2370)$ entspricht und im BESIII-Experiment ermittelt wurde. Der Mischungswinkel zwischen dem pseudoskalaren Glueball und η_C wurde ausgewertet. Er ist sehr klein und beträgt lediglich -1° . Wir haben begründet, dass das eLSM keinerlei Zerfallskanal für (axial-)vektorielle Charmonium-Zustände aufweist, wobei $\Gamma_{J/\psi} = 0$ und $\Gamma_{\chi_{c1}} = 0$. Die Ergebnisse der Zerfallsbreiten χ_{c0} und η_C stimmen gut mit experimentellen Daten überein. Dies zeigt, wie erfolgreich das eLSM im Bezug auf das Studium der Hidden-Charm- und Open-Charm-mesonischen Phänomenologie ist. Die vier bestimmten Parameter im Falle von $N_f = 3$, die zur erfolgreichen Auswertung der Massen von Open- und Hidden-Charm-Mesonen und der Zerfallsbreite des Open-Charm-Mesons dienen, sind: (i) λ_1 und h_1 , die gleich Null gesetzt werden im Falle von $N_f = 3$, da sie so klein sind und die vorherigen Resultate nicht beeinflussen. Dagegen hängt die Zerfallsbreite der Charmonium-Zustände χ_{c0} und η_C von beiden ab. Deshalb wurden diese beiden Parameter durch das Minimieren der Zerfallsbreite des χ_{c0} festgelegt, siehe Tabelle 8.2.

(ii) Der Parameter c , der im axialen Term vorkommt, wird auch durch den Fit von Gl.(8.16) bestimmt.

(iii) $c_{\tilde{G}\Phi}$, das durch die Beziehung $c_{\tilde{G}\Phi(N_f=3)}$ festgelegt wird.

Ausblick

In der modernen Hadronenphysik ist die Wiederherstellung der chiralen Symmetrie bei endlicher Temperatur und Dichte eine der fundamentalsten Fragestellungen. Das eLSM hat es im Gegensatz zu alternativen Ansätzen geschafft, den zwei-Flavor Fall bei einem chemischen Potential ungleich Null zu ergründen. All dies führt uns dazu, die Restauration der chiralen Symmetrie bei nichtverschwindender Temperatur und Dichte für $N_f = 3$ und $N_f = 4$ mithilfe des eLSM zu untersuchen. Dies bringt viele Herausforderungen mit vielen unbekanntem Parametern in sich. In Zukunft werden wir die Vakuumphänomenologie des leichten Tetraquark-Nonets und dessen Erweiterung auf $N_f = 4$ untersuchen.

Contents

1. Introduction	1
1.1. Historical Remarks	1
1.2. Standard Model	2
1.3. Quantum Chromodynamics (QCD)	4
1.4. Features of QCD	5
1.4.1. Asymptotic freedom	5
1.4.2. Quark Confinement	7
1.4.3. Chiral Symmetry	7
1.5. Evidence for colour	8
1.6. Baryons and Mesons	10
1.6.1. Charmed mesons	11
1.6.2. Glueball	12
1.7. Thesis Content	14
1.7.1. Second chapter	14
1.7.2. Third chapter	14
1.7.3. Fourth chapter	14
1.7.4. Fifth chapter	14
1.7.5. Sixth chapter	14
1.7.6. Seventh chapter	15
1.7.7. Eighth chapter	15
2. Construction of mesonic Lagrangians	17
2.1. Introduction	17
2.2. Construction of QCD Lagrangian	18
2.3. Symmetry features of QCD	20
2.3.1. $Z(N_c)$ Symmetry	20
2.3.2. Local $SU(3)_c$ colour symmetry	21
2.3.3. Scale invariance and trace anomaly	21
2.3.4. CP- symmetry	23
2.3.5. Chiral symmetry and $U(1)_A$ anomaly	24
2.4. Chiral symmetry breaking	28
2.4.1. Explicit symmetry breaking	28
2.4.2. Spontaneous symmetry breaking	28
2.5. Construction of an effective model	30
2.6. The extended Linear Sigma Model	40
3. The extended Linear Sigma Model for two- and three-flavours	43
3.1. Introduction	43

3.2.	A $U(2)_R \times U(2)_L$ interaction with nucleons	43
3.2.1.	A chirally invariant mass term	43
3.3.	The $U(3)_R \times U(3)_L$ linear sigma model	46
3.3.1.	Model Parameters	52
3.3.2.	Results	53
4.	Charmed mesons in the extended Linear Sigma Model	55
4.1.	Introduction	55
4.2.	The $U(4)_r \times U(4)_l$ linear sigma model	56
4.3.	Four-flavour linear sigma model implications	60
4.4.	Tree-level masses	65
4.4.1.	η and η' Masses	67
4.4.2.	Scalar-Isosinglet Masses	68
4.5.	The Model Parameters	70
4.6.	Results	72
4.6.1.	The w_i and the wave-function renormalization constants Z_i	72
4.6.2.	Masses of light mesons	73
4.6.3.	Masses of charmed mesons	74
5.	Particle decays	79
5.1.	Introduction	79
5.2.	Decay constants	80
5.3.	Two-body decay	81
5.4.	Three-body decay	84
6.	Decay of the pseudoscalar glueball into scalar and pseudoscalar mesons	89
6.1.	Introduction	89
6.2.	The effective Lagrangian with a pseudoscalar glueball	90
6.2.1.	Implications of the interaction Lagrangian	91
6.3.	Field assignments	92
6.4.	Decay widths of a pseudoscalar glueball into (pseudo)scalar mesons	94
6.4.1.	Results	98
6.5.	Interaction of a pseudoscalar glueball with nucleons	101
6.5.1.	Decay of a pseudoscalar glueball into two nucleons	102
7.	Decay of open charmed mesons	109
7.1.	Introduction	109
7.2.	Decay widths of open-charmed scalar mesons	109
7.2.1.	Decay Width $D_0^{*0,\pm} \rightarrow D\pi$	111
7.2.2.	Decay Width $D_{S0}^{*\pm} \rightarrow DK$	112
7.3.	Decay widths of open-charmed vector mesons	114
7.3.1.	Decay Width $D^{*0,\pm} \rightarrow D\pi$	117
7.4.	Decay widths of open charmed axial-vector mesons	119
7.4.1.	Two-body decay of D_1	121
7.4.2.	Decay Width $D_1 \rightarrow D\pi\pi$	123
7.4.3.	Decay Width $D_{S1} \rightarrow D^*K$	126

7.5. Weak decay constants of Charmed mesons	127
7.6. Summary	128
8. Decay of hidden charmed mesons	131
8.1. Introduction	131
8.2. Decay of the scalar charmonium state χ_{c0}	132
8.2.1. Parameters and results	134
8.3. Decay of the pseudoscalar charmonium state η_C	138
8.3.1. Decay of η_C into a pseudoscalar glueball	138
8.3.2. Decay of η_C into (pseudo)scalar mesons	140
8.3.3. Mixing of a pseudoscalar glueball and η_C	141
9. Conclusions and Outlook	143
Appendices	147
A. Determination of the weak decay constants	149
A.1. Pion decay constant	150
A.2. Kaon decay constant	152
A.3. Decay constant of D and D_S	153
A.4. Decay constant of η_C	156
B. Decay rates for χ_{c0}	159
B.1. Two-body decay rates for χ_{c0}	159
B.2. Three-body decay rates for χ_{c0}	169
C. Decay rates for η_C	175
C.1. Two-body decay expressions for η_C	175
C.2. Three-body decay expressions for η_C	178
Bibliography	181

1. Introduction

1.1. Historical Remarks

“The most incomprehensible thing about the universe is that it’s comprehensible at all...”

Albert Einstein

Billions of years ago, all of space was contained in a single point which, exposed to an enormous and incomprehensible explosion (the Big Bang), scattered the matter that constitutes the Universe. At that time, it was hot and dense, but within the first three minutes after the Big Bang the Universe became sufficiently cool to consist of subatomic particles, including protons, neutrons, and electrons. More than ten billion years passed before the stars and galaxies formed. After some time, planets surrounded some stars... life formed...finally, after billions of years of changes, the human being was created with a complex brain which has a deep and insatiable curiosity about the world. Humans found that understanding the world is not easy and noticed that understanding the nature of matter is an important and complementary approach to understanding the nature of reality and answering the deep and pressing questions in their minds. To answer these questions, they used the observational method which creates a lot of ideas. The Greek philosopher Empedocles surmised that everything was made from a suitable mix of four basic elements: air, fire, water, and earth. These four elements were perceived as the fundamental elements in nature. Consequently, concentration moved towards understanding the nature of the elements’ permanence. The ancient philosophers Leucippus and well-known Democritus of Greece are the earliest philosophers who conceived the idea that matter is composed entirely of various imperishable, indestructible, indivisible elements, always in motion, having empty space between them; called atoms. The name is derived from the Greek *ἄτομος* which means “indivisible”. In 1661, Robert Boyle established the atomic idea (molecules). However, this knowledge about the existence of atoms brings with it a lot of important questions: How do these atoms make molecules?... How do the molecules make gases, liquids and solids?... It must be forces that act on these atoms to keep them together in molecules, but what are these forces? They arrived at that time at the idea that the inter-atomic forces are gravity, static electricity, and magnetism. After that, there were a lot of efforts from philosophers and scientists directed towards the fundamental building blocks of matter. At the close of the 19th century, it was known that more than 100 elements exist and that all matter is composed of atoms which have an internal structure and are not indivisible, which is opposite of what Democritus foresaw of the indivisible property of the atom.

At the beginning of the 20th century, Rutherford presented the subatomic structure as a result of his experiments: an atom is composed of a dense nucleus surrounded by a cloud of

electrons. Consequently, physicists found that the nucleus decomposed into smaller particles, which they called protons and neutrons, and in turn that protons and neutrons themselves contain even smaller particles called quarks. Moreover, there are other small ingredients making up the atom, which are called leptons. These include the electron in the orbits of the nucleus, situated at (relatively) large distance from the nucleus, but not inside it. We conclude that quarks and leptons constitute all fundamental matter in the Universe [1]. This information is the starting point for understanding the formation of the Universe.

1.2. Standard Model

“Daring ideas are like chessmen moved forward; they may be detected, but they start a winning game”
Goethe

Quarks and leptons are the basic types of fundamental matter particles. Each group consists of six types of flavour. The combinations of these form the hundreds of particles discovered in the 1950s and 1960s. Two flavours each can be classified as a generation under the weak interaction, in which the first generation consists of the lightest flavours which make the most stable particles in the Universe, whereas the second and third generations contain the heavier flavours which make the less stable particles which decay quickly to the next-most stable state belonging to the previous generation. The quark generations are: the ($u \equiv up$, and the $d \equiv down$) quark flavours (the first generation), followed by the ($c \equiv charm$, and the $s \equiv strange$) quark flavours as a second generation, and the third consists of the ($t \equiv top$, and the $b \equiv bottom$) quark flavours. Concerning the electric charges of quarks, quarks carry colour charge which corresponds to the electric charge of electrons. They also carry a fractional electric charge (the u, c , and t quark flavours carry $(2/3)e$, whereas the d, s , and b quark flavours carry $(-1/3)e$). Each quark has its corresponding antiparticle with opposite charge. Similarly, there are three generations for the six lepton flavours: the $e \equiv electron$, and the $\nu_e \equiv electron\ neutrino$, the $\mu \equiv muon$, and the $\nu_\mu \equiv muon\ neutrino$, and the $\tau \equiv tau$, and the $\nu_\tau \equiv tau\ neutrino$. The three lepton flavours (the electron, the muon and the tau) have a sizable mass with charge $-e$, whereas the other three -the neutrinos- are neutral and have a small mass. (See Table 1.1 for a compilation of quarks and leptons).

Particle	Generation I	Generation II	Generation III	charge
Quarks (q)	up (u) (0.0015-0.0033)	charm (c) (1.5)	top (t) (172)	$+(2/3)e$
	down (d) (0.0035-0.006)	strange (s) (0.1)	bottom (b) (4.5)	$-(1/3)e$
Leptons (l)	electron (e) (0.0005)	muon (μ) (0.1)	tau (τ) (1.7)	-1
	electron neutrino (ν_e) (<0.000000015)	muon neutrino (ν_μ) (<0.00017)	tau neutrino (ν_τ) (<0.024)	0

Table 1.1: Summary of quarks and leptons. The numbers in parentheses are the masses in GeV.

The central rule in creating the Universe depends on the four fundamental forces. Physicists use these forces to describe quantitatively all the phenomena from the small scale of quarks and leptons to the large scale of the whole Universe. Then, what are the four fundamental forces that govern the Universe? Let us list them as follows:

(i) The gravitational force: Attracts any two pieces of matter. It has an infinite range and is the weakest force. It is responsible for keeping stars, galaxies, and planetary systems in order, but it has no significance in the particle physics realm.

(ii) The electromagnetic force: causes electric and magnetic effects. It also has infinite range, but is much stronger than gravity. This force acts only between electrically charged matter. Therefore, it governs the motion of electrons around the nucleus. Note that the relations between the spatial- and time-dependences of the electric and magnetic fields [2] were explained by James Maxwell in 1865 through his equations; the Maxwell Equations.

(iii) The nuclear force: As the name suggests, it acts only between nucleons. It is a result of the strong force which has a very short range, acting only over a range of 10^{-13} cm. It is the strongest force and has the responsibility of binding quarks together, keeping them inside protons and neutrons, and also binds the protons and neutrons together. Therefore, it is responsible for the stability of the nucleons.

(iv) The weak force: Dominates only at the level of subatomic particles. It is effective also over a very short range (see Table 1.2), and it is stronger than gravity and weaker than others.

The electromagnetic, strong, and weak forces arise from the exchange of force-carrier particles which are bosons called-gauge bosons. Each of these four fundamental forces has a different type of carrier: the electromagnetic force is carried by the massless photon (γ) which is chargeless and is known as the particle of light. The strong force has a corresponding boson, the gluon (g), which is massless and is not charged electrically, just as the photon, but which carries a different sort of charge, called colour which holds the quarks confined within nucleons. The gluon is thus related to nucleon stability. The bosons W and Z (W^\pm , Z^0) are the corresponding force-carrying particles of the weak force, these carriers are massive, having a mass about 100 times that of the proton mass. The properties of the interaction forces in the Standard Model are summarized in Table 1.2. Moreover, gravity may be carried by the “graviton”, but it has not yet been found. Note that leptons carry electromagnetic charge and weak isospin as quantum numbers, but quarks may experience all four fundamental interactions, and carry the strong charge which is also called colour charge.

Interaction	Mediator	Spin	Mass (GeV)	Range (m)	acts on
Electromagnetic	γ	1	0	∞	Quarks, Leptons, W^\pm
Weak	W^\pm	1	80.398 ± 0.025	$\leq 10^{-18}$	Quarks, Leptons
	Z^0	1	91.1876 ± 0.0021		
Strong	g	1	0	$< 10^{-15}$	Quarks, Gluons

Table 1.2: The properties of the interactions in the Standard Model.

Concerning quarks, leptons, and all their fundamental interactions, theory and experiment together produced a gauge theory called the Standard Model of elementary particles. Recently the Higgs boson which is an essential component of the standard Model was discovered by the ATLAS [3] and CMS [4] experiments at the Large Hadronic Collider (LHC)

in 2012.

The Standard Model is based on a Lagrangian density with fields as degrees of freedom. The strong and weak interactions are described by Quantum Chromodynamics (QCD) and the Glashow-Weinberg-Salam Theory of the Weak Interaction (GWS) [5], respectively. Quarks and gluons carry colour charge and have never been seen to exist as single-particle states. They couple to themselves which leads to confinement and asymptotic freedom. These can be further distinguished into baryons and mesons. Leptons do not interact by the strong force. The production of hadrons as observed in the final state of high-energy collisions, which arise due to how quarks and gluons arrange themselves, is described by the theory called quantum chromodynamics (QCD), described in the following.

1.3. Quantum Chromodynamics (QCD)

“In modern physics, there is no such thing as ‘nothing’. Even in a perfect vacuum, pairs of virtual particles are constantly being created and destroyed. The existence of these particles is no mathematical fiction. Though they cannot be directly observed, the effects they create are quite real. The assumption that they exist leads to predictions that have been confirmed by experiment to a high degree of accuracy”

Richard Morris

The dynamics of baryons and mesons (hadrons) are described by the theory of the fundamental interactions of quarks and gluons, i.e., quantum chromodynamics (QCD) [6].

The fundamental symmetry underlying QCD is an exact local $SU(3)_c$ colour symmetry. The quarks are coloured objects: $q \in 3_c$. As a consequence of the non-Abelian nature of the $SU(3)_c$ symmetry, the gauge fields of QCD - the gluons - are also coloured objects: $g \in 8_c$. Therefore, quarks and gluons interact strongly with each other. The dynamics of this interaction are described by the QCD Lagrangian, see Sec. 2.2, which implies *asymptotic freedom* and *confinement*. Perturbation theory works in the high-energy regime [7, 8], due to the asymptotically-free nature of QCD, such as for deep inelastic lepton-hadron scattering (DIS). However, at low energy (energies comparable to the low-lying hadron masses $\sim 1\text{GeV}$), perturbation theory fails due to confinement and the dynamical breaking of chiral symmetry.

The development of an effective low-energy approach to the strong interaction plays an important role in the description of the masses and the interactions of low-lying hadron resonances [9, 10], which is done by imposing chiral symmetry. One of the basic symmetries of the QCD Lagrangian in the limit of vanishing mass (the so-called chiral limit) [11, 12] is the chiral symmetry which is explicitly broken by the nonzero current quark masses, but it is also spontaneously broken by a nonzero quark condensate in the QCD vacuum [13, 14]. As a consequence, pseudoscalar (quasi-)Goldstone bosons emerge. In a world with only u and d quarks (i.e., for $N_f = 2$ quark flavours), these are the pions, while for $N_f = 3$, i.e., when also the strange quark s is considered, these are the pions, kaons, and the η meson. (The η' meson is not a Goldstone boson because of the chiral anomaly [15, 16, 17, 18]). In the present work we study the vacuum phenomenology of mesons in the framework of the extended Linear Sigma Model (eLSM) which is an effective chiral model that emulates the global symmetries of the QCD Lagrangian (see the details in Sec. 2.3). The fundamental features of QCD are described in the following section.

1.4. Features of QCD

1.4.1. Asymptotic freedom

This feature was observed by Gross, Wilczek, and Politzer in 1973 [19, 20]. (They won the Nobel Prize in Physics in 2004). Quarks behave quasi-free at small distance or at high energies (high compared to the rest mass of the proton). That means the coupling/interaction strength $\alpha_s = g^2/4\pi$ between quarks becomes weaker or smaller with increasing energy, increasing momentum, and decreasing interparticle distance. This prediction was confirmed experimentally by deep-inelastic scattering of leptons by nucleons [1]. A quark-gluon plasma was predicted for high temperature and/or baryonic chemical potential based on asymptotic freedom. Perturbation theory confirmed the existence of a quark-gluon plasma phase [21]. Furthermore, at high temperature and high density, colour charged particles are liberated from hadrons, they become deconfined.

The opposite effect occurs at low energies, which means the interaction/coupling strength between quarks becomes stronger with increasing distance. This leads to the emergence of confinement, which means that colour-charged particles are confined in colour-neutral states (hadrons).

QCD seems like an expanded version of quantum electrodynamics (QED). Both have charges: QED has electric charge and QCD has the colour charges (red, green, and blue). Therefore, just as one considers the force between two electric charges to understand and study electromagnetic physics, one can analogously consider the strong force between two colour charges to understand the strong interaction. This leads us to explain asymptotic freedom in a simple way by referring firstly to electromagnetic physics as follows [22]:

Coulomb's law describes the force between two charges q_1 and q_2 in vacuum as

$$F = \frac{1}{4\pi} \frac{q_1 q_2}{r^2}. \quad (1.1)$$

However, in a medium with dielectric constant $\epsilon > 1$, the force between them becomes

$$F = \frac{1}{4\pi\epsilon} \frac{q_1 q_2}{r^2}, \quad (1.2)$$

which has the same form as in vacuum with the effective charge $\tilde{q}_i = q_{1,2}/\sqrt{\epsilon}$.

In quantum field theory, the vacuum is the lowest energy state of a system. In QED, it is not empty but filled with electrons of negative energies. When the photon travels through the vacuum, an electron can be induced to jump from a negative to a positive energy state, which creates a virtual pair of an electron and a positron (the hole in the negative-energy continuum). That is known as a vacuum fluctuation. For this reason, the interaction force between two electrons in the vacuum becomes

$$F = \frac{e_{eff}^2}{4\pi r^2} = \frac{\alpha_{em}(r)}{r^2}, \quad (1.3)$$

where α_{em} is an effective fine structure constant and depends on the distance r or the momentum transfer $q \sim \frac{1}{r}$. The interaction strength of a low-energy photon at $r \rightarrow \infty$ or ($\equiv q \rightarrow 0$) is $\alpha_{em}(q = 0) = 1/137.035$ [23].

In QED, the coupling as a function of the momentum scale μ can be determined by the following differential equation

$$\mu \frac{\partial \alpha(\mu)}{\partial \mu} = \beta(\alpha(\mu)). \quad (1.4)$$

From perturbation theory, the β -function can be obtained at one-loop order as

$$\beta = 2 \alpha_{em}^2 / 3 \pi > 0.$$

Then the solution can be obtained as

$$\alpha_{em}(\mu) = \frac{\alpha_{em}(\mu_0)}{1 - \frac{\alpha_{em}(\mu_0)}{3\pi} \ln \frac{\mu^2}{\mu_0^2}}. \quad (1.5)$$

Now it is clear that when the distance between the two electrons becomes smaller, their interaction strength gets stronger. Therefore, QED is a strong-coupling theory at very short distance scales.

Now let us turn to QCD which has a classical scale symmetry (see the details in the next chapter). At the quantum level, this symmetry is spontaneously broken due to the energy scale which is introduced by the renormalization of quantum fluctuations. Therefore, the strong coupling g depends on the energy scale μ [24, 25, 26]:

$$g \text{ renormalization } g(\mu)$$

The beta function $\beta(g(\mu))$ of the renormalization group describes the variation of the strong coupling with energy scale μ , called running coupling. It has the same differential equation (1.4) as in QED

$$\beta(g(\mu)) = \mu \frac{\partial g(\mu)}{\partial \mu}. \quad (1.6)$$

At one-loop level in perturbation theory the beta function of QCD has the following form [19, 20]

$$\beta(g(\mu)) = \frac{-11 N_c + 2 N_f}{48 \pi^2} g^3, \quad (1.7)$$

where N_f is the number of active quark flavours and N_c the number of colours. In nature, there are six quark flavours and three colours. As seen in Eq.(1.6), if the β -function is negative ($\beta(g(\mu)) < 0$), then the QCD coupling decreases with increasing energy scale μ . The coupling constant of QCD is obtained from the solution of the differential equation (1.6) as

$$g^2(\mu) = \frac{24 \pi^2}{(11 N_c - 2 N_f) \ln(\mu/\Lambda_{\text{QCD}})}, \quad (1.8)$$

which describes clearly that, when the energy scale is increasing ($\mu \rightarrow \infty$) or the distance is decreasing ($d \rightarrow 0$), the QCD coupling constant is decreasing ($g \rightarrow 0$). This feature is called asymptotic freedom.

1.4.2. Quark Confinement

The fact that the strong coupling grows in the increasing distance leads to the confinement of quarks, which means that no isolated elementary excitations of QCD, quarks, exist in nature. Experimentally, no one has observed an isolated quark. Quarks usually clump together to form hadrons, such as baryons and mesons. In QCD, the confinement hypothesis has not been directly derived until now. Note that, at any finite order in perturbation theory, there is no confinement. Therefore, it is a nonperturbative phenomenon. Confinement has a lot of meanings. Four different meanings are considered [27]:

(i) ‘*Quarks cannot leave a certain region in space*’ [27], which is called ‘*Spatial Confinement*’. The MIT-bag model explores the consequences of spatial confinement, whereas the Chromodielectric Soliton Model [28] attempts to understand the mechanisms producing this confinement.

(ii) ‘*String confinement*’: it is especially for mesons which are produced from scattering processes. From the features of the meson spectrum, the attractive force between quark and anti-quark increases linearly with the distance of the quarks. Moreover, quark and antiquark are linked together by something which expands with increasing energy. For all of that, free quarks never appear. Note that the string breaks and new particles are created when the corresponding energy exceeds a certain critical value and the separation becomes large enough.

(iii) ‘*There are no poles in the quark propagator*’. This definition is limited to the, a priori unknown, quark propagator. Asymptotic quark states cannot appear when the full quark propagator has no poles. This means no free quarks exist.

(iv) ‘*Colour Confinement*’ means any composite particle must be a colour singlet under the strong interaction at zero temperature and density, and at distance scales larger than $1/\Lambda_{QCD}$. M. Gell-Mann is the first one who introduced this type of confinement to solve his original quark-model problem.

Finally, we have to conclude from all of this that there are no isolated quarks and gluons in nature.

1.4.3. Chiral Symmetry

Chiral symmetry and its dynamical breaking are very important features of QCD at low energy. From the dynamical breaking of chiral symmetry, an effective quark mass is generated.

What is the meaning of chirality?

Kelvin’s definition of chirality: “I call any geometrical figure, or group of points ‘*chiral*’, and say it has chirality, if its image in a plane mirror, ideally realized, cannot be brought to coincide with itself”
(Lord Kelvin, 1904, The Baltimore Lectures)

In general, *chirality* is the property of having for the same object a left-form and a right-form which are mirror images of each other.

The property of *chirality* (or “handedness”) is well-known of many physical, chemical, and

biological systems. In theoretical physics, it is demonstrated that a quantum field theory cannot be chirally symmetric if its Lagrangian density has explicit mass terms. However, comparing to the rest mass of the proton (about 1000 MeV), the current quark masses of the relevant quarks are small (about 10 MeV) in the low-energy domain of QCD which leads to an approximate realization of chiral symmetry. In the end, there is a chiral partner (with the same mass, but opposite parity and G-parity) for every eigenstate of the interaction. This is not seen in experimental data, from which it is concluded that the chiral symmetry is broken. Note that the confinement and dynamical chiral symmetry breaking cannot be obtained in a simple perturbative analysis of QCD because they are low-energy phenomena, and in this regime, perturbation theory breaks down (for more details of low-energy theorems see [11, 12, 29]). For this reason, effective chiral models are widely used to study the phenomenology of hadrons.

More details of the chiral symmetry and its spontaneous and explicit breaking are described in the next chapter.

1.5. Evidence for colour

There is experimental and theoretical evidence for the existence of colour in nature.

Experimentally:

(i) e^+e^- annihilation experiments

In 1967, the results of high-energy electron and positron annihilation experiments at the Stanford Linear Accelerator (SLAC) supported the colour charge of quarks.

The confirmation of the existence of the colour quantum number can be obtained from a comparison of the cross section of the following two processes:

$$e^+e^- \longrightarrow \mu^+\mu^- \quad \text{and} \quad e^+e^- \longrightarrow \text{hadrons}. \quad (1.9)$$

Note that hadron production occurs only when quarks are in the final state as a result of confinement. Therefore, the production of hadrons occurs through

$$e^+e^- \longrightarrow \gamma \text{ (or } Z) \longrightarrow \bar{q}q \longrightarrow \text{hadrons}.$$

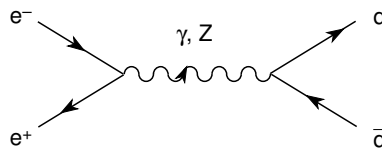


Figure 1.1.: Tree-level Feynman diagram for the e^+e^- annihilation into hadrons.

In this comparison of the cross sections, the weak production factor involving the Z for the previous process is neglected as well as for the $e^+e^- \longrightarrow \mu^+\mu^-$ process as seen in Eq.(1.9), because of the dominance of the cross section due to γ exchange amplitude at the energies

below the Z peak. The ratio of the cross sections for the processes described in Eq.(1.9) depends on the quark colour N_c [30],

$$R \equiv \frac{\sigma(e^+e^- \rightarrow \text{hadrons})}{\sigma(e^+e^- \rightarrow \mu^+\mu^-)} \simeq N_c \sum_{f=1}^{N_f} Q_f^2 = \begin{cases} \frac{5}{9}N_c = \frac{5}{3}, & \text{for } (N_f = 2 : u, d) \\ \frac{2}{3}N_c = 2, & \text{for } (N_f = 3 : u, d, s) \\ \frac{10}{9}N_c = \frac{10}{3}, & \text{for } (N_f = 4 : u, d, s, c) \\ \frac{11}{9}N_c = \frac{11}{3}, & \text{for } (N_f = 5 : u, d, s, c, t) \end{cases}, \quad (1.10)$$

where Q_f denotes the electric charge of quark flavours f . The value of the ratio, which corresponds to the experimental data of Fig. 1.2 [31] is obtained for $N_c = 3$. Therefore, there are three quark colours in the physical world.

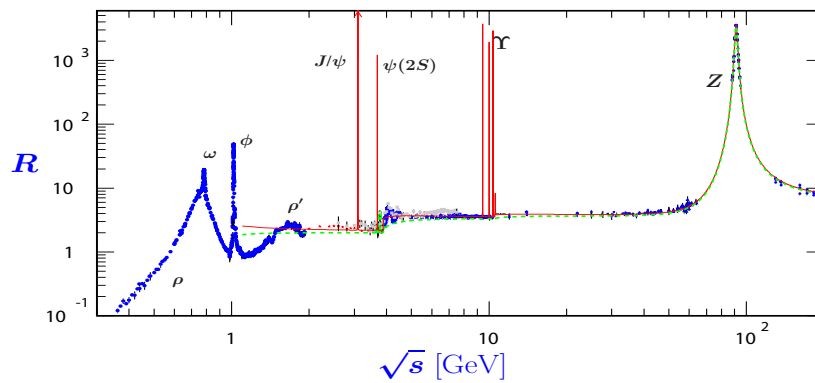


Figure 1.2.: World data on the ratio $R_{e^+e^-}$. The solid curve is the 3-loop perturbative QCD prediction. The broken lines show the naive quark model approximation with $N_c = 3$.

(ii) Decay of π^0 into 2γ

In 1967, Veltman tried to calculate the π^0 decay rate and obtained that it is forbidden [32]. Following this study, Adler, Bell, and Jackiw (1968-1970) [33, 34], using the ‘fix’ field theory, which allowed π^0 to decay, found that its decay rate is off by the factor of 9. During (1973-1974) many physicists, notably Gell-Mann and Fritzsche, used QCD with three colours and arrived at the correct result of π^0 decay. Let us explain this in more detail:

The neutral pion π^0 is a meson composed of quarks, $\pi^0 = \frac{1}{\sqrt{2}}(\bar{u}u - \bar{d}d)$. The decay width of the pion into two photons ($\pi^0 \rightarrow 2\gamma$) is determined by a triangular quark loop in the Standard Model [30] as

$$\Gamma_{\pi^0 \rightarrow 2\gamma} = \frac{\alpha^2 m_\pi^2}{64 \pi^3 f_\pi^2} \left(\frac{N_c}{3}\right)^2 \equiv \left(\frac{N_c}{3}\right)^2 7.73 \text{ eV}, \quad (1.11)$$

which depends on the number of colours and the decay constant of the pion $f_\pi = 92.4 \text{ MeV}$.

Experimental data give [23]

$$\Gamma_{\pi^0 \rightarrow 2\gamma}^{exp} = (7.83 \pm 0.37)\text{eV}. \quad (1.12)$$

These experimental data is in very good agreement with the Standard Model calculation (1.11) only when the number of colours $N_c = 3$. This is further evidence for the existence of quark colour in nature.

Theoretically: solving the spin-statistics problem

In 1965, the Δ -baryon was discovered [35, 36], which is composed of three quarks. Considering the baryon's charge $q = 2e$, spin $S = 3/2$, and angular momentum $l = 0$, there emerged a spin-statistics problem. When describing this particle in terms of u and d quarks, the spin-flavour wave function Δ^{++} had to be expressed as

$$|\Delta^{++}\rangle = |u_\uparrow u_\uparrow u_\uparrow\rangle, \quad (1.13)$$

which describes an overall symmetric state. This violated Fermi-Dirac statistics and the Pauli principle [37] as well. This paradox can be avoided by assuming the existence of colour as a degree of freedom for quarks: a quark can carry three different colours which are red (r), blue (b), green (g). Consequently, in the Δ^{++} the three u quarks combine their colours in an antisymmetric way as follows:

$$|\Delta^{++}\rangle_{\text{colour}} = \frac{1}{\sqrt{6}} |r_1 g_2 b_3 - g_1 r_2 b_3 + b_1 r_2 g_3 - b_1 g_2 r_3 + g_1 b_2 r_3 - r_1 b_2 g_3\rangle, \quad (1.14)$$

which is in accordance with the Pauli principle.

1.6. Baryons and Mesons

Baryons and mesons are hadronic particles composed of quarks and gluons bound together strongly and confined in colour singlet states (colourless states). They bear evidence for the existence of elementary (quark) constituents of matter because they come in many different forms in nature.

Baryons: These are fermionic hadronic states with half-integer spin and composed of three valence quark (qqq) or three antiquarks ($\bar{q}\bar{q}\bar{q}$). A proton and a neutron are the lightest baryons, which consist of uud and ddu , respectively. Therefore, baryons are a central part of nature and form the complex structure of the cores of atoms. The baryon number of a quark is $1/3$. Consequently, the baryon number for baryons is 1, while for antibaryons it is -1 .

The wave function of a baryon $B = qqq$ is antisymmetric under colour exchange and can thus be described as

$$|B\rangle_{\text{colour}} = \frac{1}{\sqrt{6}} |q_{1_r} q_{2_g} q_{3_b} - q_{1_g} q_{2_r} q_{3_b} + q_{1_b} q_{2_r} q_{3_g} - q_{1_b} q_{2_g} q_{3_r} + q_{1_g} q_{2_b} q_{3_r} - q_{1_r} q_{2_b} q_{3_g}\rangle, \quad (1.15)$$

which can also be written as

$$|B\rangle_{\text{colour}} = \frac{1}{\sqrt{6}} \varepsilon^{\alpha\beta\gamma} |q_{1\alpha} q_{2\beta} q_{3\gamma}\rangle, \quad (1.16)$$

where $\varepsilon^{\alpha\beta\gamma}$ is the totally antisymmetric tensor and α, β, γ refers to the three different colours (r, g, b). Furthermore, there is a hypothetical “exotic” baryon with an extra quark-antiquark pair additional to the original three quarks, which is called a pentaquark ($qqqq\bar{q}$). The $qqqg$ states, bound states of three quark and a gluon, are hybrid states and called hermaphrodite baryons. There is also a hypothetical dibaryon state which consist of six quarks and has baryon number +2.

Mesons: These are bosonic hadronic states with integer spin. Many meson types are known in nature. Most states consist of $q\bar{q}$ (a quark bound with its antiquark). The pion is the lightest meson which has a mass of about $140 \text{ MeV}/c^2$ and is the first meson to have been discovered [38, 39, 40]. The colour wave function for the $q\bar{q}$ state is antisymmetrised as

$$|M\rangle_{\text{colour}} = \frac{1}{\sqrt{3}} |r\bar{r} + g\bar{g} + b\bar{b}\rangle, \quad (1.17)$$

or,

$$|M\rangle_{\text{colour}} = \frac{1}{\sqrt{3}} \delta^{\alpha\beta} |q_{\alpha}\bar{q}_{\beta}\rangle, \quad (1.18)$$

where $\delta^{\alpha\beta}$ denotes the antisymmetric tensor and $\alpha, \beta \in \{r, g, b\}$. A meson may decay into electrons, neutrons, and photons as seen in the previous section with the decay of the pion π into two photons $\gamma\gamma$. According to the hypothesis of “exotic” mesons, there are tetraquarks, consisting of a quark pair and an antiquark pair $[qq][\bar{q}\bar{q}]$, and also glueballs, bound states of gluons (gg). The recently discovered XYZ states are candidates for tetraquarks. Moreover there are hybrid states of mesons consisting of $q\bar{q}g$, bound states of quark-antiquark and gluon, called hermaphrodite mesons. In reality, there are many particles still not known in nature and every day presents a possibility of discovery for experimental physicists. In the recent past (2012), the Higgs boson was discovered.

The main goal of the present work is the study of the vacuum properties of the pseudoscalar glueball and charmed mesons via the chirally symmetric eLSM.

1.6.1. Charmed mesons

The charm quark (c) is a special one in the quark family, as it is heavier than the first three light quarks and does not belong to the regular flavour $SU(3)$, but stands in a weak doublet with the light strange quark. Therefore, it can act as a bridge between the light and heavy flavours. There are two types of charmed mesons: (i) The heavy-light $Q\bar{q}$ and $\bar{Q}q$ mesons called open charmed mesons, where Q is a heavy quark (referring to the charm quark c) and q is a light quark (referring to u, d , and s quarks). (ii) The heavy-heavy $Q\bar{Q}$ mesons, composite states of charm and anticharm quark, are called hidden charmed mesons (charmonia). The current charm quark mass ($m_c \sim 1.3 \text{ GeV}$) is larger than the characteristic energy scale for the strong interaction ($\Lambda_{QCD} \sim 300 \text{ MeV}$), by which enter, the perturbative regime, $m_Q \gg \Lambda_{QCD}$.

Since the discovery of the charmonium/hidden charmed state J/ψ in November 1974 at the Stanford Linear Accelerator Center (SLAC) [41] and Brookhaven National Laboratory (BNL) [42], and two years later (in 1976) the discovery of open charmed states at SLAC, the study of charmed meson spectroscopy and decays has made significant experimental [43, 44, 45, 46] and theoretical progress [47, 48, 49, 50]. Therefore, we are interested to study the vacuum properties of open and hidden charmed mesons.

In present work, we show how the original $SU(3)$ flavour symmetry of hadrons can be extended to $SU(4)$ in the framework of a chirally symmetric model with charm as an extra quantum number. Twelve new charmed mesons are included in addition to the nonstrange-strange sector. The new charmed mesons of lowest mass, the D , D_s , and the higher mass η_c are quark-antiquark spin-singlet states with quantum number $J^{PC} \equiv 0^{-+}$, i.e., pseudoscalar mesons. The scalar mesons D_0^* , D_{S0}^* , and χ_{C0} are spin-singlet states with $J^{PC} = 0^{++}$. The vector mesons D^* , D_s^* , and J/ψ are quark-antiquark spin triplets with $J^{PC} = 1^{--}$. The axial-vector mesons D_1 , D_{S1} , and χ_{C1} are quark-antiquark spin triplets with $J^{PC} = 1^{+-}$. The additional charmed fields D^{*0} , D^* , D_0^{*0} , χ_{C1} , χ_{C0} , and J/ψ are assigned to the physical resonances $D^*(2007)^0$, $D^*(2010)^\pm$, $D_0^*(2400)^0$, $D_0^*(2400)^\pm$, $\chi_{C1}(1P)$, $\chi_{C0}(1P)$, and the well known ground state $J/\psi(1P)$, respectively. The isospin doublet D_1^0 is $D_1(2420)$. The D is assigned to the well-established D resonance. The isospin singlet D_{S1} can be assigned to two different physical resonances, $D_{S1}(2460)$ and $D_{S1}(2536)$ as listed by the Particle Data Group PDG [51]. The first candidate can be interpreted as a molecular or a tetraquark state as shown in Refs.[46, 52, 53, 54, 55, 56, 57], which leads us assign D_{S1} to $D_{S1}(2536)$. Finally, the strange-charmed meson D_{S0}^* is assigned to the only existing candidate $D_{S0}^*(2317)^\pm$ although it is also interpreted as a molecular or a tetraquark [47, 48, 52, 53, 58, 59] (For more details of the charmed meson assignment, see Sec. 4.2). We compute charmed meson masses, weak decay constants, and strong decay widths of (open and hidden) charmed mesons. Moreover, we calculate the decay width of a pseudoscalar ground state charmonium η_c into a pseudoscalar glueball and the decay widths of a scalar charmonium χ_{C0} into a scalar glueball. The precise description of the decays of open charmed states is important for the CBM experiment at FAIR, while the description of hidden charmed states and the pseudoscalar glueball is vital for the PANDA experiment at the upcoming FAIR facility.

1.6.2. Glueball

The bound states of gluons form colourless, or ‘white’, states which are called glueballs. The first calculations of glueball masses were based on the bag-model approach [60, 61, 62, 63, 64]. Later on, the rapid improvement of lattice QCD allowed for precise simulations of Yang-Mills theory, leading to a determination of the full glueball spectrum [65, 66, 67] (see Table 1.3). However, in full QCD (i.e., gluons plus quarks) the mixing of glueball and quark-antiquark configurations with the same quantum number occurs, rendering the identification of the resonances listed by the Particle Data Group (PDG) [23] more difficult. The search for states which are (predominantly) glueballs represents an active experimental and theoretical area of research, see Refs. [10, 68, 69, 70] and refs. therein. The reason for these efforts is that a better understanding of the glueball properties would represent an important step in the comprehension of the non-perturbative behavior of QCD. However, although up to now some glueball candidates exist (see below), no state which is (predominantly) glueball has been unambiguously identified.

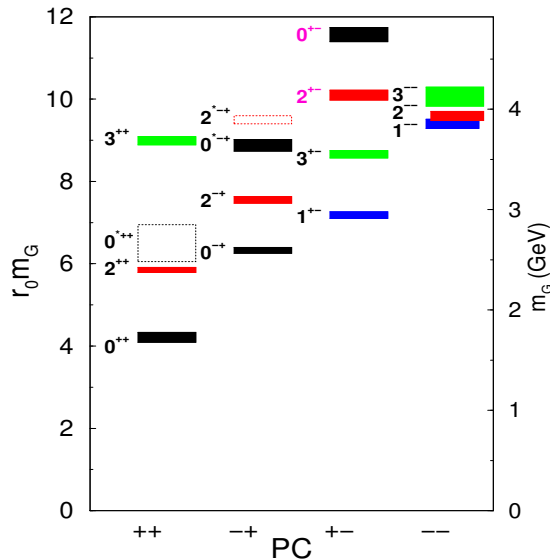


Figure 1.3: The lightest six states in the spectrum of the $SU(3)$ Yang-Mills theory [65].

In general, a glueball state should fulfill two properties regarding its decays: it exhibits ‘flavour blindness’, because the gluons couple with the same strength to all quark flavours, and it is narrow, because QCD in the large- N_c limit shows that all glueball decay widths scale as N_c^{-2} , which should be compared to the N_c^{-1} scaling law for a quark-antiquark state.

In Fig. 1.3, one can obtain that the lightest glueball state predicted by lattice QCD simulations is a scalar-isoscalar state ($J^{PC} = 0^{++}$) with a mass of about 1.7 GeV [65, 66, 67, 71]. The resonance $f_0(1500)$ shows a flavour-blind decay pattern and is narrow, thus representing an optimal candidate to be (predominantly) a scalar glueball. It has been investigated in a large variety of works, e.g. Refs. [72, 73, 74, 75, 76, 77, 78, 79, 80, 81, 82, 83] and refs. therein, in which mixing scenarios involving the scalar resonances $f_0(1370)$, $f_0(1500)$, and $f_0(1710)$ are considered. The second lightest lattice-predicted glueball state has tensor quantum numbers ($J^{PC} = 2^{++}$) and a mass of about 2.2 GeV; a good candidate could be the very narrow resonance $f_J(2200)$ [84, 85], if the total spin of the latter will be experimentally confirmed to be $J = 2$.

The third least massive glueball predicted by lattice QCD has pseudoscalar quantum numbers ($J^{PC} = 0^{-+}$) and a mass of about 2.6 GeV. Quite remarkably, most theoretical works investigating the pseudoscalar glueball did not take into account this prediction of Yang-Mills lattice studies, but concentrated their search around 1.5 GeV in connection with the isoscalar-pseudoscalar resonances $\eta(1295)$, $\eta(1405)$, and $\eta(1475)$. A candidate for a predominantly light pseudoscalar glueball is the middle-lying state $\eta(1405)$ due to the fact that it is largely produced in (gluon-rich) J/ψ radiative decays and is missing in $\gamma\gamma$ reactions [86, 87, 88, 89, 90, 91]. In this framework the resonances $\eta(1295)$ and $\eta(1475)$ represent radial excitations of the resonances η and η' . Indeed, in relation to η and η' , a lot of work has been done in determining the gluonic amount of their wave functions. The KLOE Collaboration found that the pseudoscalar glueball fraction in the mixing of the pseudoscalar-isoscalar states η and η' can be large ($\sim 14\%$) [92]. However, the theoretical work of Ref. [93] found that the glueball amount in η and η' is compatible with zero.

In this work we study the decay properties of a pseudoscalar glueball state, (see chapter 6), whose mass lies, in agreement with lattice QCD, between 2 and 3 GeV.

1.7. Thesis Content

1.7.1. Second chapter

We construct the QCD Lagrangian and discuss the symmetries of QCD and their breaking. We then construct also a chirally invariant Lagrangian for mesons, the so-called extended Linear Sigma Model (eLSM) which satisfies two requirements: (i) global chiral symmetry, and (ii) dilatation invariance. This model includes scalar and pseudoscalar mesons, as well as vector and axial-vector mesons.

1.7.2. Third chapter

We present the extended linear sigma model (eLSM) for $N_f = 2$ which describes the interaction of a scalar glueball and a tetraquark with baryonic degrees of freedom which are the nucleon N and its chiral partner N^* . We present the outline of extension of the eLSM from the two-flavour case ($N_f = 2$) to the three-flavour case ($N_f = 3$) which includes the strange sector as a new degree of freedom. We discuss the fit parameters and present the results for the light meson masses.

1.7.3. Fourth chapter

We enlarge the so-called extended linear Sigma model (eLSM) by including the charm quark to a global $U(4)_r \times U(4)_l$ chiral symmetry. Most of the parameters of the model have been determined in a previous work by fitting hadron properties involving three quark flavours. Only three new parameters, all related to the current charm quark mass, appear when introducing charmed mesons. Surprisingly, within the accuracy expected from our approach, the masses of open charmed mesons turn out to be in quantitative agreement with experimental data. On the other hand, with the exception of J/ψ , the masses of charmonia are underpredicted by about 10%. It is remarkable that our approach correctly predicts (within errors) the mass splitting between spin-0 and spin-1 negative-parity open charm states. This indicates that, although the charm quark mass breaks chiral symmetry quite strongly explicitly, this symmetry still seems to have some influence on the properties of charmed mesons.

1.7.4. Fifth chapter

In our framework we study the decays of the pseudoscalar glueball and charmed mesons. Therefore, we develop the two- and three-body decay formalisms which are used in this study. Moreover, we present a simple method for the calculation of the decay constants by using an axial transformation.

1.7.5. Sixth chapter

In this chapter we present a chirally invariant Lagrangian for $N_f = 2$ which describes the interaction of a pseudoscalar glueball, \tilde{G} , with baryonic degrees of freedom which are the

nucleon N and its chiral partner N^* . Then we consider an $N_f = 3$ chiral Lagrangian which describes the interaction between the pseudoscalar glueball, $J^{PC} = 0^{-+}$, and scalar and pseudoscalar mesons. We calculate the mesonic and baryonic decays of the pseudoscalar glueball, where we fixed its mass to 2.6 GeV, as predicted by lattice-QCD simulations, and take a closer look at the scalar-isoscalar decay channel. We present our results as branching ratios which are relevant for the future PANDA experiment at the FAIR facility. For completeness, we also repeat the calculation for a glueball mass of 2.37 GeV which corresponds to the mass of the resonance $X(2370)$ measured in the BESIII experiment.

1.7.6. Seventh chapter

In this chapter we study the OZI-dominant decays of the heavy open charmed states into light mesons within the chiral model at tree level. We also obtain the value of the charm-anticharm condensate and the values of the weak decay constants of open charmed D and D_S mesons and the charmonium state η_C . Most of the parameters in the model have been determined in the case of $N_f = 3$ by fitting hadron properties for three flavours. Only three new parameters, all related to the current charm quark mass, are fixed in the fourth chapter. The results are compatible with the experimental data, although the theoretical uncertainties are still large. The precise description of the decays of open charmed states is important for the CBM experiment at FAIR and the upcoming PANDA experiment.

1.7.7. Eighth chapter

In this chapter we expand our work of a $U(4)_r \times U(4)_l$ symmetric linear sigma model with (axial-)vector mesons by including a dilaton field, a scalar glueball, and the interaction of a pseudoscalar glueball with (pseudo)scalar mesons to study the phenomenology of charmonium states. We compute the decay channels of the scalar and pseudoscalar charmonium states $\chi_{c0}(1P)$ and $\eta_c(1S)$, respectively. We calculate the decays of χ_{c0} into the two scalar-isoscalar resonances $f_0(1370)$ and $f_0(1500)$. We also study the decay of η_C into a pseudoscalar glueball. We compute the mixing angle between a pseudoscalar glueball, with a mass of 2.6 GeV, and the hidden charmed meson η_C .

2. Construction of mesonic Lagrangians

2.1. Introduction

For many years, it has been known that chiral symmetry breaking in QCD is responsible for the low mass of pions, which leads us to describe the low-energy limit of QCD by the effective chiral Lagrangian as in Ref. [12, 29, 94]. We have to note that effective chiral models are widely used to study such phenomena because perturbative QCD calculations cannot reproduce low-energy hadronic properties due to confinement of colour charges.

Effective field theory (EFT) provides a fundamental framework to describe physical systems with quantum field theory. The chiral model is an effective field theory containing hadrons as degrees of freedom, which are colour-neutral because of the confinement hypothesis. Moreover, in effective hadronic theories the chiral symmetry of QCD can be realized in the so-called nonlinear or in the linear representations. In the nonlinear case, only the Goldstone bosons are considered [95, 96, 97, 98, 99] [in recent extensions vector mesons are also added, see e.g. Refs. [100, 101, 102, 103]]. On the contrary, in the linear case also the chiral partners of the Goldstone bosons, the scalar mesons, are retained [104, 105, 106, 107]. When extending this approach to the vector sector, both vector and axial-vector mesons are present [106, 107]. Along these lines, recent efforts have led to the construction of the so-called extended linear sigma model (eLSM), first for $N_f = 2$ [78, 108, 109] and then for $N_f = 3$ [110] (see the details in chapter 3). In the eLSM, besides chiral symmetry, a basic phenomenon of QCD in the chiral limit has been taken into account: the symmetry under dilatation transformation and its anomalous breaking (trace anomaly), see e.g. Ref. [111, 112, 113, 114, 115]. For these reasons, we have used the linear sigma model (LSM) which has also other important motivations, summarized as follows:

- (a) The LSM contains pseudoscalar states and their chiral partners from the outset.
- (b) The LSM can be extended to include a large number of different fields, i.e., quark-antiquarks with various flavours (two flavours [108, 106, 78, 116], three flavours [117, 101, 110, 116, 83], four flavours [118, 119, 120, 121, 122]), the nucleon and its chiral partner [109, 123], a pseudoscalar glueball [124, 125, 126, 127], tensor mesons, and tetraquarks ($\bar{q}\bar{q}qq$ mesons) [128].
- (c) In the LSM the properties of fields at non-zero temperatures and densities ($T \neq 0 \neq \mu$) can be studied. As seen in Refs. [129, 130, 131] the critical point of QCD at finite densities is studied, as well as the chiral phase transition.

In this chapter we will construct the QCD Lagrangian and discuss its symmetries. We then go further to construct an effective model, the extended Linear Sigma Model (eLSM), based on the global chiral symmetry and dilatation symmetry and containing the (axial-)vector mesons as well as the (pseudo-)scalar mesons. The spontaneous and explicit symmetry breaking allows us to study the phenomenology of mesons and glueballs such as masses,

decay widths, and scattering lengths, etc.

2.2. Construction of QCD Lagrangian

In this section we construct the QCD Lagrangian which is required to possess two kinds of symmetries: (i) a global chiral symmetry. (ii) a local (gauge) $SU(N_c = 3)$ symmetry [132]. The QCD Lagrangian contains quarks q_f with N_f flavours and gluons. It can be constructed by gauging the colour degrees of freedom with an $SU(3)$ –colour gauge transformation. The full QCD Lagrangian density is the sum of quark and gluon terms

$$\mathcal{L}_{QCD} = \mathcal{L}_q + \mathcal{L}_g. \quad (2.1)$$

Firstly, let us describe the quark term \mathcal{L}_q :

Quarks are spin- $\frac{1}{2}$ fermions. The Dirac-conjugate spinor is denoted as $\bar{q} \equiv q^\dagger \gamma_0$. Each quark of a particular flavour q_f is a triplet in colour space, which is given by the following 3-component quark vector

$$q_f = \begin{pmatrix} q_{f,r} \\ q_{f,g} \\ q_{f,b} \end{pmatrix}, \quad (2.2)$$

where f represents the flavour index u, d, s, \dots , whereas $r, g, \text{ and } b$ refer to the three different fundamental colour charges of quarks, *red*, *green*, and *blue*, respectively.

In the fundamental representation each quark flavour q_f separately transforms under the local colour $SU(3)_c$ group as

$$q_f(x) \rightarrow q'_f(x) = U(\theta(x)) q_f(x), \quad (2.3)$$

where $U(\theta(x))$ is a special unitary matrix, $U(\theta(x)) \in SU(3)$, acting on the colour index and requires eight real parameters. It is usually written in the form

$$U(\theta(x)) = \exp \left(-i \sum_{a=1}^8 \frac{\lambda_a}{2} \Theta^a(x) \right), \quad U^\dagger U = U U^\dagger = \mathbf{1}, \quad \det U = 1, \quad (2.4)$$

where $\Theta^a(x)$ denotes the associated local parameters and $\frac{\lambda_a}{2}$ are hermitian 3×3 matrices; the generators of the $SU(3)$ gauge group, while λ_a are the Gell-Mann matrices which can be found in the Appendix.

In general, the quarks are represented by $4N_c N_f$ – dimensional Dirac spinors. The Dirac Lagrangian for a free fermion ψ takes the following form

$$\mathcal{L}_{Dirac} = \bar{\psi} (i\gamma^\mu \partial_\mu - m_\psi) \psi, \quad (2.5)$$

which leads us to construct a Lagrangian involving the quark flavours, which is invariant under arbitrary local $SU(3)$ transformations (2.3) in colour space; with the same structure as the Dirac Lagrangian (2.5)

$$\mathcal{L}_q = \sum_{f=1}^{N_f} \bar{q}_f (i\gamma^\mu D_\mu - M_f) q_f, \quad (2.6)$$

where γ^μ are the Dirac matrices and M_f denotes the diagonal $N_f \times N_f$ quark mass matrix. The $SU(3)$ covariant derivative in Eq. (2.6) is

$$D_\mu = \partial_\mu - ig A_\mu^a \frac{\lambda_a}{2}, \quad (2.7)$$

where A_μ^a are the gauge fields (gluons), and g is the strong coupling constant.

Now let us turn to describe the gluon term \mathcal{L}_g :

Gluons are massless gauge bosons with spin-one and form an octet under the global colour $SU(3)$ group, because the gluons are described by eight real-valued functions A_μ^a . They mediate the strong interaction between quarks and do not make a distinction between different quark flavours. The gauge fields (gluons), A_μ^a , can be written as

$$A_\mu(x) = \sum_{a=1}^8 A_\mu^a(x) \frac{\lambda_a}{2}, \quad (2.8)$$

where A_μ is the matrix-valued vector potential of the non-Abelian gauge group $SU(3)$. It is a 3×3 matrix. The gluon fields transform under local $SU(3)$ transformations as follows:

$$A_\mu(x) \rightarrow A'_\mu(x) = U(\theta(x)) \left(A_\mu(x) - \frac{i}{g} \partial_\mu \right) U^\dagger(\theta(x)). \quad (2.9)$$

The gluons carry colour charge, and their self-interactions are responsible for many of the unique features of QCD. The self-interactions of the gauge fields are described by

$$G_{\mu\nu}^a(x) = \partial_\mu A_\nu^a(x) - \partial_\nu A_\mu^a(x) + gf^{abc} A_\mu^b(x) A_\nu^c(x), \quad (2.10)$$

representing the gauge-invariant gluon field strength tensor. Here, f^{abc} denote the antisymmetric structure constants of the $SU(3)$ group.

$$[t^a, t^b] = i f^{abc} t^c, \quad a, b, c = 1, \dots, 8. \quad (2.11)$$

The field strength tensor (2.10) transform as follows under local $SU(N_c)$ transformation

$$G_{\mu\nu}^a(x) \frac{\lambda_a}{2} \rightarrow \left(G_{\mu\nu}^a(x) \frac{\lambda_a}{2} \right)' = U(\theta(x)) G_{\mu\nu}^a \frac{\lambda_a}{2} U^\dagger(\theta(x)). \quad (2.12)$$

We can then construct an additional gauge-invariant term involving only gluons [133], which is identical to the Yang-Mills Lagrangian \mathcal{L}_{YM}

$$\mathcal{L}_g = -\frac{1}{4} G_{\mu\nu}^a(x) G_a^{\mu\nu}(x). \quad (2.13)$$

Therefore, we construct the $SU(3)_c$ -invariant Lagrangian of Quantum Chromodynamics (QCD) from the sum of Eq.(2.6) and Eq.(2.13)

$$\mathcal{L}_{QCD} = \sum_{f=1}^{N_f} \bar{q}_f (i\gamma^\mu D_\mu - M_f) q_f - \frac{1}{4} G_{\mu\nu}^a G_a^{\mu\nu}. \quad (2.14)$$

QCD has unique features, such as asymptotic freedom, quark confinement, and chiral symmetry breaking, which are mentioned in detail in the introduction. Beside these features there are other symmetry features of the Lagrangian (2.14), which will be discussed in the following section.

2.3. Symmetry features of QCD

In the previous section, the QCD Lagrangian has been constructed, which is the basis for all hadronic models. Therefore, all models must implement the features of the QCD Lagrangian, such as symmetries and their spontaneous and explicit breaking. For this reason let us study these features before constructing the so-called extended Linear Sigma Model (eLSM) with vector and axial-vector mesons [116].

The features of the QCD Lagrangian are as follows:

2.3.1. $Z(N_c)$ Symmetry

The Abelian group $Z(N_c)$ is the center of the $SU(N_c)$ gauge group. The special unitary $N_f \times N_f$ matrix, containing the center elements Z_n , has the following general form

$$U(\theta(x)) = Z_n \exp\left(-i\frac{\lambda_a}{2}\Theta^a(x)\right), \quad a = 1, \dots, N_f^2 - 1, \quad (2.15)$$

where

$$Z_n \equiv \exp\left(-i\frac{2\pi n}{N_c}t^0\right), \quad n = 0, 1, 2, \dots, N_c - 1, \quad (2.16)$$

where $t^0 = \lambda^0/2$. Quarks and gluon fields transform under the $Z(N_c)$ group as

$$q_f \rightarrow q'_f = Z_n q_f, \quad (2.17)$$

$$A_\mu \rightarrow A'_\mu = Z_n A_\mu Z_n^\dagger = A_\mu. \quad (2.18)$$

Consequently, these transformations leave the QCD Lagrangian \mathcal{L}_{QCD} (2.14) invariant. At large temperature, this symmetry is spontaneously broken in the gauge sector of QCD (without quarks). The spontaneous breaking of this symmetry indicates deconfinement of gluons. At nonzero temperature, the $Z(N_c)$ symmetry is explicitly broken in the presence of quarks, since the necessary antisymmetric boundary conditions are not fulfilled for the fermion field. This symmetry is important for much modern research in hadronic physics at nonzero temperature and density. The order parameter of the spontaneous symmetry breaking of the center group $Z(N_c)$ at high T is the Polyakov loop.

2.3.2. Local $SU(3)_c$ colour symmetry

The colour group $SU(3)$ corresponds to a local symmetry. As seen in Eq.(2.9), the QCD Lagrangian \mathcal{L}_{QCD} is invariant under local $SU(3)_c$ symmetry transformations. In hadronic models, this local symmetry is satisfied automatically. Hadrons are colour singlets. The $SU(N_c = 3)$ group involves also the transformation under the center elements Z_n , while the gauge fields (i.e., gluons) transform under the $Z(N_c)$ group as seen in Eq. (2.18).

2.3.3. Scale invariance and trace anomaly

Scale invariance (the so-called dilatation symmetry) is one of the most important features of QCD because the classical scale invariance is a profound phenomenon for the QCD Lagrangian. The classical QCD Lagrangian (2.14) is invariant under space-time dilatations in the limit of vanishing quark masses ($M_f \rightarrow 0$). That is clear, since no dimensionful parameters appear in the QCD Lagrangian density, which has a dimensionless coupling constant g (discussed in chapter 1).

Note that the dilatation symmetry is broken by quantum fluctuations. Let us consider the gauge sector (no quarks), which is described by the Yang-Mills (YM) Lagrangian (2.13)

$$\mathcal{L}_{YM} = -\frac{1}{4} G_{\mu\nu}^a(x) G_a^{\mu\nu}(x). \quad (2.19)$$

The scalar (or dilatation) transformation is defined as

$$x^\mu \longrightarrow x'^\mu = \lambda^{-1} x^\mu. \quad (2.20)$$

The gauge fields transform as

$$A_\mu^a(x) \longrightarrow A_\mu^{a'}(x') = \lambda A_\mu^a(x), \quad (2.21)$$

The action $S_{YM} = \int d^4x \mathcal{L}_{YM}$ is dimensionless and invariant under the scale transformations,

$$\begin{aligned} S'_{YM} &= \int d^4X' \mathcal{L}'_{YM} = -\frac{1}{4} \int d^4X' G_{\mu\nu}^{a'} G_a^{\mu\nu'} \\ &= -\frac{1}{4} \int \lambda^{-4} d^4X \lambda^2 G_{\mu\nu}^a \lambda^2 G_a^{\mu\nu} \\ &= -\frac{1}{4} \int d^4X G_{\mu\nu}^a G_a^{\mu\nu} \\ &= \int d^4X \mathcal{L}_{YM} = S_{YM}. \end{aligned} \quad (2.22)$$

Then, the scale invariance (dilatation symmetry) is fulfilled in the limit $M_f = 0$. Dilatation symmetry is continuous and leads to the conserved Noether current

$$J_{scale}^\mu = x_\nu T^{\mu\nu}, \quad (2.23)$$

where the energy-momentum tensor for the gauge field $T^{\mu\nu}$ reads

$$T^{\mu\nu} = \frac{\partial \mathcal{L}_{YM}}{\partial(\partial_\mu A_\xi)} \partial^\nu A_\xi - g^{\mu\nu} \mathcal{L}_{YM}. \quad (2.24)$$

On the classical level, the current is conserved because the action is invariant under a continuous scale transformation (as discussed above)

$$\partial_\mu J_{scale}^\mu = 0. \quad (2.25)$$

Then, the divergence

$$\begin{aligned} \partial_\mu J_{scale}^\mu &= \partial_\mu(x_\nu T^{\mu\nu}(x)) = \partial_\mu(g_{\nu\rho} x^\rho T^{\mu\nu}(x)) \\ &= g_{\nu\rho} g_\mu^\rho T^{\mu\nu}(x) + g_{\nu\rho} x^\rho \partial_\mu T^{\mu\nu}(x) \\ &= g_{\nu\mu} T^{\mu\nu}(x) = T_\mu^\mu(x), \end{aligned} \quad (2.26)$$

where the energy-momentum tensor is conserved for a time-translation invariant and homogeneous system

$$\partial_\mu T^{\mu\nu}(x) = 0. \quad (2.27)$$

A conserved scaling current leads to a vanishing trace of the energy-momentum tensor,

$$T_\mu^\mu(x) = 0. \quad (2.28)$$

Note that if all particles are massive, the scaling current would be not conserved, having a nonvanishing trace of the energy-momentum tensor.

At the quantum level, the scale current J_{scale}^μ is anomalous and the classical scale invariance is broken. This breaking is generated by a gluon condensate, i.e., a nonvanishing vacuum expectation value of $(G_{\mu\nu}^a G_a^{\mu\nu})$. From the renormalization techniques [19, 24, 25, 26] and perturbative QCD, one knows

$$\partial_\mu J_{scale}^\mu = T_\mu^\mu = \frac{\beta(g)}{4g} G_{\mu\nu}^a G_a^{\mu\nu} \neq 0, \quad (2.29)$$

where $\beta(g)$ is the β -function of QCD (1.8).

For massive quark flavours ($M_f \neq 0$), the quark fields transform under dilatation as

$$q_f \longrightarrow q'_f = \lambda^{3/2} q_f. \quad (2.30)$$

The result of explicit breaking of the scale invariance by nonvanishing quark masses gives

$$T_\mu^\mu(x) = \sum_{f=1}^{N_f} \bar{q}_f M_f q_f. \quad (2.31)$$

Therefore, the divergence of the quantum current becomes

$$\partial_\mu J_{scale}^\mu = T_\mu^\mu = \frac{\beta(g)}{4g} G_{\mu\nu}^a G_a^{\mu\nu} + \sum_{f=1}^{N_f} \bar{q}_f M_f q_f. \quad (2.32)$$

2.3.4. CP- symmetry

The charge-conjugation and parity symmetry (CP-symmetry) is one of the fundamental properties of QCD, which describes the symmetry between matter and antimatter.

CP-symmetry is the combination of a C-symmetry (charge-conjugation symmetry) and P-symmetry (parity symmetry). The strong interaction as described by the QCD Lagrangian (2.14) is invariant under the combination of CP transformations, as is the electromagnetic interaction, while CP-symmetry is violated by the weak interaction. Now, let us prove the CP-symmetry of the QCD Lagrangian (2.14):

i) *C-symmetry*: is the transformation of a particle into an antiparticle, without a change in the physical law. The charge conjugation transformation C maps matter into antimatter. This symmetry is between positive and negative charge.

The charge conjugation of quarks is

$$q \xrightarrow{C} -i\gamma^2\gamma^0\bar{q}^t = -i\gamma^2\gamma^0(\gamma^0)^t q^*, \quad (2.33)$$

where the superscript t is the transposition. Using the Dirac notation, $\delta = -i\gamma^2\gamma^0$, the previous equation becomes

$$q \xrightarrow{C} \delta\bar{q}^t = \delta(\gamma^0)^t q^*, \quad (2.34)$$

and then,

$$q^\dagger \xrightarrow{C} [\delta(\gamma^0)^t q^*]^\dagger = q^t(\gamma^0)^* \delta^\dagger. \quad (2.35)$$

Note that the properties of the Dirac notation are:

$$\delta^{-1} = \delta^\dagger \text{ (unitary transformation),}$$

$$\delta^{-1}\gamma^\mu\delta = \delta^\dagger\gamma^\mu\delta = (-\gamma^\mu)^t, \text{ and } \delta^\dagger\gamma^\mu = (-\gamma^\mu)^t\delta^{-1}.$$

Moreover, useful properties for Dirac matrices are

$$\gamma^0(\gamma^0)^\dagger = 1, \quad (\gamma^0)^*(\gamma^0)^t = [\gamma^0(\gamma^0)^\dagger]^t = 1^t = 1.$$

All of these properties are used to prove the C-symmetry of \mathcal{L}_{QCD} (2.14) (see below). Furthermore, the gluon fields in the term $(D_\mu = \partial_\mu - igA_\mu)$ transforms odd under C and the commutation of the quark fields which are fermions leads to an additional minus sign.

The QCD Lagrangian is invariant under charge-conjugation transformations.

The quark part of the QCD Lagrangian (2.14) transforms under charge conjugation as proven in Ref. [116]:

$$\begin{aligned} \mathcal{L}_q &= \bar{q}_f i\gamma^\mu D_\mu q_f - \bar{q}_f M_f q_f \\ &\xrightarrow{C} i q_f^t (\gamma^0)^* \delta^\dagger \gamma^0 \gamma^\mu (\partial_\mu + igA_\mu) \delta (\gamma^0)^t q_f^* - q_f^t (\gamma^0)^* \delta^\dagger \gamma^0 M_f \delta (\gamma^0)^t q_f^* \\ &= i \bar{q}_f \gamma^\mu D_\mu q_f - \bar{q}_f M_f q_f. \end{aligned} \quad (2.36)$$

ii) *P-symmetry*: is the symmetry under reflection of spatial coordinates. The parity transformation creates the reflection of spatial coordinates (mirror image) of a physical system.

The parity transformation for quark fields (fermions) reads

$$q(t, \vec{x}) \xrightarrow{P} \gamma^0 q(t, -\vec{x}), \quad (2.37)$$

and thus

$$q^\dagger(t, \vec{x}) \xrightarrow{P} q^\dagger(t, -\vec{x}) \gamma^0. \quad (2.38)$$

The anticommutation formula of the Dirac matrices

$$\{\gamma_\mu, \gamma_\nu\} = 2g_{\mu\nu}, \quad g_{\mu\nu} = \text{diag}(1, -1, -1, -1), \quad (2.39)$$

is used below.

The QCD Lagrangian is invariant under parity transformations.

$$\begin{aligned} \mathcal{L}_q &= \bar{q}_f(t, \vec{x}) i \gamma^i D_i q_f(t, \vec{x}) - \bar{q}_f(t, \vec{x}) M_f q_f(t, \vec{x}) \\ &\xrightarrow{P} \bar{q}_f(t, -\vec{x}) i \gamma^i D_i q_f(t, -\vec{x}) - \bar{q}_f(t, -\vec{x}) M_f q_f(t, -\vec{x}), \end{aligned} \quad (2.40)$$

where $i = 1, 2, 3$ and it is invariant when $\mu = 0$ [116]. The gauge part of the QCD Lagrangian (2.14) is also conserved under parity transformations.

From Eq.(2.36) and Eq.(2.40), we conclude that the QCD Lagrangian (2.14) has a CP-symmetry (it is invariant under the combined set of transformations CP and also separately under C and P).

2.3.5. Chiral symmetry and $U(1)_A$ anomaly

The QCD Lagrangian (2.14) for N_f flavours of massless quarks possesses a large global symmetry, namely a global chiral $U(N_f)_R \times U(N_f)_L$ symmetry [134, 135]. The notion of chirality allows us to decompose a quark spinor into two-component spinors corresponding to left- and right-handed components as

$$q_f = (\mathcal{P}_R + \mathcal{P}_L) q_f = q_{f,R} + q_{f,L}, \quad (2.41)$$

and for the Dirac-conjugate spinors :

$$\bar{q}_f = \bar{q}_f (\mathcal{P}_R + \mathcal{P}_L) = \bar{q}_{f,L} + \bar{q}_{f,R}, \quad (2.42)$$

where $\mathcal{P}_{R,L}$ are the left- and right-handed projection operators which are defined as

$$\mathcal{P}_R = \frac{1 + \gamma_5}{2}, \quad \mathcal{P}_L = \frac{1 - \gamma_5}{2}, \quad (2.43)$$

including a Dirac matrix

$$\gamma_5 = i\gamma_0\gamma^1\gamma^2\gamma^3 = \begin{pmatrix} 1 & 0 \\ 0 & -1 \end{pmatrix}.$$

The QCD Lagrangian (2.14) can be written in terms of “*right-handed quarks*”, $q_R = \mathcal{P}_R q$, and the “*left-handed quarks*”, $q_L = \mathcal{P}_L q$, by using decomposed quark fields (2.41) and (2.42) as

$$\begin{aligned} \mathcal{L}_{QCD} = & \sum_{f=1}^{N_f} i(\bar{q}_{f,L}\gamma^\mu D_\mu q_{f,L} + \bar{q}_{f,R}\gamma^\mu D_\mu q_{f,R}) \\ & - \sum_{f=1}^{N_f} (\bar{q}_{f,R}M_f q_{f,L} + \bar{q}_{f,L}M_f q_{f,R}) - \frac{1}{4} \sum_{a=1}^8 G_{\mu\nu}^a G_a^{\mu\nu}, \end{aligned} \quad (2.44)$$

which is invariant under the following global chiral $U(N_f)_R \times U(N_f)_L$ transformations of right- and left-handed quark spinors in the chiral limit (without the terms containing M_f)

$$q_{f,L} \longrightarrow q'_{f,L} = U_L q_{f,L} = \exp \left\{ -i \sum_{a=0}^{N_f^2-1} \Theta_L^a t^a \right\} q_{f,L}, \quad (2.45)$$

$$q_{f,R} \longrightarrow q'_{f,R} = U_R q_{f,R} = \exp \left\{ -i \sum_{a=0}^{N_f^2-1} \Theta_R^a t^a \right\} q_{f,R}. \quad (2.46)$$

This is the so-called *chiral symmetry* which is exact only when $M_f \rightarrow 0$, because the terms which contain masses (M_f) break the chiral symmetry explicitly. Note that *chiral symmetry* is not exact in nature. However, on the hadronic mass scale ~ 1 GeV, the current masses of up, down, and strange quarks are very small, which leads one to approximate their masses as nearly massless ($m_u = m_d = m_s \simeq 0$). Then, chiral symmetry approximately holds. Moreover, the current mass of the charm quark is already of the order of the typical hadronic mass scale, and the masses of bottom and top quark exceed the hadronic mass scale. In the chiral limit $m_u = m_d = m_s \sim 0$, the QCD Lagrangian (2.44) reads

$$\mathcal{L}_{QCD}^0 = \sum_{f=1}^{N_f} i(\bar{q}_{f,L}\gamma^\mu D_\mu q_{f,L} + \bar{q}_{f,R}\gamma^\mu D_\mu q_{f,R}) - \frac{1}{4} \sum_{a=1}^8 G_{\mu\nu}^a G_a^{\mu\nu}, \quad (2.47)$$

where the superscript 0 denotes the chiral limit. As mentioned above this Lagrangian is invariant under the chiral symmetry group $U(N_f)_R \times U(N_f)_L$. Note that if the Lagrangian contains non-vanishing quark mass terms, some of the $2N_f^2$ chiral currents are not conserved, which reveals the pattern of explicit chiral symmetry breaking, see below.

In addition, the transformation of the left- and right-handed quarks under the symmetry group $U(N_f)_A \times U(N_f)_V$ whereby the subscript A stands for “*axial vector*” and V for “*vector*” is defined as

$$q_{f,L} \rightarrow q'_{f,L} = U_V U_A^\dagger q_{f,L} = \exp(2i\theta^a t^a) \exp(-2i\tilde{\theta}^a t^a) q_{f,L}, \quad (2.48)$$

$$q_{f,R} \rightarrow q'_{f,R} = U_V U_A q_{f,R} = \exp(2i\theta^a t^a) \exp(2i\tilde{\theta}^a t^a) q_{f,R}, \quad (2.49)$$

where $U_V \in U(N_f)_V$ and $U_A \in U(N_f)_A$. This transformation is equivalent to the transformation under $U(N_f)_L \times U(N_f)_R$, if one sets

$$\theta_L^a = 2(\theta^a - \tilde{\theta}^a), \quad \theta_R^a = 2(\theta^a + \tilde{\theta}^a). \quad (2.50)$$

Therefore,

$$U(N_f)_L \times U(N_f)_R \cong U(N_f)_A \times U(N_f)_V. \quad (2.51)$$

Then, in the chiral limit, the QCD Lagrangian (2.14) is invariant also under the symmetry group $U(N_f)_A \times U(N_f)_V$. Note that, for all $V \in U(n)$ with $n \in \mathbb{N}$ there exists $U \in SU(n)$, so that

$$V = \det(V)^{\frac{1}{n}} U, \quad (2.52)$$

and for all $n \in \mathbb{N} \implies \det(V)^{\frac{1}{n}} \in U(1)$, yields

$$U(n) = U(1) \times SU(n). \quad (2.53)$$

Therefore, the unitary group can be represented as a product of a special unitary group and a complex phase as

$$\begin{aligned} U(N_f)_A \times U(N_f)_V &= [U(1)_A \times SU(N_f)_A] \times [U(1)_V \times SU(N_f)_V] \\ &= SU(N_f)_A \times SU(N_f)_V \times U(1)_A \times U(1)_V. \end{aligned} \quad (2.54)$$

Similarly,

$$U(N_f)_R \times U(N_f)_L = SU(N_f)_R \times SU(N_f)_L \times U(1)_R \times U(1)_L. \quad (2.55)$$

Using Eq.(2.51), we obtain

$$SU(N_f)_R \times SU(N_f)_L \times U(1)_R \times U(1)_L \cong SU(N_f)_R \times SU(N_f)_L \times U(1)_V \times U(1)_A, \quad (2.56)$$

which gives

$$U(N_f)_R \times U(N_f)_L \equiv SU(N_f)_R \times SU(N_f)_L \times U(1)_V \times U(1)_A. \quad (2.57)$$

In the quantized theory [94], QCD is not invariant under $U(1)_A$ anymore, as a result of the explicit breaking of axial $U(1)_A$ symmetry, which is known as the $U(1)_A$ anomaly of QCD [15, 16, 17]. Therefore the chiral symmetry is reduced to $SU(N_f)_R \times SU(N_f)_L \times U(1)_V$. However, in classical field theory, \mathcal{L}_{QCD} is invariant under $U(1)_A$. Therefore, one has to take this symmetry breaking into account when constructing the effective chiral model. Moreover, this symmetry is broken at the classical level for massive quark.

According to the Noether theorem [136], the conserved Noether current is:

$$\frac{\partial \mathcal{L}(\varphi(x), \partial_\mu \varphi(x))}{\partial(\partial_\mu \varphi(x))} \delta \varphi(x) + \delta x^\mu \mathcal{L}(\varphi(x), \partial_\mu \varphi(x)). \quad (2.58)$$

where the Lagrangian $\mathcal{L}(\varphi(x), \partial_\mu \varphi(x))$ is invariant under the transformation of the form $x \rightarrow x'(x) = x + \delta x$ and $\varphi(x) \rightarrow \varphi'(x) = \varphi(x) + \delta \varphi(x)$. This symmetry leads to the conserved left-handed and right-handed currents denoted as L_a^μ and R_a^μ , respectively,

$$R_a^\mu = \bar{q}_R \gamma^\mu t_a q_R \quad \Rightarrow \quad R^\mu = V^\mu - A^\mu, \quad (2.59)$$

$$L_a^\mu = \bar{q}_L \gamma^\mu t_a q_L \quad \Rightarrow \quad L^\mu = V^\mu + A^\mu. \quad (2.60)$$

• The vector $U(1)_V$ symmetry of the full Lagrangian (2.14) coincides with quark number conservation. According to the Noether theorem [137], the conserved $U(1)_V$ current reads

$$V_0^\mu = \frac{\partial \mathcal{L}}{\partial (\partial_\mu q_f)} \delta q_f = \bar{q}_f \gamma^\mu t_0 \delta q_f, \quad (2.61)$$

and its divergence is

$$\partial_\mu V_0^\mu = i \bar{q}_f [t_0, M_f] q_f = 0. \quad (2.62)$$

The integration over the zeroth component of V_0^μ yields the conserved baryon-number charge

$$Q = \int d^3x \bar{q}_f \gamma^0 q_f. \quad (2.63)$$

• The $SU(N_f)_V$ symmetry: the Lagrangian is symmetric under $SU(N_f)_V$ transformations only when the quark masses of all flavours are degenerate $m_1 = m_2 = \dots = m_{N_f}$. According to the Noether theorem [138], the conserved vector current is

$$V^{\mu a} = \bar{q}_f \gamma^\mu t^a q_f. \quad (2.64)$$

Its divergence reads

$$\partial_\mu V^{\mu a} = i \bar{q}_f [t^a, M_f] q_f, \quad (2.65)$$

which vanishes only for degenerate quark masses.

• The $SU(N_f)_A$ symmetry: This symmetry is broken spontaneously. The axial-vector current and its divergence (according to the Noether theorem), respectively, read

$$A^{\mu a} = \bar{q}_f \gamma^\mu \gamma^5 t^a q_f, \quad (2.66)$$

and

$$\partial_\mu A^{\mu a} = i \bar{q}_f \{t^a, M_f\} q_f, \quad (2.67)$$

which is conserved only if all quarks are massless.

From the linear combination of the left- and right-handed currents, described in Eq. (2.59) and Eq. (2.60), one can obtain the vector and axial vector currents as follows:

$$V^\mu = \frac{L^\mu + R^\mu}{2}, \quad (2.68)$$

and

$$A^\mu = \frac{L^\mu - R^\mu}{2}. \quad (2.69)$$

Using the definition of the transformation under parity

$$q(t, \mathbf{x}) \xrightarrow{P} \gamma_0 q(t, \mathbf{x}),$$

the vector and axial-vector transform under parity transformations into + or – themselves:

$$V^{\mu,0}(t, \mathbf{x}) \xrightarrow{P} PV^{\mu,0}(t, \mathbf{x})P^{-1} = +V_{\mu}^0(t, -\mathbf{x}), \quad (2.70)$$

$$V^{\mu,a}(t, \mathbf{x}) \xrightarrow{P} PV^{\mu,a}(t, \mathbf{x})P^{-1} = -V_{\mu}^a(t, -\mathbf{x}), \quad (2.71)$$

and

$$A^{\mu,0}(t, \mathbf{x}) \xrightarrow{P} PA^{\mu,0}(t, \mathbf{x})P^{-1} = -A_{\mu}^0(t, -\mathbf{x}), \quad (2.72)$$

$$A^{\mu,a}(t, \mathbf{x}) \xrightarrow{P} PV^{\mu,a}(t, \mathbf{x})P^{-1} = +A_{\mu}^a(t, -\mathbf{x}), \quad (2.73)$$

where a denotes the spatial index.

2.4. Chiral symmetry breaking

2.4.1. Explicit symmetry breaking

The chiral symmetry of QCD is completely broken in the case of non-vanishing quark masses $M_f \neq 0$, which enters the QCD Lagrangian via the mass term (combining the left- and right-handed components) as

$$\mathcal{L}_{mass} = \sum_{f=1}^{N_f} \bar{q}_f M_f q_f = \sum_{f=1}^{N_f} (\bar{q}_{f,L} M_f q_{f,R} + \bar{q}_{f,R} M_f q_{f,L}). \quad (2.74)$$

The mass term breaks the $SU(N_f)_A$ symmetry. The axial $U(N_f)_A$ symmetry of the QCD is explicitly broken even when all quark masses are equal and non-vanishing $m_1 = m_2 = \dots = M_f \neq 0$. This breaking leaves only the $SU(N_f)_V$ symmetry. Consequently, the $SU(N_f)_V$ of QCD is preserved, but only if the quark masses of all flavours are degenerate. In nature $m_u \approx m_d$ which leads to the so-called isospin symmetry. The $SU(3)_V$ flavour symmetry is also approximately preserved although it is explicitly broken due to a sizable mass of the s quark.

2.4.2. Spontaneous symmetry breaking

The central phenomenon in the low-energy hadronic realm is the spontaneous chiral symmetry breaking. This mechanism is the reason for the almost massless pions, and their weak interaction [139]. It has profound consequences for the hadron masses, especially the mass splitting of chiral partners (see below), and causes mass differences between multiplets and influences many strong decay modes.

As discussed previously, the QCD Lagrangian for massless quarks is invariant under chiral transformations. Consequently, one should expect that the approximate chiral symmetry should be evident in the mass spectrum of the lightest mesons. For $N_f = 2$, the current masses of the up and down quark flavours are small compared to the typical hadronic scale which is about 1 GeV, $m_u \simeq 0.002$ GeV and $m_d \simeq 0.005$ GeV. Therefore, these two lightest quark flavours can be considered to be approximately massless. As a consequence, the QCD Lagrangian is invariant under a global $SU(2)_R \times SU(2)_L$ transformation. One may write

the lightest mesonic states composed of up and down quarks, $q \equiv (u, d)$, (σ, π, ρ, a_1) [116] as

$$\begin{aligned}
\text{scalar singlet state :} & \quad \sigma \equiv \bar{q}q, \\
\text{pseudoscalar triplet state :} & \quad \vec{\pi} \equiv i\bar{q}\vec{\tau}\gamma_5q, \\
\text{vector triplet state :} & \quad \vec{\rho}^\mu \equiv \bar{q}\vec{\tau}\gamma^\mu q, \\
\text{axial - vector triplet state :} & \quad \vec{a}_1^\mu \equiv \bar{q}\vec{\tau}\gamma^\mu\gamma_5q.
\end{aligned} \tag{2.75}$$

The quark flavour transforms under an axial-vector transformation as

$$U(2)_A : q = q' \rightarrow e^{-i\gamma_5\frac{\vec{\tau}}{2}\cdot\vec{\Theta}}q \simeq (1 - i\gamma_5\frac{\vec{\tau}}{2}\cdot\vec{\Theta})q, \tag{2.76}$$

where τ_i are the Pauli matrices. Consequently, the states (2.75) transform under an axial-vector transformation as

$$\begin{aligned}
U(2)_A : \sigma & \rightarrow \sigma' = \sigma - \vec{\Theta} \cdot \vec{\pi}, \\
U(2)_A : \vec{\pi} & \rightarrow \vec{\pi}' = \vec{\pi} + \vec{\Theta} \cdot \vec{\pi}, \\
U(2)_A : \vec{\rho}^\mu & \rightarrow \vec{\rho}'^\mu = \vec{\rho}^\mu + \vec{\Theta} \times \vec{a}_1^\mu, \\
U(2)_A : \vec{a}_1^\mu & \rightarrow \vec{a}_1'^\mu = \vec{a}_1^\mu + \vec{\Theta} \times \vec{\rho}^\mu,
\end{aligned} \tag{2.77}$$

which gives that the scalar state σ is rotated to the pseudoscalar state π and vice versa, i.e., they are chiral partners. Likewise, the vector state $\vec{\rho}$ is rotated to its partner, the axial-vector \vec{a}_1 , and vice versa. The axial symmetry $SU(N_f)_A$ is still exact within the QCD Lagrangian. The explicit breaking of axial symmetry does not occur in the limit of small u, d quark masses. The chiral partners have the same masses. In this case, the vector state ρ is assigned to the $\rho(770)$ meson with a mass of $m_\rho = 775.49$ MeV and the axial-vector state a_1 to the $a_1(1260)$ meson with a mass of $m_{a_1} \simeq 1230$ MeV [23]. The mass difference of the chiral partners ρ and a_1 is of the order of the ρ mass itself and cannot be explained by the explicit symmetry breaking even if the nonvanishing masses of the up and down quark flavours are taken into account. However, the spontaneous symmetry breaking explains this phenomena successfully, i.e., the axial symmetry of the QCD Lagrangian is spontaneously broken in the ground state at zero temperature as

$$SU(N_f)_R \times SU(N_f)_L \rightarrow SU(N_f)_V. \tag{2.78}$$

In the case of nonvanishing quark masses, the chiral symmetry is explicitly broken by the mass term. However, even in the limit of $M_f \rightarrow 0$ the chiral symmetry is also broken, but this time spontaneously, when the ground state has a lower symmetry than the Lagrangian. The QCD vacuum has a nonvanishing expectation value for the quark condensate [140]

$$\langle \bar{q}q \rangle_{vac} = \langle \bar{q}_R q_L + \bar{q}_L q_R \rangle \neq 0. \tag{2.79}$$

According to Goldstone's theorem [141], through the spontaneous breaking of a global symmetry there emerge massless Goldstone bosons, whose number is identical to the number of broken symmetries ($N_f^2 - 1$) and which are indeed experimentally observed. In the $N_f = 2$

case, three Goldstone bosons were observed and are identified with the pions [38, 39, 40]. Their mass of about 140 MeV is small on a hadronic mass scale, but evidently they are not completely massless. The small nonvanishing mass arises from explicit chiral symmetry breaking, and thus they are named pseudo-Goldstone bosons. In the $N_f = 3$ case, additionally five pseudo-Goldstone bosons have been experimentally observed, which are named the four kaons and the η meson. In the $N_f = 4$ case, there are 15 pseudoscalar Goldstone bosons comprising pions, kaons, η 's, and charmed mesons, which consist of the fourth quark flavour; the so-called charm quark. Charm thus strongly breaks the chiral symmetry explicitly.

2.5. Construction of an effective model

The main aim of the present work is to study low-energy hadronic properties from an effective chiral model which is based on QCD. Therefore, the effective model must possess all features of the QCD Lagrangian, which are: The exact $SU(3)_c$ local gauge symmetry, the dilatation symmetry, the chiral $U(1)_A$ anomaly, CP symmetry, the global $U(N_f)_R \times U(N_f)_L$ chiral symmetry for massless quark flavours, as well as the explicit and spontaneous breaking of chiral symmetry. The relationship between these symmetries gives us an opportunity to formulate an effective model: the so-called extended Linear Sigma Model (eLSM).

In this section, we construct the eLSM [116, 142] for the (pseudo)scalar and (axial-)vector mesons as well as a dilaton field, which is valid for an arbitrary number of flavours N_f and colours N_c . Hadrons are the degrees of freedom in the eLSM; they are colour neutral as a result of the confinement hypothesis. Therefore, in the construction of the eLSM, we do not have to take into account the $SU(3)_c$ colour symmetry, it is automatically fulfilled. Note that we construct all terms of the eLSM with global chiral invariance up to naive scaling dimension four [29, 107, 143, 144]. As shown in Refs. [94, 108, 110, 116], the description of meson decay widths is quite reasonable.

The first and fundamental step for the construction of the eLSM is to define the mesonic matrix Φ which contains bound quark-antiquark states. The matrix Φ is a non-perturbative object, and one uses it to build the multiplet of the scalar and pseudoscalar mesons as

$$\Phi_{ij} \equiv \sqrt{2}\bar{q}_{j,R}q_{i,L}. \quad (2.80)$$

According to the left- and right-handed transformations of quarks (2.45) and (2.46), the mesonic matrix transforms under chiral transformations as

$$\Phi_{ij} \longrightarrow \sqrt{2}\bar{q}_{k,R}U_{kj,R}^\dagger U_{il,L}q_{l,L} \equiv U_{il,L}\Phi_{lk}U_{kj,R}^\dagger, \quad (2.81)$$

thus,

$$\Phi \longrightarrow U_L\Phi U_R^\dagger, \quad (2.82)$$

Using Eq.(2.43), Eq.(2.80) can be written as

$$\begin{aligned} \Phi_{ij} &\equiv \sqrt{2}\bar{q}_{j,R}q_{i,L} = \sqrt{2}\bar{q}_j\mathcal{P}_L\mathcal{P}_Lq_i = \sqrt{2}\bar{q}_j\mathcal{P}_Lq_i \\ &= \frac{1}{\sqrt{2}}(\bar{q}_jq_i - \bar{q}_j\gamma^5q_i) = \frac{1}{\sqrt{2}}(\bar{q}_jq_i + i\bar{q}_ji\gamma^5q_i) \\ &\equiv S_{ij} + iP_{ij}, \end{aligned} \quad (2.83)$$

where S_{ij} and P_{ij} are the scalar and the pseudoscalar quark-antiquark currents, respectively, which are defined by

$$S_{ij} \equiv \frac{1}{\sqrt{2}} \bar{q}_j q_i, \quad (2.84)$$

$$P_{ij} \equiv \frac{1}{\sqrt{2}} \bar{q}_j i \gamma^5 q_i. \quad (2.85)$$

Eventually, one can write the combination of scalar and pseudoscalar currents via the Φ matrix as

$$\Phi = S + iP, \quad (2.86)$$

The matrices S and P are Hermitian and can be expressed as follows:

$$S = S_a t_a, \quad P = P_a t_a, \quad (2.87)$$

with

$$S_a = \sqrt{2} \bar{q} t_a q, \quad P_a = \sqrt{2} \bar{q} i \gamma^5 t_a q. \quad (2.88)$$

where t^a denotes the generators of a unitary group $U(N_f)$ with $a = 0, \dots, N_f^2 - 1$.

We summarize the transformation properties of the scalar fields S , the pseudoscalar fields P , and Φ in Table 2.1.

	$S = \frac{1}{\sqrt{2}} \sum_{a=0}^8 S^a \lambda_a$	$P = \frac{1}{\sqrt{2}} \sum_{a=0}^8 P^a \lambda_a$	$\Phi = S + iP$
Elements	$S_{ij} \equiv \bar{q}_j q_i$	$P_{ij} \equiv \bar{q}_j i \gamma^5 q_i$	$\Phi_{ij} \equiv \sqrt{2} \bar{q}_{j,R} q_{i,L}$
Currents	$S^a \equiv \bar{q} \frac{\lambda_a}{\sqrt{2}} q$	$P^a \equiv \bar{q} i \gamma^5 \frac{\lambda_a}{\sqrt{2}} q$	$\Phi^a \equiv \sqrt{2} \bar{q}_R \frac{\lambda_a}{\sqrt{2}} q_L$
P	$S(t, -\mathbf{x})$	$-P(t, -\mathbf{x})$	$\Phi^\dagger(t, -\mathbf{x})$
C	S^t	P^t	Φ^t
$U(N_f)_V$	$U_V S U_V^\dagger$	$U_V P U_V^\dagger$	$U_V \Phi U_V^\dagger$
$U(N_f)_A$	$\frac{1}{2} (U_A \Phi U_A + U_A^\dagger \Phi^\dagger U_A^\dagger)$	$\frac{1}{2i} (U_A \Phi U_A - U_A^\dagger \Phi^\dagger U_A^\dagger)$	$U_A \Phi U_A$
$U(N_f)_R \times U(N_f)_L$	$\frac{1}{2} (U_L \Phi U_R^\dagger + U_R \Phi^\dagger U_L^\dagger)$	$\frac{1}{2i} (U_L \Phi U_R^\dagger - U_R \Phi^\dagger U_L^\dagger)$	$U_L \Phi U_R^\dagger$

Table 2.1: The transformation properties of S , P , and Φ [142].

The eLSM contains also the vector and axial-vector mesons, which are the basic degrees of freedom for the construction of the right- and the left-handed vector fields. Now let us define the $N_f \times N_f$ right-handed R^μ and left-handed L^μ matrices, respectively, as

$$R_{ij}^\mu \equiv \sqrt{2} \bar{q}_{j,R} \gamma^\mu q_{i,R} = \frac{1}{\sqrt{2}} (\bar{q}_j \gamma^\mu q_i - \bar{q}_j \gamma^5 \gamma^\mu q_i) \equiv V_{ij}^\mu - A_{ij}^\mu, \quad (2.89)$$

$$L_{ij}^\mu \equiv \sqrt{2} \bar{q}_{j,L} \gamma^\mu q_{i,L} = \frac{1}{\sqrt{2}} (\bar{q}_j \gamma^\mu q_i + \bar{q}_j \gamma^5 \gamma^\mu q_i) \equiv V_{ij}^\mu + A_{ij}^\mu, \quad (2.90)$$

where the vector and axial-vector currents are defined, respectively, as

$$V_{ij}^\mu \equiv \frac{1}{\sqrt{2}} \bar{q}_j \gamma^\mu q_i = V^{\mu,a} t^a; \quad V^{\mu,a} \equiv \sqrt{2} \bar{q} \gamma^\mu t^a q, \quad (2.91)$$

$$A_{ij}^\mu \equiv \frac{1}{\sqrt{2}} \bar{q}_j \gamma^5 \gamma^\mu q_i = A^{\mu,a} t^a; \quad A^{\mu,a} \equiv \sqrt{2} \bar{q} \gamma^5 \gamma^\mu t^a q, \quad (2.92)$$

which are also Hermitian matrices. The right-handed matrix and the left-handed matrix transform under the chiral transformation as

$$R^\mu \longrightarrow R^{\mu'} = U_R R^\mu U_R^\dagger, \quad (2.93)$$

and

$$L^\mu \longrightarrow L^{\mu'} = U_L L^\mu U_L^\dagger. \quad (2.94)$$

From R^μ and L^μ , we construct the right- and left-handed field-strength tensors, $R^{\mu\nu}$ and $L^{\mu\nu}$, respectively, as

$$R^{\mu\nu} = \partial^\mu R^\nu - \partial^\nu R^\mu, \quad (2.95)$$

$$L^{\mu\nu} = \partial^\mu L^\nu - \partial^\nu L^\mu, \quad (2.96)$$

which transform under chiral transformations as

$$R^{\mu\nu} \longrightarrow R^{\mu\nu'} = U_R R^{\mu\nu} U_R^\dagger, \quad (2.97)$$

$$L^{\mu\nu} \longrightarrow L^{\mu\nu'} = U_L L^{\mu\nu} U_L^\dagger. \quad (2.98)$$

We present the transformation properties of the right- and left-handed (R^μ , L^μ) fields in Table 2.2 and the vector and the axial-vector fields (V^μ , A^μ) in Table 2.3.

	$R_\mu = \frac{1}{\sqrt{2}} \sum_{a=0}^8 R_\mu^a \lambda_a$	$L_\mu = \frac{1}{\sqrt{2}} \sum_{a=0}^8 L_\mu^a \lambda_a$
Elements	$R_{ij}^\mu \equiv \sqrt{2} \bar{q}_{j,R} \gamma^\mu q_{i,R}$	$L_{ij}^\mu \equiv \sqrt{2} \bar{q}_{j,L} \gamma^\mu q_{i,L}$
Currents	$R_\mu^a \equiv \bar{q}_R \gamma^\mu \frac{\lambda_a}{\sqrt{2}} q_R$	$L_\mu^a \equiv \bar{q}_L i \gamma^\mu \frac{\lambda_a}{\sqrt{2}} q_L$
P	$g^{\mu\nu} L_\mu(t, -\mathbf{x})$	$g^{\mu\nu} R_\mu(t, -\mathbf{x})$
C	$-L_\mu^t$	R_μ^t
$U(N_f)_V$	$U_V R_\mu U_V^\dagger$	$U_V L_\mu U_V^\dagger$
$U(N_f)_A$	$U_A R_\mu U_A^\dagger$	$U_A^\dagger L_\mu U_A$
$U(N_f)_R \times U(N_f)_L$	$U_R R_\mu U_R^\dagger$	$U_L L_\mu U_L^\dagger$

Table 2.2: The transformation properties of R_μ and L_μ [142].

	$V_\mu = \frac{1}{\sqrt{2}} \sum_{a=0}^8 V_\mu^a \lambda_a$	$A_\mu = \frac{1}{\sqrt{2}} \sum_{a=0}^8 A_\mu^a \lambda_a$
Elements	$V_{ij}^\mu \equiv \sqrt{2} \bar{q}_j \gamma^\mu q_i$	$A_{ij}^\mu \equiv \sqrt{2} \bar{q}_j \gamma^5 \gamma^\mu q_i$
Currents	$V^a \equiv \bar{q} \gamma^\mu \frac{\lambda_a}{\sqrt{2}} q$	$A^a \equiv \bar{q} \gamma^5 \frac{\lambda_a}{\sqrt{2}} q$
P	$g^{\mu\nu} V_\mu(t, -\mathbf{x})$	$-g^{\mu\nu} A_\mu(t, -\mathbf{x})$
C	$-V_\mu^t$	A_μ^t

Table 2.3: The transformation properties of V_μ and A_μ [142].

The basic construction of the mesonic Lagrangian of the effective model combines several terms:

$$\mathcal{L}_{mes} = \mathcal{L}_{\Phi,AV} + \mathcal{L}_{AV} + \mathcal{L}_{U(1)_A} + \mathcal{L}_G + \mathcal{L}_{ESB}. \quad (2.99)$$

Now let us construct every term in detail.

(i) The Lagrangian density $\mathcal{L}_{\Phi,AV}$:

The chiral symmetry of QCD is exact in the chiral limit $M_f \rightarrow 0$. The Lagrangian density $\mathcal{L}_{\Phi,AV}$ fulfils the chiral symmetry exactly. It contains the (pseudo)scalar and the (axial-)vector degrees of freedom and describes the interaction between them. The covariant derivative for the coupling of the (pseudo)scalar degrees of freedom to the (axial-)vector ones has the following structure

$$D^\mu \Phi = \partial^\mu \Phi + ig_1(\Phi R^\mu - L^\mu \Phi), \quad (2.100)$$

then

$$(D^\mu \Phi)^\dagger = \partial_\mu \Phi^\dagger - ig_1(R_\mu \Phi^\dagger - \Phi^\dagger L_\mu), \quad (2.101)$$

which are invariant under global $U(N_f)_L \times U(N_f)_R$ transformations.

$$(D^\mu \Phi) \longrightarrow (D^\mu \Phi)' = U_L D^\mu \Phi U_R^\dagger. \quad (2.102)$$

and

$$(D^\mu \Phi)^\dagger \longrightarrow (D^\mu \Phi)^\dagger{}' = U_R (D^\mu \Phi)^\dagger U_L^\dagger. \quad (2.103)$$

Therefore, the chirally invariant kinetic term can be constructed as

$$\text{Tr} \left[(D^\mu \Phi)^\dagger (D^\mu \Phi) \right]. \quad (2.104)$$

The following self-interaction terms can be introduced up to naive scaling dimension four,

$$- \lambda_1 (\text{Tr}[\Phi^\dagger \Phi])^2, \quad (2.105)$$

$$- \lambda_2 \text{Tr}(\Phi^\dagger \Phi)^2, \quad (2.106)$$

which are also invariant under global chiral transformations.

Proof:

$$\begin{aligned} -\lambda_1 (\text{Tr}[\Phi^\dagger{}' \Phi'])^2 &= -\lambda_1 (\text{Tr}[U_R \Phi^\dagger U_L^\dagger U_L \Phi U_R^\dagger])^2 \\ &= -\lambda_1 (\text{Tr}[U_R \Phi^\dagger \Phi U_R^\dagger])^2 \\ &= -\lambda_1 (\text{Tr}[U_R^\dagger U_R \Phi^\dagger \Phi])^2 \\ &= -\lambda_1 (\text{Tr}[\Phi^\dagger \Phi])^2. \end{aligned} \quad (2.107)$$

Similarly,

$$- \lambda_2 \text{Tr}(\Phi^\dagger{}' \Phi')^2 = -\lambda_2 \text{Tr}(\Phi^\dagger \Phi)^2, \quad (2.108)$$

In the Lagrangian density $\mathcal{L}_{\Phi,AV}$, the fourth chirally invariant term, describes a four-body coupling of the scalar, pseudoscalar, vector, and axial-vector degrees of freedom, is constructed in the form

$$\frac{h_1}{2} \text{Tr}[\Phi^\dagger \Phi] \text{Tr}[L_\mu L^\mu + R_\mu R^\mu]. \quad (2.109)$$

While the fifth term is constructed in the following form:

$$h_2 \text{Tr}[\Phi^\dagger L_\mu L^\mu \Phi + \Phi R_\mu R^\mu \Phi]. \quad (2.110)$$

Furthermore, one can construct an additional term as follows:

$$2h_3 \text{Tr}[\Phi R_\mu \Phi^\dagger L^\mu], \quad (2.111)$$

which are invariant under global chiral transformations [145].

Finally, we obtain the full Lagrangian density $\mathcal{L}_{\Phi,AV}$ as

$$\mathcal{L}_{\Phi,AV} = \text{Tr} \left[(D^\mu \Phi)^\dagger (D^\mu \Phi) \right] - \lambda_1 (\text{Tr}[\Phi^\dagger \Phi])^2 - \lambda_2 \text{Tr}(\Phi^\dagger \Phi)^2 \quad (2.112)$$

$$+ \frac{h_1}{2} \text{Tr}[\Phi^\dagger \Phi] \text{Tr}[L_\mu L^\mu + R_\mu R^\mu] + h_2 \text{Tr}[\Phi^\dagger L_\mu L^\mu \Phi + \Phi R_\mu R^\mu \Phi^\dagger] \\ + 2h_3 \text{Tr}[\Phi R_\mu \Phi^\dagger L^\mu], \quad (2.113)$$

which contains terms up to order four in naive scaling dimension. In the Lagrangian density $\mathcal{L}_{\Phi,AV}$ (2.113), the parameters depend on the number of colours N_c [142, 146, 147, 148] as follows

$$g_1 \propto N_c^{-1/2}, \\ \lambda_1, h_1 \propto N_c^{-2}, \\ \lambda_2, h_2, h_3 \propto N_c^{-1}. \quad (2.114)$$

The quantities λ_2, h_2, h_3 scale as N_c^{-1} because it describes a four-point interaction of the quark-antiquark states. The quantities λ_1, h_1 are suppressed by an additional N_c and scale as N_c^{-2} because these terms are the product of two separate traces. At the microscopic quark gluon level, one needs further large- N_c suppressed transversal gluons to generate these terms. The quantity g_1 scales as $N_c^{-1/2}$.

(ii) The term \mathcal{L}_{AV} :

The Lagrangian density \mathcal{L}_{AV} includes the (axial-)vector degrees of freedom. The construction of this Lagrangian follows the same principles as in the (pseudo)scalar sector with additional terms of naive scaling dimension four. The mass term can be constructed as

$$\frac{m_1^2}{2} \text{Tr} [(L^\mu)^2 + (R^\mu)^2]. \quad (2.115)$$

Using Eq.(2.95) and Eq.(2.96), one can construct the kinetic term of the vector degrees of freedom as

$$- \frac{1}{4} \text{Tr} [(L^{\mu\nu})^2 + (R^{\mu\nu})^2]. \quad (2.116)$$

From the transformation (2.93, 2.94) and (2.97, 2.98), one can obtain that the mass term (2.115) and the kinetic term (2.116) are invariant under chiral transformations. Moreover, the Lagrangian density \mathcal{L}_{AV} involves also additional terms with 3- and 4-point vertices of

the (axial-)vector degrees of freedom. The full Lagrangian L_{AV} has the following form:

$$\begin{aligned} \mathcal{L}_{AV} = & \frac{m_1^2}{2} \text{Tr} [(L^\mu)^2 + (R^\mu)^2] - \frac{1}{4} \text{Tr} [(L^{\mu\nu})^2 + (R^{\mu\nu})^2] \\ & - i \frac{g_2}{2} \{ \text{Tr}(L_{\mu\nu}[L^\mu, L^\nu]) + \text{Tr}(R_{\mu\nu}[R^\mu, R^\nu]) \} + g_3 [\text{Tr}(L_\mu L_\nu L^\mu L^\nu) + \text{Tr}(R_\mu R_\nu R^\mu R^\nu)] \\ & + g_4 [\text{Tr}(L_\mu L^\mu L_\nu L^\nu) + \text{Tr}(R_\mu R^\mu R_\nu R^\nu)] + g_5 \text{Tr}(L_\mu L^\mu) \text{Tr}(R_\nu R^\nu) \\ & + g_6 [\text{Tr}(L_\mu L^\mu) \text{Tr}(L_\nu L^\nu) + \text{Tr}(R_\mu R^\mu) \text{Tr}(R_\nu R^\nu)] , \end{aligned} \quad (2.117)$$

with the large- N_c dependence of the parameters as

$$\begin{aligned} g_2 & \propto N_c^{-1/2}, \\ g_3, g_4 & \propto N_c^{-1}, \\ g_5, g_6 & \propto N_c^{-2}. \end{aligned} \quad (2.118)$$

(iii) **The term $\mathcal{L}_{U(1)_A}$:**

The Lagrangian density $\mathcal{L}_{U(1)_A}$ contains only the chiral anomaly term [16, 18],

$$\mathcal{L}_{U(1)_A} = c \left(\det \Phi^\dagger - \det \Phi \right)^2. \quad (2.119)$$

which contributes to the mass of the isoscalar-pseudoscalar bosons. Their mass also does not disappear in the chiral limit. These fields are therefore no Goldstone bosons. This term is invariant under $SU(N_f)_R \times SU(N_f)_L$, but not under $U(1)_A$, as shown in the following :

Proof:

$$\begin{aligned} c \left(\det \Phi^{\dagger'} - \det \Phi' \right)^2 & = c \left[\det(U_R \Phi^\dagger U_L^\dagger) - \det(U_L \Phi U_R^\dagger) \right]^2 \\ & = c \left[\det(e^{i\theta_R^a t_a} \Phi^\dagger e^{-i\theta_L^a t_a}) - \det(e^{i\theta_L^a t_a} \Phi e^{-i\theta_R^a t_a}) \right]^2 \\ & = c \left[\det(e^{-i\theta_A^a t_a} \Phi^\dagger) - \det(e^{i\theta_A^a t_a} \Phi) \right]^2 \\ & = c \left[\det(e^{-i \sum_{a=1}^{N_f^2-1} \theta_A^a t_a}) \det(e^{-i\theta_A^0 t_0}) \det \Phi^\dagger \right. \\ & \quad \left. - \det(e^{i \sum_{a=1}^{N_f^2-1} \theta_A^a t_a}) \det(e^{i\theta_A^0 t_0}) \det \Phi \right]^2 \\ & = c \left[\det(e^{-i\theta_A^0 t_0}) \det \Phi^\dagger - \det(e^{i\theta_A^0 t_0}) \det \Phi \right]^2 \\ & = c \left[e^{-i\theta_A^0 N_f} \det \Phi^\dagger - e^{i\theta_A^0 N_f} \det \Phi \right]^2 \\ & \neq c \left[\det \Phi^\dagger - \det \Phi \right]^2 . \end{aligned} \quad (2.120)$$

The parameter c scales in the large- N_c limit [142] as

$$c \propto N_c^{-N_f/2}, \quad (2.121)$$

i.e., it has a dependence on the number of quark flavours (N_f) in this model. For $N_f \geq 2$, the parameter c vanishes which leads to neglect the anomaly for large N_c . The corresponding meson is then a Goldstone boson for $N_c \gg 1$. Note that for $N_f \neq 4$, the parameter c is dimensionfull. This is an exception of the discussed rule. Which is possible since the anomaly also comes from the gauge sector.

(iv) The term \mathcal{L}_G :

The last field entering the model is the dilaton field /scalar glueball G through the Lagrangian density \mathcal{L}_G which consists of the dilaton Lagrangian \mathcal{L}_{dil} and the coupling of the dilaton field with (pseudo)scalar and (axial-)vector degrees of freedom.

Firstly, let us discuss the dilaton Lagrangian

As shown in Eq.(2.22), the Yang-Mills (YM) sector of QCD (which is described by \mathcal{L}_{YM}) is classically invariant under dilatations. However, this symmetry is broken at the quantum level. This scale invariance and its anomalous breaking is one of the essential features of our effective model. From the trace of the energy-momentum tensor $T_{YM}^{\mu\nu}$ of the YM Lagrangian (2.19), one can write the divergence of the dilatation (Noether) current as follows:

$$\partial_\mu J_{YM,dil}^\mu = (T_{YM})_\mu^\mu = \frac{\beta(g)}{2g} \left(\frac{1}{2} G_{\mu\nu}^a G_a^{\mu\nu} \right) \neq 0, \quad (2.122)$$

which does not vanish. The β -function is defined in Eq.(1.6), and $g = g(\mu)$ is the renormalised coupling constant at the scale μ . At the one-loop level,

$$\beta(g) = \frac{-11 N_c}{48\pi^2} g^3. \quad (2.123)$$

This implies

$$g^2(\mu) = \left[2 \frac{11 N_c}{48\pi^2} \ln \left(\frac{\mu}{\Lambda_{YM}} \right) \right]^{-1}, \quad (2.124)$$

where Λ_{YM} is the YM scale and has a value of about ($\simeq 200$ MeV). The non-vanishing expectation value of the trace anomaly represents the gluon condensate

$$\langle T_\mu^\mu \rangle = \frac{-11 N_c}{48} \left\langle \frac{\alpha_s}{\pi} G_{\mu\nu}^a G_a^{\mu\nu} \right\rangle = \frac{-11 N_c}{48} C^4, \quad (2.125)$$

where

$$\left\langle \frac{\alpha_s}{\pi} G_{\mu\nu}^a G_a^{\mu\nu} \right\rangle \equiv C^4. \quad (2.126)$$

The numerical values of C^4 have been computed from lattice-QCD simulations (higher range of the interval) [149] and QCD sum rules (lower range of the interval) [150]:

$$C^4 \approx [(300 - 600) MeV]^4, \quad (2.127)$$

whereas, in the lattice-QCD simulation of Ref. [151], its value has been found to be $C \approx 610$ MeV.

The effective theory of the YM sector of QCD can be built by introducing a scalar dilaton/scalar field G at the composite level. The Lagrangian density of the dilaton reads [111, 112, 113, 114, 115, 151]

$$\mathcal{L}_{dil}(G) = \frac{1}{2}(\partial^\mu G)^2 - V_{dil}(G), \quad (2.128)$$

where the dilaton potential is

$$V_{dil}(G) = \frac{1}{4} \frac{m_G^2}{\Lambda^2} \left(G^4 \ln \left| \frac{G}{\Lambda} \right| - \frac{G^4}{4} \right). \quad (2.129)$$

The value $G_0 = \Lambda$ corresponds to the minimum of the dilaton potential $\mathcal{V}_{dil}(G)$. The particle mass m_G emerges upon shifting $G \rightarrow G_0 + G$. This particle is interpreted as the scalar glueball and its mass has been evaluated as $m_G \approx (1500 - 1700)$ MeV by lattice QCD [65, 66, 71]. The scale invariance is broken explicitly by the logarithmic term of the potential. The divergence of the dilatation current reads

$$\langle T_{dil,\mu}^\mu \rangle = \left\langle -\frac{1}{4} \frac{m_G^2}{\Lambda^2} G^4 \right\rangle = -\frac{1}{4} \frac{m_G^2}{\Lambda^2} G_0^4 = -\frac{1}{4} m_G^2 \Lambda^2, \quad (2.130)$$

where G is set to be equal to the minimum of the potential G_0 . By comparing Eq.(2.125) and Eq.(2.130), one obtains

$$\Lambda = \frac{\sqrt{11}}{2m_G} C^2. \quad (2.131)$$

When $m_G = 1500$ MeV and $C \approx 610$ MeV [152], the parameter Λ has the value $\Lambda = 400$ MeV. Note that a narrow glueball is possible only if $\Lambda \gtrsim 1000$ MeV.

Now let us turn to couple the dilaton field/scalar glueball with the (pseudo)scalar and (axial-)vector degrees of freedom. This coupling must be scale invariance.

We assume that, a part from the $U(1)_A$ anomaly and terms related to quark masses, only the dilaton term breaks the dilatation invariance and generates the scale anomaly in the effective model. Note that the mass term for the (axial-)vector mesons (2.115) break the symmetry explicitly. It does not has dilatation symmetry, since each scale with λ^2 . In order to achieve scale invariance, one should write down the mass term of the scalar degrees of freedom as follows

$$- a G^2 \text{Tr} [\Phi^\dagger \Phi], \quad (2.132)$$

with the scalar mass parameter

$$m_0^2 = a G_0^2, \quad (2.133)$$

where a is a dimensionless constant larger than 0, which represents the spontaneous symmetry breaking. The mass term for the vector mesons should be written in the same way. Now let us modify both mass terms by including the scalar glueball as

$$- m_0^2 \text{Tr} [\Phi^\dagger \Phi] \longrightarrow - m_0^2 \left(\frac{G}{G_0} \right)^2 \text{Tr} [\Phi^\dagger \Phi], \quad (2.134)$$

and similarly,

$$\frac{m_1^2}{2} \text{Tr} [(L^\mu)^2 + (R^\mu)^2] \longrightarrow \frac{m_1^2}{2} \left(\frac{G}{G_0} \right)^2 \text{Tr} [(L^\mu)^2 + (R^\mu)^2], \quad (2.135)$$

which implements the scale-invariance [as proven in Ref. [145]]. From Eqs.(2.128, 2.129, 2.134, 2.135), we get the full structure of the Lagrangian density \mathcal{L}_G in the effective model as

$$\begin{aligned} \mathcal{L}(G) = & \frac{1}{2} (\partial^\mu G)^2 - \frac{1}{4} \frac{m_G^2}{\Lambda^2} \left(G^4 \ln \left| \frac{G}{\Lambda} \right| - \frac{G^4}{4} \right) \\ & - m_0^2 \left(\frac{G}{G_0} \right)^2 \text{Tr} [\Phi^\dagger \Phi] + \frac{m_1^2}{2} \left(\frac{G}{G_0} \right)^2 \text{Tr} [(L^\mu)^2 + (R^\mu)^2]. \end{aligned} \quad (2.136)$$

The Large- N_c dependence of the parameter is given as

$$\begin{aligned} m_G & \propto N_c^0, \\ \Lambda_G & \propto N_c. \end{aligned} \quad (2.137)$$

(v) The term \mathcal{L}_{ESB} :

The chiral symmetry is explicitly broken by the quark masses. Two additional terms appear in the Lagrangian density \mathcal{L}_{ESB} , to describe this breaking separately for the (pseudo)scalar and (axial-)vector fields. We discuss these separately: In the (pseudo)scalar sector, pions are not really massless because of the explicit breaking of the $SU(N_f)_V \times SU(N_f)_A$ -symmetry. Therefore the following term is introduced to break this symmetry explicitly

$$\text{Tr}[H(\Phi^\dagger + \Phi)], \quad (2.138)$$

where

$$H = \text{diag}[h_1, h_2, \dots, h_{N_f}], \quad (2.139)$$

is the diagonal matrix with h_0^N proportional the mass of the quark flavour number. For example: $N_f = 1 \Rightarrow h_1 \propto m_u$ and $N_f = 2 \Rightarrow h_2 \propto m_d, \dots$ etc.

For the (axial-)vector sector, one can construct the following mass term which breaks the chiral symmetry explicitly

$$\text{Tr}[\Delta(L_\mu^2 + R_\mu^2)], \quad (2.140)$$

where

$$\Delta = \text{diag}[\delta_u, \delta_d, \dots, \delta_{N_f}], \quad (2.141)$$

which is also proportional to the quark mass terms as

$$\delta_u, \delta_d, \dots, \delta_{N_f} \propto m_u^2, m_d^2, \dots, m_{N_f}^2$$

Thus, the Lagrangian density \mathcal{L}_{ESB} is obtained as

$$\mathcal{L}_{ESB} = \text{Tr}[H(\Phi^\dagger + \Phi)] + \text{Tr}[\Delta(L_\mu^2 + R_\mu^2)]. \quad (2.142)$$

The large- N_c dependence of the parameters in the previous Lagrangian density is given as

$$\begin{aligned} h_i &\propto N_c^{1/2}, \\ \delta_i &\propto N_c^0. \end{aligned} \tag{2.143}$$

Spontaneous symmetry breaking

The spontaneous breaking of the chiral symmetry is an important requirement for all phenomena linked to hadrons in low-energy QCD. One can discuss this point from the following potential of the mesonic Lagrangian \mathcal{L}_{mes} along the axis $\Phi = \sigma t^0$

$$V(G, \sigma) = V_{dil}(G) + m_0^2 \sigma^2 + (\lambda_1 + \lambda_2) \sigma^4. \tag{2.144}$$

The symmetry is broken spontaneously by non-trivial minima, which are in the present case at

$$G_0 \neq 0, \sigma_0 \neq 0, \text{ for } m_0^2 < 0,$$

and

$$\sigma_0 = 0, G_0 \neq 0, \text{ for } m_0^2 > 0,$$

which means that the vacuum is not invariant under $SU(N_f)_A$ transformations. The dilatation symmetry is broken explicitly which is an important source for the phenomenology in the vacuum. Note that the conservation of parity and $SU(N_f)_V$ symmetry are required, whereas the $U(1)_A$ anomaly is neglected here. The only state that can condense in the vacuum is the scalar-isosinglet state, because this state is the only one which has the same quantum numbers as the vacuum.

Now let us summarize the full Lagrangian of the effective model, the so-called extended Linear Sigma Model (eLSM), for a generic number N_f of flavours in the following section.

2.6. The extended Linear Sigma Model

In this subsection we present the chirally symmetric linear sigma model Lagrangian which is essentially constructed with two requirements stemming from the underlying theory QCD: (i) global chiral symmetry $U(N)_R \times U(N)_L$. (ii) dilatation invariance (with the exceptions of the scale anomaly, the $U(1)_A$ anomaly and terms proportional to quark masses). It is also invariant under the discrete symmetries charge conjugation C , parity P , and time reversal T . It has the following form for a generic number N_f of flavours [108, 110, 116]:

$$\begin{aligned}
\mathcal{L} = & \mathcal{L}_{dil} + \text{Tr}[(D_\mu \Phi)^\dagger (D_\mu \Phi)] - m_0^2 \left(\frac{G}{G_0} \right)^2 \text{Tr}(\Phi^\dagger \Phi) - \lambda_1 [\text{Tr}(\Phi^\dagger \Phi)]^2 - \lambda_2 \text{Tr}(\Phi^\dagger \Phi)^2 \\
& - \frac{1}{4} \text{Tr}[(L^{\mu\nu})^2 + (R^{\mu\nu})^2] + \text{Tr} \left\{ \left[\left(\frac{G}{G_0} \right)^2 \frac{m_1^2}{2} + \Delta \right] [(L^\mu)^2 + (R^\mu)^2] \right\} + \text{Tr}[H(\Phi + \Phi^\dagger)] \\
& + c(\det \Phi - \det \Phi^\dagger)^2 + \frac{h_1}{2} \text{Tr}(\Phi^\dagger \Phi) \text{Tr}(L_\mu^2 + R_\mu^2) + h_2 \text{Tr}[|L_\mu \Phi|^2 + |\Phi R_\mu|^2] \\
& + 2h_3 \text{Tr}(L_\mu \Phi R^\mu \Phi^\dagger) + i \frac{g_2}{2} \{ \text{Tr}(L_{\mu\nu} [L^\mu, L^\nu]) + \text{Tr}(R_{\mu\nu} [R^\mu, R^\nu]) \} \\
& + g_3 [\text{Tr}(L_\mu L_\nu L^\mu L^\nu) + \text{Tr}(R_\mu R_\nu R^\mu R^\nu)] + g_4 [\text{Tr}(L_\mu L^\mu L_\nu L^\nu) + \text{Tr}(R_\mu R^\mu R_\nu R^\nu)] \\
& + g_5 \text{Tr}(L_\mu L^\mu) \text{Tr}(R_\nu R^\nu) + g_6 [\text{Tr}(L_\mu L^\mu) \text{Tr}(L_\nu L^\nu) + \text{Tr}(R_\mu R^\mu) \text{Tr}(R_\nu R^\nu)] . \quad (2.145)
\end{aligned}$$

Here, G is the dilaton field/scalar glueball and the dilaton Lagrangian \mathcal{L}_{dil} [112, 114, 151] reads

$$\mathcal{L}_{dil} = \frac{1}{2} (\partial_\mu G)^2 - \frac{1}{4} \frac{m_G^2}{\Lambda^2} \left(G^4 \ln \left| \frac{G}{\Lambda} \right| - \frac{G^4}{4} \right), \quad (2.146)$$

which mimics the trace anomaly of QCD [111, 116]. The dimensionful parameter $\Lambda_G \sim N_c \Lambda_{QCD}$ sets the energy scale of low-energy QCD; in the chiral limit it is the only dimensionful parameter besides the coefficient of the term representing the axial anomaly. All other interaction terms of the Lagrangian are described by dimensionless coupling constants. The minimum of the dilaton potential in Eq.(2.129) is given by $G_0 = \Lambda$. A massive particle will arise after shifting the dilaton field $G \rightarrow G_0 + G$, where the dilaton field G is interpreted as the scalar glueball which consists of two gluons ($G \equiv |gg\rangle$). The value of G_0 is related to the gluon condensate of QCD. According to lattice QCD the glueball mass m_G , in the quenched approximation (no quarks), is about 1.5-1.7 GeV [65]. As mentioned above, the identification of G is still uncertain, the two most likely candidates are $f_0(1500)$ and $f_0(1710)$ and/or admixtures of them. Note that, we include the scalar glueball because it is conceptually important to guarantee dilatation invariance of the model (thus constraining the number of possible terms that the Lagrangian can have). We do not make an assignment for the scalar glueball in the framework of the strange and nonstrange ($N_f = 2$ and $N_f = 3$) cases (see chapter 3) and it does not affect the results of the study of the $N_f = 4$ case for the masses of open and hidden charmed mesons as well as the decay of open charmed mesons. Therefore, the scalar glueball is a frozen field in these investigations, whereas it becomes a dynamical field in the study of the decay of hidden charmed states as we will see in chapter 8. The logarithmic term of the dilaton potential breaks the dilatation symmetry explicitly, $x^\mu \rightarrow \Lambda^{-1} x^\mu$, which leads to the divergence of the corresponding current:

$$\partial_\mu J_{dil}^\mu = T_{dil, \mu}^\mu = -\frac{1}{4} m_G^2 \Lambda^2 . \quad (2.147)$$

The model has also mesonic fields described as quark-antiquark fields. We have to note that when working in the so-called large- N_c limit [147, 148]: (i) the glueball self-interaction term vanishes, (ii) the glueball becomes a free field, (iii) the masses are N_c -independent, (iv) the widths scale as N_c^{-1} .

Let us now turn to the question: **How can we introduce a pseudoscalar glueball into the chiral model (2.145)?**

The structure of the chiral anomaly term, $ic(\det\Phi - \det\Phi^\dagger)^2$, allows one to incorporate a pseudoscalar glueball field \tilde{G} into the model in a simple way, of the form

$$ic_{\tilde{G}\Phi}\tilde{G}(\det\Phi - \det\Phi^\dagger).$$

This form describes the interaction of the pseudoscalar field \tilde{G} with the scalar and pseudoscalar fields by a dimensionless coupling constant $c_{\tilde{G}\Phi}$. Through this term one can study the phenomenology of a pseudoscalar glueball. The details of the introduction of the pseudoscalar glueball in the extended Linear Sigma Model are presented in chapter 6. Furthermore, it is relevant in the decay of hidden charmed mesons, see chapter 8 below.

3. The extended Linear Sigma Model for two- and three-flavours

3.1. Introduction

In the last decades, effective low-energy approaches to the strong interaction have been developed by imposing chiral symmetry, one of the basic symmetries of the QCD Lagrangian in the limit of vanishing quark masses (the so-called chiral limit) [11, 12]. Chiral symmetry is explicitly broken by the nonzero current quark masses, but is also spontaneously broken by a nonzero quark condensate in the QCD vacuum [13]. As a consequence, pseudoscalar (quasi-)Goldstone bosons emerge, as discussed in details in the previous chapter. We develop the eLSM to study the vacuum properties of mesons and glueballs. In the case of $N_f = 2$ quark flavours, there are only mesons made of u and d quarks. However, the nucleons can also be taken into account in the context of a chiral model. The interaction of nucleons with mesons, tetraquarks, and glueballs in the chiral model for $N_f = 2$ will be described in the present chapter. Furthermore, in the case $N_f = 3$, mesons are made of up, down and strange quarks. It is for the first time possible to describe (pseudo)scalar as well as (axial-)vector meson nonets in a chiral framework: masses and decay widths turn out to be in very good agreement with the results listed by the Particle Data Group (PDG) [51]. In this chapter, we thus present the extension of the eLSM from non-strange hadrons ($N_f = 2$) [78, 106, 108, 109, 116] to strange hadrons ($N_f = 3$) [83, 101, 110, 116, 117]. Consequently, we investigate the vacuum properties of the three-flavour case [110, 116].

3.2. A $U(2)_R \times U(2)_L$ interaction with nucleons

In this section we present the chirally symmetric linear sigma model in the case of $N_f = 2$ [109]. It contains (pseudo)scalar and (axial-)vector fields, as well as nucleons and their chiral partners. Then we describe how the pseudoscalar glueball interacts with the nucleon and its chiral partner. This allows us to compute the decay widths of a pseudoscalar glueball into two nucleons (see Sec. 6.5).

3.2.1. A chirally invariant mass term

The mesonic Lagrangian for the Linear Sigma Model with global chiral $U(2)_R \times U(2)_L$ symmetry has the same form of the Lagrangian (2.145).

In this case, the matrix Φ reads

$$\Phi = \sum_{a=0}^3 \phi_a t_a = (\sigma + i\eta_N) t^0 + (\vec{a}_0 + i\vec{\pi}) \cdot \vec{t}, \quad (3.1)$$

and includes scalar and pseudoscalar fields. The eta meson η_N contains only non-strange degrees of freedom. Under the global $U(2)_R \times U(2)_L$ chiral symmetry, Φ transforms as $\Phi \rightarrow U_L \Phi^\dagger U_R$. The vector and axial-vector fields are described as

$$V^\mu = \sum_{a=0}^3 V_a^\mu t_a = \omega^\mu t^0 + \vec{\rho}^\mu \cdot \vec{t}, \quad (3.2)$$

and

$$A^\mu = \sum_{a=0}^3 A_a^\mu t_a = f_1^\mu t^0 + \vec{a}_1^\mu \cdot \vec{t}, \quad (3.3)$$

respectively, where the generators of $U(2)$ are $\vec{t} = \vec{\tau}/2$, with the vector of Pauli matrices $\vec{\tau}$ and $t^0 = \mathbf{1}_2/2$. Under global $U(2)_R \times U(2)_L$ transformations, these fields behave as $R^\mu \rightarrow U_R R^\mu U_R^\dagger$, $L^\mu \rightarrow U_L L^\mu U_L^\dagger$.

The mesonic Lagrangian (2.145) is invariant under $U(2)_R \times U(2)_L$ transformations for $c = h_0 = 0$ whereas for $h_0 \neq 0$, this symmetry is explicitly broken to the vectorial subgroup $U(2)_V$ [109], where $V = L + R$. Moreover, the $U(1)_A$ symmetry, where $A = L - R$, is explicitly broken for $c \neq 0$. The spontaneous chiral symmetry breaking is implemented by shifting the scalar-isoscalar field σ by its vacuum expectation value φ as $\sigma \rightarrow \sigma + \varphi$, where the chiral condensate $\varphi = \langle 0 | \sigma | 0 \rangle = Z f_\pi$. The parameter $f_\pi = 92.4$ MeV is the pion decay constant and Z is the wave function renormalization constant of the pseudoscalar fields [108, 153].

The meson fields of the model (2.145) [108, 109] are assigned to the following resonances listed by the PDG [51]:

- (i) The pseudoscalar fields $\vec{\pi}$ and η_N correspond to the pion and the $SU(2)$ counterpart of the η meson, $\eta_N \equiv |\bar{u}u + \bar{d}d\rangle/\sqrt{2}$, with a mass of about 700 MeV which can be obtained by “unmixin” the physical η and η' mesons. In the case of $N_f = 3$ [110] this mixing is calculated and the results are presented in the next section, where the model contains also contributions from strange quarks.
- (ii) The vector fields ω^μ and $\vec{\rho}^\mu$ represent the $\omega(782)$ and $\rho(770)$ vector mesons, respectively.
- (iii) The axial-vector fields f_1^μ and \vec{a}_1^μ represent the $f_1(1285)$ and $a_1(1260)$, respectively. The physical ω and f_1 states contain $\bar{s}s$ contributions which are negligibly small.
- (iv) The scalar fields σ and \vec{a}_0 are assigned to the physical $f_0(1370)$ and $a_0(1450)$ resonances.

We now turn to the baryonic sector in the eLSM for two flavours. The baryon sector involves two baryon doublets ψ_1 and ψ_2 , where ψ_1 has positive parity and ψ_2 has negative parity. In the so-called mirror assignment [154, 155, 156] they transform under chiral transformation as:

$$\Psi_{1R} \rightarrow U_R \Psi_{1R}, \quad \Psi_{1L} \rightarrow U_L \Psi_{1L}, \quad \Psi_{2R} \rightarrow U_L \Psi_{2R}, \quad \Psi_{2L} \rightarrow U_R \Psi_{2L}. \quad (3.4)$$

While ψ_1 transforms as usual, ψ_2 transforms in a “mirror way” [156, 157]. These field transformations allow us to write the following baryonic Lagrangian for $N_f = 2$ with a chirally invariant mass term \mathcal{L}_{mas} for the fermions [109]:

$$\begin{aligned} \mathcal{L}_{\text{bar}} = & \bar{\Psi}_{1L} i \gamma_\mu D_{1L}^\mu \Psi_{1L} + \bar{\Psi}_{1R} i \gamma_\mu D_{1R}^\mu \Psi_{1R} + \bar{\Psi}_{2L} i \gamma_\mu D_{2R}^\mu \Psi_{2L} + \bar{\Psi}_{2R} i \gamma_\mu D_{2L}^\mu \Psi_{2R} \\ & - \hat{g}_1 \left(\bar{\Psi}_{1L} \Phi \Psi_{1R} + \bar{\Psi}_{1R} \Phi^\dagger \Psi_{1L} \right) - \hat{g}_2 \left(\bar{\Psi}_{2L} \Phi^\dagger \Psi_{2R} + \bar{\Psi}_{2R} \Phi \Psi_{2L} \right) + \mathcal{L}_{\text{mass}}, \end{aligned} \quad (3.5)$$

where

$$D_{1R}^\mu = \partial^\mu - ic_1 R^\mu, \quad D_{1L}^\mu = \partial^\mu - ic_1 L^\mu,$$

and

$$D_{2R}^\mu = \partial^\mu - ic_2 R^\mu, \quad D_{2L}^\mu = \partial^\mu - ic_2 L^\mu,$$

are the covariant derivatives for the nucleonic fields, with the coupling constants c_1 and c_2 . Note that the three coupling constants c_1 , c_2 , and g_1 are equal in the case of local chiral symmetry. The interaction of the baryonic fields with the scalar and (pseudo)scalar mesons is parameterized by \widehat{g}_1 and \widehat{g}_2 . The chirally invariant mass term \mathcal{L}_{mass} for fermions parameterized by μ_0 , reads

$$\begin{aligned} \mathcal{L}_{mass} &= -\mu_0(\overline{\Psi}_{1L}\Psi_{2R} - \overline{\Psi}_{1R}\Psi_{2L} - \overline{\Psi}_{2L}\Psi_{1R} + \overline{\Psi}_{2R}\Psi_{1L}) \\ &= -\mu_0(\overline{\Psi}_2\gamma_5\Psi_1 - \overline{\Psi}_1\gamma_5\Psi_2), \end{aligned} \quad (3.6)$$

where μ_0 has the dimension of mass. This mass term plays an important role in generating the nucleon mass. The physical fields are the nucleon N and its chiral partner N^* . They engender by diagonalizing the baryonic part of the Lagrangian. As a result [109] we have

$$\begin{pmatrix} N \\ N^* \end{pmatrix} = \widehat{M} \begin{pmatrix} \Psi_1 \\ \Psi_2 \end{pmatrix} = \frac{1}{\sqrt{2 \cosh \delta}} \begin{pmatrix} e^{\delta/2} & \gamma_5 e^{-\delta/2} \\ \gamma_5 e^{-\delta/2} & -e^{\delta/2} \end{pmatrix} \begin{pmatrix} \Psi_1 \\ \Psi_2 \end{pmatrix}, \quad (3.7)$$

where δ measures the intensity of the mixing and is related to the parameter μ_0 and the physical masses of N and N^* by the expression:

$$\cosh \delta = \frac{m_N + m_{N^*}}{2m_0}. \quad (3.8)$$

The masses of nucleon and its partner [109] read

$$m_{N,N^*} = \sqrt{m_0^2 + \left[\frac{1}{4}(\widehat{g}_1 + \widehat{g}_2)\varphi\right]^2} \pm \frac{1}{4}(\widehat{g}_1 - \widehat{g}_2)\varphi. \quad (3.9)$$

The coupling constants $\widehat{g}_{1,2}$ are determined by the masses of nucleon (m_N), its partner (m_{N^*}), and the parameter m_0 ,

$$\widehat{g}_{1,2} = \frac{1}{\varphi} \left[\pm(m_N - m_{N^*}) + \sqrt{(m_N + m_{N^*})^2 - 4m_0^2} \right]. \quad (3.10)$$

The masses of the nucleon and its partner turn into be degenerate, $m_N = m_{N^*} = m_0$, in the chirally restored phase where $\varphi \rightarrow 0$ as observed from Eq. (3.9). The breaking of chiral symmetry, $\varphi \neq 0$, generates the mass splitting.

Note that the mass term (3.6) is not dilatation invariant but we can modify this term to restore the dilatation symmetry by coupling it to the chirally invariant dilaton field G and a tetraquark field $\chi \equiv [\bar{u}, \bar{d}][u, d]$ in an $U(2)_R \times U(2)_L$ invariant way. Then we obtain the dilatation invariant mass term as follows:

$$\mathcal{L}_{mass} = -(\alpha\chi + \beta G)(\overline{\Psi}_2\gamma_5\Psi_1 - \overline{\Psi}_1\gamma_5\Psi_2), \quad (3.11)$$

where α and β are dimensionless coupling constants. The term \mathcal{L}_{mass} would not be possible if the field ψ_2 would transform as ψ_1 . If both scalar fields are shifted around their vacuum expectation values $\chi \rightarrow \chi_0 + \chi$ and $G \rightarrow G_0 + G$, there emerges a nonvanishing chiral mass

$$m_0 = \alpha \chi_0 + \beta G_0, \quad (3.12)$$

where χ_0 and G_0 are the tetraquark and gluon condensates, respectively. m_0 is the mass contribution to the nucleon which does not stem from the chiral $(q\bar{q})$ condensate $\sigma = \phi$. In Ref. [109] the quantitative value for the parameter m_0 has been obtained by a fit to vacuum properties as

$$m_0 = (460 \pm 136) \text{ MeV}. \quad (3.13)$$

Under the simplifying assumption $\beta = 0$, as seen in the Ref. [158], the parameter m_0 is saturated by the tetraquark condensate, where χ is identified with the resonance $f_0(600)$ while for N^* there are two candidates with quantum numbers $(J^P = \frac{1}{2}^-)$, which are the lightest state $N(1535)$ and the heavier state $N(1650)$ [123]. But in the present section, we are interested in studying the case $\alpha = 0$, when the parameter m_0 is saturated by the glueball condensate. The fermions involved are represented by the spinors Ψ_1 and Ψ_2 . Then we obtain the following interaction term for the glueball with a nucleon

$$\mathcal{L}_{G\text{-baryons}} = \beta G (\bar{\Psi}_2 \gamma_5 \Psi_1 - \bar{\Psi}_1 \gamma_5 \Psi_2), \quad (3.14)$$

where β is a dimensionless coupling constant. The physical fields N and N^* are related to the spinors Ψ_1 and Ψ_2 according to Eq. (3.7) by the following relations:

$$\Psi_1 = \frac{1}{\sqrt{2 \cosh \delta}} \left(N e^{\delta/2} + \gamma_5 N^* e^{-\delta/2} \right), \quad (3.15)$$

$$\Psi_2 = \frac{1}{\sqrt{2 \cosh \delta}} \left(\gamma_5 N e^{-\delta/2} - N^* e^{\delta/2} \right), \quad (3.16)$$

$$\bar{\Psi}_1 = \frac{1}{\sqrt{2 \cosh \delta}} \left(\bar{N} e^{\delta/2} - \bar{N}^* \gamma_5 e^{-\delta/2} \right), \quad (3.17)$$

and

$$\bar{\Psi}_2 = \frac{1}{\sqrt{2 \cosh \delta}} \left(-\bar{N} \gamma_5 e^{-\delta/2} - \bar{N}^* e^{\delta/2} \right). \quad (3.18)$$

3.3. The $U(3)_R \times U(3)_L$ linear sigma model

In this section we present the extended linear sigma model (eLSM) including the strange sector, $N_f = 3$, and its implications which have been investigated in Refs. [110, 116].

In the case $N_f = 3$, all quark-antiquark mesons in the Lagrangian (2.145) are assigned to the light (i.e., with mass $\lesssim 2$ GeV) resonances in the strange-nonstrange sector. The pseudoscalar fields P and the scalar fields S read

$$P = \frac{1}{\sqrt{2}} \begin{pmatrix} \frac{\eta_N + \pi^0}{\sqrt{2}} & \pi^+ & K^+ \\ \pi^- & \frac{\eta_N - \pi^0}{\sqrt{2}} & K^0 \\ K^- & K^0 & \eta_S \end{pmatrix}, \quad (3.19)$$

and

$$S = \frac{1}{\sqrt{2}} \begin{pmatrix} \frac{\sigma_N + a_0^0}{\sqrt{2}} & a_0^+ & K_0^{*+} \\ a_0^- & \frac{\sigma_N - a_0^0}{\sqrt{2}} & K_0^{*0} \\ K_0^{*-} & \bar{K}_0^{*0} & \sigma_S \end{pmatrix}, \quad (3.20)$$

which together form the matrix Φ describing the multiplet of the scalar and pseudoscalar mesons, as follows

$$\Phi = \sum_{a=0}^8 (S_a + iP_a) T_a = \frac{1}{\sqrt{2}} \begin{pmatrix} \frac{(\sigma_N + a_0^0) + i(\eta_N + \pi^0)}{\sqrt{2}} & a_0^+ + i\pi^+ & K_0^{*+} + iK^+ \\ a_0^- + i\pi^- & \frac{(\sigma_N - a_0^0) + i(\eta_N - \pi^0)}{\sqrt{2}} & K_0^{*0} + iK^0 \\ K_0^{*-} + iK^- & \bar{K}_0^{*0} + i\bar{K}^0 & \sigma_S + i\eta_S \end{pmatrix}, \quad (3.21)$$

$$(3.22)$$

and the adjoint matrix Φ^\dagger is

$$\Phi^\dagger = \sum_{a=0}^8 (S_a - iP_a) T_a = \frac{1}{\sqrt{2}} \begin{pmatrix} \frac{(\sigma_N + a_0^0) - i(\eta_N + \pi^0)}{\sqrt{2}} & a_0^+ - i\pi^+ & K_0^{*+} - iK^+ \\ a_0^- - i\pi^- & \frac{(\sigma_N - a_0^0) - i(\eta_N - \pi^0)}{\sqrt{2}} & K_0^{*0} - iK^0 \\ K_0^{*-} - iK^- & \bar{K}_0^{*0} - i\bar{K}^0 & \sigma_S - i\eta_S \end{pmatrix}, \quad (3.23)$$

where T_a ($a = 0, \dots, 8$) denote the generators of $U(3)$. The assignment of the quark-antiquark fields is as follows:

(i) In the pseudoscalar sector the fields $\vec{\pi}$ and K represent the pions and the kaons, respectively [51]. The bare fields $\eta_N \equiv |\bar{u}u + \bar{d}d\rangle/\sqrt{2}$ and $\eta_S \equiv |\bar{s}s\rangle$ are the non-strange and strange contributions of the physical states η and η' [51]:

$$\eta = \eta_N \cos \varphi + \eta_S \sin \varphi, \quad (3.24)$$

$$\eta' = -\eta_N \sin \varphi + \eta_S \cos \varphi, \quad (3.25)$$

where $\varphi \simeq -44.6^\circ$ is the mixing angle [110] between η and η' . There are other values for the mixing angle, e.g. $\varphi = -36^\circ$ [159] or $\varphi = -41.4^\circ$, as determined by the KLOE Collaboration [92], but using these affects the presented results only marginally.

(ii) In the scalar sector we assign the field \vec{a}_0 to the physical isotriplet state $a_0(1450)$ and the scalar kaon fields K_0^* to the resonance $K_0^*(1430)$. Finally, the non-strange and strange bare fields $\sigma_N \equiv |\bar{u}u + \bar{d}d\rangle/\sqrt{2}$ and $\sigma_S \equiv |\bar{s}s\rangle$ mix with a scalar glueball $G \equiv gg\rangle$ and generate the three physical isoscalar resonances $f_0(1370)$, $f_0(1500)$ and $f_0(1710)$. As seen in Ref. [83] that $f_0(1370)$, $f_0(1500)$ and $f_0(1710)$ are predominantly a σ_N , σ_S , and a glueball state, respectively. The mixing of the bare fields σ_N and σ_S is small [110, 116] (in agreement with large- N_c arguments) and is neglected in this work.

Now let us turn to the vector fields V (with quantum numbers $J^{PC} = 1^{--}$) and the axial-vector fields A (with quantum numbers $J^{PC} = 1^{+-}$) which are summarized in the following 3×3 matrices, respectively:

$$V^\mu = \frac{1}{\sqrt{2}} \begin{pmatrix} \frac{\omega_N^\mu + \rho^{\mu 0}}{\sqrt{2}} & \rho^{\mu+} & K^{*\mu+} \\ \rho^{\mu-} & \frac{\omega_N^\mu - \rho^{\mu 0}}{\sqrt{2}} & K^{*\mu 0} \\ K^{*\mu-} & \bar{K}^{*\mu 0} & \omega_S^\mu \end{pmatrix}, \quad (3.26)$$

and

$$A^\mu = \frac{1}{\sqrt{2}} \begin{pmatrix} \frac{f_{1N}^\mu + a_1^{\mu 0}}{\sqrt{2}} & a_1^{\mu+} & K_1^{\mu+} \\ a_1^{\mu-} & \frac{f_{1N}^\mu - a_1^{\mu 0}}{\sqrt{2}} & K_1^{\mu 0} \\ K_1^{\mu-} & \bar{K}_1^{\mu 0} & f_{1S}^\mu \end{pmatrix}, \quad (3.27)$$

which are combined into right-handed and left-handed vector fields as follows:

$$R^\mu = \sum_{a=0}^8 (V_a^\mu - A_a^\mu) T_a = \frac{1}{\sqrt{2}} \begin{pmatrix} \frac{\omega_N + \rho^0}{\sqrt{2}} - \frac{f_{1N} + a_1^0}{\sqrt{2}} & \rho^+ - a_1^+ & K^{*+} - K_1^+ \\ \rho^- - a_1^- & \frac{\omega_N - \rho^0}{\sqrt{2}} - \frac{f_{1N} - a_1^0}{\sqrt{2}} & K^{*0} - K_1^0 \\ K^{*-} - K_1^- & \bar{K}^{*0} - \bar{K}_1^0 & \omega_S - f_{1S} \end{pmatrix}^\mu, \quad (3.28)$$

$$L^\mu = \sum_{a=0}^8 (V_a^\mu + A_a^\mu) T_a = \frac{1}{\sqrt{2}} \begin{pmatrix} \frac{\omega_N + \rho^0}{\sqrt{2}} + \frac{f_{1N} + a_1^0}{\sqrt{2}} & \rho^+ + a_1^+ & K^{*+} + K_1^+ \\ \rho^- + a_1^- & \frac{\omega_N - \rho^0}{\sqrt{2}} + \frac{f_{1N} - a_1^0}{\sqrt{2}} & K^{*0} + K_1^0 \\ K^{*-} + K_1^- & \bar{K}^{*0} + \bar{K}_1^0 & \omega_S + f_{1S} \end{pmatrix}^\mu, \quad (3.29)$$

Note that the so-called strange-nonstrange basis in the $(0-8)$ vector is used [110], which is defined as

$$\begin{aligned} \varphi_N &= \frac{1}{\sqrt{3}} \left(\sqrt{2} \varphi_0 + \varphi_8 \right), \\ \varphi_S &= \frac{1}{\sqrt{3}} \left(\varphi_0 - \sqrt{2} \varphi_8 \right), \quad \varphi \in (S_a, P_a, V_a^\mu, A_a^\mu), \end{aligned} \quad (3.30)$$

The quark-antiquark (axial-)vector fields in the matrices (3.26, 3.27) are assigned as follows: (i) In the vector sector the fields ω_N and ρ represent the $\omega(782)$ and $\rho(770)$ vector mesons, respectively, while the ω_S and K^* fields correspond to the physical $\phi(1020)$ and $K^*(892)$ resonances, respectively.

(ii) In the axial-vector sector we assign the fields f_{1N}^μ and \vec{a}_1^μ to the physical resonances $f_1(1285)$ and $a_1(1260)$ mesons, respectively. The strange fields f_{1S} and K_1 correspond to the $f_1(1420)$ and K_{1270} [or $K_1(1400)$] mesons, respectively. [The details of this assignment are given in Ref. [110]].

The matrices H and Δ are defined as

$$H = H_0 T_0 + H_8 T_8 = \begin{pmatrix} \frac{h_{0N}}{2} & 0 & 0 \\ 0 & \frac{h_{0N}}{2} & 0 \\ 0 & 0 & \frac{h_{0S}}{\sqrt{2}} \end{pmatrix}, \quad (3.31)$$

$$\Delta = \Delta_0 T_0 + \Delta_8 T_8 = \begin{pmatrix} \frac{\tilde{\delta}_N}{2} & 0 & 0 \\ 0 & \frac{\tilde{\delta}_N}{2} & 0 \\ 0 & 0 & \frac{\tilde{\delta}_S}{\sqrt{2}} \end{pmatrix} \equiv \begin{pmatrix} \delta_N & 0 & 0 \\ 0 & \delta_N & 0 \\ 0 & 0 & \delta_S \end{pmatrix}, \quad (3.32)$$

where $h_N \sim m_u$, $h_S \sim m_s$, $\delta_N \sim m_u^2$, $\delta_S \sim m_s^2$. The matrices H (3.31) and Δ (3.32) enter the terms $\text{Tr}[H(\Phi + \Phi^\dagger)]$ and $\text{Tr}[\Delta(L_\mu^2 + R_\mu^2)]$ which explicitly break the global symmetry, $U(3)_R \times U(3)_L [= U(3)_V \times U(3)_A]$, in the (pseudo)scalar and (axial-)vector sectors due to different nonzero values for the quark masses. They break $U(3)_A$, if $H_0, \Delta_0 \neq 0$, and $U(3)_V \rightarrow SU(2)_V \times U(1)_V$, if $H_8, \Delta_8 \neq 0$, for details see Ref. [117].

The spontaneous symmetry breaking of the chiral symmetry is implemented by condensing the scalar-isosinglet states which are $\sigma_N \equiv (\bar{u}u + \bar{d}d)/\sqrt{2}$ and $\sigma_S \equiv \bar{s}s$. We shift these fields by their vacuum expectation values ϕ_N and ϕ_S ,

$$\sigma_N \rightarrow \sigma_N + \phi_N \text{ and } \sigma_S \rightarrow \sigma_S + \phi_S, \quad (3.33)$$

where the condensates ϕ_N and ϕ_S are functions of the pion decay constant f_π and the kaon decay constant f_K , respectively, (the detailed calculation is presented in the Appendix)

$$\phi_N = Z_\pi f_\pi, \quad (3.34)$$

$$\phi_S = \frac{2Z_K f_K - \phi_N}{\sqrt{2}}, \quad (3.35)$$

Thus leads to the mixing between (axial-)vector and (pseudo)scalar states in the Lagrangian (2.145),

$$\begin{aligned} & -g_1 \phi_N (f_{1N}^\mu \partial_\mu \eta_N + \vec{a}_1^\mu \cdot \partial_\mu \vec{\pi}) - \sqrt{2} g_1 \phi_S f_{1S}^\mu \partial_\mu \eta_S \\ & - i \frac{g_1}{2} (\phi_N - \phi_S) (\bar{K}^{*\mu 0} \partial_\mu K_0^{*0} + K^{*\mu -} \partial_\mu K_0^{*+}) \\ & + i \frac{g_1}{2} (\phi_N - \sqrt{2} \phi_S) (K^{*\mu 0} \partial_\mu \bar{K}_0^{*0} + K^{*\mu +} \partial_\mu K_0^{*-}) \\ & - \frac{g_1}{2} (\phi_N + \sqrt{2} \phi_S) (K_1^{\mu 0} \partial_\mu \bar{K}^0 + K_1^{\mu +} \partial_\mu K^- + \bar{K}_1^{\mu 0} \partial_\mu K^0 + K_1^{\mu -} \partial_\mu K^+). \end{aligned} \quad (3.36)$$

In order to eliminate this mixing, one performs shifts of the (axial-)vector fields as follows

$$f_{1N/S}^\mu \longrightarrow f_{1N/S}^\mu + Z_{\eta_{N/S}} w_{f_{1N/S}} \partial^\mu \eta_{N/S}, \quad (3.37)$$

$$a_1^{\mu \pm, 0} \longrightarrow a_1^{\mu \pm, 0} + Z_\pi w_{a_1} \partial^\mu \pi^{\pm, 0}, \quad (3.38)$$

$$K_1^{\mu \pm, 0, \bar{0}} \longrightarrow K_1^{\mu \pm, 0, \bar{0}} + Z_K w_{K_1} \partial^\mu K^{\pm 0, \bar{0}}, \quad (3.39)$$

$$K^{*\mu \pm, 0, \bar{0}} \longrightarrow K^{*\mu \pm, 0, \bar{0}} + Z_{K^*} w_{K^*} \partial^\mu K_0^{*\pm, 0, \bar{0}}. \quad (3.40)$$

which produce additional kinetic terms for the (pseudo)scalar fields. The shift (3.37) was performed in the case $N_f = 2$ in Ref. [108], and the shifts (3.38 - 3.40) were performed in the case $N_f = 3$ Ref. [110]. The wave-function renormalization constants have been introduced to retain the canonical normalization

$$\pi^{\pm,0} \rightarrow Z_\pi \pi^{\pm,0}, \quad (3.41)$$

$$K^{\pm,0,\bar{0}} \rightarrow Z_K K^{\pm,0,\bar{0}}, \quad (3.42)$$

$$\eta_{N/S} \rightarrow Z_{\eta_N/\eta_S} \eta_{N/S}, \quad (3.43)$$

$$K_0^{*\mu\pm,0,\bar{0}} \rightarrow Z_{K_0^*} K_0^{*\mu\pm,0,\bar{0}}. \quad (3.44)$$

Note that for simplicity the isotriplet states have been grouped together with the notation $\pi^{\pm,0}, a_1^{\mu\pm,0}$ and the isodoublet states with the notation $K^{\pm,0,\bar{0}}, K_0^{*\mu\pm,0,\bar{0}}$, where $\bar{0}$ refers to \bar{K}^0 . The explicit expressions for the coefficients w_i are obtained after some straightforward calculation (for details see Ref. [116]) as

$$w_{f_{1N}} = w_{a_1} = \frac{g_1 \phi_N}{m_{a_1}^2}, \quad (3.45)$$

$$w_{f_{1S}} = \frac{\sqrt{2} g_1 \phi_S}{m_{f_{1S}}^2}, \quad (3.46)$$

$$w_{K^*} = \frac{i g_1 (\phi_N - \sqrt{2} \phi_S)}{2 m_{K^*}^2}, \quad (3.47)$$

$$w_{K_1} = \frac{g_1 (\phi_N + \sqrt{2} \phi_S)}{2 m_{K_1}^2}. \quad (3.48)$$

The wave-function renormalization constants Z_i , introduced in Eq. (3.37-3.40), are determined such that one obtains the canonical normalization of the π, η_N, η_S, K and K_0^* . Their explicit expressions read [110, 116]:

$$Z_\pi = Z_{\eta_N} = \frac{m_{a_1}}{\sqrt{m_{a_1}^2 - g_1^2 \phi_N^2}}, \quad (3.49)$$

$$Z_K = \frac{2 m_{K_1}}{\sqrt{4 m_{K_1}^2 - g_1^2 (\phi_N + \sqrt{2} \phi_S)^2}}, \quad (3.50)$$

$$Z_{K_S} = \frac{2 m_{K^*}}{\sqrt{4 m_{K^*}^2 - g_1^2 (\phi_N - \sqrt{2} \phi_S)^2}}, \quad (3.51)$$

$$Z_{\eta_S} = \frac{m_{f_{1S}}}{\sqrt{m_{f_{1S}}^2 - 2 g_1^2 \phi_S^2}}, \quad (3.52)$$

which are always larger than one. After some straightforward calculation the tree-level

(squared) masses for all nonets in the chiral Lagrangian (2.145) are given[110, 116] by

$$m_\pi^2 = Z_\pi^2 \left[m_0^2 + \left(\lambda_1 + \frac{\lambda_2}{2} \right) \phi_N^2 + \lambda_1 \phi_S^2 \right] \equiv \frac{Z_\pi^2 h_{0N}}{\phi_N}, \quad (3.53)$$

$$m_K^2 = Z_K^2 \left[m_0^2 + \left(\lambda_1 + \frac{\lambda_2}{2} \right) \phi_N^2 - \frac{\lambda_2}{\sqrt{2}} \phi_N \phi_S + (\lambda_1 + \lambda_2) \phi_S^2 \right], \quad (3.54)$$

$$m_{\eta_N}^2 = Z_\pi^2 \left[m_0^2 + \left(\lambda_1 + \frac{\lambda_2}{2} \right) \phi_N^2 + \lambda_1 \phi_S^2 + c_1 \phi_N^2 \phi_S^2 \right] \equiv Z_\pi^2 \left(\frac{h_{0N}}{\phi_N} + c_1 \phi_N^2 \phi_S^2 \right), \quad (3.55)$$

$$m_{\eta_S}^2 = Z_{\eta_S}^2 \left[m_0^2 + \lambda_1 \phi_N^2 + (\lambda_1 + \lambda_2) \phi_S^2 + \frac{c_1}{4} \phi_N^4 \right] \equiv Z_{\eta_S}^2 \left(\frac{h_{0S}}{\phi_S} + \frac{c_1}{4} \phi_N^4 \right), \quad (3.56)$$

$$m_{\eta_{NS}}^2 = Z_\pi Z_{\pi_S} \frac{c_1}{2} \phi_N^3 \phi_S, \quad (3.57)$$

for the (squared) pseudoscalar masses, while

$$m_{a_0}^2 = m_0^2 + \left(\lambda_1 + \frac{3}{2} \lambda_2 \right) \phi_N^2 + \lambda_1 \phi_S^2, \quad (3.58)$$

$$m_{K_0^*}^2 = Z_{K_0^*}^2 \left[m_0^2 + \left(\lambda_1 + \frac{\lambda_2}{2} \right) \phi_N^2 + \frac{\lambda_2}{\sqrt{2}} \phi_N \phi_S + (\lambda_1 + \lambda_2) \phi_S^2 \right], \quad (3.59)$$

$$m_{\sigma_N}^2 = m_0^2 + 3 \left(\lambda_1 + \frac{\lambda_2}{2} \right) \phi_N^2 + \lambda_1 \phi_S^2, \quad (3.60)$$

$$m_{\sigma_S}^2 = m_0^2 + \lambda_1 \phi_N^2 + 3 (\lambda_1 + \lambda_2) \phi_S^2, \quad (3.61)$$

$$m_{\sigma_{NS}}^2 = 2\lambda_1 \phi_N \phi_S, \quad (3.62)$$

are the (squared) scalar masses. Moreover, the (squared) vector masses are obtained as

$$m_\rho^2 = m_1^2 + \frac{1}{2} (h_1 + h_2 + h_3) \phi_N^2 + \frac{h_1}{2} \phi_S^2 + 2\delta_N, \quad (3.63)$$

$$m_{K^*}^2 = m_1^2 + \frac{1}{4} (g_1^2 + 2h_1 + h_2) \phi_N^2 + \frac{1}{\sqrt{2}} \phi_N \phi_S (h_3 - g_1^2) + \frac{1}{2} (g_1^2 + h_1 + h_2) \phi_S^2 + \delta_N + \delta_S, \quad (3.64)$$

$$m_{\omega_N}^2 = m_\rho^2, \quad (3.65)$$

$$m_{\omega_S}^2 = m_1^2 + \frac{h_1}{2} \phi_N^2 + \left(\frac{h_1}{2} + h_2 + h_3 \right) \phi_S^2 + 2\delta_S, \quad (3.66)$$

while the (squared) axial-vector meson masses are

$$m_{a_1}^2 = m_1^2 + \frac{1}{2} (2g_1^2 + h_1 + h_2 - h_3) \phi_N^2 + \frac{h_1}{2} \phi_S^2 + 2\delta_N, \quad (3.67)$$

$$m_{K_1}^2 = m_1^2 + \frac{1}{4} (g_1^2 + 2h_1 + h_2) \phi_N^2 - \frac{1}{\sqrt{2}} \phi_N \phi_S (h_3 - g_1^2) + \frac{1}{2} (g_1^2 + h_1 + h_2) \phi_S^2 + \delta_N + \delta_S, \quad (3.68)$$

$$m_{f_{1N}}^2 = m_{a_1}^2, \quad (3.69)$$

$$m_{f_{1S}}^2 = m_1^2 + \frac{h_1}{2} \phi_N^2 + \left(2g_1^2 + \frac{h_1}{2} + h_2 - h_3 \right) \phi_S^2 + 2\delta_S. \quad (3.70)$$

All previous expressions coincide with Refs. [110, 116].

3.3.1. Model Parameters

The chirally symmetric model Eq.(2.145) contains 18 parameters which are: m_0^2 , m_1^2 , c_1 , δ_N , δ_S , g_1 , g_2 , g_3 , g_4 , g_5 , g_6 , h_{0N} , h_{0S} , h_1 , h_2 , h_3 , λ_1 , λ_2 . Note that the coupling of the glueball with the other mesons has been neglected. The parameters g_3 , g_4 , g_5 , and g_6 are not considered in the fit because they do not influence any decay channels in the case of the $N_f = 3$ [110] investigation. The explicit symmetry breaking in the vector and axial-vector channel is described by δ_N and δ_S . The ESB arises from non-vanishing quark masses, which leads us to the correspondence $\delta_N \propto m_{u,d}^2$ and $\delta_S \propto m_S^2$. The linear combination $m_1^2/2 + \delta_{N/S}$ appears in the vector-meson mass term $\text{Tr}[(m_1^2/2 + \Delta)(L_\mu^2 + R_\mu^2)]$. We can redefine $m_1^2/2 \rightarrow m_1^2/2 - \delta_N$ which leads to the appearance of only the combination $\delta_S - \delta_N$ in the mass formulas. This difference is determined by the fit of the (axial-)vector masses. Without loss of generality, we may take $\delta_N \equiv 0$. Then the unknown parameters are decreased to 13 in the chiral Lagrangian (or the so-called the extended Linear Sigma Model) [110]: m_0^2 , m_1^2 , c_1 , δ_S , g_1 , g_2 , h_{0N} , h_{0S} , h_1 , h_2 , h_3 , λ_1 , λ_2 .

Moreover, the experimental quantities that are used in the fit do not depend on all previous 13 parameters. The following two linear combinations have been used in the fit rather than the parameters m_0 , λ_1 , m_1 , h_1 separately.

$$\begin{aligned} C_1 &= m_0^2 + \lambda_1 (\phi_N^2 + \phi_S^2) , \\ C_2 &= m_1^2 + \frac{h_1}{2} (\phi_N^2 + \phi_S^2) . \end{aligned} \quad (3.71)$$

The condensates ϕ_N and ϕ_S are used instead of the parameters h_{0N} and h_{0S} which are determined by the masses of pion and η_S , as presented in Eqs. (3.53), (3.56). Consequently, there are eleven parameters left:

$$C_1, C_2, c_1, \delta_S, g_1, g_2, \phi_N, \phi_S, h_2, h_3, \lambda_2 .$$

The eleven parameters are fitted by 21 experimental quantities as seen in Ref. [116]. The parameter values are obtained with $\chi^2 \simeq 1$ [110] as summarized in the Table 3.1.

Parameter	Value
C_1	$(-0.9183 \pm 0.0006) \text{ GeV}^2$
C_2	$(0.4135 \pm 0.0147) \text{ GeV}^2$
c_1	$(450.5420 \pm 7.0339) \text{ GeV}^{-2}$
δ_S	$(0.1511 \pm 0.0038) \text{ GeV}^2$
g_1	5.8433 ± 0.0176
g_2	3.0250 ± 0.2329
ϕ_N	$(0.1646 \pm 0.0001) \text{ GeV}$
ϕ_S	$(0.1262 \pm 0.0001) \text{ GeV}$
h_2	9.8796 ± 0.6627
h_3	4.8667 ± 0.0864
λ_2	68.2972 ± 0.0435

Table 3.1.: Parameters and their errors.

Note that the parameters λ_1 and h_1 are set to zero because the fit uses all scalar mass terms except m_{σ_N} and m_{σ_S} , due to the well-known ambiguities regarding the assignment of scalar mesons. The parameter λ_1 is expressed via the bare mass parameter m_0^2 which is allowed due to the knowledge of the mentioned linear combination. Moreover the parameter h_1 is suppressed in large- N_c as well as λ_1 .

3.3.2. Results

The fit results for masses [110] are interesting because they prove that a chiral framework is applicable for the study of hadron vacuum phenomenology up to 1.7 GeV, (as listed in Table 3.1)

Observable	Fit [MeV]	Experiment [MeV]
m_π	141.0 ± 5.8	137.3 ± 6.9
m_K	485.6 ± 3.0	495.6 ± 24.8
m_η	509.4 ± 3.0	547.9 ± 27.4
$m_{\eta'}$	962.5 ± 5.6	957.8 ± 47.9
m_ρ	783.1 ± 7.0	775.5 ± 38.8
m_{K^*}	885.1 ± 6.3	893.8 ± 44.7
m_ϕ	975.1 ± 6.4	1019.5 ± 51.0
m_{a_1}	1186 ± 6	1230 ± 62
$m_{f_1(1420)}$	1372.5 ± 5.3	1426.4 ± 71.3
m_{a_0}	1363 ± 1	1474 ± 74
$m_{K_0^*}$	1450 ± 1	1425 ± 71

Table 3.2.: Best-fit results for masses compared with experiment (from Ref. [110]).

The mass results of the (pseudo)scalar and (axial-)vector sectors are in good agreement with experimental results as seen in Table 3.2. The resonances $a_0(1450)$ and $K_0^*(1430)$ are well described as quark-antiquark fields. The scalar-isoscalar mesons are not included in the fit. The decay pattern and the masses suggest that $f_0(1370)$ and $f_0(1710)$ are (predominantly) the non-strange and strange scalar-isoscalar fields. In the Refs.[110, 116] there are further results for the decay widths for light mesons in the chiral model (2.145) which are also in a good agreement with experiment.

4. Charmed mesons in the extended Linear Sigma Model

“Research is to see what everybody has seen and to think what nobody else has thought”

Albert Szent-Györgi

4.1. Introduction

In this chapter we investigate the eLSM model in the four-flavour case ($N_f = 4$), i.e., by considering mesons which contain at least one charm quark. This chapter is based on Refs.[118, 119, 120, 121, 122]. This study is a straightforward extension of Sec 3.3 [110]: the Lagrangian has the same structure as in the $N_f = 3$ case, except that all (pseudo)scalar and (axial-)vector meson fields are now parametrized in terms of 4×4 (instead of 3×3) matrices. These now also include the charmed degrees of freedom. Since low-energy (i.e., nonstrange and strange) hadron phenomenology was described very well [110], we retain the values for the parameters that already appear in the three-flavour sector. Then, extending the model to $N_f = 4$, three additional parameters enter, all of which are related to the current charm quark mass (two of them in the (pseudo)scalar sector and one in the (axial-)vector sector).

Considering that the explicit breaking of chiral and dilatation symmetries by the current charm quark mass, $m_c \simeq 1.275$ GeV, are quite large, one may wonder whether it is at all justified to apply a model based on chiral symmetry. Related to this, the charmed mesons entering our model have a mass up to about 3.5 GeV, i.e., they are strictly speaking no longer part of the low-energy domain of the strong interaction. Naturally, we do not expect to achieve the same precision as refined potential models [47, 48, 49, 160, 161, 162, 163, 164], lattice-QCD calculations [165, 166, 167], and heavy-quark effective theories [50, 168, 169, 170, 171, 172, 173, 174, 175, 176, 177, 178, 179] [see also the review of Ref. [59] and refs. therein]. Nevertheless, it is still interesting to see how a successful model for low-energy hadron phenomenology based on chiral symmetry and dilatation invariance fares when extending it to the high-energy charm sector. Quite surprisingly, a quantitative agreement with experimental values for the open charmed meson masses is obtained by fitting just the three additional parameters mentioned above (with deviations of the order of 150 MeV, i.e., $\sim 5\%$). On the other hand, with the exception of J/ψ , the charmonium states turn out to be about 10% too light when compared to experimental data. Nevertheless, the main conclusion is that it is, to first approximation, not unreasonable to delegate the strong breaking of chiral and dilatation symmetries to three mass terms only and still have chirally and dilatation invariant interaction terms. Moreover, our model correctly predicts the mass splitting between spin-0 and spin-1 negative-parity open charm states, i.e., naturally incorporates the right amount of breaking of the heavy-quark spin symmetry.

4.2. The $U(4)_r \times U(4)_l$ linear sigma model

In this section we extend the eLSM [110, 116] to the four-flavour case. To this end, we introduce 4×4 matrices which contain, in addition to the usual nonstrange and strange mesons, also charmed states. The matrix of pseudoscalar fields P (with quantum numbers $J^{PC} = 0^{-+}$) reads

$$P = \frac{1}{\sqrt{2}} \begin{pmatrix} \frac{1}{\sqrt{2}}(\eta_N + \pi^0) & \pi^+ & K^+ & D^0 \\ \pi^- & \frac{1}{\sqrt{2}}(\eta_N - \pi^0) & K^0 & D^- \\ K^- & \bar{K}^0 & \eta_S & D_S^- \\ \bar{D}^0 & D^+ & D_S^+ & \eta_c \end{pmatrix} \sim \frac{1}{\sqrt{2}} \begin{pmatrix} \bar{u}\Gamma u & \bar{d}\Gamma u & \bar{s}\Gamma u & \bar{c}\Gamma u \\ \bar{u}\Gamma d & \bar{d}\Gamma d & \bar{s}\Gamma d & \bar{c}\Gamma d \\ \bar{u}\Gamma s & \bar{d}\Gamma s & \bar{s}\Gamma s & \bar{c}\Gamma s \\ \bar{u}\Gamma c & \bar{d}\Gamma c & \bar{s}\Gamma c & \bar{c}\Gamma c \end{pmatrix}, \quad (4.1)$$

where, for sake of clarity, we also show the quark-antiquark content of the mesons (in the pseudoscalar channel $\Gamma = i\gamma^5$). In the nonstrange-strange sector (the upper left 3×3 matrix) the matrix P contains the pion triplet $\vec{\pi}$, the four kaon states K^+ , K^- , K^0 , \bar{K}^0 , and the isoscalar fields $\eta_N = \sqrt{1/2}(\bar{u}u + \bar{d}d)$ and $\eta_S = \bar{s}s$, see Eq. (3.19). The latter two fields mix and generate the physical fields η (3.24) and η' (3.25) [see details in Ref. [110]]. In the charm sector (fourth line and fourth column) the matrix P contains the open charmed states D^+ , D^- , D^0 , \bar{D}^0 , which correspond to the well-established D resonance, the open strange-charmed states D_S^\pm , and, finally, the hidden charmed state η_c , which represents the well-known pseudoscalar ground state charmonium $\eta_c(1S)$.

The matrix of scalar fields S (with quantum numbers $J^{PC} = 0^{++}$) reads

$$S = \frac{1}{\sqrt{2}} \begin{pmatrix} \frac{1}{\sqrt{2}}(\sigma_N + a_0^0) & a_0^+ & K_0^{*+} & D_0^{*0} \\ a_0^- & \frac{1}{\sqrt{2}}(\sigma_N - a_0^0) & K_0^{*0} & D_0^{*-} \\ K_0^{*-} & \bar{K}_0^{*0} & \sigma_S & D_{S0}^{*-} \\ \bar{D}_0^{*0} & D_0^{*+} & D_{S0}^{*+} & \chi_{c0} \end{pmatrix}. \quad (4.2)$$

The quark-antiquark content is the same as in Eq. (4.1), but using $\Gamma = 1_4$. A long debate about the correct assignment of light scalar states has taken place in the last decades. Present results [9, 10, 72, 73, 74], which have been independently confirmed in the framework of the eLSM [110], show that the scalar quarkonia have masses between 1-2 GeV. In particular, the isotriplet \vec{a}_0 is assigned to the resonance $a_0(1450)$ (and not to the lighter state $a_0(980)$). Similarly, the kaonic states K_0^{*+} , K_0^{*-} , K_0^{*0} , \bar{K}_0^{*0} are assigned to the resonance $K_0^*(1430)$ (and not to the $K_0^*(800)$ state). The situation in the scalar-isoscalar sector is more complicated, due to the presence of a scalar glueball state G , see Ref. [78] and below. Then, σ_N , σ_S , G mix and generate the three resonances $f_0(1370)$, $f_0(1500)$, and $f_0(1710)$. There is evidence [83] that $f_0(1370)$ is predominantly a $\sqrt{1/2}(\bar{u}u + \bar{d}d)$ state, while $f_0(1500)$ is predominantly a $\bar{s}s$ state and $f_0(1710)$ predominantly a glueball state. As a consequence, the light scalar states $f_0(500)$ and $f_0(980)$ are not quarkonia (but, arguably, tetraquark or molecular states) [128, 180, 181, 182, 183, 184, 185, 186, 187, 188]. In the open charm sector, we assign the charmed states D_0^* to the resonances $D_0^*(2400)^0$ and $D_0^*(2400)^\pm$ (the latter state has not yet been unambiguously established). In the strange-charm sector we assign the state $D_{S0}^{*\pm}$ to the only existing candidate $D_{S0}^*(2317)^\pm$; it should, however, be stressed that the latter state has also been interpreted as a tetraquark or molecular state because it is too light when compared to quark-model predictions, see Refs. [47, 48, 52, 53, 58, 59, 189, 190, 191]. In

the next section, we discuss in more detail the possibility that a heavier, very broad (and therefore not yet discovered) scalar charmed state exists. In the hidden charm sector the resonance χ_{c0} corresponds to the ground-state scalar charmonium $\chi_{c0}(1P)$.

The matrices P and S are used to construct the matrix Φ as follows,

$$\Phi = S + iP = \frac{1}{\sqrt{2}} \begin{pmatrix} \frac{(\sigma_N + a_0^0) + i(\eta_N + \pi^0)}{\sqrt{2}} & a_0^+ + i\pi^+ & K_0^{*+} + iK^+ & D_0^{*0} + iD^0 \\ a_0^- + i\pi^- & \frac{(\sigma_N - a_0^0) + i(\eta_N - \pi^0)}{\sqrt{2}} & K_0^{*0} + iK^0 & D_0^{*-} + iD^- \\ K_0^{*-} + iK^- & \bar{K}_0^{*0} + i\bar{K}^0 & \sigma_S + i\eta_S & D_{S0}^{*-} + iD_S^- \\ \bar{D}_0^{*0} + i\bar{D}^0 & D_0^{*+} + iD^+ & D_{S0}^{*+} + iD_S^+ & \chi_{c0} + i\eta_C \end{pmatrix}, \quad (4.3)$$

and the adjoint matrix Φ^\dagger reads

$$\Phi^\dagger = S - iP = \frac{1}{\sqrt{2}} \begin{pmatrix} \frac{(\sigma_N + a_0^0) - i(\eta_N + \pi^0)}{\sqrt{2}} & a_0^+ - i\pi^+ & K_0^{*+} - iK^+ & D_0^{*0} - iD^0 \\ a_0^- - i\pi^- & \frac{(\sigma_N - a_0^0) - i(\eta_N - \pi^0)}{\sqrt{2}} & K_0^{*0} - iK^0 & D_0^{*-} - iD^- \\ K_0^{*-} - iK^- & \bar{K}_0^{*0} - i\bar{K}^0 & \sigma_S - i\eta_S & D_{S0}^{*-} - iD_S^- \\ \bar{D}_0^{*0} - i\bar{D}^0 & D_0^{*+} - iD^+ & D_{S0}^{*+} - iD_S^+ & \chi_{c0} - i\eta_C \end{pmatrix}. \quad (4.4)$$

The multiplet matrix Φ transforms as $\Phi \rightarrow U_L \Phi U_R^\dagger$ under $U_L(4) \times U_R(4)$ chiral transformations, where $U_{L(R)} = e^{-i\theta_{L(R)}^a t^a}$ is an element of $U(4)_{R(L)}$, under parity, $\Phi(t, \vec{x}) \rightarrow \Phi^\dagger(t, -\vec{x})$, and under charge conjugate $\Phi \rightarrow \Phi^\dagger$. The determinant of Φ is invariant under $SU(4)_L \times SU(4)_R$, but not under $U(1)_A$ because $\det \Phi \rightarrow \det U_A \Phi U_A = e^{-i\theta_A^0 \sqrt{2N_f}} \det \Phi \neq \det \Phi$.

We now turn to the vector sector. The matrix V^μ which includes the vector degrees of freedom is:

$$V^\mu = \frac{1}{\sqrt{2}} \begin{pmatrix} \frac{1}{\sqrt{2}}(\omega_N + \rho^0) & \rho^+ & K^*(892)^+ & D^{*0} \\ \rho^- & \frac{1}{\sqrt{2}}(\omega_N - \rho^0) & K^*(892)^0 & D^{*-} \\ K^*(892)^- & \bar{K}^*(892)^0 & \omega_S & D_S^{*-} \\ \bar{D}^{*0} & D^{*+} & D_S^{*+} & J/\psi \end{pmatrix}^\mu. \quad (4.5)$$

The quark-antiquark content is that shown in Eq. (4.1), setting $\Gamma = \gamma^\mu$. The isotriplet field $\vec{\rho}$ corresponds to the ρ meson, the four kaonic states correspond to the resonance $K^*(892)$, the isoscalar states ω_N and ω_S correspond to the ω and ϕ mesons, respectively. [No mixing between strange and nonstrange isoscalars is present in the eLSM; this mixing is small anyway [192].] In the charm sector, the fields D^{*0} , \bar{D}^{*0} , D^{*+} , and D^{*-} correspond to the vector charmed resonances $D^*(2007)^0$ and $D^*(2010)^\pm$, respectively, while the strange-charmed $D_S^{*\pm}$ corresponds to the resonance $D_S^{*\pm}$ (with mass $M_{D_S^{*\pm}} = (2112.3 \pm 0.5)$ MeV; note, however, that the quantum numbers $J^P = 1^-$ are not yet fully established). Finally, J/ψ is the very well-known lowest vector charmonium state $J/\psi(1S)$.

The matrix A^μ describing the axial-vector degrees of freedom is given by:

$$A^\mu = \frac{1}{\sqrt{2}} \begin{pmatrix} \frac{1}{\sqrt{2}}(f_{1,N} + a_1^0) & a_1^+ & K_1^+ & D_1^0 \\ a_1^- & \frac{1}{\sqrt{2}}(f_{1,N} - a_1^0) & K_1^0 & D_1^- \\ K_1^- & \bar{K}_1^0 & f_{1,S} & D_{S1}^- \\ \bar{D}_1^0 & D_1^+ & D_{S1}^+ & \chi_{c,1} \end{pmatrix}^\mu. \quad (4.6)$$

The quark-antiquark content is that shown in Eq. (4.1), setting $\Gamma = \gamma^\mu \gamma^5$. The isotriplet field \bar{a}_1 corresponds to the field $a_1(1260)$, the four kaonic states K_1 correspond (predominantly) to the resonance $K_1(1200)$ [but also to $K_1(1400)$, because of mixing between axial-vector and pseudovector states, see Refs. [193, 194, 195, 196, 197] and ref. therein]. The isoscalar fields $f_{1,N}$ and $f_{1,S}$ correspond to $f_1(1285)$ and $f_1(1420)$, respectively. In the charm sector, the D_1 field is chosen to correspond to the resonances $D_1(2420)^0$ and $D_1(2420)^\pm$. (Another possibility would be the not yet very well established resonance $D_1(2430)^0$, or, due to mixing between axial- and pseudovector states, to a mixture of $D_1(2420)$ and $D_1(2430)$. Irrespective of this uncertainty, the small mass difference between these states would leave our results virtually unchanged.) The assignment of the strange-charmed doublet D_{S1}^\pm is not yet settled, the two possibilities listed by the PDG are the resonances $D_{S1}(2460)^\pm$ and $D_{S1}(2536)^\pm$ [51]. According to various studies, the latter option is favored, while the former can be interpreted as a molecular or a tetraquark state [46, 52, 53, 56, 57, 58, 198]. Thus, we assign our quark-antiquark D_1 state to the resonance $D_{S1}(2536)^\pm$. Finally, the charm-anticharm state $\chi_{c,1}$ can be unambiguously assigned to the charm-anticharm resonance $\chi_{c,1}(1P)$.

From the matrices V^μ and A^μ we construct the left-handed and right-handed vector fields as follows:

$$L^\mu = V^\mu + A^\mu = \frac{1}{\sqrt{2}} \begin{pmatrix} \frac{\omega_N + \rho^0}{\sqrt{2}} + \frac{f_{1N} + a_1^0}{\sqrt{2}} & \rho^+ + a_1^+ & K^{*+} + K_1^+ & D^{*0} + D_1^0 \\ \rho^- + a_1^- & \frac{\omega_N - \rho^0}{\sqrt{2}} + \frac{f_{1N} - a_1^0}{\sqrt{2}} & K^{*0} + K_1^0 & D^{*-} + D_1^- \\ K^{*-} + K_1^- & \bar{K}^{*0} + \bar{K}_1^0 & \omega_S + f_{1S} & D_S^{*-} + D_{S1}^- \\ \bar{D}^{*0} + \bar{D}_1^0 & D^{*+} + D_1^+ & D_S^{*+} + D_{S1}^+ & J/\psi + \chi_{C1} \end{pmatrix}^\mu, \quad (4.7)$$

$$R^\mu = V^\mu - A^\mu = \frac{1}{\sqrt{2}} \begin{pmatrix} \frac{\omega_N + \rho^0}{\sqrt{2}} - \frac{f_{1N} + a_1^0}{\sqrt{2}} & \rho^+ - a_1^+ & K^{*+} - K_1^+ & D^{*0} - D_1^0 \\ \rho^- - a_1^- & \frac{\omega_N - \rho^0}{\sqrt{2}} - \frac{f_{1N} - a_1^0}{\sqrt{2}} & K^{*0} - K_1^0 & D^{*-} - D_1^- \\ K^{*-} - K_1^- & \bar{K}^{*0} - \bar{K}_1^0 & \omega_S - f_{1S} & D_S^{*-} - D_{S1}^- \\ \bar{D}^{*0} - \bar{D}_1^0 & D^{*+} - D_1^+ & D_S^{*+} - D_{S1}^+ & J/\psi - \chi_{C1} \end{pmatrix}^\mu, \quad (4.8)$$

which transform under chiral transformations as $L^\mu \rightarrow U_L L^\mu U_L^\dagger$ and $R^\mu \rightarrow U_R R^\mu U_R^\dagger$.

The Lagrangian of the $N_f = 4$ model with global chiral invariance has an analogous form as the corresponding eLSM Lagrangian for $N_f = 3$ [110, 116], which is discussed in Sec. 2.6 and described in Eq.(2.145), with the additional mass term

$$-2 \text{Tr}[E\Phi^\dagger\Phi]$$

which has been added to account for the mass of the charm quark, as well as to obtain a better fit to the masses.

The terms involving the matrices H , E , and Δ break the dilatation symmetry explicitly, because they involve dimensionful coupling constants, and chiral symmetry due to nonzero current quark masses in the (pseudo)scalar and (axial-)vector sectors. They are of particular importance when the charmed mesons are considered, because the charm quark mass is large. In the light sectors, these terms are surely subleading when the quarks u and d are considered (unless one is studying some particular isospin-breaking processes), while the quark s is somewhat on the border between light and heavy. We describe these terms separately:

(i) The term $\text{Tr}[H(\Phi + \Phi^\dagger)]$ with

$$H = \frac{1}{2} \begin{pmatrix} h_U & 0 & 0 & 0 \\ 0 & h_D & 0 & 0 \\ 0 & 0 & \sqrt{2}h_S & 0 \\ 0 & 0 & 0 & \sqrt{2}h_C \end{pmatrix}, \quad (4.9)$$

describes the usual explicit symmetry breaking (tilting of the Mexican-hat potential). The constants h_i are proportional to the current quark masses, $h_i \propto m_i$. Here we work in the isospin limit, $h_U = h_D = h_N$. The pion mass, for instance, turns out to be $m_\pi^2 \propto m_u$, in agreement with the Gell-Mann–Oakes–Renner (GOR) relation [199]. The parameter h_C is one of the three new parameters entering the $N_f = 4$ version of the model when compared to the $N_f = 3$ case of Ref. [110].

(ii) The term $-2 \text{Tr}[E\Phi^\dagger\Phi]$ with

$$E = \begin{pmatrix} \varepsilon_U & 0 & 0 & 0 \\ 0 & \varepsilon_D & 0 & 0 \\ 0 & 0 & \varepsilon_S & 0 \\ 0 & 0 & 0 & \varepsilon_C \end{pmatrix}, \quad (4.10)$$

where $\varepsilon_i \propto m_i^2$, is the next-to-leading order correction in the current quark-mass expansion. In the isospin-symmetric limit $\varepsilon_U = \varepsilon_D = \varepsilon_N$ one can subtract from ε a matrix proportional to the identity in such a way that the parameter ε_N can be absorbed in the parameter m_0^2 . Thus, without loss of generality we can set $\varepsilon_N = 0$. Following Ref. [110], for the sake of simplicity we shall here also set $\varepsilon_S = 0$, while we keep ε_C nonzero. This is the second additional parameter with respect to Ref. [110].

(iii) The term $\text{Tr}[\Delta(L^{\mu 2} + R^{\mu 2})]$ with

$$\Delta = \begin{pmatrix} \delta_U & 0 & 0 & 0 \\ 0 & \delta_D & 0 & 0 \\ 0 & 0 & \delta_S & 0 \\ 0 & 0 & 0 & \delta_C \end{pmatrix}, \quad (4.11)$$

where $\delta_i \sim m_i^2$, describes the current quark-mass contribution to the masses of the (axial-)vector mesons. Also in this case, in the isospin-symmetric limit it is possible to set $\delta_U =$

$\delta_D = \delta_N = 0$ because an identity matrix can be absorbed in the term proportional to m_1^2 . The parameter δ_S is taken from Ref. [110]. The third new parameter with respect to Ref. [110] is δ_C . Note that in the present effective model the mass parameters δ_C and ε_C are not to be regarded as the second-order contribution in an expansion in powers of m_C . They simply represent the direct, and in this case dominant, contribution $\sim m_C^2$ of a charm quark to the masses of charmed (pseudo)scalar and (axial-)vector mesons.

Another important term in the Lagrangian (2.145) is $c(\det\Phi - \det\Phi^\dagger)^2$, which is responsible for the large η' mass. Care is needed, because a determinant changes when the number of flavours changes.

We conclude this section with a few remarks on how to extend the Lagrangian (2.145) in order to improve the description of hadron vacuum properties. First of all, note that the requirement of dilatation invariance restricts the interaction terms in the Lagrangian to have naive scaling dimension four: higher-order dilatation-invariant terms would have to contain inverse powers of G , and thus would be non-analytic in this field. In this sense, our Lagrangian is complete and cannot be systematically improved by the inclusion of higher-order interaction terms, such as in theories with nonlinearly realized chiral symmetry. However, one may add further terms that violate dilatation invariance (which is already broken by the mass terms $\sim H, \varepsilon, \Delta$, and the $U(1)_A$ -violating term $\sim c$) to improve the model.

Another possibility is to sacrifice chiral symmetry. For instance, since the explicit breaking of chiral symmetry by the charm quark mass is large (which is accounted for by the terms $\sim h_C, \varepsilon_C, \delta_C$), one could also consider chiral-symmetry violating interaction terms, e.g. replace

$$\lambda_2 \text{Tr}(\Phi^\dagger \Phi)^2 \longrightarrow \lambda_2 \text{Tr}(\Phi^\dagger \Phi)^2 + \delta\lambda_2 \text{Tr}(\mathbb{P}_C \Phi^\dagger \Phi)^2 \quad (4.12)$$

where $\mathbb{P}_C = \text{diag}\{0, 0, 0, 1\}$ is a projection operator onto the charmed states. A value $\delta\lambda_2 \neq 0$ explicitly breaks the symmetry of this interaction term from $U_R(4) \times U_L(4)$ to $U_R(3) \times U_L(3)$. One could modify the interaction terms proportional to $\lambda_1, c, g_1, g_2, h_1, h_2$, and h_3 in Eq. (2.145) in a similar manner.

4.3. Four-flavour linear sigma model implications

The Lagrangian (2.145) induces spontaneous symmetry breaking if $m_0^2 < 0$: as a consequence, the scalar-isoscalar fields G, σ_N, σ_S , and χ_{C0} develop nonzero vacuum expectation values. One has to perform the shifts as

$$G_0 \rightarrow G + G_0, \quad \sigma_N \rightarrow \sigma_N + \phi_N, \quad \sigma_S \rightarrow \sigma_S + \phi_S, \quad (4.13)$$

as obtained in Eq.(3.33) and in Refs. [116], and similarly for χ_{C0} ,

$$\chi_{C0} \rightarrow \chi_{C0} + \phi_C, \quad (4.14)$$

to implement this breaking. The quantity G_0 is proportional to the gluon condensate [78], while the quantities ϕ_N, ϕ_S , and ϕ_C correspond to the nonstrange, strange and charm quark-antiquark condensates.

The relations between the nonstrange, strange, and charm condensates with the pion decay constant f_π and the kaon decay constant f_K are presented in Eq.(3.34) and Eq.

(3.35), respectively, whereas the decay constants of the pseudoscalar D , D_S , and η_C mesons, f_D , f_{D_s} , and f_{η_C} are

$$f_D = \frac{\phi_N + \sqrt{2}\phi_C}{\sqrt{2}Z_D}, \quad (4.15)$$

$$f_{D_S} = \frac{\phi_S + \phi_C}{Z_{D_S}}, \quad (4.16)$$

$$f_{\eta_C} = \frac{2\phi_C}{Z_{\eta_C}}. \quad (4.17)$$

where the detailed calculation is presented in Appendices A.3 and A.4. The chiral condensates $\phi_{N,S,C}$ lead to the mixing between (axial)vector and (pseudo)scalar states in the Lagrangian (2.145), with the additional term $-2\text{Tr}[E\Phi^\dagger\Phi]$, with bilinear mixing terms involving the light mesons $\eta_N - f_{1N}$, $\vec{\pi} - \vec{a}_1$ [116], $\eta_S - f_{1S}$, $K_S - K^*$, and $K - K_1$, which are presented in Eq.(3.36). In addition, for charmed mesons similar mixing terms of the type $D - D_1$, $D_0^* - D^*$, $D_S - D_{S1}$, $D_{S0}^* - D_S^*$, and $\eta_C - \chi_{C1}$ are present:

$$\begin{aligned} & -g_1\phi_C\chi_{C1}^\mu\partial_\mu\eta_C - \frac{g_1}{\sqrt{2}}g_1\phi_S(D_{S1}^{\mu-}\partial_\mu D_S^+ + D_{S1}^{\mu+}\partial_\mu D_S^-) \\ & + i\frac{g_1}{\sqrt{2}}\phi_S(D_S^{*\mu-}\partial_\mu D_{S0}^{*+} - D_S^{*\mu+}\partial_\mu D_{S0}^{*-}) \\ & + i\frac{g_1}{2}\phi_N(D^{*\mu-}\partial_\mu D_0^{*+} - D^{*\mu+}\partial_\mu D_0^{*-} + D^{*\mu 0}\partial_\mu \bar{D}_0^{*0} - \bar{D}^{*\mu 0}\partial_\mu D_0^{*0}) \\ & - \frac{g_1}{2}\phi_N(D_1^{0\mu}\partial_\mu \bar{D}^0 + \bar{D}_1^{\mu 0}\partial_\mu D^0 + D_1^{\mu+}\partial_\mu D^- + D_1^{\mu-}\partial_\mu D^+) . \end{aligned} \quad (4.18)$$

Note that the Lagrangian (2.145) is real despite the imaginary $K_S - K^*$, $D_{S0}^* - D_{S1}^*$, $D_S - D_{S1}$ and $D_0^* - D^*$ coupling because these mixing terms are equal to their Hermitian conjugates.

The mixing terms (3.36) are removed by performing field transformations of the (axial-)vector states as presented in Eqs.(3.37-3.40). The mixing terms (4.18) are removed by performing field transformations of the (axial-)vector states as follows

$$\chi_{C1}^\mu \rightarrow \chi_{C1}^\mu + w_{\chi_{C1}} Z_{\eta_C} \partial^\mu \eta_C, \quad (4.19)$$

$$D_{S1}^{\mu\pm} \rightarrow D_{S1}^{\mu\pm} + w_{D_{S1}} Z_{D_S} \partial^\mu D_S^\pm, \quad (4.20)$$

$$D_S^{*\mu-} \rightarrow D_S^{*\mu-} + w_{D_S^*} Z_{D_{S0}^*} \partial^\mu D_{S0}^{*-}, \quad (4.21)$$

$$D_S^{*\mu+} \rightarrow D_S^{*\mu+} + w_{D_S^*}^* Z_{D_{S0}^*} \partial^\mu D_{S0}^{*+}, \quad (4.22)$$

$$D^{*\mu+} \rightarrow D^{*\mu+} + w_{D^*}^* Z_{D_0^*} \partial^\mu D_0^{*+}, \quad (4.23)$$

$$D^{*\mu-} \rightarrow D^{*\mu-} + w_{D^*} Z_{D_0^*} \partial^\mu D_0^{*-}, \quad (4.24)$$

$$\bar{D}^{*\mu 0} \rightarrow \bar{D}^{*\mu 0} + w_{D^{*0}}^* Z_{D_0^{*0}} \partial^\mu \bar{D}_0^{*0}, \quad (4.25)$$

$$D^{*\mu 0} \rightarrow D^{*\mu 0} + w_{D^{*0}} Z_{D_0^{*0}} \partial^\mu D_0^{*0}, \quad (4.26)$$

$$D_1^{\mu\pm,0,\bar{0}} \rightarrow D_1^{\mu\pm,0,\bar{0}} + w_{D_1} Z_D \partial^\mu D^{\pm,0,\bar{0}}. \quad (4.27)$$

These shifts produce additional kinetic terms for the open and hidden (pseudo)scalar charmed fields. Furthermore, one has to rescale the strange-nonstrange (pseudo)scalar fields

as described in Eqs.(3.41-3.41) as well as the open and hidden charmed pseudoscalar fields as

$$D^{\pm,0,\bar{0}} \rightarrow Z_D D^{\pm,0,\bar{0}}, \quad (4.28)$$

$$D_0^{*\pm} \rightarrow Z_{D_0^*} D_0^{*\pm}, \quad (4.29)$$

$$D_0^{*0,\bar{0}} \rightarrow Z_{D_0^{*0}} D_0^{*0,\bar{0}}, \quad (4.30)$$

$$D_{S_0}^{*\pm} \rightarrow Z_{D_{S_0}^*} D_{S_0}^{*\pm}, \quad (4.31)$$

$$\eta_C \rightarrow Z_{\eta_C} \eta_C. \quad (4.32)$$

Note that for the sake of simplicity we have grouped together the isodoublet states with the notation $D^{\pm,0,\bar{0}}$, and $D_0^{*0,\bar{0}}$, where $\bar{0}$ refers to \bar{D}^0 and \bar{D}_0^{*0} . The coefficients w_i and Z_i are determined in order to eliminate the mixing terms and to obtain the canonical normalization of the D , D_0^* , $D_{S_0}^*$, and η_C fields. This is described next.

The quantities $w_{f_{1N}}$, w_{a_1} , $w_{f_{1S}}$, w_{K^*} , w_{K_1} , are given in Eqs. (3.37-3.40), while $w_{\chi_{C1}}$, $w_{D_{S1}}$, $w_{D_S^*}$, w_{D^*} , $w_{D^{*0}}$, and w_{D_1} are calculated from the condition that the mixing terms (4.18) vanish once the shifts of the (axial-)vectors have been implemented:

$$\left[-g_1 \phi_N + \frac{1}{2}(2g_1^2 + h_1 + h_2 - h_3)w_{f_{1N}} \phi_N^2 + (m_1^2 + 2\delta_N)w_{f_{1N}} + \frac{h_1}{2}w_{f_{1N}} \phi_S^2 + \frac{h_1}{2}w_{f_{1N}} \phi_C^2 \right] \times (f_{1N}^\mu \partial_\mu \eta_N + \vec{a}_1^\mu \cdot \partial_\mu \vec{\pi}) = 0, \quad (4.33)$$

$$\left[-\sqrt{2}g_1 \phi_S + (2g_1^2 + \frac{h_1}{2} + h_2 - h_3)w_{f_{1S}} \phi_S^2 + (m_1^2 + 2\delta_S)w_{f_{1S}} + \frac{h_1}{2}w_{f_{1S}} \phi_N^2 + \frac{h_1}{2}w_{f_{1S}} \phi_C^2 \right] \times f_{1S}^\mu \partial_\mu \eta_S = 0, \quad (4.34)$$

$$\left[i\frac{g_1}{\sqrt{2}}\phi_S + \frac{h_3 - g_1^2}{\sqrt{2}}w_{K^*}\phi_N\phi_S + \frac{g_1^2 + h_1 + h_2}{2}w_{K^*}\phi_S^2 + (m_1^2 + \delta_N + \delta_S)w_{K^*} - i\frac{g_1}{2}\phi_N + \frac{1}{4}(g_1^2 + 2h_1 + h_2)w_{K^*}\phi_N^2 + \frac{h_1}{2}w_{K^*}\phi_C^2 \right] (\bar{K}^{*\mu 0} \partial_\mu K_S^0 + K^{*\mu -} \partial_\mu K_S^+) = 0, \quad (4.35)$$

$$\left[-i\frac{g_1}{\sqrt{2}}\phi_S + \frac{h_3 - g_1^2}{\sqrt{2}}w_{K^*}^*\phi_N\phi_S + \frac{g_1^2 + h_1 + h_2}{2}w_{K^*}^*\phi_S^2 + (m_1^2 + \delta_N + \delta_S)w_{K^*}^* + i\frac{g_1}{2}\phi_N + \frac{1}{4}(g_1^2 + 2h_1 + h_2)w_{K^*}^*\phi_N^2 + \frac{h_1}{2}w_{K^*}^*\phi_C^2 \right] (K^{*\mu 0} \partial_\mu \bar{K}_S^0 + K^{*\mu +} \partial_\mu K_S^-) = 0, \quad (4.36)$$

$$\left[-\frac{g_1}{\sqrt{2}}\phi_S + \frac{g_1^2 - h_3}{\sqrt{2}}w_{K_1}\phi_N\phi_S + \frac{g_1^2 + h_1 + h_2}{2}w_{K_1}\phi_S^2 + (m_1^2 + \delta_N + \delta_S)w_{K_1} - \frac{g_1}{2}\phi_N + \frac{1}{4}(g_1^2 + 2h_1 + h_2)w_{K_1}\phi_N^2 + \frac{h_1}{2}w_{K_1}\phi_C^2 \right] (K_1^{\mu 0} \partial_\mu \bar{K}^0 + K_1^{\mu +} \partial_\mu K^- + \bar{K}_1^{\mu 0} \partial_\mu K^0 + K_1^{\mu -} \partial_\mu K^+) = 0, \quad (4.37)$$

$$\left[-\frac{g_1}{\sqrt{2}}\phi_S + (g_1^2 - h_3)w_{D_{S1}}\phi_S\phi_C + \frac{g_1^2 + h_1 + h_2}{2}w_{D_{S1}}\phi_S^2 + (m_1^2 + \delta_S + \delta_C)w_{D_{S1}} - \frac{g_1}{\sqrt{2}}\phi_C + \frac{g_1^2 + h_1 + h_2}{2}w_{D_{S1}}\phi_C^2 + \frac{h_1}{2}w_{D_{S1}}\phi_N^2 \right] (D_{S1}^{\mu-} \partial_\mu D_S^+ + D_{S1}^{\mu+} \partial_\mu D_S^-) = 0, \quad (4.38)$$

$$\left[-i\frac{g_1}{\sqrt{2}}\phi_S + (h_3 - g_1^2)w_{D_{S1}^*}\phi_S\phi_C + \frac{g_1^2 + h_1 + h_2}{2}w_{D_{S1}^*}\phi_S^2 + (m_1^2 + \delta_S + \delta_C)w_{D_{S1}^*} + i\frac{g_1}{\sqrt{2}}\phi_C + \frac{g_1^2 + h_1 + h_2}{2}w_{D_{S1}^*}\phi_C^2 + \frac{h_1}{2}w_{D_{S1}^*}\phi_N^2 \right] D_{S1}^{*\mu+} \partial_\mu D_{S0}^{*-} = 0, \quad (4.39)$$

$$\left[i\frac{g_1}{\sqrt{2}}\phi_S + (h_3 - g_1^2)w_{D_{S1}^*}\phi_S\phi_C + \frac{g_1^2 + h_1 + h_2}{2}w_{D_{S1}^*}\phi_S^2 + (m_1^2 + \delta_S + \delta_C)w_{D_{S1}^*} - i\frac{g_1}{\sqrt{2}}\phi_C + \frac{g_1^2 + h_1 + h_2}{2}w_{D_{S1}^*}\phi_C^2 + \frac{h_1}{2}w_{D_{S1}^*}\phi_N^2 \right] D_{S1}^{*\mu-} \partial_\mu D_{S0}^{*+} = 0, \quad (4.40)$$

$$\left[-i\frac{g_1}{2}\phi_N + \frac{h_3 - g_1^2}{\sqrt{2}}w_{D^*}\phi_N\phi_C + \frac{1}{4}(g_1^2 + 2h_1 + h_2)w_{D^*}\phi_N^2 + (m_1^2 + \delta_N + \delta_C)w_{D^*} + i\frac{g_1}{\sqrt{2}}\phi_C + \frac{g_1^2 + h_1 + h_2}{2}w_{D^*}\phi_C^2 + \frac{h_1}{2}w_{D^*}\phi_S^2 \right] D^{*\mu+} \partial_\mu D_0^{*-} = 0, \quad (4.41)$$

$$\left[i\frac{g_1}{2}\phi_N + \frac{h_3 - g_1^2}{\sqrt{2}}w_{D^*}\phi_N\phi_C + \frac{1}{4}(g_1^2 + 2h_1 + h_2)w_{D^*}\phi_N^2 + (m_1^2 + \delta_N + \delta_C)w_{D^*} - i\frac{g_1}{\sqrt{2}}\phi_C + \frac{g_1^2 + h_1 + h_2}{2}w_{D^*}\phi_C^2 + \frac{h_1}{2}w_{D^*}\phi_S^2 \right] D^{*\mu-} \partial_\mu D_0^{*+} = 0, \quad (4.42)$$

$$\left[-i\frac{g_1}{2}\phi_N + \frac{h_3 - g_1^2}{\sqrt{2}}w_{D^{*0}}\phi_N\phi_C + \frac{1}{4}(g_1^2 + 2h_1 + h_2)w_{D^{*0}}\phi_N^2 + (m_1^2 + \delta_N + \delta_C)w_{D^{*0}} + i\frac{g_1}{\sqrt{2}}\phi_C + \frac{g_1^2 + h_1 + h_2}{2}w_{D^{*0}}\phi_C^2 + \frac{h_1}{2}w_{D^{*0}}\phi_S^2 \right] \bar{D}^{*\mu 0} \partial_\mu D_0^{*0} = 0, \quad (4.43)$$

$$\left[i\frac{g_1}{2}\phi_N + \frac{h_3 - g_1^2}{\sqrt{2}}w_{D^{*0}}\phi_N\phi_C + \frac{1}{4}(g_1^2 + 2h_1 + h_2)w_{D^{*0}}\phi_N^2 + (m_1^2 + \delta_N + \delta_C)w_{D^{*0}} - i\frac{g_1}{\sqrt{2}}\phi_C + \frac{g_1^2 + h_1 + h_2}{2}w_{D^{*0}}\phi_C^2 + \frac{h_1}{2}w_{D^{*0}}\phi_S^2 \right] D^{*\mu 0} \partial_\mu \bar{D}_0^{*0} = 0, \quad (4.44)$$

$$\left[-\frac{g_1}{2}\phi_N + \frac{g_1^2 - h_3}{\sqrt{2}}w_{D_1}\phi_N\phi_C + \frac{1}{4}(g_1^2 + 2h_1 + h_2)w_{D_1}\phi_N^2 + (m_1^2 + \delta_N + \delta_C)w_{D_1} - \frac{g_1}{\sqrt{2}}\phi_C + \frac{g_1^2 + h_1 + h_2}{2}w_{D_1}\phi_C^2 + \frac{h_1}{2}w_{D_1}\phi_S^2 \right] (D_1^{0\mu} \partial_\mu \bar{D}^0 + \bar{D}_1^{\mu 0} \partial_\mu D^0 + D_1^{\mu+} \partial_\mu D^- + D_1^{\mu-} \partial_\mu D^+) = 0, \quad (4.45)$$

$$\left[-\sqrt{2}g_1\phi_C + (2g_1^2 + \frac{h_1}{2} + h_2 - h_3)w_{\chi_{c1}}\phi_C^2 + (m_1^2 + 2\delta_C)w_{\chi_{c1}} + \frac{h_1}{2}w_{\chi_{c1}}\phi_N^2 + \frac{h_1}{2}w_{\chi_{c1}}\phi_S^2 \right] \times \chi_{C1}^\mu \partial_\mu \eta_C = 0, \quad (4.46)$$

Equations (4.33) - (4.37) correspond to the mixing terms (3.36) obtained in the case of strange-nonstrange investigation [116]. Equations (4.33)-(4.46) are fulfilled only if we define

$$w_{\chi_{c1}} = \frac{\sqrt{2}g_1\phi_C}{m_{\chi_{c1}}^2}, \quad (4.47)$$

$$w_{D_{S1}} = \frac{g_1(\phi_S + \phi_C)}{\sqrt{2}m_{D_{S1}}^2}, \quad (4.48)$$

$$w_{D_S^*} = \frac{ig_1(\phi_S - \phi_C)}{\sqrt{2}m_{D_S^*}^2}, \quad (4.49)$$

$$w_{D^*} = \frac{ig_1(\phi_N - \sqrt{2}\phi_C)}{2m_{D^*}^2}, \quad (4.50)$$

$$w_{D^{*0}} = \frac{ig_1(\phi_N - \sqrt{2}\phi_C)}{2m_{D^{*0}}^2}, \quad (4.51)$$

$$w_{D_1} = \frac{g_1(\phi_N + \sqrt{2}\phi_C)}{2m_{D_1}^2}. \quad (4.52)$$

The wave-function renormalization constants of the strange-nonstrange fields are given in Eqs.(3.49-3.52) [110, 116]. For the charmed fields, they read

$$Z_{\eta_C} = \frac{m_{\chi_{c1}}}{\sqrt{m_{\chi_{c1}}^2 - 2g_1^2\phi_C^2}}, \quad (4.53)$$

$$Z_{D_S} = \frac{\sqrt{2}m_{D_{S1}}}{\sqrt{2m_{D_{S1}}^2 - g_1^2(\phi_S + \phi_C)^2}}, \quad (4.54)$$

$$Z_{D_{S0}^*} = \frac{\sqrt{2}m_{D_S^*}}{\sqrt{2m_{D_S^*}^2 - g_1^2(\phi_S - \phi_C)^2}}, \quad (4.55)$$

$$Z_{D_0^*} = \frac{2m_{D^*}}{\sqrt{4m_{D^*}^2 - g_1^2(\phi_N - \sqrt{2}\phi_C)^2}}, \quad (4.56)$$

$$Z_{D_0^{*0}} = \frac{2m_{D^{*0}}}{\sqrt{4m_{D^{*0}}^2 - g_1^2(\phi_N - \sqrt{2}\phi_C)^2}}, \quad (4.57)$$

$$Z_D = \frac{2m_{D_1}}{\sqrt{4m_{D_1}^2 - g_1^2(\phi_N + \sqrt{2}\phi_C)^2}}. \quad (4.58)$$

It is obvious from Eqs.(3.49-3.52) and Eqs.(4.53)-(4.58) that all the renormalization coefficients will have values larger than one.

4.4. Tree-level masses

In this section we present the squared meson masses of all mesons in the model after having performed the transformation above as well as transforming the unphysical fields to the physical fields, e.g. for the pseudoscalar mesons η_N, η_S to η, η' , and the scalar mesons σ_N, σ_S to σ_1, σ_2 due to the mixing terms of these fields.

We obtain the tree-level masses of nonstrange-strange mesons in the eLSM:

(i) Pseudoscalar mesons:

$$m_\pi^2 = Z_\pi^2 \left[m_0^2 + \left(\lambda_1 + \frac{\lambda_2}{2} \right) \phi_N^2 + \lambda_1 \phi_S^2 + \lambda_1 \phi_C^2 \right], \quad (4.59)$$

$$m_K^2 = Z_K^2 \left[m_0^2 + \left(\lambda_1 + \frac{\lambda_2}{2} \right) \phi_N^2 - \frac{\lambda_2}{\sqrt{2}} \phi_N \phi_S + (\lambda_1 + \lambda_2) \phi_S^2 + \lambda_1 \phi_C^2 \right], \quad (4.60)$$

$$m_{\eta_N}^2 = Z_{\eta_N}^2 \left[m_0^2 + \left(\lambda_1 + \frac{\lambda_2}{2} \right) \phi_N^2 + \lambda_1 \phi_S^2 + \lambda_1 \phi_C^2 + \frac{c}{2} \phi_N^2 \phi_S^2 \phi_C^2 \right], \quad (4.61)$$

$$m_{\eta_S}^2 = Z_{\eta_S}^2 \left[m_0^2 + \lambda_1 \phi_N^2 + (\lambda_1 + \lambda_2) \phi_S^2 + \lambda_1 \phi_C^2 + \frac{c}{8} \phi_N^4 \phi_C^2 \right]. \quad (4.62)$$

(ii) Scalar mesons:

$$m_{a_0}^2 = m_0^2 + \left(\lambda_1 + \frac{3}{2} \lambda_2 \right) \phi_N^2 + \lambda_1 \phi_S^2 + \lambda_1 \phi_C^2, \quad (4.63)$$

$$m_{K_0^*}^2 = Z_{K_0^*}^2 \left[m_0^2 + \left(\lambda_1 + \frac{\lambda_2}{2} \right) \phi_N^2 + \frac{\lambda_2}{\sqrt{2}} \phi_N \phi_S + (\lambda_1 + \lambda_2) \phi_S^2 + \lambda_1 \phi_C^2 \right], \quad (4.64)$$

$$m_{\sigma_N}^2 = m_0^2 + 3 \left(\lambda_1 + \frac{\lambda_2}{2} \right) \phi_N^2 + \lambda_1 \phi_S^2 + \lambda_1 \phi_C^2, \quad (4.65)$$

$$m_{\sigma_S}^2 = m_0^2 + \lambda_1 \phi_N^2 + 3(\lambda_1 + \lambda_2) \phi_S^2 + \lambda_1 \phi_C^2. \quad (4.66)$$

(iii) Vector mesons:

$$m_\rho^2 = m_{\omega_N}^2, \quad (4.67)$$

$$m_{\omega_N}^2 = m_1^2 + 2\delta_N + \frac{\phi_N^2}{2} (h_1 + h_2 + h_3) + \frac{h_1}{2} \phi_S^2 + \frac{h_1}{2} \phi_C^2, \quad (4.68)$$

$$m_{\omega_S}^2 = m_1^2 + 2\delta_S + \frac{h_1}{2} \phi_N^2 + \left(\frac{h_1}{2} + h_2 + h_3 \right) \phi_S^2 + \frac{h_1}{2} \phi_C^2, \quad (4.69)$$

$$m_{K^*}^2 = m_1^2 + \delta_N + \delta_S + \frac{\phi_N^2}{2} \left(\frac{g_1^2}{2} + h_1 + \frac{h_2}{2} \right) + \frac{1}{\sqrt{2}} \phi_N \phi_S (h_3 - g_1^2) + \frac{\phi_S^2}{2} (g_1^2 + h_1 + h_2) + \frac{h_1}{2} \phi_C^2. \quad (4.70)$$

(iv) Axial-vector mesons:

$$m_{f_{1N}}^2 = m_{a_1}^2, \quad (4.71)$$

$$m_{a_1}^2 = m_1^2 + 2\delta_N + g_1^2 \phi_N^2 + \frac{\phi_N^2}{2}(h_1 + h_2 - h_3) + \frac{h_1}{2} \phi_S^2 + \frac{h_1}{2} \phi_C^2, \quad (4.72)$$

$$m_{f_{1S}}^2 = m_1^2 + 2\delta_S + \frac{h_1}{2} \phi_N^2 + \frac{h_1}{2} \phi_C^2 + 2g_1^2 \phi_S^2 + \phi_S^2 \left(\frac{h_1}{2} + h_2 - h_3 \right), \quad (4.73)$$

$$m_{K_1}^2 = m_1^2 + \delta_N + \delta_S + \frac{\phi_N^2}{2} \left(\frac{g_1^2}{2} + h_1 + \frac{h_2}{2} \right) + \frac{1}{\sqrt{2}} \phi_N \phi_S (g_1^2 - h_3) \\ + \frac{\phi_S^2}{2} (g_1^2 + h_1 + h_2) + \frac{h_1}{2} \phi_C^2. \quad (4.74)$$

Note that all the squared strange-nonstrange mesons masses have the same expressions obtained in the $N_f = 3$ case as shown in Sec. 3.3, but with an additional term related to the charm sector. However, this term will not affect the results because it is multiplied by a vanishing parameter as we will see below in the results section.

The masses of (open and hidden) charmed mesons are as follows:

(i) Pseudoscalar charmed mesons:

$$m_{\eta_C}^2 = Z_{\eta_C}^2 [m_0^2 + \lambda_1 \phi_N^2 + \lambda_1 \phi_S^2 + (\lambda_1 + \lambda_2) \phi_C^2 + \frac{c}{8} \phi_N^4 \phi_S^2 + 2\varepsilon_C], \quad (4.75)$$

$$m_{D^-}^2 = Z_D^2 \left[m_0^2 + \left(\lambda_1 + \frac{\lambda_2}{2} \right) \phi_N^2 + \lambda_1 \phi_S^2 - \frac{\lambda_2}{\sqrt{2}} \phi_N \phi_C + (\lambda_1 + \lambda_2) \phi_C^2 + \varepsilon_C \right], \quad (4.76)$$

$$m_{D_S^-}^2 = Z_{D_S}^2 [m_0^2 + \lambda_1 \phi_N^2 + (\lambda_1 + \lambda_2) \phi_S^2 - \lambda_2 \phi_C \phi_S + (\lambda_1 + \lambda_2) \phi_C^2 + \varepsilon_C]. \quad (4.77)$$

(ii) Scalar charmed mesons:

$$m_{\chi_D^0}^2 = m_0^2 + \lambda_1 \phi_N^2 + \lambda_1 \phi_S^2 + 3(\lambda_1 + \lambda_2) \phi_C^2 + 2\varepsilon_C, \quad (4.78)$$

$$m_{D_0^*}^2 = Z_{D_0^*}^2 \left[m_0^2 + \left(\lambda_1 + \frac{\lambda_2}{2} \right) \phi_N^2 + \lambda_1 \phi_S^2 + \frac{\lambda_2}{\sqrt{2}} \phi_C \phi_N + (\lambda_1 + \lambda_2) \phi_C^2 + \varepsilon_C \right], \quad (4.79)$$

$$m_{D_0^{*0}}^2 = Z_{D_0^{*0}}^2 \left[m_0^2 + \left(\lambda_1 + \frac{\lambda_2}{2} \right) \phi_N^2 + \lambda_1 \phi_S^2 + \frac{\lambda_2}{\sqrt{2}} \phi_N \phi_C + (\lambda_1 + \lambda_2) \phi_C^2 + \varepsilon_C \right], \quad (4.80)$$

$$m_{D_{S0}^*}^2 = Z_{D_{S0}^*}^2 [m_0^2 + \lambda_1 \phi_N^2 + (\lambda_1 + \lambda_2) \phi_S^2 + \lambda_2 \phi_C \phi_S + (\lambda_1 + \lambda_2) \phi_C^2 + \varepsilon_C]. \quad (4.81)$$

(iii) Vector charmed mesons:

$$m_{D^*}^2 = m_1^2 + \delta_N + \delta_C + \frac{\phi_N^2}{2} \left(\frac{g_1^2}{2} + h_1 + \frac{h_2}{2} \right) + \frac{1}{\sqrt{2}} \phi_N \phi_C (h_3 - g_1^2) \\ + \frac{\phi_C^2}{2} (g_1^2 + h_1 + h_2) + \frac{h_1}{2} \phi_S^2, \quad (4.82)$$

$$m_{J/\psi}^2 = m_1^2 + 2\delta_C + \frac{h_1}{2} \phi_N^2 + \frac{h_1}{2} \phi_S^2 + \left(\frac{h_1}{2} + h_2 + h_3 \right) \phi_C^2, \quad (4.83)$$

$$m_{D_S^*}^2 = m_1^2 + \delta_S + \delta_C + \frac{\phi_S^2}{2} (g_1^2 + h_1 + h_2) + \phi_S \phi_C (h_3 - g_1^2) \\ + \frac{\phi_C^2}{2} (g_1^2 + h_1 + h_2) + \frac{h_1}{2} \phi_N^2. \quad (4.84)$$

(iv) Axial-vector charmed mesons:

$$m_{D_{S1}}^2 = m_1^2 + \delta_S + \delta_C + \frac{\phi_S^2}{2}(g_1^2 + h_1 + h_2) + \phi_S \phi_C (g_1^2 - h_3) + \frac{\phi_C^2}{2}(g_1^2 + h_1 + h_2) + \frac{h_1}{2} \phi_N^2, \quad (4.85)$$

$$m_{D_1}^2 = m_1^2 + \delta_N + \delta_C + \frac{\phi_N^2}{2} \left(\frac{g_1^2}{2} + h_1 + \frac{h_2}{2} \right) + \frac{1}{\sqrt{2}} \phi_N \phi_C (g_1^2 - h_3) + \frac{\phi_C^2}{2}(g_1^2 + h_1 + h_2) + \frac{h_1}{2} \phi_S^2, \quad (4.86)$$

$$m_{\chi_{C1}}^2 = m_1^2 + 2\delta_C + \frac{h_1}{2} \phi_N^2 + \frac{h_1}{2} \phi_S^2 + 2g_1^2 \phi_C^2 + \phi_C^2 \left(\frac{h_1}{2} + h_2 - h_3 \right). \quad (4.87)$$

Further interesting quantities are also the following mass differences, in which the explicit dependence on the parameters ε_C and δ_C cancels:

$$m_{D_1}^2 - m_{D^*}^2 = \sqrt{2}(g_1^2 - h_3)\phi_N\phi_C, \quad (4.88)$$

$$m_{\chi_{C1}}^2 - m_{J/\psi}^2 = 2(g_1^2 - h_3)\phi_C^2, \quad (4.89)$$

$$m_{D_{S1}}^2 - m_{D_S^*}^2 = 2(g_1^2 - h_3)\phi_S\phi_C. \quad (4.90)$$

4.4.1. η and η' Masses

From the Lagrangian (2.145), we obtain mixing between the pure non-strange and strange fields $\eta_N \equiv (\bar{u}u - \bar{d}d)/\sqrt{2}$ and $\eta_S \equiv \bar{s}s$ as

$$\mathcal{L}_{\eta_N\eta_S} = -\frac{c}{4}Z_{\eta_S}Z_\pi\phi_N^3\phi_S\phi_C^2\eta_N\eta_S. \quad (4.91)$$

which has the same formula for $N_f = 3$ case, as seen in Ref. [116], but it includes charm quark-antiquark condensate (ϕ_C).

The generate part of the η_N - η_S Lagrangian [116] has the form

$$\mathcal{L}_{\eta_N\eta_S, \text{full}} = \frac{1}{2}(\partial_\mu\eta_N)^2 + \frac{1}{2}(\partial_\mu\eta_S)^2 - \frac{1}{2}m_{\eta_N}^2\eta_N^2 - \frac{1}{2}m_{\eta_S}^2\eta_S^2 + \Upsilon_\eta\eta_N\eta_S, \quad (4.92)$$

where Υ_η defines the mixing term of the pure states η_N and η_S .

By comparing Eqs. (4.91) and (4.92) we obtain the mixing term Υ_η as follows

$$\Upsilon_\eta = -\frac{c}{4}Z_{\eta_S}Z_\pi\phi_N^3\phi_S\phi_C^2, \quad (4.93)$$

We can determine the physical states η and η' as mixtures of the pure non-strange and strange fields η_N and η_S , see the details in Ref. [116], as

$$\begin{pmatrix} \eta \\ \eta' \end{pmatrix} = \begin{pmatrix} \cos\varphi_\eta & \sin\varphi_\eta \\ -\sin\varphi_\eta & \cos\varphi_\eta \end{pmatrix} \begin{pmatrix} \eta_N \\ \eta_S \end{pmatrix}, \quad (4.94)$$

which gives

$$\eta = \cos\varphi_\eta\eta_N + \sin\varphi_\eta\eta_S, \quad (4.95)$$

$$\eta' = -\sin\varphi_\eta\eta_N + \cos\varphi_\eta\eta_S, \quad (4.96)$$

where $\varphi_\eta = 44.6$ is the $\eta - \eta'$ mixing angle [110].

By overturning Eqs. (4.95) and (4.96), one obtain the pure states η_N and η_S as

$$\eta_N = \cos \varphi_\eta \eta - \sin \varphi_\eta \eta' , \quad (4.97)$$

$$\eta_S = \sin \varphi_\eta \eta + \cos \varphi_\eta \eta' , \quad (4.98)$$

By substituting η_N and η_S by η and η' in the Lagrangian Eq. (4.92), we get [116]

$$\begin{aligned} \mathcal{L}_{\eta\eta'} &= \frac{1}{2}[(\partial_\mu \eta)^2 \cos^2 \varphi_\eta + (\partial_\mu \eta')^2 \sin^2 \varphi_\eta - \sin(2\varphi_\eta) \partial_\mu \eta \partial^\mu \eta'] \\ &+ \frac{1}{2}[(\partial_\mu \eta)^2 \sin^2 \varphi_\eta + (\partial_\mu \eta')^2 \cos^2 \varphi_\eta + \sin(2\varphi_\eta) \partial_\mu \eta \partial^\mu \eta'] \\ &- \frac{1}{2} m_{\eta_N}^2 [\eta^2 \cos^2 \varphi_\eta + (\eta')^2 \sin^2 \varphi_\eta - \sin(2\varphi_\eta) \eta \eta'] \\ &- \frac{1}{2} m_{\eta_S}^2 [\eta^2 \sin^2 \varphi_\eta + (\eta')^2 \cos^2 \varphi_\eta + \sin(2\varphi_\eta) \eta \eta'] \\ &+ \Upsilon_\eta \{[\eta^2 - (\eta')^2] \sin \varphi_\eta \cos \varphi_\eta + \cos(2\varphi_\eta) \eta \eta'\} \\ &= \frac{1}{2} (\partial_\mu \eta)^2 + \frac{1}{2} (\partial_\mu \eta')^2 - \frac{1}{2} [m_{\eta_N}^2 \cos^2 \varphi_\eta + m_{\eta_S}^2 \sin^2 \varphi_\eta - \Upsilon_\eta \sin(2\varphi_\eta)] \eta^2 \\ &- \frac{1}{2} [m_{\eta_N}^2 \sin^2 \varphi_\eta + m_{\eta_S}^2 \cos^2 \varphi_\eta + \Upsilon_\eta \sin(2\varphi_\eta)] (\eta')^2 \\ &- \frac{1}{2} [(m_{\eta_S}^2 - m_{\eta_N}^2) \sin(2\varphi_\eta) - 2\Upsilon_\eta \cos(2\varphi_\eta)] \eta \eta' , \end{aligned} \quad (4.99)$$

which gives the masses of the physical states η and η' , m_η and $m_{\eta'}$, in terms of the pure non-strange and strange, η_N and η_S , mass terms:

$$m_\eta^2 = m_{\eta_N}^2 \cos^2 \varphi_\eta + m_{\eta_S}^2 \sin^2 \varphi_\eta - \Upsilon_\eta \sin(2\varphi_\eta), \quad (4.100)$$

$$m_{\eta'}^2 = m_{\eta_N}^2 \sin^2 \varphi_\eta + m_{\eta_S}^2 \cos^2 \varphi_\eta + \Upsilon_\eta \sin(2\varphi_\eta) . \quad (4.101)$$

where the mass terms m_{η_N} and m_{η_S} are known from Eqs. (4.61) and (4.62).

4.4.2. Scalar-Isosinglet Masses

There is a mixing between the pure states $\sigma_N \equiv (\bar{u}u + \bar{d}d)/\sqrt{2}$ and $\sigma_S \equiv \bar{s}s$ in the Lagrangian (2.145) with the mixing term given by

$$\mathcal{L}_{\sigma_N \sigma_S} = -2\lambda_1 \phi_N \phi_S \sigma_N \sigma_S . \quad (4.102)$$

Notice that the mixing term (4.102) of σ_N and σ_S does not depend on the charm quark-antiquark condensate ϕ_C . So it is the same mixing term in the case of $N_f = 3$ [116].

The generate part of the σ_N - σ_S Lagrangian has the form

$$\mathcal{L}_{\sigma_N \sigma_S, \text{full}} = \frac{1}{2} (\partial_\mu \sigma_N)^2 + \frac{1}{2} (\partial_\mu \sigma_S)^2 - \frac{1}{2} m_{\sigma_N}^2 \sigma_N^2 - \frac{1}{2} m_{\sigma_S}^2 \sigma_S^2 + \Upsilon_\sigma \sigma_N \sigma_S , \quad (4.103)$$

where Υ_σ is the mixing term of the σ_N and σ_S fields,

$$\Upsilon_\sigma = -2\lambda_1\phi_N\phi_S . \quad (4.104)$$

The mixing between the states σ_N and σ_S yields σ_1 and σ_2 fields [see Ref. [116]]:

$$\begin{pmatrix} \sigma_1 \\ \sigma_2 \end{pmatrix} = \begin{pmatrix} \cos \varphi_\sigma & \sin \varphi_\sigma \\ -\sin \varphi_\sigma & \cos \varphi_\sigma \end{pmatrix} \begin{pmatrix} \sigma_N \\ \sigma_S \end{pmatrix} . \quad (4.105)$$

which can be written as

$$\sigma_1 = \cos \varphi_\sigma \sigma_N + \sin \varphi_\sigma \sigma_S , \quad (4.106)$$

$$\sigma_2 = -\sin \varphi_\sigma \sigma_N + \cos \varphi_\sigma \sigma_S , \quad (4.107)$$

where φ_σ is the σ_N - σ_S mixing angle.

By overturning Eqs. (4.106) and (4.107), one obtain the pure states σ_N and σ_S as

$$\sigma_N = \cos \varphi_\sigma \sigma_1 - \sin \varphi_\sigma \sigma_2 , \quad (4.108)$$

$$\sigma_S = \sin \varphi_\sigma \sigma_1 + \cos \varphi_\sigma \sigma_2 , \quad (4.109)$$

Substituting from Eqs. (4.108) and (4.109) into Eq. (4.103), one obtain the $\sigma_1 - \sigma_2$ Lagrangian as follows:

$$\begin{aligned} \mathcal{L}_{\sigma_1\sigma_2} &= \frac{1}{2}[(\partial_\mu\sigma_1)^2 \cos^2 \varphi_\sigma + (\partial_\mu\sigma_2)^2 \sin^2 \varphi_\sigma - \sin(2\varphi_\sigma)\partial_\mu\sigma_1\partial^\mu\sigma_2] \\ &+ \frac{1}{2}[(\partial_\mu\sigma_1)^2 \sin^2 \varphi_\sigma + (\partial_\mu\sigma_2)^2 \cos^2 \varphi_\sigma + \sin(2\varphi_\sigma)\partial_\mu\sigma_1\partial^\mu\sigma_2] \\ &- \frac{1}{2}m_{\sigma_N}^2[\sigma_1^2 \cos^2 \varphi_\sigma + (\sigma_2)^2 \sin^2 \varphi_\sigma - \sin(2\varphi_\sigma)\sigma_1\sigma_2] \\ &- \frac{1}{2}m_{\sigma_S}^2[\sigma_1^2 \sin^2 \varphi_\sigma + (\sigma_2)^2 \cos^2 \varphi_\sigma + \sin(2\varphi_\sigma)\sigma_1\sigma_2] \\ &+ \Upsilon_\sigma\{[\sigma_1^2 - (\sigma_2)^2] \sin \varphi_\sigma \cos \varphi_\sigma + \cos(2\varphi_\sigma)\sigma_1\sigma_2\} \\ &= \frac{1}{2}(\partial_\mu\sigma)^2 + \frac{1}{2}(\partial_\mu\sigma')^2 - \frac{1}{2}[m_{\sigma_N}^2 \cos^2 \varphi_\sigma + m_{\sigma_S}^2 \sin^2 \varphi_\sigma - \Upsilon_\sigma \sin(2\varphi_\sigma)]\sigma_1^2 \\ &- \frac{1}{2}[m_{\sigma_N}^2 \sin^2 \varphi_\sigma + m_{\sigma_S}^2 \cos^2 \varphi_\sigma + \Upsilon_\sigma \sin(2\varphi_\sigma)](\sigma_2)^2 \\ &- \frac{1}{2}[(m_{\sigma_S}^2 - m_{\sigma_N}^2) \sin(2\varphi_\sigma) - 2\Upsilon_\sigma \cos(2\varphi_\sigma)]\sigma_1\sigma_2 , \end{aligned} \quad (4.110)$$

We then obtain the mass terms of σ_1 and σ_2 fields as

$$m_{\sigma_1}^2 = m_{\sigma_N}^2 \cos^2 \varphi_\sigma + m_{\sigma_S}^2 \sin^2 \varphi_\sigma - \Upsilon_\sigma \sin(2\varphi_\sigma), \quad (4.111)$$

$$m_{\sigma_2}^2 = m_{\sigma_N}^2 \sin^2 \varphi_\sigma + m_{\sigma_S}^2 \cos^2 \varphi_\sigma + \Upsilon_\sigma \sin(2\varphi_\sigma), \quad (4.112)$$

where m_{σ_N} and m_{σ_S} known from Eq. (4.65) and Eq. (4.66), respectively. While the mixing term Υ_σ is

$$\Upsilon_\sigma = \frac{1}{2}(m_{\sigma_S}^2 - m_{\sigma_N}^2) \tan(2\varphi_\sigma) . \quad (4.113)$$

The resonances σ_1 and σ_2 will be assigned to the physical states $f_0(1370)$ and $f_0(1710)$ [116], respectively.

One can determine the $\sigma_1 - \sigma_2$ mixing angle φ_σ from Eqs. (4.104) and (4.113) [116] as

$$\begin{aligned}\varphi_\sigma &= -\frac{1}{2} \arctan \left(\frac{4\lambda_1 \phi_N \phi_S}{m_{\sigma_S}^2 - m_{\sigma_N}^2} \right) \\ &= \frac{1}{2} \arctan \left[\frac{8\lambda_1 \phi_N \phi_S}{(4\lambda_1 + 3\lambda_2)\phi_N^2 - (4\lambda_1 + 6\lambda_2)\phi_S^2} \right],\end{aligned}\quad (4.114)$$

In the large- N_c limit, one sets $\lambda_1 = 0$, as shown in Ref. [116] for the case $N_f = 3$. Therefore we get from Eq.(4.114) that the mixing angle φ_σ between $\sigma_1 - \sigma_2$ is zero. Naturally the mixing angle between $\sigma_1 - \sigma_2$ is very small, which is in agreement with our result. Then φ_σ does not affect the results in this framework.

4.5. The Model Parameters

The Lagrangian (2.145) contains the following 15 free parameters: m_0^2 , λ_1 , λ_2 , m_1 , g_1 , c_1 , h_1 , h_2 , h_3 , δ_S , δ_C , ε_C , h_N , h_S , and h_C . For technical reasons, instead of the parameters h_N , h_S , and h_C entering Eq. (4.9), it is easier to use the condensates ϕ_N , ϕ_S , ϕ_C . This is obviously equivalent, because ϕ_N , ϕ_S , and ϕ_C form linearly independent combinations of the parameters.

We can obtain the relation between c and its counterpart in the three-flavour case $c_{N_f=3}$ of Ref. [110] as follows:

The axial-anomaly term as described in the Lagrangian (2.145) in the case of $N_f = 3$ can be written as

$$\mathcal{L}_{ca3} = c_{N_f=3} (\det \Phi_{N_f=3} - \det \Phi_{N_f=3}^\dagger)^2, \quad (4.115)$$

and in the case of $N_f = 4$

$$\mathcal{L}_{ca4} = c (\det \Phi - \det \Phi^\dagger)^2, \quad (4.116)$$

The (pseudo)scalar multiplet matrix, Φ , in the case of $N_f = 4$, which includes the 3×3 (pseudo)scalar multiplet matrix, $\Phi_{N_f=3}$, can be written as

$$\Phi = \begin{pmatrix} & & & 0 \\ & \Phi_{N_f=3} & & 0 \\ & & & 0 \\ 0 & 0 & 0 & \frac{\phi_C}{\sqrt{2}} \end{pmatrix}. \quad (4.117)$$

By using Eq.(4.117) to calculate the determinant of Φ , we obtain

$$\det \Phi = \frac{\phi_C}{\sqrt{2}} \det \Phi_{N_f=3}, \quad (4.118)$$

The axial-anomaly term in the case of $N_f = 3$, Eq. (4.115), can be transformed to the case of $N_f = 4$ by using Eq.(4.117) as follows:

$$\mathcal{L}_{ca4} = \frac{2c_{N_f=3}}{\phi_C^2} (\det\Phi - \det\Phi^\dagger)^2, \quad (4.119)$$

Comparing between Eq.(4.116) and Eq.(4.119), we get

$$c = \frac{2c_{N_f=3}}{\phi_C^2}. \quad (4.120)$$

Thus, the parameter c can be determined once the condensate ϕ_C is obtained.

In the large- N_c limit, one sets $h_1 = \lambda_1 = 0$. Then, as shown in Ref. [110] for the case $N_f = 3$, ten parameters can be determined by a fit to masses and decay widths of mesons below 1.5 GeV as shown in Table 1. In the following we use these values for our numerical calculations. As a consequence, the masses and the decay widths of the nonstrange-strange mesons are – by construction – identical to the results of Ref. [110] (see Table 2 and Fig. 1 in that ref.). Note also that, in virtue of Eq. (4.120), the parameter combination $\phi_C^2 c/2$ is determined by the fit of Ref. [110].

Parameter	Value	Parameter	Value
m_1^2	$0.413 \times 10^6 \text{ MeV}^2$	m_0^2	$-0.918 \times 10^6 \text{ MeV}^2$
$\phi_C^2 c/2$	$450 \cdot 10^{-6} \text{ MeV}^{-2}$	δ_S	$0.151 \times 10^6 \text{ MeV}^2$
g_1	5.84	h_1	0
h_2	9.88	h_3	3.87
ϕ_N	164.6 MeV	ϕ_S	126.2 MeV
λ_1	0	λ_2	68.3

Table 4.1.: Values of the parameters (from Ref. [110])

For the purposes of the present work, we are left with three unknown parameters: $\phi_C, \varepsilon_C, \delta_C$. We determine these by performing a fit to twelve experimental (hidden and open) charmed meson masses listed by the PDG [51], minimizing

$$\chi^2 \equiv \sum_i^{12} \left(\frac{M_i^{th} - M_i^{exp}}{\xi M_i^{exp}} \right)^2, \quad (4.121)$$

where ξ is a constant. We do not use the experimental errors for the masses, because we do not expect to reach the same precision with our effective model, which (besides other effects) already neglects isospin breaking. In Ref. [110], we required a minimum error of 5% for experimental quantities entering our fit, and obtained a reduced χ^2 of about 1.23. Here, we slightly change our fit strategy: we choose the parameter ξ such that the reduced χ^2 takes the value $\chi^2/(12 - 3) = 1$, which yields $\xi = 0.07$. This implies that we enlarge the experimental errors to 7% of the respective masses.

The parameters (together with their theoretical errors) are:

Parameter	Value
ϕ_C	$176 \pm 28 \text{ MeV}$
δ_C	$(3.91 \pm 0.36) \times 10^6 \text{ MeV}^2$
ε_C	$(2.23 \pm 0.71) \times 10^6 \text{ MeV}$
c	$(2.91 \pm 0.94) \times 10^{-8} \text{ MeV}^{-4}$

Table 4.2.: Values of the unknown parameters.

4.6. Results

In this section we present the w_i and the wave-function renormalization constants Z_i values which are important parameters for the determination of the masses and the decay widths of mesons. We present also the masses of light mesons as well as (open and hidden) charmed mesons.

4.6.1. The w_i and the wave-function renormalization constants Z_i

All 15 parameter have been determined as shown in the previous section. Then, the parameters w_i can be determined from Eqs. (3.46 - 3.49) and (4.45 - 4.50) and the wave-function renormalization constants from Eqs. (3.49-3.52) as summarized in Table 4.3:

parameter	value	parameter	value
w_{a1}	0.00068384	$w_{f_{1N}}$	0.00068384
$w_{f_{1S}}$	0.0005538	w_{K1}	0.000609921
w_{K^*}	-0.0000523i	$w_{D_{S1}}$	0.000203
$w_{D^*} = w_{D^{*0}}$	-0.0000523i	$w_{D_0^*}$	-0.0000423i
w_{D_1}	0.00020	$w_{\chi_{C1}}$	0.000138
$Z_\pi = Z_{\eta_N}$	1.70927	Z_{η_S}	1.53854
Z_K	1.60406	Z_{K_S}	1.00105
Z_{η_C}	1.11892	Z_D	1.15256
Z_{D_S}	1.15716	$Z_{D_{S0}^*}$	1.00437
$Z_{D_0^*} = Z_{D_0^{*0}}$	1.00649	$Z_{D_0^{*0}}$	1.00649

Table 4.3.: w_i and the wave-function renormalization constants Z_i values.

As seen in Table 4.3, all wave-function renormalization constants have values larger than one. The parameter w_{D^*} is equal to $w_{D^{*0}}$ and the parameter $w_{D_0^*}$ is equal to $w_{D_0^{*0}}$ for isospin symmetry reasons.

4.6.2. Masses of light mesons

The results for the light meson masses are reported in Table 4.4. By construction, one finds the same values as in Refs. [110, 116].

observable	J^P	theoretical value [MeV]	experimental value [MeV]
m_π	0^-	141	139.57018 ± 0.00035
m_η	0^-	509	547.853 ± 0.024
$m_{\eta'}$	0^-	962	957.78 ± 0.06
m_K	0^-	485	493.677 ± 0.016
m_{a_0}	0^+	1363	1474 ± 19
m_{σ_1}	0^+	1362	$(1200-1500)-i(150-250)$
m_{σ_2}	0^+	1531	1720 ± 60
$m_{K_0^*}$	0^+	1449	1425 ± 50
m_{ω_N}	1^-	783	782.65 ± 0.12
m_{ω_S}	1^-	975	1019.46 ± 0.020
m_ρ	1^-	783	775.5 ± 38.8
m_{K^*}	1^-	885	891.66 ± 0.26
$m_{f_{1N}}$	1^+	1186	1281.8 ± 0.6
m_{a_1}	1^+	1185	1230 ± 40
$m_{f_{1S}}$	1^+	1372	1426.4 ± 0.9
m_{K_1}	1^+	1281	1272 ± 7

Table 4.4.: Light meson masses.

Note that the values of the light mesons are the same as in the case of $N_f = 3$, shown in Table 3.2, as they are not affected by the charm sector because $\lambda_1 = h_1 = 0$.

4.6.3. Masses of charmed mesons

In Table 4.5 we present the results of our fit for the masses of the open and hidden charmed mesons, by comparing the theoretically computed with the experimentally measured masses [see also Ref. [118] for preliminary results]. For the nonstrange-charmed states we use the masses of the neutral members of the multiplet in the fit, because the corresponding resonances have been clearly identified and the masses have been well determined for all quantum numbers. In view of the fact that the employed model is built as a low-energy chiral model and that only three parameters enter the fit, the masses are quite well described. The mismatch grows for increasing masses because Eq. (4.121) imposes, by construction, a better precision for low masses. For comparison, in the right column of Table 4.5 we also show the value $0.07M_i^{exp}$ which represents the ‘artificial experimental error’ that we have used in our fit.

Resonance	Quark content	J^P	Our Value [MeV]	Experimental Value [MeV]	7% of the exp. value [MeV]
D^0	$u\bar{c}, \bar{u}c$	0^-	1981 ± 73	1864.86 ± 0.13	130
D_S^\pm	$s\bar{c}, \bar{s}c$	0^-	2004 ± 74	1968.50 ± 0.32	138
$\eta_c(1S)$	$c\bar{c}$	0^-	2673 ± 118	2983.7 ± 0.7	209
$D_0^*(2400)^0$	$u\bar{c}, \bar{u}c$	0^+	2414 ± 77	2318 ± 29	162
$D_{S0}^*(2317)^\pm$	$s\bar{c}, \bar{s}c$	0^+	2467 ± 76	2317.8 ± 0.6	162
$\chi_{c0}(1P)$	$c\bar{c}$	0^+	3144 ± 128	3414.75 ± 0.31	239
$D^*(2007)^0$	$u\bar{c}, \bar{u}c$	1^-	2168 ± 70	2006.99 ± 0.15	140
D_s^*	$s\bar{c}, \bar{s}c$	1^-	2203 ± 69	2112.3 ± 0.5	148
$J/\psi(1S)$	$c\bar{c}$	1^-	2947 ± 109	3096.916 ± 0.011	217
$D_1(2420)^0$	$u\bar{c}, \bar{u}c$	1^+	2429 ± 63	2421.4 ± 0.6	169
$D_{S1}(2536)^\pm$	$s\bar{c}, \bar{s}c$	1^+	2480 ± 63	2535.12 ± 0.13	177
$\chi_{c1}(1P)$	$c\bar{c}$	1^+	3239 ± 101	3510.66 ± 0.07	246

Table 4.5.: Masses of charmed mesons used in the fit.

The following remarks about our results are in order:

(i) Remembering that our model is a low-energy effective approach to the strong interaction, it is quite surprising that the masses of the open charmed states are in good quantitative agreement (within the theoretical error) with experiment data. In particular, when taking into account the 7% range (right column of Table 2), almost all the results are within 1σ or only slightly above it. Clearly, our results cannot compete with the precision of other approaches, but show that a connection to low-energy models is possible.

(ii) With the exception of J/ψ , the masses of the charmonia states are somewhat underestimated as is particularly visible for the resonance $\eta_c(1S)$. On the one hand, this is due to the way the fit has been performed; on the other hand, it points to the fact that unique values of the parameters h_C , δ_C , and ε_C are not sufficient for a precise description of both open and hidden charmed states over the whole energy range. One way to improve the fit of the charmonium masses would be to include non-zero values for λ_1, h_1 . Another way is explicitly breaking the chiral symmetry as discussed at the end of Sec. 4.2.

However, since the description of open charm states is already reasonable, we only need to consider the charmonium states. For the (pseudo)scalar charmonia, we would thus modify the second term in Eq. (4.12) by introducing another projection operator under the trace, $\text{Tr}(\mathbb{P}_C \Phi^\dagger \Phi)^2 \rightarrow \text{Tr}(\mathbb{P}_C \Phi^\dagger \mathbb{P}_C \Phi)^2$. A similar consideration could be done for the (axial-)vector charmonia.

(iii) The experimental value for the mass of the charged scalar state $D_0^*(2400)^\pm$, which is $(2403 \pm 14 \pm 35)$ MeV, is in fair agreement with our theoretical result, although the existence of this resonance has not yet been unambiguously established.

(iv) The theoretically computed mass of the strange-charmed scalar state $D_{S0}^{*\pm}$ turns out to be larger than that of the charmed state $D_0^*(2400)^0$. In this respect, the experimental result is puzzling because the mass of $D_{S0}^*(2317)^\pm$ is smaller than that of $D_0^*(2400)^0$. A possibility is that the resonance $D_{S0}^*(2317)$ is not a quarkonium, or that the current mass of the quarkonium field is diminished by quantum fluctuations [see e.g. Ref. [200, 201, 202].]

(v) The theoretical mass of the axial-vector strange-charmed state D_{S1} reads 2480 MeV, which lies in between the two physical states $D_{S1}(2460)^\pm$ and $D_{S1}(2536)^\pm$. We shall re-analyze the scalar and the axial-vector strange-charmed states in light of the results for the decay widths, see chapter 7.

The theoretical results for the squared charmed vector and axial-vector mass differences, in which the explicit dependence on the parameters ε_C and δ_C cancels and which were presented in Eqs.(4.88-4.90) are

mass difference	theoretical value MeV ²	experimental value MeV ²
$m_{D_1}^2 - m_{D^*}^2$	$(1.2 \pm 0.6) \times 10^6$	1.82×10^6
$m_{\chi_{C1}}^2 - m_{J/\psi}^2$	$(1.8 \pm 1.3) \times 10^6$	2.73×10^6
$m_{D_{S1}}^2 - m_{D_S^*}^2$	$(1.2 \pm 0.6) \times 10^6$	1.97×10^6

Table 4.6.: Mass differences.

Here we compare them also with the experimental results (the experimental error is omitted because, being of the order of 10^3 MeV², they are very small w.r.t. the theoretical ones). The agreement is fairly good, which shows that our determination of the charm condensate ϕ_C is compatible with the experiment, although it still has a large uncertainty. Note that a similar determination of ϕ_C via the weak decay constants of charmed mesons determined via the PCAC relations has been presented in Ref. [203]. Their result is $\phi_C/\phi_N \simeq 1.35$, which is compatible to our ratio of about 1.07 ± 0.20 . Previously, Ref. [204] determined $\phi_C/\phi_N \simeq 1.08$ in the framework of the NJL model, which is in perfect agreement with our result.

From a theoretical point of view, it is instructive to study the behavior of the condensate ϕ_C as function of the heavy quark mass m_C . To this end, we recall that the equation determining ϕ_C is of the third-order type and reads (for $\lambda_1 = 0$)

$$h_{0,C} = (m_0^2 + 2\varepsilon_C)\phi_C + \lambda_2\phi_C^3. \quad (4.122)$$

By imposing the scaling behaviors $h_{0,C} = m_C \tilde{h}_{0,C}$ and $\varepsilon_C = \tilde{\varepsilon}_C m_C^2$, the solution for large values of m_C reads $\phi_C \simeq h_{0,C}/2\varepsilon_C \propto 1/m_C$, which shows that the mass differences of Eqs.

(4.88-4.90) vanish in the heavy-quark limit. However, the fact that the value of the charm condensate turns out to be quite large implies that the charm quark is not yet that close to the heavy-quark limit. To show this aspect, we plot in Fig. 4.1 the condensate ϕ_C as function of m_c by keeping all other parameters fixed. Obviously, this is a simplifying assumption, but the main point of this study is a qualitative demonstration that the chiral condensate of charm-anticharm quarks is non-negligible.

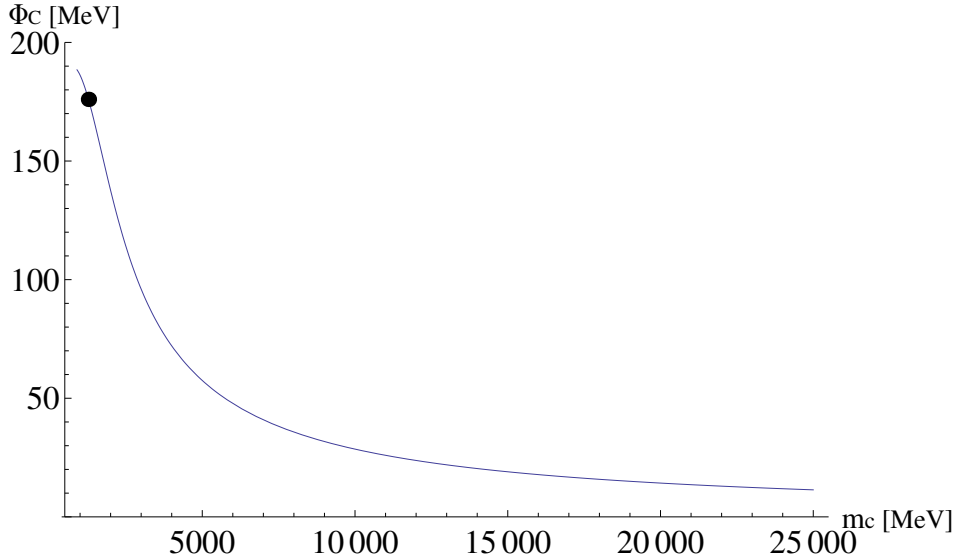


Figure 4.1.: Condensate ϕ_C as function of the quark mass m_C . The dot corresponds to the physical value $m_C = 1.275$ GeV [51].

Note that, in contrast to the demands of heavy-quark spin symmetry, our chiral approach does not necessarily imply an equal mass of the vector and pseudoscalar states and of scalar and axial-vector states. Namely, for a very large heavy quark mass one has $m_D^2 \simeq \varepsilon_C$ and $m_{D^*}^2 \simeq \delta_C$. Thus, in order to obtain a degeneracy of these mesons, as predicted by heavy-quark symmetry [50, 168, 169, 170, 171, 172], we should additionally impose that $\varepsilon_C = \delta_C$. Numerically, the values have indeed the same order of magnitude, but differ by a factor of two, see Table 4.2. Nevertheless, the differences of masses $m_{D^*} - m_D \simeq 180$ MeV of the spin-0 and spin-1 negative-parity open charm states turns out to be (at least within theoretical errors) in quantitative agreement with the experiment. Thus, at least for negative-parity mesons, our chiral approach seems to correctly predict the amount of breaking of the heavy-quark spin symmetry. For the mass difference $m_{D_1} - m_{D_0^*}$ of spin-0 and spin-1 mesons with positive parity, our model underpredicts the experimental values by an order of magnitude, i.e., our approach based on chiral symmetry follows the predictions of heavy-quark symmetry even more closely than nature!

We conclude our discussion of the charmed meson masses by remarking that chiral symmetry (and its breaking) may still have a sizable influence in the charm sector. In this context it is interesting to note that in the theoretical works of Refs. [174, 175, 176, 177, 178] the degeneracy of vector and axial-vector charmed states in the heavy-quark limit [see Eqs.

(4.88-4.90)] as well as of scalar and pseudoscalar charmed states was obtained by combining the heavy-quark and the (linear) chiral symmetries.

5. Particle decays

5.1. Introduction

The study of decays of resonances plays a central role in understanding hadron phenomenology. One can describe the behaviour and the inner structure of subatomic particles in mathematical expressions of decays based on Feynman diagrams, which are applications of quantum field theory.

An unstable particle transforms spontaneously into other more stable particles, with less mass. This can be followed by another transformation, until one arrives at the lightest particles. These transformations occur according to some conservation rules and are called decays. There are three types of decays: strong, weak, and electromagnetic. Strong decays occur when an unstable meson (quark-antiquark state with gluons mediating the interaction) decay into lighter mesons. Weak decays occur when a quark couples to the massive bosons W^\pm and Z^0 due to weak interactions. A famous electromagnetic decay is that of the neutral pion into two photons ($\pi^0 \rightarrow 2\gamma$), but not into objects consisting of charged subcomponents.

In the 1960s, Okubo, Zweig, and Iizuka explained independently the reason why certain decay modes appear less frequently than otherwise might be expected. This is summarized in their famous rule (OZI rule) [205, 206, 207] which states that decays whose Feynman diagrams contain disconnected quark lines (which occur by cutting internal gluon lines) are suppressed.

The probability of a decay's occurrence can be computed. For a particle with rest mass M with energy and momentum (E, \vec{P}) , the survival probability $\mathbb{P}(t)$ (the probability that the particle survives for a time t before decaying) [51] is

$$\mathbb{P}(t) = e^{-t/\gamma\tau} = e^{-Mt\Gamma/E}. \quad (5.1)$$

where $\tau(\equiv 1/\Gamma)$ is the mean life time and Γ is the decay width. After the particle moves a distance x , the probability is

$$\mathbb{P}(t) = e^{-t/\gamma\tau} = e^{-Mx\Gamma/|\vec{P}|}. \quad (5.2)$$

In this chapter, we will study two-body decays of mesons. Also three-body decays of mesons will be analyzed. Moreover, the decay constant of mesons will be calculated. Therefore, in the present chapter, we develop formalisms for computing the corresponding decay constants and for both the two- and three-body decays.

5.2. Decay constants

In this section we develop the general formula for the decay constant by using the transformation method. As seen in Sec. 2.5 the matrix Φ is a combination of scalar and pseudoscalar currents:

$$\Phi = S + iP. \quad (5.3)$$

The hermitian conjugate is

$$\Phi^\dagger = S - iP, \quad (5.4)$$

which transforms as

$$\Phi^\dagger \rightarrow U_R \Phi^\dagger U_L^\dagger. \quad (5.5)$$

The pseudoscalar matrix can be written as

$$P = \frac{1}{2i}(\Phi - \Phi^\dagger), \quad (5.6)$$

which transforms as

$$P \rightarrow \frac{1}{2i}(U_L \Phi U_R^\dagger - U_R \Phi^\dagger U_L^\dagger), \quad (5.7)$$

with

$$U_L \in U(N_f)_L, \quad U_R \in U(N_f)_R. \quad (5.8)$$

The chiral symmetry group of QCD is

$$U(N_f)_L \times U(N_f)_R \equiv U(1)_V \times SU(N_f)_V \times U(1)_A \times SU(N_f)_A. \quad (5.9)$$

The $U(1)_V$ transformation corresponds to

$$U_1 = U_L = U_R = e^{i\theta t^0}, \quad (5.10)$$

while an $SU(N_f)_V$ transformation corresponds to

$$U_V = U_L = U_R = e^{i\theta_a^V t^a}, \quad (5.11)$$

and an $SU(N_f)_A$ transformation corresponds to

$$U_A = U_L = U_R^\dagger = e^{i\theta_a^A t^a}, \quad (5.12)$$

where $\theta_a^{V,A}$ are the parameters, and t^a are the generators of the group, with $a = 1, \dots, N_f^2 - 1$. For $N_f = 2$, $t_0 = \frac{1}{2}1_2$ and $t_i = \frac{1}{2}\tau_i$ where τ_i are the Pauli matrices. Note that the matrices of the scalar mesons S and of the pseudoscalar mesons in the model (2.88) are hermitian. Therefore they can be decomposed in terms of generators t^a of a unitary group $U(N_f)$ with $a = 0, \dots, N_f^2 - 1$. For small parameters

$$U = 1 + i\theta_a t^a, \quad (5.13)$$

Under a $U_A(N_f)$ transformation, the pseudoscalar matrix becomes

$$P \rightarrow \frac{1}{2i}(U_A \Phi U_A - U_A^\dagger \Phi^\dagger U_A^\dagger). \quad (5.14)$$

Using Eqs.(5.3), (5.6), and (5.13), we obtain the transformation of fields

$$P \rightarrow P + \theta_a^A \{t_a, S\}, \quad (5.15)$$

Introducing the wave-function renormalization of the fields

$$Z_i P \rightarrow Z_i P + \theta_a^A \{t_a, S\}, \quad (5.16)$$

which can be written as

$$P \rightarrow P + \theta_a^A \frac{\{t_a, S\}}{Z_i}, \quad (5.17)$$

The weak decay constants take the following form

$$f_i = \frac{\{t_a, S\}}{Z_i}. \quad (5.18)$$

5.3. Two-body decay

In this section, we investigate various aspects of the decay of a particle into a two-particle final state [208].

Consider a particle with four-momenta P described by $P(M, 0)$, in its rest frame, which decays into two particles with momenta p_i and masses m_i , where $i = 1, 2$, with $M > m_1 + m_2$. This two-body decay is described by the Feynman diagram in Fig. 5.1.

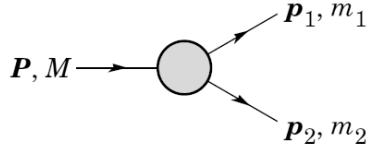


Figure 5.1.: Feynman diagram of a two-body decay [51].

The initial state of the decaying particle and the final state can be defined as

$$|in\rangle = b_P^\dagger |0\rangle, \quad (5.19)$$

$$|fin\rangle = a_{p_1}^\dagger a_{p_2}^\dagger |0\rangle. \quad (5.20)$$

Assume that the decaying particle and the decay products are confined in a ‘box’ with length L and volume $V = L^3$. The three-momenta are quantized in the box, as known from quantum mechanics, as $P = 2\pi n_P/L$ and $p_{1,2} = 2\pi n_{p_{1,2}}/L$. The corresponding energies of

these particles are described by $w_P = \sqrt{M^2 + P^2}$ and $w_{p_1, p_2} = \sqrt{m_{1,2}^2 + p_{1,2}^2}$.

The corresponding matrix element of the scattering matrix in terms of the initial and final states is

$$\langle fin|S^{(1)}|in \rangle = \frac{S}{V^{3/2}} \frac{-i\mathcal{M}}{\sqrt{2\omega_{p_1}2\omega_{p_2}2\omega_P}} (2\pi)^4 \delta^4(P - p_1 - p_2), \quad (5.21)$$

where S refers to a symmetrization factor, $\delta^4(P - p_1 - p_2)$ denotes the delta distribution which describes the energy-momentum conservation for each vertex, and \mathcal{M} is the corresponding tree-level decay amplitude.

The squared modulus of the scattering matrix (5.21) gives the probability for the particle decaying from the initial state $|in \rangle$ state to the final $|fin \rangle$ as:

$$|\langle fin|S^{(1)}|in \rangle|^2 = \frac{1}{V^3} \frac{|-i\mathcal{M}|^2}{\sqrt{2\omega_{p_1}2\omega_{p_2}2\omega_P}} (2\pi)^8 (\delta^4(P - p_1 - p_2))^2. \quad (5.22)$$

Using the ‘‘Fermi trick’’ [209], the square of the delta distribution can be obtained as follows:

$$\begin{aligned} (2\pi)^8 (\delta^4(P - p_1 - p_2))^2 &= (2\pi)^4 \delta^4(P - p_1 - p_2) \int d^4x e^{ix(\mathbf{P} - p_1 - p_2)} \\ &= (2\pi)^4 \delta^4(P - p_1 - p_2) \int d^4x \\ &= (2\pi)^4 \delta^4(P - p_1 - p_2) \int_V d^3x \int_0^t dt \\ &= (2\pi)^4 \delta^4(P - p_1 - p_2) Vt, \end{aligned} \quad (5.23)$$

where x is the Minkowski space-time vector. Consequently, the probability of the two-body decay (5.22) can be written as

$$|\langle fin|S^{(1)}|in \rangle|^2 = \frac{1}{V^3} \frac{|-i\mathcal{M}|^2}{\sqrt{2\omega_{p_1}2\omega_{p_2}2\omega_P}} (2\pi)^4 \delta^4(P - p_1 - p_2) Vt. \quad (5.24)$$

The number of final states is obtained as the factor $V \frac{d^3p_1}{(2\pi)^3} V \frac{d^3p_2}{(2\pi)^3}$ when the three-momenta of the outgoing particles lie between $(p_1, p_1 + d^3p_1)$ and $(p_2, p_2 + d^3p_2)$. Consequently, the probability for the decay in the momentum range becomes

$$\begin{aligned} |\langle fin|S^{(1)}|in \rangle|^2 V \frac{d^3p_1}{(2\pi)^3} V \frac{d^3p_2}{(2\pi)^3} &= \frac{S|-i\mathcal{M}|^2}{2\omega_{p_1}2\omega_{p_2}2\omega_P} \\ &\quad \times (2\pi)^4 \delta^4(P - p_1 - p_2) \times \frac{d^3p_1}{(2\pi)^3} \times \frac{d^3p_2}{(2\pi)^3} t. \end{aligned} \quad (5.25)$$

By integrating over all possible final momenta (p_1 and p_2), we obtain the definition of the decay rate Γ of the two-body decay as

$$\Gamma = S \int \frac{d^3p_1}{(2\pi)^3} \frac{d^3p_2}{(2\pi)^3} \frac{|-i\mathcal{M}|^2}{2\omega_{p_1}2\omega_{p_2}2\omega_P} (2\pi)^4 \delta^4(P - p_1 - p_2). \quad (5.26)$$

The probability to obtain the two particles as decay products at any instant t is

$$\mathbb{P}_d(t) = \Gamma t. \quad (5.27)$$

Consequently, the probability of the initial particle surviving at the same instant is

$$\mathbb{P}_s(t) = 1 - \Gamma t. \quad (5.28)$$

which holds only when $t \ll \Gamma^{-1}$. The mean-life time is

$$\tau = \Gamma^{-1}. \quad (5.29)$$

Now, let us turn to the evaluation of the decay rate (5.26) of the two-body decay:

$$\Gamma = \frac{S}{2(2\pi)^2} \int d^3 p_1 d^3 p_2 \frac{|-i\mathcal{M}|^2}{2\omega_{p_1} 2\omega_{p_2} 2\omega_P} \delta^4(P - p_1 - p_2). \quad (5.30)$$

Consider the two outgoing particles to have the same mass ($m_1 = m_2$) and note that, in the rest frame of the decaying particle the four momentum is $P = (M, 0)$. Therefore, the delta function can be obtained as

$$\begin{aligned} \delta^4(P - p_1 - p_2) &= \delta^3(p_1 + p_2) \delta(M - \omega_{p_1} - \omega_{p_2}) \\ &= \delta^3(p_1 + p_2) \delta(M - 2\omega_{p_1}). \end{aligned} \quad (5.31)$$

Using the Dirac delta function to solve the integral over $d^3 p_2$, we obtain

$$\Gamma = \frac{S}{2(2\pi)^2} \int d^3 p_1 \frac{|-i\mathcal{M}|^2}{(2\omega_{p_1})^2 2M} \delta(M - 2\omega_{p_1}). \quad (5.32)$$

When we use the generic identity $\delta(g(x)) = \sum_i \delta(x - x_i)/|g'(x_i)|$, where $g(x_i) = 0$, the δ distribution can be written as

$$\delta(M - 2\omega_{p_1}) = \frac{4M}{k_f} \delta(|p_1| - k_f), \quad (5.33)$$

where the energy-momentum conservation gives

$$|p_1| = \sqrt{\frac{M^2}{4} - m_{1,2}^2} \equiv k_f, \quad \text{for } (m_1 = m_2). \quad (5.34)$$

Using the spherical coordinates $d^3 p_1 \equiv p_1^2 d\Omega d|p_1|$ and integrating over $d|p_1|$, the decay rate (5.32) becomes

$$\Gamma = \frac{S k_f}{32 \pi^2 M^2} \int d\Omega |-i\mathcal{M}|^2, \quad (5.35)$$

When the decay amplitude does not depend on the angle, we obtain the general formula [116, 208] of the two-body decay rate as

$$\Gamma_{A \rightarrow BC} = I \frac{S k_f}{8\pi M^2} |-i\mathcal{M}|^2, \quad (5.36)$$

with the center-of-mass momentum of the two decay particles

$$k_f = \frac{1}{2M} \sqrt{M^4 + (m_1^2 - m_2^2)^2 - 2M^2(m_1^2 + m_2^2)\theta(M - m_1 - m_2)}, \quad (5.37)$$

and the symmetrization factor S equals 1 if the outgoing particles are different, and 2 for two identical outgoing particles (because of the inter change ability of outgoing particles lines). The isospin factor I considers all subchannels of a particular decay channel. The decay threshold is encoded by the θ function.

5.4. Three-body decay

In this section we expand our investigation to various aspects of the decay into a three-body final state which is more complicated than the two-body decay, as we will see in the following.

Consider a particle A with four-momentum P in its rest frame, with $P = (M, 0)$, decaying into three particles (B_1, B_2, B_3) with momenta p_i and mass m_i , where $i = 1, 2, 3$, with $M > m_1 + m_2 + m_3$. This decay is confined in a “box” that has length L with volume $V = L^3$. The momenta of the decaying particle and the three outgoing particles are quantized in the box as $P = 2\pi n_P/L$ and $p_{1,2,3} = 2\pi n_{p_{1,2,3}}/L$, respectively. The corresponding energies for the decaying particle are $\omega_P = \sqrt{M^2 + P^2}$ whereas those for the produced particles are $\omega_{p_{1,2,3}} = \sqrt{m_{1,2,3}^2 + p_{1,2,3}^2}$. The Feynman diagram that describes the three-body decay is presented in Fig. 5.2.

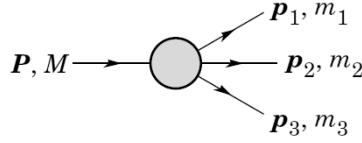


Figure 5.2.: Feynman diagram of the three body decay [51].

The initial and final states read

$$|in\rangle = b_P^\dagger |0\rangle, \quad (5.38)$$

$$|fin\rangle = a_{p_1}^\dagger a_{p_2}^\dagger a_{p_3}^\dagger |0\rangle, \quad (5.39)$$

and the corresponding element of the scattering matrix is

$$\begin{aligned} \langle fin | S^{(1)} | in \rangle &= \frac{1}{V^{3/2}} \frac{1}{\sqrt{2\omega_{p_1} 2\omega_{p_2} 2\omega_{p_3} 2\omega_P}} (2\pi)^4 \\ &\times \delta^4(P - p_1 - p_2 - p_3) (-i\mathcal{M}_{A \rightarrow B_1 B_2 B_3}), \end{aligned} \quad (5.40)$$

where $-i\mathcal{M}_1$ is the invariant amplitude of the vertex function that enters into the Feynman rule for the vertex $A - B_1 B_2 B_3$. The probability for the process $A \rightarrow B_1 B_2 B_3$ can be computed by squaring the amplitude (5.40)

$$|\langle fin|S^{(1)}|in\rangle|^2 = \frac{1}{V^3} \frac{1}{\sqrt{2\omega_{p_1}2\omega_{p_2}2\omega_{p_3}2\omega_P}} (2\pi)^8 \times (\delta^4(P - p_1 - p_2 - p_3))^2 | -i\mathcal{M}_{A \rightarrow B_1 B_2 B_3} |^2. \quad (5.41)$$

Due to the Fermi Trick [209], we simplify the delta squared as

$$\begin{aligned} (2\pi)^8 (\delta^4(P - p_1 - p_2 - p_3))^2 &= (2\pi)^4 \delta^4(P - p_1 - p_2 - p_3) \int d^4x e^{ix(P - p_1 - p_2 - p_3)} \\ &= (2\pi)^4 \delta^4(P - p_1 - p_2 - p_3) \int d^4x \\ &= (2\pi)^4 \delta^4(P - p_1 - p_2 - p_3) \int_V d^3x \int_0^t dt \\ &= (2\pi)^4 \delta^4(P - p_1 - p_2 - p_3) Vt, \end{aligned} \quad (5.42)$$

where $x = (t, x_1, x_2, x_3)$. The probability for the decay $A \rightarrow B_1 B_2 B_3$ when the three particles B_1 , B_2 , and B_3 have momenta between $(\mathbf{p}_1, \mathbf{p}_1 + d^3p_1)$, $(\mathbf{p}_2, \mathbf{p}_2 + d^3p_2)$ and $(\mathbf{p}_3, \mathbf{p}_3 + d^3p_3)$, respectively, is given by

$$|\langle fin|S^{(1)}|in\rangle|^2 V \frac{d^3p_1}{(2\pi)^3} V \frac{d^3p_2}{(2\pi)^3} V \frac{d^3p_3}{(2\pi)^3}, \quad (5.43)$$

where $V d^3p_i / (2\pi)^3$ describes the number of states with four momenta between $(\mathbf{p}_1, \mathbf{p}_1 + d^3p_1)$. Using Eqs. (5.41) and (5.42), the probability of the three-body decay Eq.(5.43) becomes

$$\begin{aligned} |\langle fin|S^{(1)}|in\rangle|^2 V \frac{d^3p_1}{(2\pi)^3} V \frac{d^3p_2}{(2\pi)^3} V \frac{d^2p_3}{(2\pi)^3} \\ = \frac{1}{2\omega_{p_1}2\omega_{p_2}2\omega_{p_3}2\omega_P} \times (2\pi)^4 \delta^4(P - p_1 - p_2 - p_3) \\ \times \frac{d^3p_1}{(2\pi)^3} \frac{d^3p_2}{(2\pi)^3} \frac{d^2p_3}{(2\pi)^3} | -i\mathcal{M}_{A \rightarrow B_1 B_2 B_3} |^2 t, \end{aligned} \quad (5.44)$$

which does not depend on the normalization volume V . By integrating over all possible final momenta, we can obtain the decay rate Γ as:

$$\Gamma = \int \frac{d^3p_1}{(2\pi)^3} \frac{d^3p_2}{(2\pi)^3} \frac{d^3p_3}{(2\pi)^3} \frac{| -i\mathcal{M}_{A \rightarrow B_1 B_2 B_3} |^2}{2\omega_{p_1}2\omega_{p_2}2\omega_{p_3}2\omega_P} (2\pi)^4 \delta^4(P - p_1 - p_2 - p_3), \quad (5.45)$$

which can be written as

$$\Gamma = \frac{1}{(2\pi)^5} \int d^3p_1 d^3p_2 d^3p_3 \frac{| -i\mathcal{M}_{A \rightarrow B_1 B_2 B_3} |^2}{2\omega_{p_1}2\omega_{p_2}2\omega_{p_3}2\omega_P} \delta^4(P - p_1 - p_2 - p_3). \quad (5.46)$$

In the rest frame of the decaying particle with $P = (M, 0)$ we have

$$\delta^4(P - p_1 - p_2 - p_3) = \delta^3(p_1 + p_2 + p_3) \delta(M - \omega_{p_1} - \omega_{p_2} - \omega_{p_3}). \quad (5.47)$$

Substituting Eq.(5.47) into Eq.(5.46), we obtain

$$\Gamma = \frac{1}{16(2\pi)^5} \int d^3 p_1 d^3 p_2 d^3 p_3 \frac{|-i\mathcal{M}_{A \rightarrow B_1 B_2 B_3}(p_1, p_2, p_3)|^2}{\omega_{p_1} \omega_{p_2} \omega_{p_3} M} \times \delta^3(p_1 + p_2 + p_3) \delta(M - \omega_{p_1} - \omega_{p_2} - \omega_{p_3}), \quad (5.48)$$

solving the integral over $d^3 p_3$ (by use of the Dirac delta function), we get

$$\Gamma = \frac{1}{16(2\pi)^5} \int d^3 p_1 d^3 p_2 \frac{|-i\mathcal{M}_{A \rightarrow B_1 B_2 B_3}(p_1, p_2, -(p_1 + p_2))|^2}{\omega_{p_1} \omega_{p_2} \omega_{p_3} M} \delta(M - \omega_{p_1} - \omega_{p_2} - \omega_{p_3}), \quad (5.49)$$

where $\omega_{p_3} = (p_3^2 + m_{B_3}^2)^{1/2}$ and now p_3 is a notation for $-(p_1 + p_2)$. The matrix element depends on the angle θ between p_1 and p_2 , and so Eq. (5.49) becomes

$$\Gamma = \frac{1}{8(2\pi)^3} \int \frac{p_1 dp_1 \cdot p_2 dp_2}{\omega_{p_1} \omega_{p_2} \omega_{p_3} M} p_1 p_2 d \cos \theta | -i\mathcal{M}_{A \rightarrow B_1 B_2 B_3}\{p_1, p_2, -(p_1 + p_2)\} |^2 \times \delta(M - \omega_{p_1} - \omega_{p_2} - \omega_{p_3}), \quad (5.50)$$

but

$$\begin{aligned} \omega_{p_1}^2 = p_1^2 + m_{B_1}^2 &\Rightarrow 2\omega_{p_1} d\omega_{p_1} = 2p_1 dp_1, \\ \therefore \omega_{p_1} d\omega_{p_1} &= p_1 dp_1. \end{aligned} \quad (5.51)$$

Similarly,

$$\omega_{p_2} d\omega_{p_2} = p_2 dp_2, \quad (5.52)$$

$$\omega_{p_3}^2 = (\vec{p}_1 + \vec{p}_2)^2 + m_{B_3}^2 = p_1^2 + p_2^2 + 2p_1 p_2 \cos \theta + m_{B_3}^2,$$

At p_1 and p_2 fixed, we have

$$2\omega_{p_3} d\omega_{p_3} = 2p_1 p_2 d \cos \theta, \quad (5.53)$$

Substituting Eqs.(5.51 - 5.53) into Eq.(5.50), we obtain

$$\Gamma = \frac{1}{8(2\pi)^3} \int \frac{d\omega_{p_1} d\omega_{p_2} d\omega_{p_3}}{M} | -i\mathcal{M}_{A \rightarrow B_1 B_2 B_3} |^2 \delta(M - \omega_{p_1} - \omega_{p_2} - \omega_{p_3}), \quad (5.54)$$

Using the Dirac delta to eliminate ω_{p_3}

$$\begin{aligned} \Gamma &= \frac{1}{(2\pi)^3} \frac{1}{8M} \int | -i\mathcal{M}_{A \rightarrow B_1 B_2 B_3} |^2 d\omega_{p_1} d\omega_{p_2}, \\ &= \frac{1}{(2\pi)^3} \frac{1}{32M^3} \int | -i\mathcal{M}_{A \rightarrow B_1 B_2 B_3} |^2 dm_{12}^2 dm_{23}^2, \end{aligned} \quad (5.55)$$

which is the standard form for the Dalitz plot [51].

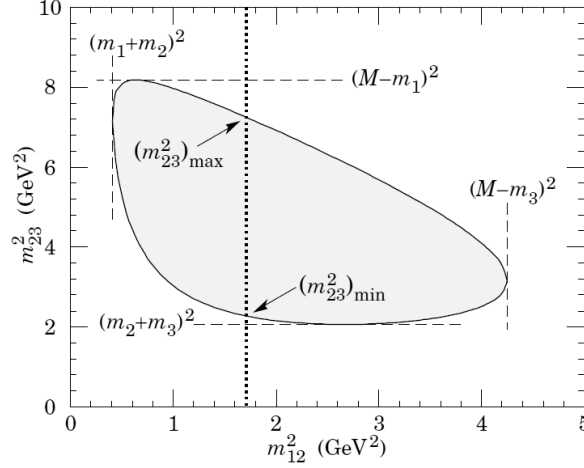


Figure 5.3.: Dalitz plot for a three-body final state [51].

The limits of integration can be determined from the Dalitz plot [51], which leads to the following formula for the decay rate of A into B_1 , B_2 , B_3

$$\Gamma_{A \rightarrow B_1 B_2 B_3} = \frac{S_{A \rightarrow B_1 B_2 B_3}}{32(2\pi)^3 M^3} \int_{(m_1+m_2)^2}^{(M-m_3)^2} \int_{(m_{23}^2)_{\min}}^{(m_{23}^2)_{\max}} |-i\mathcal{M}_{A \rightarrow B_1 B_2 B_3}|^2 dm_{23}^2 dm_{12}^2. \quad (5.56)$$

Integrating over m_{23}^2 , we obtain

$$\Gamma_{A \rightarrow B_1 B_2 B_3} = \frac{S_{A \rightarrow B_1 B_2 B_3}}{32(2\pi)^3 M^3} \int_{(m_1+m_2)^2}^{(M-m_3)^2} |-i\mathcal{M}_{A \rightarrow B_1 B_2 B_3}|^2 [(m_{23}^2)_{\max} - (m_{23}^2)_{\min}] dm_{12}^2. \quad (5.57)$$

The range of m_{23}^2 is determined by the value of m_{12}^2 when p_2 is parallel or antiparallel to p_3 as follows [51]

$$(m_{23}^2)_{\min} = (E_2^* + E_3^*)^2 - \left(\sqrt{E_2^{*2} - m_2^2} + \sqrt{E_3^{*2} - m_3^2} \right)^2, \quad (5.58)$$

$$(m_{23}^2)_{\max} = (E_2^* + E_3^*)^2 - \left(\sqrt{E_2^{*2} - m_2^2} - \sqrt{E_3^{*2} - m_3^2} \right)^2, \quad (5.59)$$

where E_2^* and E_3^* are the energies of particles B_2 and B_3 , respectively, in the m_{12} rest frame,

$$\begin{aligned} E_2^* &= \frac{m_{12}^2 - m_1^2 + m_2^2}{2m_{12}}, \\ E_3^* &= \frac{M^2 - m_{12}^2 - m_3^2}{2m_{12}}. \end{aligned} \quad (5.60)$$

Finally, the explicit expression for the three-body decay rate for the process $A \rightarrow B_1 B_2 B_3$

is:

$$\begin{aligned}
\Gamma_{A \rightarrow B_1 B_2 B_3} &= \frac{S_{A \rightarrow B_1 B_2 B_3}}{32(2\pi)^3 M^3} \int_{(m_1+m_2)^2}^{(M-m_3)^2} | -i\mathcal{M}_{A \rightarrow B_1 B_2 B_3} |^2 \\
&\times \sqrt{\frac{(-m_1 + m_{12} - m_2)(m_1 + m_{12} - m_2)(-m_1 + m_{12} + m_2)(m_1 + m_{12} + m_2)}{m_{12}^2}} \\
&\times \sqrt{\frac{(-M + m_{12} - m_3)(M + m_{12} - m_3)(-M + m_{12} + m_3)(M + m_{12} + m_3)}{m_{12}^2}} dm_{12}^2,
\end{aligned} \tag{5.61}$$

where $\mathcal{M}_{A \rightarrow B_1 B_2 B_3}$ is the corresponding tree-level decay amplitude, and $S_{A \rightarrow B_1 B_2 B_3}$ is a symmetrization factor (it is equal to 1 if B_1 , B_2 , and B_3 are all different, and equal to 2 for two identical particles in the final state, and equal to 6 for three identical particles in the final state).

6. Decay of the pseudoscalar glueball into scalar and pseudoscalar mesons

“The most exciting phrase to hear in science, the one that heralds new discoveries, is not ‘Eureka’ (I found it), but ‘that’s funny’...”

Isaac Asimov

6.1. Introduction

The fundamental symmetry underlying Quantum Chromodynamics (QCD), the theory of strong interactions, is the exact local $SU(3)_c$ colour symmetry. As a consequence of the non-Abelian nature of this symmetry the gauge fields of QCD (the gluons) are coloured objects and therefore interact strongly with each other. Because of confinement, one expects that gluons can also form colourless, or ‘white’, states which are called glueballs.

In this chapter we study the decay properties of a pseudoscalar glueball state whose mass lies, in agreement with lattice QCD, between 2 and 3 GeV. Following Ref. [111, 113, 210, 211] we write down an effective chiral Lagrangian which couples the pseudoscalar glueball field (denoted as \tilde{G}) to scalar and pseudoscalar mesons. We can thus evaluate the widths for the decays $\tilde{G} \rightarrow PPP$ and $\tilde{G} \rightarrow PS$, where P and S stand for pseudoscalar and scalar quark-antiquark states. The pseudoscalar state P refers to the well-known light pseudoscalars $\{\pi, K, \eta, \eta'\}$, while the scalar state S refers to the quark-antiquark nonet of scalars above 1 GeV: $\{a_0(1450), K_0^*(1430), f_0(1370), f_0(1710)\}$. The reason for the latter assignment is a growing consensus that the chiral partners of the pseudoscalar states should not be identified with the resonances below 1 GeV, see Refs. [78, 108, 110] for results within the extended linear sigma model, see also other theoretical works in Refs. [72, 73, 74, 75, 76, 77, 131, 212, 213, 214, 215, 216, 217] (and refs. therein).

The chiral Lagrangian that we construct contains one unknown coupling constant which cannot be determined without experimental data. However, the branching ratios can be unambiguously calculated and may represent a useful guideline for an experimental search of the pseudoscalar glueball in the energy region between 2 to 3 GeV. In this respect, the planned PANDA experiment at the FAIR facility [218] will prove fruitful, since it will be capable of scanning the mass region above 2.5 GeV. The experiment is based on proton-antiproton scattering, thus the pseudoscalar glueball \tilde{G} can be directly produced as an intermediate state. We shall therefore present our results for the branching ratios for a putative pseudoscalar glueball with a mass of 2.6 GeV.

In addition to the vacuum properties of a pseudoscalar glueball, we describe (to our knowledge [124, 125, 126, 127] for the first time) the interaction of \tilde{G} with baryons: we introduce the chiral effective Lagrangian which couples \tilde{G} to the nucleon field and its chiral partner.

This Lagrangian describes also the proton-antiproton conversion process $\bar{p}p \rightarrow \tilde{G}$, which allow us to study the decay of a pseudoscalar glueball into two nucleons.

Additionally, it is possible that the pseudoscalar glueball \tilde{G} has a mass that is slightly lower than the lattice-QCD prediction and that it has been already observed in the BESIII experiment where pseudoscalar resonances have been investigated in J/ψ decays [219, 220, 221]. In particular, the resonance $X(2370)$ which has been clearly observed in the $\pi^+\pi^-\eta'$ channel represents a good candidate, because it is quite narrow (~ 80 MeV) and its mass lies just below the lattice-QCD prediction. For this reason we repeat our calculation for a pseudoscalar glueball mass of 2.37 GeV, and thus make predictions for the resonance $X(2370)$, which can be tested in the near future.

6.2. The effective Lagrangian with a pseudoscalar glueball

In this section we consider an $N_f = 3$ chiral Lagrangian which describes the interaction between the pseudoscalar glueball and (pseudo)scalar mesons. We calculate the decay widths of the pseudoscalar glueball, where we fixed its mass to 2.6 GeV, as predicted by lattice-QCD simulations, and take a closer look at the scalar-isoscalar decay channel. We present our results as branching ratios which are relevant for the future PANDA experiment at the FAIR facility.

We introduce a chiral Lagrangian which couples the pseudoscalar glueball $\tilde{G} \equiv |gg\rangle$ with quantum numbers $J^{PC} = 0^{-+}$ to scalar and pseudoscalar mesons as in Refs. [111, 124, 125, 126, 127, 211]

$$\mathcal{L}_{\tilde{G}-mesons}^{int} = ic_{\tilde{G}\Phi} \tilde{G} (\det\Phi - \det\Phi^\dagger) , \quad (6.1)$$

where $c_{\tilde{G}\Phi}$ is a (unknown) dimensionless coupling constant.

$$\Phi = (S^a + iP^a)t^a \quad (6.2)$$

represents the multiplet of scalar and pseudoscalar quark-antiquark states, and t^a are the generators of the group $U(N_f)$. In the present case $N_f = 3$ the explicit representation of the scalar and pseudoscalar mesons reads [110, 116]:

$$\Phi = \frac{1}{\sqrt{2}} \begin{pmatrix} \frac{(\sigma_N + a_0^0) + i(\eta_N + \pi^0)}{\sqrt{2}} & a_0^+ + i\pi^+ & K_0^{*+} + iK^+ \\ a_0^- + i\pi^- & \frac{(\sigma_N - a_0^0) + i(\eta_N - \pi^0)}{\sqrt{2}} & K_0^{*0} + iK^0 \\ K_0^{*-} + iK^- & \bar{K}_0^{*0} + i\bar{K}^0 & \sigma_S + i\eta_S \end{pmatrix} . \quad (6.3)$$

Let us consider the symmetry properties [9, 10] of the effective Lagrangian (6.1). The pseudoscalar glueball \tilde{G} consists of gluons and is therefore a chirally invariant object. Under $U(3)_L \times U(3)_R$ chiral transformations the multiplet Φ transforms as $\Phi \rightarrow U_L \Phi U_R^\dagger$ where $U_{L(R)} = e^{-i\theta_{L(R)}^a t^a}$ is an element of the group of $U(3)_{R(L)}$ matrices. Performing these transformations on the determinant of Φ it is easy to prove that this object is invariant under $SU(3)_L \times SU(3)_R$, but not under the axial $U(1)_A$ transformation,

$$\det\Phi \rightarrow \det(U_A \Phi U_A) = e^{-i\theta_A^0 \sqrt{2N_f}} \det\Phi \neq \det\Phi .$$

This is in agreement with the so-called axial anomaly. Consequently the effective Lagrangian (6.1) possesses only an $SU(3)_L \times SU(3)_R$ symmetry. Further essential symmetries

of the strong interaction are the parity P and charge conjugation C . The pseudoscalar glueball and the multiplet Φ transform under parity as

$$\tilde{G}(t, \vec{x}) \rightarrow -\tilde{G}(t, -\vec{x}),$$

$$\Phi(t, \vec{x}) \rightarrow \Phi^\dagger(t, -\vec{x}).$$

Performing the discrete transformations P and C on the effective Lagrangian (6.1) leave it unchanged. In conclusion, one can say that the symmetries of the effective Lagrangian (6.1) are in agreement with the symmetries of the QCD Lagrangian. The rest of the mesonic Lagrangian which describes the interactions of Φ and also includes (axial-)vector degrees of freedom is presented in Sec. 3.3.

6.2.1. Implications of the interaction Lagrangian

We have to consider that when $m_0^2 < 0$ spontaneous chiral symmetry breaking occurs and the scalar-isoscalar fields condense. When this breaking takes place, we need to shift the scalar-isoscalar fields by their vacuum expectation values ϕ_N and ϕ_S ,

$$\sigma_N \rightarrow \sigma_N + \phi_N, \quad (6.4)$$

and

$$\sigma_S \rightarrow \sigma_S + \phi_S. \quad (6.5)$$

In addition, when (axial-)vector mesons are present in the Lagrangian, one also has to ‘shift’ the (axial-)vector fields and to define the wave-function renormalization constants of the (pseudo)scalar fields:

$$\begin{aligned} \vec{\pi} &\rightarrow Z_\pi \vec{\pi}, \\ K^i &\rightarrow Z_K K^i, \\ \eta_j &\rightarrow Z_{\eta_j} \eta_j, \\ K_0^{*i} &\rightarrow Z_{K_0^*} K_0^{*i}, \end{aligned} \quad (6.6)$$

where $i = 1, 2, 3, 4$ runs over the four kaonic fields and $j = N, S$. Once the field transformations in Eqs. (6.5) and (6.6) have been performed, the Lagrangian (6.1) contains the relevant

tree-level vertices for the decay processes of \tilde{G} , and takes the form [124]:

$$\begin{aligned}
\mathcal{L}_{\tilde{G}-mesons}^{int} = & \frac{c_{\tilde{G}\Phi}}{2\sqrt{2}}\tilde{G}(\sqrt{2}Z_{K_0^*}Z_K a_0^0 K_0^{*0}\bar{K}^0 + \sqrt{2}Z_K Z_{K_0^*} a_0^0 K^0 \bar{K}_0^{*0} - 2Z_{K_0^*}Z_K a_0^+ K_0^{*0} K^- \\
& - 2Z_{K_0^*}Z_K a_0^+ K_0^{*-} K^0 - 2Z_{K_0^*}Z_K a_0^- \bar{K}_0^{*0} K^+ - \sqrt{2}Z_{K_0^*}Z_K a_0^0 K_0^{*-} K^+ \\
& - \sqrt{2}Z_K^2 Z_{\eta_N} K^0 \bar{K}^0 \eta_N + \sqrt{2}Z_{K_S}^2 Z_{\eta_N} K_S^0 \bar{K}_S^0 \eta_N + 2Z_{\eta_S} a_0^- a_0^+ \eta_S \\
& - \sqrt{2}Z_K^2 Z_{\eta_N} K^- K^+ \eta_N - \sqrt{2}Z_K^2 Z_{\pi} K^0 \bar{K}^0 \pi^0 + \sqrt{2}Z_{K_0^*}^2 Z_{\pi} K_0^{*0} \bar{K}_0^{*0} \pi^0 \\
& + \sqrt{2}Z_K^2 Z_{\pi} K^- K^+ \pi^0 + Z_{\eta_S} a_0^0 \eta_S + Z_{\eta_N}^2 Z_{\eta_S} \eta_N^2 \eta_S - Z_{\eta_S} Z_{\pi}^2 \eta_S \pi^0 \\
& + 2Z_K^2 Z_{\pi} \bar{K}^0 K^+ \pi^- + 2Z_K^2 Z_{\pi} K^0 K^- \pi^+ - 2Z_{K_0^*}^2 Z_{\pi} K_0^{*0} K_0^{*-} \pi^+ \\
& - 2Z_{\eta_S} Z_{\pi}^2 \eta_S \pi^- \pi^+ - 2Z_{K_0^*} Z_K a_0^- K_0^{*+} \bar{K}^0 + \sqrt{2}Z_{K_0^*}^2 Z_{\eta_N} K_0^{*+} K_0^{*-} \eta_N \\
& - \sqrt{2}Z_{K_0^*}^2 Z_{\pi} K_0^{*+} K_0^{*-} \pi^0 - 2Z_{K_0^*}^2 Z_{\pi} K_0^{*+} \bar{K}_0^{*0} \pi^- + 2Z_{\pi} a_0^0 \pi^0 \phi_S \\
& + 2Z_{\pi} a_0^0 \pi^0 \sigma_S - \sqrt{2}Z_{K_0^*} Z_K a_0^0 K_0^{*+} K^- + \sqrt{2}Z_K Z_{K_0^*} K^- K_0^{*+} \phi_N \\
& + \sqrt{2}Z_K Z_{K_0^*} K^- K_0^{*+} \sigma_N + \sqrt{2}Z_{K_0^*} Z_K K_0^{*0} \bar{K}^0 \phi_N - 2Z_{\eta_N} \eta_N \phi_N \phi_S \\
& + \sqrt{2}Z_{K_0^*} Z_K K_0^{*0} \bar{K}^0 \sigma_N + \sqrt{2}Z_K Z_{K_0^*} K^0 \bar{K}_0^{*0} \phi_N - Z_{\eta_S} \eta_S \phi_N^2 \\
& + \sqrt{2}Z_K Z_{K_0^*} K^0 \bar{K}_0^{*0} \sigma_N + \sqrt{2}Z_{K_0^*} Z_K K_0^{*-} K^+ \phi_N \\
& - Z_{\eta_S} \eta_S \sigma_N^2 - 2Z_{\eta_S} \eta_S \phi_N \sigma_N + \sqrt{2}Z_{K_0^*} Z_K K_0^{*-} K^+ \sigma_N \\
& + 2Z_{\pi} a_0^+ \pi^- \phi_S + 2Z_{\pi} a_0^+ \pi^- \sigma_S + 2Z_{\pi} a_0^- \pi^+ \phi_S + 2Z_{\pi} a_0^- \pi^+ \sigma_S \\
& - 2Z_{\eta_N} \eta_N \phi_N \sigma_S - 2Z_{\eta_N} \eta_N \sigma_N \phi_S - 2Z_{\eta_N} \eta_N \sigma_N \sigma_S). \tag{6.7}
\end{aligned}$$

which is used to determine the coupling of the field \tilde{G} to the scalar and pseudoscalar mesons.

6.3. Field assignments

The assignment of the quark-antiquark fields in Eq. (6.1) or (6.3) is as follows:

(i) In the pseudoscalar sector the fields $\vec{\pi}$ and K represent the pions and the kaons, respectively [23]. The bare fields $\eta_N \equiv |\bar{u}u + \bar{d}d\rangle/\sqrt{2}$ and $\eta_S \equiv |\bar{s}s\rangle$ are the non-strange and strange contributions of the physical states η and η' [23]:

$$\begin{aligned}
\eta &= \eta_N \cos \varphi + \eta_S \sin \varphi, \\
\eta' &= -\eta_N \sin \varphi + \eta_S \cos \varphi, \tag{6.8}
\end{aligned}$$

where $\varphi \simeq -44.6^\circ$ is the mixing angle [110]. Using other values for the mixing angle, e.g. $\varphi = -36^\circ$ [159] or $\varphi = -41.4^\circ$, as determined by the KLOE Collaboration [92], affects the presented results only marginally. In the effective Lagrangian (6.1) there exists a mixing between the bare pseudoscalar glueball \tilde{G} and both bare fields η_N and η_S , but due to the large mass difference between the pseudoscalar glueball and the pseudoscalar quark-antiquark fields, it turns out that this mixing is very small and is therefore negligible.

(ii) In the scalar sector the field \vec{a}_0 corresponds to the physical isotriplet state $a_0(1450)$ and the scalar kaon field K_0^* to the physical isodoublet state $K_0^*(1430)$ [23]. The field

$\sigma_N \equiv (\bar{u}u + \bar{d}d)/\sqrt{2}$ is the bare nonstrange isoscalar field and it corresponds to the resonance $f_0(1370)$ [110, 80]. The field $\sigma_S \equiv \bar{s}s$ is the bare strange isoscalar field and the debate about its assignment to a physical state is still ongoing; in a first approximation it can be assigned to the resonance $f_0(1710)$ [110] or $f_0(1500)$ [80]. (Scalars below 1 GeV are predominantly tetraquarks or mesonic molecular states, as seen in Refs. [212, 213, 214, 222, 216, 223, 224, 225, 226, 227, 228], which are not considered here). In order to properly take into account mixing effects in the scalar-isoscalar sector, we have also used the results of Refs. [79, 80]. The mixing takes the form:

$$\begin{pmatrix} f_0(1370) \\ f_0(1500) \\ f_0(1710) \end{pmatrix} = B \cdot \begin{pmatrix} \sigma_N \equiv \bar{n}n = (\bar{u}u + \bar{d}d)/\sqrt{2} \\ G \equiv gg \\ \sigma_S \equiv \bar{s}s \end{pmatrix}, \quad (6.9)$$

where $G \equiv gg$ is a scalar glueball field which is absent in this study and B is an orthogonal (3×3) matrix which has three solutions. The solution 1 and 2 from Ref. [79] is:

$$B_1 = \begin{pmatrix} 0.86 & 0.45 & 0.24 \\ -0.45 & 0.89 & -0.06 \\ -0.24 & -0.06 & 0.97 \end{pmatrix}, \quad (6.10)$$

$$B_2 = \begin{pmatrix} 0.81 & 0.54 & 0.19 \\ -0.49 & 0.49 & 0.72 \\ 0.30 & -0.68 & 0.67 \end{pmatrix}, \quad (6.11)$$

and the solution 3 from Ref. [80]:

$$B_3 = \begin{pmatrix} 0.78 & -0.36 & 0.51 \\ -0.54 & 0.03 & 0.84 \\ 0.32 & 0.93 & 0.18 \end{pmatrix}. \quad (6.12)$$

In the solution 1 of Ref. [79] the resonance $f_0(1370)$ is predominantly an $\bar{n}n$ state, the resonance $f_0(1500)$ is predominantly a glueball, and $f_0(1710)$ is predominantly a strange $\bar{s}s$ state. In the solution 2 of Ref. [79] and in the solution of Ref. [80] the resonance $f_0(1370)$ is still predominantly a nonstrange $\bar{n}n$ state, but $f_0(1710)$ is now predominantly a glueball, and $f_0(1500)$ predominantly a strange $\bar{s}s$ state.

Note that the experimental values of the fields are used, which are summarized with the numerical values of the renormalization constants Z_i [110], the vacuum expectation values of σ_N and σ_S which are ϕ_N (3.34) and ϕ_S (3.35), respectively, and the decay constants of pion (f_π) and kaon (f_K) [51] in the following Table 6.1

Observable	Experiment ([51])[MeV]	constants	Value
m_π	137.3 ± 6.9	Z_π	1.709
m_K	495.6 ± 24.8	Z_K	1.604
m_η	547.9 ± 27.4	Z_{K_S}	1.001
$m_{\eta'}$	957.8 ± 47.9	Z_{η_N}	1.709
m_{a_0}	1474 ± 74	Z_{η_S}	1.539
m_{K_S}	893.8 ± 44.7	ϕ_N	158 MeV
$m_{f_1(1370)}$	$(1200 - 1500) - i(150 - 250)$	ϕ_S	138 MeV
$m_{f_1(1500)}$	1505 ± 6	f_π	92.2 MeV
$m_{f_1(1710)}$	1722^{+6}_{-5}	f_K	110 MeV

Table 6.1.: Masses and wave-function renormalization constants.

6.4. Decay widths of a pseudoscalar glueball into (pseudo)scalar mesons

The chiral Lagrangian (6.7) describes the two- and three-body decays of a pseudoscalar glueball, \tilde{G} , into scalar and pseudoscalar mesons. All the decay rates depend on the unknown coupling constant $c_{\tilde{G}\Phi}$. The decay widths for the two- and three-body decays of a pseudoscalar glueball are listed in the following:

Firstly, let us list the two-body decay widths for a pseudoscalar glueball, \tilde{G} . Performing the two-body decay-width calculation Eq.(5.36), the decay widths for every channel can be obtain as follows:

$$\begin{aligned} \Gamma_{\tilde{G} \rightarrow KK^*} &= \Gamma_{\tilde{G} \rightarrow K^- K_0^{*+}} + \Gamma_{\tilde{G} \rightarrow \bar{K}^0 K_0^{*0}} + \Gamma_{\tilde{G} \rightarrow K^0 \bar{K}_0^{*0}} + \Gamma_{\tilde{G} \rightarrow K^+ K_0^{*-}} \\ &= \frac{Z_K^2 \phi_N^2 c_{\tilde{G}\phi}^2}{16 \pi m_{\tilde{G}}^3} [m_{\tilde{G}}^4 + (m_K^2 - m_{K_0^*}^2)^2 - 2(m_K^2 + m_{K_0^*}^2) m_{\tilde{G}}^2]^{1/2}, \end{aligned} \quad (6.13)$$

$$\begin{aligned} \Gamma_{\tilde{G} \rightarrow a_0 \pi} &= \Gamma_{\tilde{G} \rightarrow a_0^0 \pi^0} + \Gamma_{\tilde{G} \rightarrow a_0^+ \pi^-} + \Gamma_{\tilde{G} \rightarrow a_0^- \pi^+} \\ &= \frac{3 Z_\pi^2 \phi_S^2 c_{\tilde{G}\phi}^2}{32 \pi m_{\tilde{G}}^3} [m_{\tilde{G}}^4 + (m_{a_0}^2 - m_\pi^2)^2 - 2(m_{a_0}^2 + m_\pi^2) m_{\tilde{G}}^2]^{1/2}, \end{aligned} \quad (6.14)$$

$$\Gamma_{\tilde{G} \rightarrow \eta \sigma_N} = \frac{Z_{\eta_S}^2 \phi_N^2 c_{\tilde{G}\phi}^2 \sin^2 \varphi}{32 \pi m_{\tilde{G}}^3} [m_{\tilde{G}}^4 + (m_\eta^2 - m_{\sigma_N}^2)^2 - 2(m_\eta^2 + m_{\sigma_N}^2) m_{\tilde{G}}^2]^{1/2}, \quad (6.15)$$

$$\Gamma_{\tilde{G} \rightarrow \eta' \sigma_N} = \frac{Z_{\eta_S}^2 \phi_N^2 c_{\tilde{G}\phi}^2 \cos^2 \varphi}{32 \pi m_{\tilde{G}}^3} [m_{\tilde{G}}^4 + (m_{\eta'}^2 - m_{\sigma_N}^2)^2 - 2(m_{\eta'}^2 + m_{\sigma_N}^2) m_{\tilde{G}}^2]^{1/2}, \quad (6.16)$$

$$\Gamma_{\tilde{G} \rightarrow \eta \sigma_S} = \frac{Z_{\eta_N}^2 \phi_N^2 c_{\tilde{G}\phi}^2 \cos^2 \varphi}{32 \pi m_{\tilde{G}}^3} [m_{\tilde{G}}^4 + (m_\eta^2 - m_{\sigma_S}^2)^2 - 2(m_\eta^2 + m_{\sigma_S}^2) m_{\tilde{G}}^2]^{1/2}, \quad (6.17)$$

$$\Gamma_{\tilde{G} \rightarrow \eta' \sigma_S} = \frac{Z_{\eta_N}^2 \phi_N^2 c_{\tilde{G}\phi}^2 \sin^2 \varphi}{32 \pi m_{\tilde{G}}^3} [m_{\tilde{G}}^4 + (m_{\eta'}^2 - m_{\sigma_S}^2)^2 - 2(m_{\eta'}^2 + m_{\sigma_S}^2) m_{\tilde{G}}^2]^{1/2}. \quad (6.18)$$

Secondly, let us turn to the three-body decay widths for a pseudoscalar glueball, \tilde{G} . We use the three-body decay-width expression Eq.(5.61), which reads in the present case for the decay of \tilde{G} into three pseudoscalar mesons \bar{P}_1 , \bar{P}_2 , and \bar{P}_3 ,

$$\begin{aligned} \Gamma_{\tilde{G} \rightarrow \bar{P}_1 \bar{P}_2 \bar{P}_3} &= \frac{S_{\tilde{G} \rightarrow \bar{P}_1 \bar{P}_2 \bar{P}_3}}{32(2\pi)^3 m_{\tilde{G}}^3} \int_{(m_1+m_2)^2}^{(m_{\tilde{G}}-m_3)^2} |-i\mathcal{M}_{\tilde{G} \rightarrow \bar{P}_1 \bar{P}_2 \bar{P}_3}|^2 dm_{12}^2 \\ &\times \sqrt{\frac{(-m_1 + m_{12} - m_2)(m_1 + m_{12} - m_2)(-m_1 + m_{12+m_2})(m_1 + m_{12} + m_2)}{m_{12}^2}} \\ &\times \sqrt{\frac{(-m_{\tilde{G}} + m_{12} - m_3)(m_{\tilde{G}} + m_{12} - m_3)(-m_{\tilde{G}} + m_{12} + m_3)(m_{\tilde{G}} + m_{12} + m_3)}{m_{12}^2}}, \quad (6.19) \end{aligned}$$

The quantities m_1 , m_2 , m_3 are the masses of \bar{P}_1 , \bar{P}_2 , and \bar{P}_3 , $\mathcal{M}_{\tilde{G} \rightarrow \bar{P}_1 \bar{P}_2 \bar{P}_3}$ is the tree-level decay amplitude, and $S_{\tilde{G} \rightarrow \bar{P}_1 \bar{P}_2 \bar{P}_3}$ is a symmetrization factor (it is equal to 1 if \bar{P}_1 , \bar{P}_2 , and \bar{P}_3 are all different, equal to 2 for two identical particles in the final state, and equal to 6 for three identical particles in the final state). The decay channels can be obtained as follows:

(1) The full decay width into the channel $KK\eta$ results from the sum

$$\Gamma_{\tilde{G} \rightarrow KK\eta} = \Gamma_{\tilde{G} \rightarrow K^0 \bar{K}^0 \eta} + \Gamma_{\tilde{G} \rightarrow K^- K^+ \eta} = 2\Gamma_{\tilde{G} \rightarrow K^- K^+ \eta}, \quad (6.20)$$

with the modulus squared decay amplitude

$$|-i\mathcal{M}_{\tilde{G} \rightarrow K^- K^+ \eta}|^2 = \frac{1}{4} c_{\tilde{G}\Phi}^2 Z_K^2 Z_{\eta_N}^2 \cos^2 \varphi,$$

where $m_1 = m_2 = m_K$ and $m_3 = m_\eta$.

(2) The full decay width into the channel $KK\eta'$ results from the sum

$$\Gamma_{\tilde{G} \rightarrow KK\eta'} = \Gamma_{\tilde{G} \rightarrow K^0 \bar{K}^0 \eta'} + \Gamma_{\tilde{G} \rightarrow K^- K^+ \eta'} = 2\Gamma_{\tilde{G} \rightarrow K^- K^+ \eta'}, \quad (6.21)$$

with the modulus squared decay amplitude

$$|-i\mathcal{M}_{\tilde{G} \rightarrow K^- K^+ \eta'}|^2 = \frac{1}{4} c_{\tilde{G}\Phi}^2 Z_K^2 Z_{\eta_N}^2 \sin^2 \varphi,$$

where $m_1 = m_2 = m_K$, and $m_3 = m_\eta$.

(3) The decay width into the channel $\eta\eta\eta$ has as modulus squared decay amplitude

$$|-i\mathcal{M}_{\tilde{G} \rightarrow \eta\eta\eta}|^2 = \frac{1}{8} c_{\tilde{G}\Phi}^2 Z_{\eta_N}^4 Z_{\eta_S}^2 \cos^4 \varphi \sin^2 \varphi,$$

where $m_1 = m_2 = m_3 = m_\eta$ and the symmetrization factor $S_{\tilde{G} \rightarrow \eta\eta\eta} = 6$.

(4) The decay width into the channel $\eta\eta\eta'$ has as modulus squared decay amplitude

$$|-i\mathcal{M}_{\tilde{G} \rightarrow \eta\eta\eta'}|^2 = \frac{1}{8} c_{\tilde{G}\Phi}^2 Z_{\eta_N}^4 Z_{\eta_S}^2 (\cos^3 \varphi - 2 \cos \varphi \sin^2 \varphi)^2,$$

where $m_1 = m_2 = m_\eta$, $m_3 = m_{\eta'}$ and the symmetrization factor $S_{\tilde{G} \rightarrow \eta\eta\eta'} = 2$.

(5) The decay width into the channel $\eta\eta'\eta'$ has as modulus squared decay amplitude

$$|-i\mathcal{M}_{\tilde{G} \rightarrow \eta\eta'\eta'}|^2 = \frac{1}{8} c_{\tilde{G}\Phi}^2 Z_{\eta_N}^4 Z_{\eta_S}^2 (\sin^3 \varphi - 2 \cos^2 \varphi \sin \varphi)^2,$$

where $m_1 = m_\eta$, $m_2 = m_3 = m_{\eta'}$ and the symmetrization factor $S_{\tilde{G} \rightarrow \eta\eta'\eta'} = 2$.

(6) The full decay width into the channel $\eta\pi\pi$ is computed from the sum

$$\Gamma_{\tilde{G} \rightarrow \eta\pi\pi} = \Gamma_{\tilde{G} \rightarrow \eta\pi^0\pi^0} + \Gamma_{\tilde{G} \rightarrow \eta\pi^-\pi^+} = \frac{3}{2} \Gamma_{\tilde{G} \rightarrow \eta\pi^-\pi^+}, \quad (6.22)$$

with the modulus squared decay amplitude

$$|-i\mathcal{M}_{\tilde{G} \rightarrow \eta\pi^-\pi^+}|^2 = \frac{1}{8} c_{\tilde{G}\Phi}^2 Z_\pi^4 Z_{\eta_S}^2 \sin^2 \varphi,$$

where $m_1 = m_\eta$ and $m_2 = m_3 = m_\pi$.

(7) The full decay width into the channel $\eta'\pi\pi$ is computed from the sum

$$\Gamma_{\tilde{G} \rightarrow \eta'\pi\pi} = \Gamma_{\tilde{G} \rightarrow \eta'\pi^0\pi^0} + \Gamma_{\tilde{G} \rightarrow \eta'\pi^-\pi^+} = \frac{3}{2} \Gamma_{\tilde{G} \rightarrow \eta'\pi^-\pi^+}, \quad (6.23)$$

with the modulus squared decay amplitude

$$|-i\mathcal{M}_{\tilde{G} \rightarrow \eta'\pi^-\pi^+}|^2 = \frac{1}{8} c_{\tilde{G}\Phi}^2 Z_\pi^4 Z_{\eta_S}^2 \cos^2 \varphi,$$

where $m_1 = m_{\eta'}$ and $m_2 = m_3 = m_\pi$.

(8) In the case $\tilde{G} \rightarrow K^-K^+\pi^0$ one has:

$$|-i\mathcal{M}_{\tilde{G} \rightarrow K^-K^+\pi^0}|^2 = \frac{1}{4} c_{\tilde{G}\Phi}^2 Z_K^4 Z_\pi^2,$$

where $m_1 = m_2 = m_K$ and $m_3 = m_{\pi^0}$. Then:

$$\Gamma_{\tilde{G} \rightarrow K^-K^+\pi^0} = 0.00041 c_{\tilde{G}\Phi}^2 [\text{GeV}]. \quad (6.24)$$

The full decay width into the channel $KK\pi$ results from the sum

$$\begin{aligned} \Gamma_{\tilde{G} \rightarrow KK\pi} &= \Gamma_{\tilde{G} \rightarrow K^-K^+\pi^0} + \Gamma_{\tilde{G} \rightarrow K^0\bar{K}^0\pi^0} + \Gamma_{\tilde{G} \rightarrow \bar{K}^0K^+\pi^-} + \Gamma_{\tilde{G} \rightarrow K^0K^-\pi^+} \\ &= 6\Gamma_{\tilde{G} \rightarrow K^-K^+\pi^0}. \end{aligned} \quad (6.25)$$

There exists an interesting and subtle issue: a decay channel which involves some scalar states which decay further into two pseudoscalar ones. For instance, $K_0^* \equiv K_0^*(1430)$ decays into $K\pi$. There are then two possible decay amplitudes for the process $\tilde{G} \rightarrow KK\pi$: one is the direct decay mechanism reported in Table 6.2, and the other is the decay chain $\tilde{G} \rightarrow KK_0^* \rightarrow KK\pi$. The immediate question is, if interference effects emerge which spoil the results presented in Table 6.2 and 6.3. Namely, simply performing the sum of the direct three-body decay (Table 6.2) and the corresponding two-body decay (Table 6.3) is not correct.

We now describe this point in more detail using the neutral channel $\tilde{G} \rightarrow K^0 \bar{K}^0 \pi$ as an illustrative case. To this end, we describe the coupling K_0^* to $K\pi$ via the Lagrangian

$$\mathcal{L}_{K_0^* K \pi} = g K_0^* \bar{K}^0 \pi^0 + \sqrt{2} g K_0^* K^- \pi^+ + h.c. . \quad (6.26)$$

The coupling constant $g = 2.73$ GeV is obtained by using the experimental value for the total decay width $\Gamma_{K_0^*} = 270$ MeV [23]. The full amplitude for the process $\tilde{G} \rightarrow K^0 \bar{K}^0 \pi^0$ will result from the sum

$$\mathcal{M}_{\tilde{G} \rightarrow K^0 \bar{K}^0 \pi^0}^{\text{full}} = \mathcal{M}_{\tilde{G} \rightarrow K^0 \bar{K}^0 \pi^0}^{\text{direct}} + \mathcal{M}_{\tilde{G} \rightarrow \bar{K}^0 K_0^{*0} \rightarrow K^0 \bar{K}^0 \pi^0}^{\text{via } K_0^*} + \mathcal{M}_{\tilde{G} \rightarrow K^0 \bar{K}_0^{*0} \rightarrow K^0 \bar{K}^0 \pi^0}^{\text{via } \bar{K}_0^*} . \quad (6.27)$$

Thus for the decay width we obtain

$$\begin{aligned} \Gamma_{\tilde{G} \rightarrow K^0 \bar{K}^0 \pi^0}^{\text{full}} &= \Gamma_{\tilde{G} \rightarrow K^0 \bar{K}^0 \pi^0}^{\text{direct}} + \Gamma_{\tilde{G} \rightarrow K^0 K_0^{*0} \rightarrow K^0 \bar{K}^0 \pi^0}^{\text{via } K_0^*} + \\ &\Gamma_{\tilde{G} \rightarrow K^0 \bar{K}_0^{*0} \rightarrow K^0 \bar{K}^0 \pi^0}^{\text{via } \bar{K}_0^*} + \Gamma_{\tilde{G} \rightarrow K^0 \bar{K}^0 \pi^0}^{\text{mix}} , \end{aligned} \quad (6.28)$$

where $\Gamma_{\tilde{G} \rightarrow K^0 \bar{K}^0 \pi^0}^{\text{mix}}$ is the sum of all interference terms. We can then investigate the magnitude of the mixing term Γ_{mix} , and thus the error incurred when it is neglected. The explicit calculation for the $K^0 \bar{K}^0 \pi^0$ case gives a relative error of

$$\left| \frac{\Gamma_{\tilde{G} \rightarrow K^0 \bar{K}^0 \pi^0}^{\text{mix}}}{\Gamma_{\tilde{G} \rightarrow K^0 \bar{K}^0 \pi^0}^{\text{direct}} + \Gamma_{\tilde{G} \rightarrow K^0 K_0^{*0} \rightarrow K^0 \bar{K}^0 \pi^0}^{\text{via } K_0^*} + \Gamma_{\tilde{G} \rightarrow K^0 \bar{K}_0^{*0} \rightarrow K^0 \bar{K}^0 \pi^0}^{\text{via } \bar{K}_0^*}} \right| \approx \begin{array}{l} 7.3 \% (g > 0) \\ 2.2 \% (g < 0) \end{array} . \quad (6.29)$$

Present results from the model in Ref. [110] show that $g < 0$: the estimates presented in Ref. [124] may be regarded as upper limits. We thus conclude that the total error for the channel $\tilde{G} \rightarrow K^0 \bar{K}^0 \pi^0$ is not large and can be neglected at this stage. However, in any future, more detailed and precise theoretical calculation, these interference effects should also be taken into account.

6.4.1. Results

The branching ratios of \tilde{G} for the decays into three pseudoscalar mesons are reported in Table 6.2 for both choices of the pseudoscalar masses, 2.6 and 2.37 GeV (relevant for PANDA and BESIII experiments, respectively). The branching ratios are presented relative to the total decay width of the pseudoscalar glueball $\Gamma_{\tilde{G}}^{tot}$.

Quantity	Case (i): $m_{\tilde{G}} = 2.6$ GeV	Case (ii): $m_{\tilde{G}} = 2.37$ GeV
$\Gamma_{\tilde{G} \rightarrow KK\eta} / \Gamma_{\tilde{G}}^{tot}$	0.049	0.043
$\Gamma_{\tilde{G} \rightarrow KK\eta'} / \Gamma_{\tilde{G}}^{tot}$	0.019	0.011
$\Gamma_{\tilde{G} \rightarrow \eta\eta\eta} / \Gamma_{\tilde{G}}^{tot}$	0.016	0.013
$\Gamma_{\tilde{G} \rightarrow \eta\eta\eta'} / \Gamma_{\tilde{G}}^{tot}$	0.0017	0.00082
$\Gamma_{\tilde{G} \rightarrow \eta\eta'\eta'} / \Gamma_{\tilde{G}}^{tot}$	0.00013	0
$\Gamma_{\tilde{G} \rightarrow KK\pi} / \Gamma_{\tilde{G}}^{tot}$	0.47	0.47
$\Gamma_{\tilde{G} \rightarrow \eta\pi\pi} / \Gamma_{\tilde{G}}^{tot}$	0.16	0.17
$\Gamma_{\tilde{G} \rightarrow \eta'\pi\pi} / \Gamma_{\tilde{G}}^{tot}$	0.095	0.090

Table 6.2.: Branching ratios for the decay of the pseudoscalar glueball \tilde{G} into three pseudoscalar mesons.

Next we turn to the decay process $\tilde{G} \rightarrow PS$. The results, for both choices of $m_{\tilde{G}}$, are reported in Table 6.3 for the cases in which the bare resonance σ_S is assigned to $f_0(1710)$ or to $f_0(1500)$.

Quantity	Case (i): $m_{\tilde{G}} = 2.6$ GeV	Case (ii): $m_{\tilde{G}} = 2.37$ GeV
$\Gamma_{\tilde{G} \rightarrow KK_S} / \Gamma_{\tilde{G}}^{tot}$	0.060	0.070
$\Gamma_{\tilde{G} \rightarrow a_0\pi} / \Gamma_{\tilde{G}}^{tot}$	0.083	0.10
$\Gamma_{\tilde{G} \rightarrow \eta\sigma_N} / \Gamma_{\tilde{G}}^{tot}$	0.0000026	0.0000030
$\Gamma_{\tilde{G} \rightarrow \eta'\sigma_N} / \Gamma_{\tilde{G}}^{tot}$	0.039	0.026
$\Gamma_{\tilde{G} \rightarrow \eta\sigma_S} / \Gamma_{\tilde{G}}^{tot}$	0.012 (0.015)	0.0094 (0.017)
$\Gamma_{\tilde{G} \rightarrow \eta'\sigma_S} / \Gamma_{\tilde{G}}^{tot}$	0 (0.0082)	0 (0)

Table 6.3.: Branching ratios for the decay of the pseudoscalar glueball \tilde{G} into a scalar and a pseudoscalar meson. In the last two rows σ_S is assigned to $f_0(1710)$ or to $f_0(1500)$ (values in parentheses).

Note that the results are presented as branching ratios because of the as of yet undetermined coupling constant $c_{\tilde{G}\Phi}$. Concerning the decays involving scalar-isoscalar mesons, one should go beyond the results of Table 6.3 by including the full mixing pattern above 1 GeV, in which the resonances $f_0(1370)$, $f_0(1500)$, and $f_0(1710)$ are mixed states of the

bare quark-antiquark contributions $\sigma_N \equiv |\bar{u}u + \bar{d}d\rangle/\sqrt{2}$, $\sigma_S = \bar{s}s$, and a bare scalar glueball field G . This mixing is described by an orthogonal (3×3) matrix, see Eq. (6.9) [72, 73, 74, 75, 76, 77, 78, 79, 80, 81, 82]. In view of the fact that a complete evaluation of this mixing in the framework of our chiral approach has not yet been done, we use the two solutions for the mixing matrix of Ref. [79] and the solution of Ref. [80] in order to evaluate the decays of the pseudoscalar glueball into the three scalar-isoscalar resonances $f_0(1370)$, $f_0(1500)$, and $f_0(1710)$. In all three solutions $f_0(1370)$ is predominantly described by the bare configuration $\sigma_N \equiv |\bar{u}u + \bar{d}d\rangle/\sqrt{2}$, but the assignments for the other resonances vary: in the first solution of Ref. [79] the resonance $f_0(1500)$ is predominantly gluonic, while in the second solution of Ref. [79] and the solution of Ref. [80] the resonance $f_0(1710)$ has the largest gluonic content. The results for the decay of the pseudoscalar glueball into scalar-isoscalar resonances are reported in Table 6.4.

Quantity	Sol. 1 of Ref. [79]	Sol. 2 of Ref. [79]	Sol. of Ref. [80]
$\Gamma_{\tilde{G} \rightarrow \eta f_0(1370)} / \Gamma_{\tilde{G}}^{tot}$	0.00093 (0.0011)	0.00058 (0.00068)	0.0044 (0.0052)
$\Gamma_{\tilde{G} \rightarrow \eta f_0(1500)} / \Gamma_{\tilde{G}}^{tot}$	0.000046 (0.000051)	0.0082 (0.0090)	0.011 (0.012)
$\Gamma_{\tilde{G} \rightarrow \eta f_0(1710)} / \Gamma_{\tilde{G}}^{tot}$	0.011 (0.0089)	0.0053 (0.0042)	0.00037 (0.00029)
$\Gamma_{\tilde{G} \rightarrow \eta' f_0(1370)} / \Gamma_{\tilde{G}}^{tot}$	0.038 (0.026)	0.033 (0.022)	0.043 (0.029)
$\Gamma_{\tilde{G} \rightarrow \eta' f_0(1500)} / \Gamma_{\tilde{G}}^{tot}$	0.0062 (0)	0.00020 (0)	0.00013 (0)
$\Gamma_{\tilde{G} \rightarrow \eta' f_0(1710)} / \Gamma_{\tilde{G}}^{tot}$	0 (0)	0 (0)	0 (0)

Table 6.4.: Branching ratios for the decays of the pseudoscalar glueball \tilde{G} into η and η' , respectively, and one of the scalar-isoscalar states: $f_0(1370)$, $f_0(1500)$, and $f_0(1710)$ by using three different mixing scenarios of these scalar-isoscalar states reported in Refs [79, 80]. The mass of the pseudoscalar glueball is $m_{\tilde{G}} = 2.6$ GeV and $m_{\tilde{G}} = 2.37$ GeV (values in parentheses), respectively.

In Fig. 6.1 we show the behavior of the total decay width $\Gamma_{\tilde{G}}^{tot} = \Gamma_{\tilde{G} \rightarrow PPP} + \Gamma_{\tilde{G} \rightarrow PS}$ as function of the coupling constant $c_{\tilde{G}\Phi}$ for both choices of the pseudoscalar glueball mass. (We assume here that other decay channels, such as decays into vector mesons or baryons are negligible.) In the case of $m_{\tilde{G}} = 2.6$ GeV, one expects from large- N_c considerations that the total decay width $\Gamma_{\tilde{G}}^{tot} \lesssim 100$ MeV. In fact, as discussed in the Introduction, the scalar glueball candidate $f_0(1500)$ is roughly 100 MeV broad and the tensor candidate $f_J(2220)$ is even narrower. In the present work, the condition $\Gamma_{\tilde{G}}^{tot} \lesssim 100$ MeV implies that $c_{\tilde{G}\Phi} \lesssim 5$. Moreover, in the case of $m_{\tilde{G}} = 2.37$ GeV for which the identification $\tilde{G} \equiv X(2370)$ has been made, we can indeed use the experimental knowledge of the full decay width [$\Gamma_{X(2370)} = 83 \pm 17$ MeV [219, 220, 221]] to determine the coupling constant to be $c_{\tilde{G}\Phi} = 4.48 \pm 0.46$. (However, we also refer to the recent work of Ref. [229], where the possibility of a broad pseudoscalar glueball is discussed.)

Some comments are in order:

(i) The results depend only slightly on the glueball mass. Thus, the two columns of Table 6.2 and 6.3 are similar. It turns out that the channel $KK\pi$ is the dominant one (almost 50%), and also that the $\eta\pi\pi$ and $\eta'\pi\pi$ channels are sizable. On the other hand, the two-body decays are subdominant and reach only 20% of the full mesonic decay width.

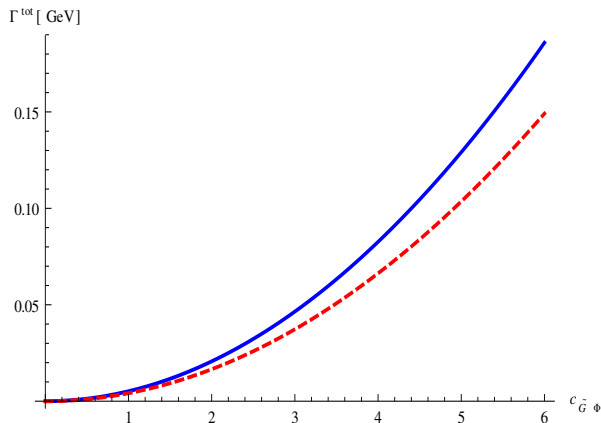


Figure 6.1.: Solid (blue) line: Total decay width of the pseudoscalar glueball with the bare mass $M_{\tilde{G}} = 2.6$ GeV as function of the coupling $c_{\tilde{G}\Phi}$. Dashed (red) line: Same curve for $M_{\tilde{G}} = 2.37$ GeV.

- (ii) The decay of the pseudoscalar glueball into three pions vanishes:

$$\Gamma_{\tilde{G} \rightarrow \pi\pi\pi} = 0. \quad (6.30)$$

This result represents a further testable prediction of our approach.

(iii) The decays of the pseudoscalar glueball into a scalar-isoscalar meson amount only to 5% of the total decay width. Moreover, the mixing pattern in the scalar-isoscalar sector has a negligible influence on the total decay width of \tilde{G} . Nevertheless, in the future it may represent an interesting and additional test for scalar-isoscalar states.

(iv) Once the shifts of the scalar fields have been performed, there are also bilinear mixing terms of the form $\tilde{G}\eta_N$ and $\tilde{G}\eta_S$ which lead to a non-diagonal mass matrix. In principle, one should take these terms into account (in addition to the already-mentioned $\eta_N\eta_S$ mixing) and solve a three-state mixing problem in order to determine the masses of the pseudoscalar particles. This will also affect the calculation of the decay widths. However, due to the large mass difference of the bare glueball fields \tilde{G} in contrast to the other quark-antiquark pseudoscalar fields, the mixing of \tilde{G} turns out to be very small in the present work, and can be safely neglected. For instance, it turns out that the mass of the mixed state which is predominantly glueball is (at most) just 0.002 GeV larger than the bare mass $m_{\tilde{G}} = 2.6$ GeV.

(v) If a standard linear sigma model without (axial-)vector mesons is studied, the replacements $Z_\pi = Z_K = Z_{\eta_N} = Z_{\eta_S} = 1$ need to be performed. Most of the results of the branching ratios for the three-body decay are qualitatively (but not quantitatively) similar to the values of Table 6.2 (variations of about 25-30%). However, the branching ratios for the two-body decay change sizably w.r.t. the results of Table 6.3. This fact shows once more that the inclusion of (axial-)vector degrees of freedom has sizable effects also concerning the decays of the pseudoscalar glueball.

(vi) In principle, the three-body final states for the decays shown in Table 6.2 can also be reached through a sequential decay from the two-body final states shown in Table 6.3, where the scalar particle S further decays into PP , for instance, $K_0^*(1430) \rightarrow K\pi$. There

are then two possible decay amplitudes: One from the direct three-body decay, and one from the sequential decay, which have to be added coherently before taking the modulus square to obtain the total three-body decay width. Summing the results shown in Table 6.2 and 6.3 gives a first estimate (which neglects interference terms) for the magnitude of the total three-body decay width. We have verified that the correction from the interference term to this total three-body decay width in a given channel is at most of the order of 10% for $m_{\tilde{G}} = 2.6$ GeV and 15% for $m_{\tilde{G}} = 2.37$ GeV. For a full understanding of the contribution of the various decay amplitudes to the final three-body state, one needs to perform a detailed study of the Dalitz plot for the three-body decay.

6.5. Interaction of a pseudoscalar glueball with nucleons

In this section we compute the decay width of the pseudoscalar glueball into a nucleon and an antinucleon and we present the result as a branching ratio to remove the effects of the undetermined coupling constant.

A $U(2)_R \times U(2)_L$ Lagrangian of the interaction of a pseudoscalar glueball \tilde{G} with the baryon fields Ψ_1 and Ψ_2 [126, 230] is

$$\mathcal{L}_{\tilde{G}\text{-baryons}}^{int} = i c_{\tilde{G}\Psi} \tilde{G} (\bar{\Psi}_2 \Psi_1 - \bar{\Psi}_1 \Psi_2). \quad (6.31)$$

This interaction Lagrangian (6.31) describes the fusion of a proton and an antiproton, which is hermitian and invariant under $SU(2)_R \times SU(2)_L$, parity ($\tilde{G} \rightarrow -\tilde{G}$), and charge conjugation as proved in Ref. [230]. Now let us write the interaction Lagrangian with the physical fields N and N^* which refer to the nucleon and its partner [230], respectively. By substituting Eqs. (3.15-3.18) into Eq.(6.31), we obtain

$$\begin{aligned} \mathcal{L}_{\tilde{G}\text{-nucleons}}^{int} &= \frac{c_{\tilde{G}\Psi}}{2 \cosh \delta} \tilde{G} (-i\bar{N}\gamma_5 N - i\bar{N}^* N e^\delta - i\bar{N} N^* e^{-\delta} - i\bar{N}^* \gamma_5 N^* \\ &\quad - i\bar{N}\gamma_5 N + i\bar{N} N^* e^\delta + i\bar{N}^* N e^{-\delta} - i\bar{N}^* \gamma_5 N^*) \\ &= \frac{c_{\tilde{G}\Psi}}{2 \cosh \delta} \tilde{G} (-2i\bar{N}\gamma_5 N + i\bar{N} N^* [e^\delta - e^{-\delta}] \\ &\quad + i\bar{N}^* N [e^{-\delta} - e^\delta] - 2i\bar{N}^* \gamma_5 N^*) \\ &= \frac{-i c_{\tilde{G}\Psi}}{\cosh \delta} \tilde{G} (\bar{N}\gamma_5 N + \sinh \delta \bar{N}^* N - \sinh \delta \bar{N} N^* + \bar{N}^* \gamma_5 N^*). \end{aligned} \quad (6.32)$$

We consider first the pseudoscalar field \tilde{G} and the nucleon fields N , N^* , \bar{N} , and \bar{N}^* as confined in a cube of length L and volume $V = L^3$. The four-momenta of \tilde{G} , N , and \bar{N} are denoted as p , k_1 , and k_2 , respectively: From Quantum Mechanics it is known that their 3-momenta are quantized as $\mathbf{p} = 2\pi\mathbf{n}_p/L$, $\mathbf{k}_1 = 2\pi\mathbf{n}_{k_1}/L$, and $\mathbf{k}_2 = 2\pi\mathbf{n}_{k_2}$. Using a Fourier transformation the field operators [230] can be obtained as

$$\tilde{G}(X) = \frac{1}{\sqrt{V}} \sum_{\vec{p}} \frac{1}{\sqrt{2E_p}} (a_p e^{-iP \cdot X} + a_p^\dagger e^{iP \cdot X}), \quad (6.33)$$

$$\bar{N}(X) = \frac{1}{\sqrt{V}} \sum_{\vec{k}_1, s} \sqrt{\frac{m_N}{E_{k_1}}} \left(d_{\vec{k}_1, s} \bar{v}(\vec{p}, s) e^{-iK_1 \cdot X} + b_{\vec{k}_1, s}^\dagger \bar{u}(\vec{k}_1, s) e^{iK_1 \cdot X} \right), \quad (6.34)$$

and

$$N(X) = \frac{1}{\sqrt{V}} \sum_{\vec{k}_2, r} \sqrt{\frac{m_N}{E_{k_2}}} \left(b_{\vec{k}_2, r} u(\vec{k}_2, r) e^{-iK_2 \cdot X} + d_{\vec{k}_2, r}^\dagger v(\vec{k}_2, r) e^{iK_2 \cdot X} \right). \quad (6.35)$$

where, as known from Quantum Field Theory, the glueball and the two fermionic fields were decomposed in terms of annihilation and creation operators, a_p , b , d , and a_p^\dagger , b^\dagger , d^\dagger , respectively.

In Eq. (6.32) the coupling constant $c_{\tilde{G}\Psi}$ cannot be determined, but it is easy to calculate the ratio of the decay of the pseudoscalar glueball \tilde{G} into a nucleon and an antinucleon and of the decay into \bar{N}^* and N [230],

$$Q = \frac{\Gamma_{\tilde{G} \rightarrow \bar{N}N}}{\Gamma_{\tilde{G} \rightarrow \bar{N}^*N+h.c.}} = \frac{\Gamma_{\tilde{G} \rightarrow \bar{N}N}}{2\Gamma_{\tilde{G} \rightarrow \bar{N}^*N}}. \quad (6.36)$$

6.5.1. Decay of a pseudoscalar glueball into two nucleons

Let us calculate the decay process of $\Gamma_{\tilde{G} \rightarrow \bar{N}N}$ which is described by the first term in Eq.(6.32),

$$\mathcal{L}_1 = \frac{-ig}{\cosh \delta} \tilde{G} \bar{N} \gamma_5 N. \quad (6.37)$$

The \tilde{G} resonance represents the initial state $|i\rangle$

$$|i\rangle = a_{\vec{p}}^\dagger |0\rangle, \quad (6.38)$$

whereas the final state is

$$|f\rangle = b_{\vec{k}_1, s'}^\dagger d_{\vec{k}_2, r'}^\dagger |0\rangle, \quad (6.39)$$

The corresponding matrix element of the scattering matrix reads

$$\langle f|S|i\rangle, \quad (6.40)$$

We now calculate the expectation value S_{fi} in terms of the initial and final states:

$$S_{fi} = \langle f|S|i\rangle = \langle f|i \int d^4X \mathcal{L}_1 |i\rangle, \quad (6.41)$$

Inserting Eqs. (6.33), (6.34), (6.35), and (6.37) into (6.41) and performing a time-ordered

product of creation and annihilation operators [230] we obtain

$$\begin{aligned}
\langle f|S|i\rangle &= \frac{-ig\sqrt{m_N^2}}{\cosh\delta V^{\frac{3}{2}}\sqrt{2E_{k_2}E_pE_{k_1}}}\langle 0|b_{\vec{k}_1,s'}^{\rightarrow}d_{\vec{k}_2,r'}^{\rightarrow}\int d^4X \\
&\times\sum_{\vec{p}}\left(a_{\vec{p}}e^{-iP\cdot X}+a_{\vec{p}}^\dagger e^{iP\cdot X}\right) \\
&\times\sum_{\vec{k}_1,s}\left(d_{\vec{k}_1,s}^{\rightarrow}\bar{v}\left(\vec{k}_1,s\right)e^{-iK_1\cdot X}+b_{\vec{k}_1,s}^\dagger\bar{u}\left(\vec{k}_1,s\right)e^{iK_1\cdot X}\right)\gamma_5 \\
&\times\sum_{\vec{k}_2,r}\left(b_{\vec{k}_2,r}^{\rightarrow}u\left(\vec{k}_2,r\right)e^{-iK_2\cdot X}+d_{\vec{k}_2,r}^\dagger v\left(\vec{k}_2,r\right)e^{iK_2\cdot X}\right)a_{\vec{p}'}^\dagger|0\rangle \\
&\propto\langle 0|b_{\vec{k}_1,s'}^{\rightarrow}d_{\vec{k}_2,r'}^{\rightarrow}b_{\vec{k}_1,s}^\dagger d_{\vec{k}_2,r}^\dagger a_{\vec{p}}a_{\vec{p}'}^\dagger e^{-i(P-K_2-K_1)X}\bar{u}\gamma_5 v|0\rangle \\
&\propto\langle 0|b_{\vec{k}_1,s'}^{\rightarrow}d_{\vec{k}_2,r'}^{\rightarrow}b_{\vec{k}_1,s}^\dagger d_{\vec{k}_2,r}^\dagger\left(\delta_{\vec{p}\vec{p}'}+a_{\vec{p}}^\dagger a_{\vec{p}}\right)|0\rangle e^{-i(P-K_2-K_1)X}\bar{u}\gamma_5 v \\
&=\langle 0|\left(\delta_{\vec{k}_1\vec{k}_1}\delta_{ss'}-\delta_{\vec{k}_1,s}^\dagger b_{\vec{k}_1,s'}^{\rightarrow}\right)d_{\vec{k}_2}^{\rightarrow}d_{\vec{k}_2}^\dagger\delta_{\vec{p}\vec{p}'}|0\rangle e^{-i(P-K_2-K_1)X}\bar{u}\gamma_5 v \\
&=\langle 0|\delta_{\vec{k}_1\vec{k}_1}\delta_{ss'}\delta_{\vec{p}\vec{p}'}\left(\delta_{\vec{k}_2\vec{k}_2}\delta_{rr'}-d_{\vec{k}_2,r'}^{\rightarrow}d_{\vec{k}_2,r}^{\rightarrow}\right)|0\rangle e^{-i(P-K_2-K_1)X}\bar{u}\gamma_5 v \\
&=\delta_{\vec{k}_1\vec{k}_1}\delta_{ss'}\delta_{\vec{p}\vec{p}'}\delta_{\vec{k}_2\vec{k}_2}\delta_{rr'}e^{-i(P-K_2-K_1)X}\bar{u}\gamma_5 v. \tag{6.42}
\end{aligned}$$

We therefore obtain

$$\begin{aligned}
\langle f|S|i\rangle &= \frac{m_N}{V^{\frac{3}{2}}\sqrt{2E_{k_2}E_pE_{k_1}}}\int d^4X i\mathcal{M}e^{-i(P-K_2-K_1)X} \\
&= \frac{m_N}{V^{\frac{3}{2}}\sqrt{2E_{k_2}E_pE_{k_1}}}i\mathcal{M}(2\pi)^4\delta^4(K_1+K_2-p), \tag{6.43}
\end{aligned}$$

where V is the volume of the ‘box’ which contains the fields and $i\mathcal{M}$ is the invariant amplitude which is given by

$$i\mathcal{M}\equiv\frac{g}{\cosh\delta}\bar{u}\left(\vec{k}_1,s\right)\gamma_5 v\left(\vec{k}_2,r\right). \tag{6.44}$$

To find the lifetime of \tilde{G} we have to take the square of the amplitude, which is the probability for the process,

$$\begin{aligned}
\langle f|S|i\rangle^2 &= \frac{m_N^2}{V^3 2E_{k_2}E_pE_{k_1}}|i\mathcal{M}|^2(2\pi)^8(\delta^4(K_1+K_2-p))^2 \\
&= \frac{m_N^2}{V^3 2E_pE_{k_1}E_{k_2}}|i\mathcal{M}|^2(2\pi)^4(\delta^4(p-K_1-K_2))^2 Vt, \tag{6.45}
\end{aligned}$$

where

$$(2\pi)^8(\delta^4(K_1+K_2-p))^2=(2\pi)^4(\delta^4(p-K_1-K_2))^2 Vt.$$

This is proved in Sec.5.3. The probability for the decay, when the two particles \bar{N} , N have momenta between $(\mathbf{k}_1, \mathbf{k}_1+d^3k_1)$ and $(\mathbf{k}_2, \mathbf{k}_2+d^3k_2)$, is given by

$$|\langle f|S|i\rangle|^2 V\frac{d^3k_1}{(2\pi)^3}V\frac{d^3k_2}{(2\pi)^3}. \tag{6.46}$$

By integrating over all possible final momenta, summing over all final spin orientations and division by t , one can calculate the decay rate as

$$\Gamma = \frac{m_N^2}{(2\pi)^2} \sum_{r,s} \int d^3k_1 \int d^3k_2 \frac{|i\mathcal{M}|^2}{2E_p E_{k_1} E_{k_2}} \delta^4(P - K_1 + K_2). \quad (6.47)$$

In the rest frame of the decaying particle, $p = (m_{\tilde{G}}, \mathbf{0})$, one finds

$$\delta^4(P - K_1 + K_2) = \delta^3(\mathbf{k}_1 + \mathbf{k}_2) \delta(m_{\tilde{G}} - E_{k_1} - E_{k_2}). \quad (6.48)$$

Solving the integral over d^3k_2 (by using the Dirac delta function) we are left with

$$\Gamma = \frac{m_N^2}{(2\pi)^2} \sum_{r,s} \int d^3k_1 \frac{|i\mathcal{M}|^2}{2E_{k_1}^2 m_{\tilde{G}}} \delta(m_{\tilde{G}} - 2E_{k_1}). \quad (6.49)$$

We can write

$$\delta(m_{\tilde{G}} - 2E_{k_1}) = \frac{m_{\tilde{G}}}{4k_f} \delta(|k_1| - k_f), \quad (6.50)$$

where

$$k_f = \sqrt{\frac{m_{\tilde{G}}^2}{4} - m_N^2} \quad (6.51)$$

is the modulus of the momenta of the outgoing particles. Using the spherical coordinates, $d^3k_1 = d\Omega |k_1|^2 d|k_1|$ and solving the integral over dk_1 , one obtains the decay rate as

$$\Gamma = \frac{m_N^2}{2\pi m_{\tilde{G}}^2} \sum_{r,s} |i\mathcal{M}|^2 k_f. \quad (6.52)$$

For the computation of $\sum_{r,s} |i\mathcal{M}|^2$, one should use the following two identities [230] :

$$\sum_s u_\alpha(\vec{k}, s) \bar{u}_\beta(\vec{k}, s) = \left(\frac{\gamma^\mu K_\mu + m_N}{2m_N} \right)_{\alpha\beta}, \quad (6.53)$$

and

$$\sum_s v_{\alpha\beta}(\vec{k}, s) \bar{v}_\beta(\vec{k}, s) = \left(\frac{-\gamma^\mu K_\mu + m_N}{2m_N} \right)_{\alpha\beta}. \quad (6.54)$$

The averaged modulus squared amplitude will thus be

$$\begin{aligned}
\sum_{r,s} |i\mathcal{M}|^2 &= \frac{g^2}{\cosh^2 \delta} \times \sum_{r,s} \bar{u}(\vec{k}_1, s) \gamma_5 v(\vec{k}_2, r) \left[\bar{u}(\vec{k}_1, s) \gamma_5 v(\vec{k}_2, r) \right]^\dagger \\
&= \frac{g^2}{\cosh^2 \delta} \times - \sum_r (\gamma_5)_{\alpha\beta} v_\beta(\vec{k}_2, r) \bar{v}_\mu(\vec{k}_2, r) \sum_s (\gamma_5)_{\mu\nu} u_\nu(\vec{k}_1, s) \bar{u}_\alpha(\vec{k}_1, s) \\
&= \frac{g^2}{\cosh^2 \delta} \times (\gamma_5)_{\alpha\beta} \left(\frac{-\gamma^\mu K_{2\mu} + m_N}{2m_N} \right)_{\beta\mu} (\gamma_5)_{\mu\nu} \left(\frac{\gamma^\mu K_{1\mu} + m_N}{2m_N} \right)_{\nu\alpha} \\
&= \frac{g^2}{\cosh^2 \delta} \times \text{Tr} \left[\gamma_5 \left(\frac{-\gamma^\mu K_{2\mu} + m_N}{2m_N} \right) \gamma_5 \left(\frac{\gamma^\mu K_{1\mu} + m_N}{2m_N} \right) \right] \\
&= \frac{g^2}{\cosh^2 \delta} \times \frac{1}{4m_N^2} (4K_1 \cdot K_2 + 4m_N^2) \\
&= \frac{g^2}{\cosh^2 \delta} \times \frac{m_G^2 - 2m_N^2 + 2m_N^2}{2m_N^2} \\
&= \frac{g^2}{\cosh^2 \delta} \times \left(\frac{m_G^2}{2m_N^2} \right),
\end{aligned}$$

where

$$K_1 \cdot K_2 = \frac{m_G^2 - 2m_N^2}{2}.$$

Then we obtain the final result of the decay rate $\Gamma_{\tilde{G} \rightarrow \bar{N}N}$ as follows

$$\Gamma_{\tilde{G} \rightarrow \bar{N}N} = \frac{g^2}{4\pi \cosh^2 \delta} k_f. \quad (6.55)$$

Similarly, we now proceed to calculate the rate for the decay process $\tilde{G} \rightarrow \bar{N}^* N$, which is described in Eq.(6.32) by the term

$$\mathcal{L}_2 = \frac{-i \sinh \delta}{\cosh \delta} g \tilde{G} \bar{N}^* N = -\tanh \delta g \tilde{G} \bar{N}^* N. \quad (6.56)$$

The corresponding matrix element can be obtained by

$$\begin{aligned}
S_{fi} &= \langle f|S|i\rangle = \langle f|i \int d^4 X \mathcal{L}_2|i\rangle \\
&= \frac{-ig \tanh \delta \sqrt{m_N m_{N^*}}}{V^{\frac{3}{2}} \sqrt{2E_{k_2} E_p E_{k_1}}} \langle 0|\tilde{b}_{\vec{k}_1, s'} d_{\vec{k}_2, r'} \int d^4 X \\
&\quad \times \sum_{\vec{p}} \left(a_{\vec{p}} e^{-iP \cdot X} + a_{\vec{p}}^\dagger e^{iP \cdot X} \right) \\
&\quad \times \sum_{\vec{k}_1, s} \left(\tilde{d}_{\vec{k}_1, s} \bar{v}(\vec{k}_1, s) e^{-iK_1 \cdot X} + \tilde{b}_{\vec{k}_1, s}^\dagger \bar{u}(\vec{k}_1, s) e^{iK_1 \cdot X} \right) \\
&\quad \times \sum_{\vec{k}_2, r} \left(b_{\vec{k}_2, r} u(\vec{k}_2, r) e^{-iK_2 \cdot X} + d_{\vec{k}_2, r}^\dagger v(\vec{k}_2, r) e^{iK_2 \cdot X} \right) a_{\vec{p}}^\dagger |0\rangle \\
&\propto \delta_{\vec{k}_1 \vec{k}_1} \delta_{s s'} \delta_{\vec{p} \vec{p}} \delta_{\vec{k}_2 \vec{k}_2} \delta_{r r'} \bar{u} v e^{-i(P - K_1 - K_2)X}, \quad (6.57)
\end{aligned}$$

which can be written as:

$$\langle f|S|i\rangle = \frac{\sqrt{m_N m_{N^*}}}{V^{\frac{3}{2}} \sqrt{2E_{k_2} E_p E_{k_1}}} \int d^4 X i\mathcal{M} e^{-i(P-K_2-K_1)X}, \quad (6.58)$$

where

$$i\mathcal{M} \equiv g \tanh \delta \bar{u}(\vec{k}_1, s) v(\vec{k}_2, r). \quad (6.59)$$

The decay rate of the pseudoscalar glueball into $\bar{N}^* N$ is obtained as

$$\Gamma_{\tilde{G} \rightarrow \bar{N}^* N} = \frac{m_{N^*} m_N}{2\pi M^2} \sum_{r,s} |i\mathcal{M}|^2 k'_f, \quad (6.60)$$

where

$$k'_f = \pm \sqrt{\frac{m_{N^*}^4 + m_N^4 + m_{\tilde{G}}^4 - 2m_N^2 m_{N^*}^2 - 2m_{N^*}^2 m_{\tilde{G}}^2 - 2m_N^2 m_{\tilde{G}}^2}{4m_{\tilde{G}}^2}}, \quad (6.61)$$

which is proved in Ref. [230]. The averaged modulus squared decay amplitude is

$$\begin{aligned} \sum_{r,s} |i\mathcal{M}|^2 &= g^2 \tanh^2 \delta \sum_{r,s} \bar{u}(\vec{k}_1, s) v(\vec{k}_2, r) \left[\bar{u}(\vec{k}_1, s) v(\vec{k}_2, r) \right]^\dagger \\ &= - \left(\frac{\gamma^\mu K_{1\mu} + m_{N^*}}{2m_{N^*}} \right)_{\beta\alpha} \left(\frac{-\gamma^\mu K_{2\mu} + m_N}{2m_N} \right)_{\alpha\beta} g^2 \tanh^2 \delta \\ &= -\text{Tr} \left[\left(\frac{\gamma^\mu K_{1\mu} + m_{N^*}}{2m_{N^*}} \right) \left(\frac{-\gamma^\mu K_{2\mu} + m_N}{2m_N} \right) \right] g^2 \tanh^2 \delta \\ &= \frac{1}{4m_N m_{N^*}} (4K_1 \cdot K_2 - 4m_N m_{N^*}) g^2 \tanh^2 \delta \\ &= \frac{1}{2m_N m_{N^*}} \left[m_{\tilde{G}}^2 - (m_N + m_{N^*})^2 \right] g^2 \tanh^2 \delta. \end{aligned} \quad (6.62)$$

We obtain the final result of the decay width $\Gamma_{\tilde{G} \rightarrow \bar{N}^* N}$ as

$$\Gamma_{\tilde{G} \rightarrow \bar{N}^* N} = \frac{g^2 \tanh^2 \delta}{4\pi m_{\tilde{G}}^2} \left[m_{\tilde{G}}^2 - (m_N + m_{N^*})^2 \right] k'_f. \quad (6.63)$$

The mass of the nucleon and its partner are $m_N = 938$ MeV and $m_{N^*} = 1535$ MeV, respectively [23], whereas the mass of the lightest pseudoscalar glueball is predicted from lattice calculations to be about 2.6 GeV. The moduli of the momenta of the outgoing particles are $k_f = 900$ MeV and $k_{f'} = 390.6$ MeV. From Eq.(6.55) and Eq.(6.63) we obtain the branching ratio (6.36) of the pseudoscalar glueball decay processes $\tilde{G} \rightarrow \bar{N}N$ and $\tilde{G} \rightarrow \bar{N}^*N$ [126, 230]:

$$\begin{aligned}
Q &= \frac{\Gamma_{\tilde{G} \rightarrow \bar{N}N}}{2\Gamma_{\tilde{G} \rightarrow \bar{N}^*N}} \\
&= \frac{k_f m_{\tilde{G}}^2}{2 \sinh^2 \delta [m_{\tilde{G}}^2 - (m_N + m_{N^*})] k'_f} \\
&= 1.94,
\end{aligned} \tag{6.64}$$

which can be tested by the upcoming PANDA experiment at the FAIR facility in Darmstadt.

7. Decay of open charmed mesons

7.1. Introduction

Charm physics is an experimentally and theoretically active field of hadronic physics [231]. The study of strong decays of the heavy mesons into light pseudoscalar mesons is useful to classify the charmed states. In this chapter, which is based in the paper [119], we study the strong OZI-dominant decays of the open heavy charmed states into light mesons. In this way, our model acts as a bridge between the high- and low-energy sector of the strong interaction. It turns out that the OZI-dominant decays are in agreement with current experimental results, although the theoretical uncertainties for some of them are still very large. Nevertheless, since our decay amplitudes depend on the parameters of the low-energy sector of the theory, there seems to be an important influence of chiral symmetry in the determination of the decay widths of charmed states. As a by-product of our analysis, we also obtain the value of the charm-anticharm condensate and the values of the weak decay constants of D mesons. Moreover, in the light of our results we shall discuss the interpretation of the enigmatic scalar strange-charmed meson $D_{S0}^*(2317)$ and the axial-vector strange-charmed mesons $D_{S1}(2460)$ and $D_{S1}(2536)$ [59, 189, 190, 191]. We show the explicit form of open-charmed decay widths which were obtained from the Lagrangian (2.145) at tree level. The formulas are organized according to the type of decaying particle. The precise description of the decays of open charmed states is important for the CBM experiment at FAIR.

7.2. Decay widths of open-charmed scalar mesons

In this section we study the phenomenology of the open charmed mesons in the scalar sector. The Lagrangian (2.145) contains two open charmed scalar mesons which are D_0^* and D_{S0}^* . The neutral scalar state D_0^{*0} and the charged $D_0^{*\pm}$ decay into $D\pi$, while the strange-charmed state $D_{S0}^{*\pm}$ decays into DK . The corresponding interaction Lagrangian from Eq.(2.145) for the nonstrange-charmed meson D_0^* with $D\pi$ and the strange-charmed meson with DK has the same structure, as we shall see below. Then, we shall calculate the general decay width of a scalar state in this case.

We consider a generic decay process of a scalar state S into two pseudoscalar states \tilde{P} , i.e., $S \rightarrow \tilde{P}_1 \tilde{P}_2$. The interaction Lagrangian for the neutral scalar state will be given in the following general simple form:

$$\begin{aligned} \mathcal{L}_{SPP} = & A_{SPP} S^0 \tilde{P}_1^0 \tilde{P}_2^0 + B_{SPP} S^0 \partial_\mu \tilde{P}_1^0 \partial^\mu \tilde{P}_2^0 \\ & + C_{SPP} \partial_\mu S^0 \partial^\mu \tilde{P}_1^0 \tilde{P}_2^0 + E_{SPP} \partial_\mu S^0 \tilde{P}_1^0 \partial^\mu \tilde{P}_2^0. \end{aligned} \quad (7.1)$$

Firstly, to calculate the decay amplitude for this process we denote the momenta of S , \tilde{P}_1 , and \tilde{P}_2 as P , P_1 , and P_2 , respectively. Then, (upon substituting $\partial^\mu \rightarrow -iP^\mu$ for the

decaying particles and $\partial^\mu \rightarrow i\tilde{P}_{1,2}^\mu$ for the decay products) we obtain the Lorentz-invariant $S\tilde{P}_1\tilde{P}_2$ decay amplitude $-i\mathcal{M}_{S\rightarrow\tilde{P}_1\tilde{P}_2}$ as

$$-i\mathcal{M}_{S\rightarrow\tilde{P}_1\tilde{P}_2} = i(A_{SPP} - B_{SPP}P_1 \cdot P_2 + C_{SPP}P \cdot P_1 + E_{SPP}P \cdot P_2). \quad (7.2)$$

Using energy momentum conservation on the vertex, $P = P_1 + P_2$, we obtain

$$-i\mathcal{M}_{S\rightarrow\tilde{P}_1\tilde{P}_2} = i[A_{SPP} - B_{SPP}P_1 \cdot P_2 + C_{SPP}(P_1^2 + P_1 \cdot P_2) + E_{SPP}(P_2^2 + P_1 \cdot P_2)]. \quad (7.3)$$

In the decay process, the two pseudoscalar mesons \tilde{P}_1^0 and \tilde{P}_2^0 are on-shell; therefore $P_1^2 = m_{\tilde{P}_1}^2$ and $P_2^2 = m_{\tilde{P}_2}^2$. Moreover,

$$P_1 \cdot P_2 = \frac{P^2 - P_1^2 - P_2^2}{2} \equiv \frac{m_S^2 - m_{\tilde{P}_1}^2 - m_{\tilde{P}_2}^2}{2}. \quad (7.4)$$

Therefore, the decay amplitude (7.3) can be written as

$$\begin{aligned} -i\mathcal{M}_{S\rightarrow\tilde{P}_1\tilde{P}_2} = & i[A_{SPP} + (C_{SPP} + E_{SPP} - B_{SPP})\frac{m_S^2 - m_{\tilde{P}_1}^2 - m_{\tilde{P}_2}^2}{2} \\ & + C_{SPP}m_{\tilde{P}_1}^2 + E_{SPP}m_{\tilde{P}_2}^2]. \end{aligned} \quad (7.5)$$

The decay width $\Gamma_{S\rightarrow\tilde{P}_1\tilde{P}_2}$ then reads

$$\Gamma_{S\rightarrow\tilde{P}_1\tilde{P}_2} = \frac{k(m_S, m_{\tilde{P}_1}, m_{\tilde{P}_2})}{8\pi m_S^2} | -i\mathcal{M}_{S\rightarrow\tilde{P}_1\tilde{P}_2} |^2. \quad (7.6)$$

A non-singlet scalar field will possess also charged decay channels. We then have to consider the contribution of the charged modes from the process $S \rightarrow \tilde{P}_1^\pm \tilde{P}_2^\mp$ to the full decay width. By multiplying the neutral-mode decay width of Eq.(7.6) with an isospin factor I , we obtain

$$\Gamma_{S\rightarrow\tilde{P}_1\tilde{P}_2} = \Gamma_{S\rightarrow\tilde{P}_1^0\tilde{P}_2^0} + \Gamma_{S\rightarrow\tilde{P}_1^\pm\tilde{P}_2^\mp} \equiv I\Gamma_{S\rightarrow\tilde{P}_1\tilde{P}_2}. \quad (7.7)$$

The full decay width can be written as

$$\Gamma_{S\rightarrow\tilde{P}_1\tilde{P}_2} = I \frac{k(m_S, m_{\tilde{P}_1}, m_{\tilde{P}_2})}{8\pi m_S^2} | -i\mathcal{M}_{S\rightarrow\tilde{P}_1\tilde{P}_2} |^2, \quad (7.8)$$

where I is determined from isospin deliberations, or from the interaction Lagrangian of a given decay process.

Note that usually the contribution of the charged modes, is twice the contribution of the neutral modes, which, as we will see in the explicit interaction Lagrangian below, leads us to write the general decay width of S into charged modes, $\tilde{P}_1^\pm \tilde{P}_2^\mp$, as follows:

$$\Gamma_{S\rightarrow\tilde{P}_1^\pm\tilde{P}_2^\mp} = 2 \frac{k(m_S, m_{\tilde{P}_1}, m_{\tilde{P}_2})}{8\pi m_S^2} | -i\mathcal{M}_{S\rightarrow\tilde{P}_1\tilde{P}_2} |^2. \quad (7.9)$$

Using this general structures of the decay process of a scalar into two pseudoscalar states, $S \rightarrow \tilde{P}_1\tilde{P}_2$, in the following we compute the decay width of the nonstrange-charmed scalar state $D_0^{*0,\pm}$ into $D\pi$ and the strange-charmed scalar state $D_{S0}^{*\pm}$ into DK .

7.2.1. Decay Width $D_0^{*0,\pm} \rightarrow D\pi$

Firstly, we study the phenomenology of the scalar doublet charmed mesons $D_0^{*0,\pm}$ which are assigned to $D_0^*(2400)^{0,\pm}$. These open-charmed mesons are known to decay into $D\pi$ [119, 120, 122]. The corresponding interaction Lagrangian from Eq.(2.145), for only the neutral and positively-charged components (the other ones like $D_0^{*0,-}$ possess analogous forms) reads

$$\begin{aligned} \mathcal{L}_{D_0^*D\pi} = & A_{D_0^*D\pi} D_0^{*0} (\bar{D}^0 \pi^0 + \sqrt{2} D^+ \pi^-) + B_{D_0^*D\pi} D_0^{*0} (\partial_\mu \bar{D}^0 \partial^\mu \pi^0 + \sqrt{2} \partial_\mu D^+ \partial^\mu \pi^-) \\ & + C_{D_0^*D\pi} \partial_\mu D_0^{*0} (\pi^0 \partial^\mu \bar{D}^0 + \sqrt{2} \pi^- \partial^\mu D^+) + E_{D_0^*D\pi} \partial_\mu D_0^{*0} (\bar{D}^0 \partial^\mu \pi^0 + \sqrt{2} D^+ \partial^\mu \pi^-) \\ & + A_{D_0^*D\pi} D_0^{*+} (D^- \pi^0 - \sqrt{2} D^0 \pi^-) + B_{D_0^*D\pi} D_0^{*+} (\partial_\mu D^- \partial^\mu \pi^0 - \sqrt{2} \partial_\mu D^0 \partial^\mu \pi^-) \\ & + C_{D_0^*D\pi} \partial_\mu D_0^{*+} (\pi^0 \partial^\mu D^- - \sqrt{2} \pi^- \partial^\mu D^0) + E_{D_0^*D\pi} \partial_\mu D_0^{*+} (D^- \partial^\mu \pi^0 - \sqrt{2} D^0 \partial^\mu \pi^-), \end{aligned} \quad (7.10)$$

where the coefficients read

$$A_{D_0^*D\pi} = -\frac{Z_\pi Z_D Z_{D_0^*0}}{\sqrt{2}} \lambda_2 \phi_C, \quad (7.11)$$

$$\begin{aligned} B_{D_0^*D\pi} = & \frac{Z_\pi Z_D Z_{D_0^*0}}{4} w_{a_1} w_{D_1} [g_1^2 (3\phi_N + \sqrt{2}\phi_C) - 2g_1 \frac{w_{a_1} + w_{D_1}}{w_{a_1} w_{D_1}} \\ & + h_2 (\phi_N + \sqrt{2}\phi_C) - 2h_3 \phi_N], \end{aligned} \quad (7.12)$$

$$C_{D_0^*D\pi} = -\frac{Z_\pi Z_D Z_{D_0^*0}}{2} w_{D^{*0}} w_{D_1} [\sqrt{2} i g_1^2 \phi_C - g_1 \frac{w_{D_1} + i w_{D^{*0}}}{w_{D^{*0}} w_{D_1}} - \sqrt{2} i h_3 \phi_C], \quad (7.13)$$

$$\begin{aligned} E_{D_0^*D\pi} = & \frac{Z_\pi Z_D Z_{D_0^*0}}{4} w_{D^{*0}} w_{a_1} [i g_1^2 (3\phi_N - \sqrt{2}\phi_C) + 2g_1 \frac{w_{a_1} - i w_{D^{*0}}}{w_{D^{*0}} w_{a_1}} \\ & + i h_2 (\phi_N - \sqrt{2}\phi_C) - 2i h_3 \phi_N], \end{aligned} \quad (7.14)$$

$$A_{D_0^*D\pi} = \frac{Z_\pi Z_D Z_{D_0^*}}{\sqrt{2}} \lambda_2 \phi_C, \quad (7.15)$$

$$\begin{aligned} B_{D_0^*D\pi} = & -\frac{Z_\pi Z_D Z_{D_0^*}}{4} w_{a_1} w_{D_1} [g_1^2 (3\phi_N + \sqrt{2}\phi_C) - 2g_1 \frac{w_{a_1} + w_{D_1}}{w_{a_1} w_{D_1}} \\ & + h_2 (\phi_N + \sqrt{2}\phi_C) - 2h_3 \phi_N], \end{aligned} \quad (7.16)$$

$$C_{D_0^*D\pi} = \frac{Z_\pi Z_D Z_{D_0^*}}{2} w_{D^*} w_{D_1} \left[\sqrt{2} i g_1^2 \phi_C - g_1 \frac{w_{D_1} + i w_{D^*}}{w_{D^*} w_{D_1}} - \sqrt{2} i h_3 \phi_C \right], \quad (7.17)$$

$$\begin{aligned} E_{D_0^*D\pi} = & -\frac{Z_\pi Z_D Z_{D_0^*}}{4} w_{D^*} w_{a_1} [i g_1^2 (3\phi_N - \sqrt{2}\phi_C) + 2g_1 \frac{w_{a_1} - i w_{D^*}}{w_{D^*} w_{a_1}} \\ & + i h_2 (\phi_N - \sqrt{2}\phi_C) - 2i h_3 \phi_N]. \end{aligned} \quad (7.18)$$

Note that the parameters w_{D^*} and $w_{D^{*0}}$ are imaginary as shown in Eqs. (4.48) and (4.49), respectively, which means that the coefficients containing the imaginary unit are real. Furthermore the wave-function renormalisation factors $Z_{D_0^{*0}}$ and $Z_{D_0^*}$ are equal, as well as the parameters $w_{D^{*0}}$ and w_{D^*} (for isospin symmetry reasons), which leads to

$$A_{D_0^* D\pi} = A_{D_0^{*0} D\pi}^*, \quad B_{D_0^* D\pi} = B_{D_0^{*0} D\pi}^*, \quad C_{D_0^* D\pi} = C_{D_0^{*0} D\pi}^*, \quad E_{D_0^* D\pi} = E_{D_0^{*0} D\pi}^*.$$

In the interaction Lagrangian (7.10), the considered decays are that of the neutral state D_0^{*0} and the positively charged state D_0^{*+} . Both have two relevant decay channels.

Firstly, let us focus on the decay of D_0^{*0} which decays into neutral modes $D^0\pi^0$ and charged modes $D^+\pi^-$. The explicit expression for the decay process $D_0^{*0} \rightarrow D^0\pi^0$ is similar to Eq.(7.1) as seen in Eq.(7.10); when using Eq.(7.6) upon identifying the mesons S , \tilde{P}_1 , and \tilde{P}_2 with the scalar meson D_0^{*0} , and the pseudoscalar mesons as D^0 and π^0 , respectively. The coefficients A_{SPP} , B_{SPP} , C_{SPP} , and D_{SPP} refer to $A_{D_0^{*0} D\pi}$, $B_{D_0^{*0} D\pi}$, $C_{D_0^{*0} D\pi}$, and $E_{D_0^{*0} D\pi}$, respectively. We then obtain $\Gamma_{D_0^{*0} \rightarrow D^0\pi^0}$ as follows:

$$\begin{aligned} \Gamma_{D_0^{*0} \rightarrow D^0\pi^0} &= \frac{1}{8\pi m_{D_0^{*0}}} \left[\frac{(m_{D_0^{*0}}^2 - m_{D^0}^2 - m_{\pi^0}^2)^2 - 4m_{\pi^0}^2 m_{D^0}^2}{4m_{D_0^{*0}}^4} \right]^{1/2} \\ &\times \left[A_{D_0^{*0} D\pi} + (C_{D_0^{*0} D\pi} + E_{D_0^{*0} D\pi} - B_{D_0^{*0} D\pi}) \frac{m_{D_0^{*0}}^2 - m_{D^0}^2 - m_{\pi^0}^2}{2} \right. \\ &\left. + C_{D_0^{*0} D\pi} m_{D^0}^2 + E_{D_0^{*0} D\pi} m_{\pi^0}^2 \right]^2. \end{aligned} \quad (7.19)$$

The decay width for $D_0^{*0} \rightarrow D^+\pi^-$ has the same expression as (7.19) but is multiplied by an isospin factor 2, which can be seen in Eq.(7.9). All the parameters entering Eqs.(7.19) have been fixed as presented in Tables 4.1, 4.2, and 4.3. The value of $\Gamma_{D_0^{*0} \rightarrow D\pi}$ is then determined as follows:

$$\Gamma_{D_0^*(2400)^0 \rightarrow D\pi} = \Gamma_{D_0^{*0} \rightarrow D^0\pi^0} + \Gamma_{D_0^{*0} \rightarrow D^+\pi^-} \quad (7.20)$$

$$= 139_{-114}^{+243} \text{ MeV}. \quad (7.21)$$

Now let us turn to the positively charged scalar state D_0^{*+} which decays into $D^+\pi^0$ and $D^0\pi^+$. The explicit expression for the decay process $D_0^{*+} \rightarrow D^0\pi^+$ is also similar to Eq.(7.1) as seen in Eq.(7.10), when using Eq.(7.6) (upon identifying the mesons S , \tilde{P}_1 , and \tilde{P}_2 with D_0^{*+} , D^+ , and π^0 , respectively). One may proceed in a similar manner for the decay width of $D_0^{*+} \rightarrow D^0\pi^+$, where an overall isospin factor 2 is also present. Then we obtain the value for $\Gamma_{D_0^{*+} \rightarrow D\pi}$:

$$\Gamma_{D_0^*(2400)^+ \rightarrow D\pi} = \Gamma_{D^+\pi^0} + \Gamma_{D^0\pi^+} \quad (7.22)$$

$$= 51_{-51}^{+182} \text{ MeV}. \quad (7.23)$$

7.2.2. Decay Width $D_{S_0}^{*\pm} \rightarrow DK$

We turn here to the phenomenology of the scalar state $D_{S_0}^{*\pm}$ which is assigned to $D_{S_0}^*(2317)^\pm$. This open strange-charmed meson decays into D^+K^0 and D^0K^+ [119] as known from [51]. The corresponding interaction Lagrangian from Eq.(2.145) reads

$$\begin{aligned}
\mathcal{L}_{D_{S_0}^* DK} = & A_{D_{S_0}^* DK} D_{S_0}^{*+} (D^- \bar{K}^0 + D^0 K^-) + B_{D_{S_0}^* DK} D_{S_0}^{*+} (\partial_\mu D^- \partial^\mu \bar{K}^0 + \partial_\mu D^0 \partial^\mu K^-) \\
& + C_{D_{S_0}^* DK} \partial_\mu D_{S_0}^{*+} (\bar{K}^0 \partial^\mu D^- + \partial_\mu D^0 K^-) + E_{D_{S_0}^* DK} \partial_\mu D_{S_0}^{*+} (D^- \partial^\mu \bar{K}^0 + D^0 \partial^\mu K^-) \\
& + A_{D_{S_0}^* DK} D_{S_0}^{*-} (D^+ K^0 + \bar{D}^0 K^+) + B_{D_{S_0}^* DK} D_{S_0}^{*-} (\partial_\mu D^+ \partial^\mu K^0 + \partial_\mu \bar{D}^0 \partial^\mu K^+) \\
& + C_{D_{S_0}^* DK} \partial_\mu D_{S_0}^{*-} (K^0 \partial^\mu D^+ + \partial_\mu \bar{D}^0 K^+) + E_{D_{S_0}^* DK} \partial_\mu D_{S_0}^{*-} (D^+ \partial^\mu K^0 + \bar{D}^0 \partial^\mu K^+),
\end{aligned} \tag{7.24}$$

with the following coefficients

$$A_{D_{S_0}^* DK} = \frac{Z_K Z_D Z_{D_{S_0}^*}}{\sqrt{2}} \lambda_2 \left[\phi_N + \sqrt{2}(\phi_S - \phi_C) \right], \tag{7.25}$$

$$\begin{aligned}
B_{D_{S_0}^* DK} = & \frac{Z_K Z_D Z_{D_{S_0}^*}}{2} w_{K_1} w_{D_1} \left[-\sqrt{2} g_1 \frac{w_{K_1} + w_{D_1}}{w_{K_1} w_{D_1}} \right. \\
& \left. + \sqrt{2}(g_1^2 - h_3) \phi_N + (g_1^2 + h_2)(\phi_S + \phi_C) \right],
\end{aligned} \tag{7.26}$$

$$\begin{aligned}
C_{D_{S_0}^* DK} = & \frac{Z_K Z_D Z_{D_{S_0}^*}}{2} w_{D_1} w_{D_S^*} \left[\sqrt{2} g_1 \frac{w_{D_1} + i w_{D_S^*}}{w_{D_1} w_{D_S^*}} - \frac{i}{\sqrt{2}} (g_1^2 + h_2) \phi_N \right. \\
& \left. + i(g_1^2 + h_2) \phi_S + 2i(h_3 - g_1^2) \phi_C \right],
\end{aligned} \tag{7.27}$$

$$\begin{aligned}
E_{D_{S_0}^* DK} = & \frac{Z_K Z_D Z_{D_{S_0}^*}}{2} w_{K_1} w_{D_S^*} \left[\sqrt{2} g_1 \frac{w_{K_1} - i w_{D_S^*}}{w_{K_1} w_{D_S^*}} + \frac{i}{\sqrt{2}} (g_1^2 + h_2) \phi_N \right. \\
& \left. - + 2i(g_1^2 - h_3) \phi_S i(g_1^2 + h_2) \phi_C \right].
\end{aligned} \tag{7.28}$$

As seen in Eq.(7.24) the explicit expression of $D_{S_0}^{*-}$ has a form analogous to that of $D_{S_0}^{*+}$ for isospin symmetry reasons. The decay width of the process $D_{S_0}^{*+} \rightarrow D^+ K^0$ is obtained from Eq.(7.8) when using Eq.(7.5) upon identifying S , \tilde{P}_1 , and \tilde{P}_2 with $D_{S_0}^{*+}$, D^+ , and K^0 and upon replacing $A_{SPP} \rightarrow A_{D_{S_0}^* DK}$, $B_{SPP} \rightarrow B_{D_{S_0}^* DK}$, $C_{SPP} \rightarrow C_{D_{S_0}^* DK}$, $E_{SPP} \rightarrow E_{D_{S_0}^* DK}$. The decay width for the process $D_{S_0}^{*+} \rightarrow D^0 K^+$ has an analogous analytic expression. The full decay width of $D_{S_0}^*$ with a mass of about 2467 MeV into DK [119], see Table 4.5, is then

$$\Gamma_{D_{S_0}^* \rightarrow DK} \simeq 3 \text{ GeV}.$$

7.3. Decay widths of open-charmed vector mesons

In this section we describe the phenomenology of open-charmed vector mesons $D^{*0,+}$. The neutral state D^{*0} is assigned to $D^*(2007)^0$ while the positively charged state D^{*+} to $D^*(2010)^+$. These resonances decay into two pseudoscalar states $D\pi$ [51]. Let us now consider the decay of a vector state V into two pseudoscalar states \tilde{P} , i.e., $V \rightarrow \tilde{P}_1 \tilde{P}_2$, in general. The general simple form of the interaction Lagrangian, as obtained from Eq.(2.145), reads

$$\mathcal{L}_{VPP} = A_{VPP} V_\mu^0 \tilde{P}_1^0 \partial^\mu \tilde{P}_2^0 + B_{VPP} V_\mu^0 \partial^\mu \tilde{P}_1^0 \tilde{P}_2^0 + C_{VPP} \partial_\nu V_\mu^0 (\partial^\nu \tilde{P}_1^0 \partial^\mu \tilde{P}_2^0 - \partial^\mu \tilde{P}_1^0 \partial^\nu \tilde{P}_2^0). \quad (7.29)$$

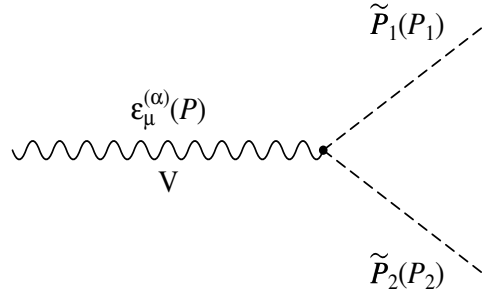


Figure 7.1.: Decay process $V \rightarrow \tilde{P}_1 \tilde{P}_2$

We denote the momenta of V , \tilde{P}_1 , and \tilde{P}_2 as P , P_1 , and P_2 , respectively, and compute the decay amplitude for this process. We consider the polarization vector $\varepsilon_\mu^{(\alpha)}(P)$ for the vector state. Then, upon substituting $\partial^\mu \rightarrow -iP^\mu$ for the decaying particle and $\partial^\mu \rightarrow iP_{1,2}^\mu$ for the decay products, we obtain the following Lorentz-invariant $V\tilde{P}_1\tilde{P}_2$ scattering amplitude $-i\mathcal{M}_{V\rightarrow\tilde{P}_1\tilde{P}_2}^{(\alpha)}$ from the Lagrangian (7.29):

$$-i\mathcal{M}_{V\rightarrow\tilde{P}_1\tilde{P}_2}^{(\alpha)} = \varepsilon_\mu^{(\alpha)}(P) h_{VPP}^\mu, \quad (7.30)$$

with

$$h_{VPP}^\mu = -\{A_{VPP} P_2^\mu + B_{VPP} P_1^\mu + C_{VPP} [P_2^\mu (P \cdot P_1) - P_1^\mu (P \cdot P_2)]\}, \quad (7.31)$$

where h_{VPP}^μ denotes the $V\tilde{P}_1\tilde{P}_2$ vertex.

The calculation of the decay width requires the determination of the modulus square of the scattering amplitude. The scattering amplitude in Eq. (7.30) depends on the polarization vector $\varepsilon_\mu^{(\alpha)}(P)$.

For a general scattering amplitude, one has to calculate $|\overline{-i\mathcal{M}_{V\rightarrow\tilde{P}_1\tilde{P}_2}}|^2$ of a process containing one vector state with mass m_V . The calculation reads as follows:

$$-i\mathcal{M}_{V\rightarrow\tilde{P}_1\tilde{P}_2}^{(\alpha)} = \varepsilon_\mu^{(\alpha)}(P)h_{VPP}^\mu \Rightarrow \quad (7.32)$$

$$\begin{aligned} \Rightarrow |\overline{-i\mathcal{M}_{V\rightarrow\tilde{P}_1\tilde{P}_2}}|^2 &= \frac{1}{3} \sum_{\alpha=1}^3 | -i\mathcal{M}_{V\rightarrow\tilde{P}_1\tilde{P}_2}^{(\alpha)} |^2 \\ &= \frac{1}{3} \sum_{\alpha=1}^3 \varepsilon_\mu^{(\alpha)}(P)\varepsilon_\nu^{(\alpha)}(P)h_{VPP}^\mu h_{VPP}^\nu \\ &= \frac{1}{3} \left(-g_{\mu\nu} + \frac{P_\mu P_\nu}{m^2} \right) h_{VPP}^\mu h_{VPP}^\nu \\ &= \frac{1}{3} \left[- (h_{VPP}^\mu)^2 + \frac{(P_\mu h_{VPP}^\mu)^2}{m_V^2} \right], \end{aligned} \quad (7.33)$$

where

$$\sum_{\alpha=1}^3 \varepsilon_\mu^{(\alpha)}(P)\varepsilon_\nu^{(\alpha)}(P) = -g_{\mu\nu} + \frac{P_\mu P_\nu}{m_V^2}. \quad (7.34)$$

Eq.(7.33) contains the metric tensor $g_{\mu\nu} = \text{diag}(1, -1, -1, -1)$. Note that, if the vector particle decays, then $P_\mu = (m_V, 0)$ in the rest frame of the decaying particle and thus

$$\frac{(P_\mu h^\mu)^2}{m_V^2} \equiv \frac{(m_V h^0)^2}{m_V^2} = (h^0)^2. \quad (7.35)$$

Therefore, we have to calculate the squared vertex $(h_{VPP}^\mu)^2$ using Eq.(7.31):

$$\begin{aligned} (h_{VPP}^\mu)^2 &= A_{VPP}^2 m_{\tilde{P}_2}^2 + B_{VPP}^2 m_{\tilde{P}_1}^2 + C_{VPP}^2 [P_2^\mu (P \cdot P_1) - P_1^\mu (P \cdot P_2)]^2 \\ &\quad + 2A_{VPP} B_{VPP} P_1 \cdot P_2 + 2A_{VPP} C_{VPP} [(P \cdot P_1) m_{\tilde{P}_2}^2 - (P_1 \cdot P_2)(P \cdot P_2)] \\ &\quad + 2B_{VPP} C_{VPP} [(P_1 \cdot P_2)(P \cdot P_1) - (P \cdot P_2) m_{\tilde{P}_1}^2]. \end{aligned} \quad (7.36)$$

Now let us compute the squared vertex at rest (also using Eq. (7.31)):

$$\begin{aligned} (h_{VPP}^0)^2 &= A_{VPP}^2 E_{\tilde{P}_2}^2 + B_{VPP}^2 E_{\tilde{P}_1}^2 + C_{VPP}^2 [E_{\tilde{P}_2}(P \cdot P_1) - E_{\tilde{P}_1}(P \cdot P_2)]^2 \\ &\quad + 2A_{VPP} B_{VPP} E_{\tilde{P}_1} E_{\tilde{P}_2} + 2A_{VPP} C_{VPP} [(P \cdot P_1) E_{\tilde{P}_2}^2 - E_{\tilde{P}_1} E_{\tilde{P}_2} (P \cdot P_2)] \\ &\quad + 2B_{VPP} C_{VPP} [E_{\tilde{P}_1} E_{\tilde{P}_2} (P \cdot P_1) - (P \cdot P_2) E_{\tilde{P}_1}^2]. \end{aligned} \quad (7.37)$$

From Eqs. (7.33), (7.36), and (7.37) we obtain

$$\begin{aligned}
|\overline{-i\mathcal{M}_{V\rightarrow PP}}|^2 &= \frac{1}{3}\{(A_{VPP}^2 + B_{VPP}^2)k^2(m_V, m_{\tilde{P}_2}, m_{\tilde{P}_1}) \\
&\quad + C_{VPP}^2\{k^2(m_V, m_{\tilde{P}_1}, m_{\tilde{P}_1})[(P \cdot P_1)^2 + (P \cdot P_2)^2] \\
&\quad - 2(P \cdot P_1)(P \cdot P_2)(E_{\tilde{P}_1} E_{\tilde{P}_2} - P_1 \cdot P_2)\} \\
&\quad + 2A_{VPP}B_{VPP}(E_{\tilde{P}_1} E_{\tilde{P}_2} - P_1 \cdot P_2) \\
&\quad + 2A_{VPP}C_{VPP}[k^2(m_V, m_{\tilde{P}_2}, m_{\tilde{P}_2})P \cdot P_1 - (P \cdot P_2)(E_{\tilde{P}_1} E_{\tilde{P}_2} - P_1 \cdot P_2)] \\
&\quad + 2B_{VPP}C_{VPP}[(P \cdot P_1)(E_{\tilde{P}_1} E_{\tilde{P}_2} - P_1 \cdot P_2) - k^2(m_V, m_{\tilde{P}_2}, m_{\tilde{P}_1})(P \cdot P_2)]\} \\
&= \frac{1}{3}\{\{A_{VPP}^2 + B_{VPP}^2 + C_{VPP}^2[(P \cdot P_1)^2 + (P \cdot P_2)^2] \\
&\quad + 2C_{VPP}[A_{VPP}(P \cdot P_1) - B_{VPP}(P \cdot P_2)]\}k^2(m_V, m_{\tilde{P}_2}, m_{\tilde{P}_1}) \\
&\quad + 2\{A_{VPP}B_{VPP} - C_{VPP}^2(P \cdot P_1)(P \cdot P_2) + C_{VPP}(B_{VPP}P \cdot P_1 \\
&\quad - A_{VPP}P \cdot P_2)\}(E_{\tilde{P}_1} E_{\tilde{P}_2} - P_1 \cdot P_2)\} . \tag{7.38}
\end{aligned}$$

The vertex h_{VPP}^μ from Eq.(7.31) can be transformed as

$$\begin{aligned}
h_{VPP}^\mu &= -[A_{VPP}P_2^\mu + B_{VPP}P_1^\mu + C_{VPP}(m_V E_{\tilde{P}_1} P_2^\mu - m_V E_{\tilde{P}_2} P_1^\mu)] \\
&= -(B_{VPP} - C_{VPP}m_V E_{\tilde{P}_2})P_1^\mu - (A_{VPP} + C_{VPP}m_V E_{\tilde{P}_1})P_2^\mu , \tag{7.39}
\end{aligned}$$

where

$$P_1 \cdot P = m_V E_{\tilde{P}_1} \quad \text{and} \quad P_2 \cdot P = m_V E_{\tilde{P}_2} . \tag{7.40}$$

We can then write Eq.(7.38) in a slightly different (but equivalent) form, by inserting Eq.(7.39) into Eq. (7.33) as follows:

$$\begin{aligned}
|\overline{-i\mathcal{M}_{V\rightarrow PP}}|^2 &= \frac{1}{3}\{-(B_{VPP} - C_{VPP}m_V E_{\tilde{P}_2})P_1^\mu + (A_{VPP} + C_{VPP}m_V E_{\tilde{P}_1})P_2^\mu\}^2 \\
&\quad + \frac{1}{m_V^2}\{(B_{VPP} - C_{VPP}m_V E_{\tilde{P}_2})P_{1\mu}P^\mu \\
&\quad + (A_{VPP} + C_{VPP}m_V E_{\tilde{P}_1})P_{2\mu}P^\mu\}^2 . \tag{7.41}
\end{aligned}$$

Using Eq.(7.40), $k^2(m_V, m_{\tilde{P}_2}, m_{\tilde{P}_1}) = E_{\tilde{P}_2}^2 - m_{\tilde{P}_2}^2$, and $k^2(m_V, m_{\tilde{P}_2}, m_{\tilde{P}_1}) = E_{\tilde{P}_1}^2 - m_{\tilde{P}_1}^2$, we obtain that Eq.(7.41) can be written as

$$\begin{aligned}
|\overline{-i\mathcal{M}_{V\rightarrow \tilde{P}_1 \tilde{P}_2}}|^2 &= \frac{1}{3}[(B_{VPP} - C_{VPP}m_V E_{\tilde{P}_2})^2 + (A_{VPP} + C_{VPP}m_V E_{\tilde{P}_1})^2 \\
&\quad - 2(A_{VPP} + C_{VPP}m_V E_{\tilde{P}_1})(B_{VPP} - C_{VPP}m_V E_{\tilde{P}_2})]k^2(m_V, m_{\tilde{P}_2}, m_{\tilde{P}_1}) \\
&= \frac{1}{3}[A_{VPP} - B_{VPP} + C_{VPP}m_V(E_{\tilde{P}_1} + E_{\tilde{P}_2})]^2 k^2(m_V, m_{\tilde{P}_2}, m_{\tilde{P}_1}) \\
&= \frac{1}{3}(A_{VPP} - B_{VPP} + C_{VPP}m_V^2)^2 k^2(m_V, m_{\tilde{P}_2}, m_{\tilde{P}_1}) . \tag{7.42}
\end{aligned}$$

The decay width for a vector meson decaying into two pseudoscalar mesons $\Gamma_{V \rightarrow \tilde{P}_1 \tilde{P}_2}$ (as obtained from Eq. (7.29)) can be computed with the following formula:

$$\Gamma_{V \rightarrow \tilde{P}_1 \tilde{P}_2} = I \frac{k(m_V, m_{\tilde{P}_2}, m_{\tilde{P}_1})}{8\pi m_V^2} |-i\mathcal{M}_{V \rightarrow \tilde{P}_1 \tilde{P}_2}|^2, \quad (7.43)$$

where I is an isospin factor and the modulus square of the decay amplitude $|-i\bar{\mathcal{M}}_{V \rightarrow \tilde{P}_1 \tilde{P}_2}|^2$ is given in Eq. (7.42) or, equivalently, Eq. (7.38). Now let us apply this result to calculate the decay width of the vector meson $D^{*0,+}$ into $D\pi$ from the Lagrangian (2.145).

7.3.1. Decay Width $D^{*0,\pm} \rightarrow D\pi$

The $D^*D\pi$ interaction Lagrangian from Eq.(2.145) reads

$$\begin{aligned} \mathcal{L}_{D^*D\pi} = & A_{D^*D\pi} D_\mu^{*0} (\pi^0 \partial^\mu \bar{D}^0 + \sqrt{2} \pi^- \partial^\mu D^+) + B_{D^*D\pi} D_\mu^{*0} (\bar{D}^0 \partial^\mu \pi^0 + \sqrt{2} D^+ \partial^\mu \pi^-) \\ & + C_{D^*D\pi} \partial_\nu D_\mu^{*0} (\partial^\mu \bar{D}^0 \partial^\nu \pi^0 + \sqrt{2} \partial^\mu D^+ \partial^\nu \pi^-) \\ & + C_{D^*D\pi}^* \partial_\nu D_\mu^{*0} (\partial^\mu \pi^0 \partial^\nu \bar{D}^0 + \sqrt{2} \partial^\mu \pi^- \partial^\nu D^+) \\ & + A_{D^*D\pi}^* \bar{D}_\mu^{*0} (\pi^0 \partial^\mu D^0 + \sqrt{2} \pi^+ \partial^\mu D^-) + B_{D^*D\pi}^* \bar{D}_\mu^{*0} (D^0 \partial^\mu \pi^0 + \sqrt{2} D^- \partial^\mu \pi^+) \\ & + C_{D^*D\pi}^* \partial_\nu \bar{D}_\mu^{*0} (\partial^\mu D^0 \partial^\nu \pi^0 + \sqrt{2} \partial^\mu D^- \partial^\nu \pi^+) \\ & + C_{D^*D\pi} \partial_\nu \bar{D}_\mu^{*0} (\partial^\mu \pi^0 \partial^\nu D^0 + \sqrt{2} \partial^\mu \pi^+ \partial^\nu D^-) \\ & + A_{D^*D\pi} D_\mu^{*+} (\pi^0 \partial^\mu D^- - \sqrt{2} \pi^- \partial^\mu D^0) + B_{D^*D\pi} D_\mu^{*+} (D^- \partial^\mu \pi^0 - \sqrt{2} D^0 \partial^\mu \pi^-) \\ & + C_{D^*D\pi} \partial_\nu D_\mu^{*+} (\partial^\mu D^- \partial^\nu \pi^0 - \sqrt{2} \partial^\mu D^0 \partial^\nu \pi^-) \\ & + C_{D^*D\pi}^* \partial_\nu D_\mu^{*+} (\partial^\mu \pi^0 \partial^\nu D^- - \sqrt{2} \partial^\mu \pi^- \partial^\nu D^0) \\ & + A_{D^*D\pi}^* D_\mu^{*-} (\pi^0 \partial^\mu D^+ - \sqrt{2} \pi^+ \partial^\mu \bar{D}^0) + B_{D^*D\pi}^* D_\mu^{*-} (D^+ \partial^\mu \pi^0 - \sqrt{2} \bar{D}^0 \partial^\mu \pi^+) \\ & + C_{D^*D\pi}^* \partial_\nu D_\mu^{*-} (\partial^\mu D^+ \partial^\nu \pi^0 - \sqrt{2} \partial^\mu \bar{D}^0 \partial^\nu \pi^+) \\ & + C_{D^*D\pi} \partial_\nu D_\mu^{*-} (\partial^\mu \pi^0 \partial^\nu D^+ - \sqrt{2} \partial^\mu \pi^+ \partial^\nu \bar{D}^0), \end{aligned} \quad (7.44)$$

with the following coefficients

$$A_{D^*D\pi} = \frac{i}{2} Z_\pi Z_D \left[g_1 + \sqrt{2} w_{D_1} (h_3 - g_1^2) \phi_C \right], \quad (7.45)$$

$$B_{D^*D\pi} = -\frac{i}{4} Z_\pi Z_D \left[2g_1 - w_{a_1} (3g_1^2 + h_2 - 2h_3) \phi_N + \sqrt{2} w_{a_1} (g_1^2 + h_2) \phi_C \right], \quad (7.46)$$

$$C_{D^*D\pi} = \frac{i}{2} Z_\pi Z_D w_{a_1} w_{D_1} g_2. \quad (7.47)$$

Note that the Lagrangian in Eq. (7.44) contains the parameter combinations $A_{D^*D\pi}$, $B_{D^*D\pi}$, and $C_{D^*D\pi}$ and their complex conjugates. Thus, it is certain that the Lagrangian is hermitian; so we obtain $\mathcal{L}_{D^*D\pi}^\dagger = \mathcal{L}_{D^*D\pi}$.

In the following we will focus only on the decays $D^{*0} \rightarrow D\pi$ and $D^{*+} \rightarrow D\pi$, where the corresponding decay of \bar{D}^{*0} and $D^{*-} \rightarrow D\pi$ yields the same result due to isospin symmetry.

The interaction Lagrangian (7.44) has two decay channels for the neutral charmed-vector meson D^{*0} , which are $D^{*0} \rightarrow D^0\pi^0$ and $D^{*0} \rightarrow D^+\pi^-$. We have to note that the decay of D^{*0} into $D^+\pi^-$ is impossible because, in this situation, the sum of the decay product masses is larger than the mass of the decay particle, so

$$\Gamma_{D^{*0} \rightarrow D^+\pi^-} = 0.$$

This result shows very good agreement with the experiment result: experimentally it is not seen, as listed by the Particle Data Group [51]. Then the decay of the neutral state D^{*0} into the neutral modes $D^0\pi^0$ is the only possible decay in the eLSM (2.145). To compute $\Gamma_{D^{*0} \rightarrow D^0\pi^0}$, we use Eqs. (7.42) and (7.43) upon identifying V , \tilde{P}_1 , and \tilde{P}_2 with D^{*0} , π^0 , and D^0 and the coefficients A_{VPP} , B_{VPP} , and C_{VPP} with $A_{D^*D\pi}$, $B_{D^*D\pi}$, and $C_{D^*D\pi}$, respectively. We then obtain the corresponding expression

$$\Gamma_{D^{*0} \rightarrow D^0\pi^0} = \frac{1}{24\pi} \left[\frac{(m_{D^{*0}}^2 - m_{\pi^0}^2 - m_{D^0}^2)^2 - 4m_{\pi^0}^2 m_{D^0}^2}{4m_{D^{*0}}^4} \right]^{3/2} \times (A_{D^*D\pi} - B_{D^*D\pi} + C_{D^*D\pi} m_{D^{*0}}^2)^2. \quad (7.48)$$

The parameters entering Eq.(7.44) have been determined uniquely from the fit (see Tables 4.1, 4.2, and 4.3). Therefore we can calculate the value of the decay width immediately:

$$\Gamma_{D^{*(2007)0} \rightarrow D^0\pi^0} = (0.025 \pm 0.003)\text{MeV}, \quad (7.49)$$

where the experimental value reads $\Gamma_{D^{*(2007)0} \rightarrow D^0\pi^0}^{\text{exp}} < 1.3 \text{ MeV}$ as listed in Ref. [51].

Now let us turn to the phenomenology of the positively charged state $D^{*(2010)+}$, which can decay into $D^0\pi^+$ and $D^+\pi^0$. The decay width of the channel $D^{*(2010)+} \rightarrow D^0\pi^+$ has an analogous analytic expression as $\Gamma_{D^{*0} \rightarrow D^0\pi^0}$, which is described in Eq.(7.48), whereas concerning the decay $D^{*(2010)+} \rightarrow D^+\pi^0$ Eq. (7.48) holds upon multiplication with an isospin factor 2. We then obtain the following results:

$$\Gamma_{D^{*(2010)+} \rightarrow D^+\pi^0} = (0.018_{-0.003}^{+0.002}) \text{MeV}, \quad (7.50)$$

$$\Gamma_{D^{*(2010)+} \rightarrow D^0\pi^+} = (0.038_{-0.004}^{+0.005}) \text{MeV}. \quad (7.51)$$

The experimental values [51] read

$$\Gamma_{D^{*(2010)+} \rightarrow D^+\pi^0}^{\text{exp}} = (0.029 \pm 0.008)\text{MeV}$$

and

$$\Gamma_{D^{*(2010)+} \rightarrow D^0\pi^+}^{\text{exp}} = (0.065 \pm 0.017)\text{MeV}.$$

7.4. Decay widths of open charmed axial-vector mesons

In this section we turn to the study of the phenomenology of axial-vector charmed mesons, i.e., the two- and three-body decays of D_1 and the two-body decays of the strange D_{S1} . The nonstrange-charmed field D_1 corresponds to the resonances $D_1(2420)^{0,\pm}$ while the strange-charmed doublet D_{S1}^\pm is assigned to the resonance $D_{S1}(2536)^\pm$. Firstly let us focus on the two-body decays of the axial-vector charmed mesons D_1, D_{S1} . The nonstrange-charmed D_1 decays into vector-charmed and light pseudoscalar mesons, $D_1 \rightarrow D^*\pi$, while the strange-charmed doublet D_{S1} decays into D^*K , which also contains a vector-charmed meson and a light pseudoscalar meson. Therefore, both decays have the same structure of the corresponding expression for the decay amplitude. This leads us to consider the general case of the two-body decay process of an axial-vector meson A into a vector V and a pseudoscalar state \tilde{P} , i.e., $A \rightarrow V\tilde{P}$. The following interaction Lagrangian describes the decay of the axial-vector state into neutral modes:

$$\begin{aligned} \mathcal{L}_{AV\tilde{P}} = & A_{AV\tilde{P}} A^{\mu 0} V_\mu^0 \tilde{P}^0 \\ & + B_{AV\tilde{P}} [A^{\mu 0} (\partial_\nu V_\mu^0 - \partial_\mu V_\nu^0) \partial^\nu \tilde{P}^0 + \partial^\nu A^{\mu 0} (V_\nu^0 \partial_\mu \tilde{P}^0 - V_\mu^0 \partial_\nu \tilde{P}^0)] . \end{aligned} \quad (7.52)$$

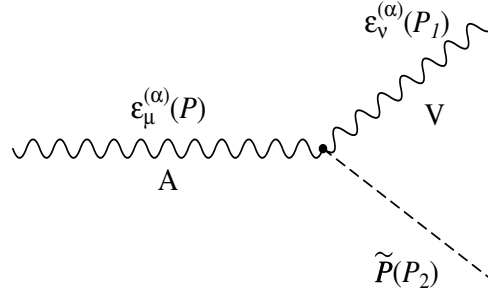


Figure 7.2.: Decay process $A \rightarrow V\tilde{P}$.

Let us study a generic decay process of the form $A \rightarrow V^0\tilde{P}^0$. The 4-momenta of $A, V,$ and \tilde{P} are denoted as $P, P_1,$ and $P_2,$ respectively. We have to consider the corresponding polarization vectors because there are two vector states involved in the decay process $A \rightarrow V^0\tilde{P}^0$, i.e., A and V . These we denote as $\varepsilon_\mu^{(\alpha)}(P)$ for A and $\varepsilon_\nu^{(\beta)}(P_1)$ for V . Using the substitutions $\partial^\mu \rightarrow -iP^\mu$ for the decaying particle and $\partial^\mu \rightarrow iP_{1,2}^\mu$ for the decay products, we obtain the Lorentz-invariant $AV\tilde{P}$ scattering amplitude $-i\mathcal{M}_{A \rightarrow V^0\tilde{P}^0}^{(\alpha,\beta)}$ as follows:

$$-i\mathcal{M}_{A \rightarrow V^0\tilde{P}^0}^{(\alpha,\beta)} = \varepsilon_\mu^{(\alpha)}(P)\varepsilon_\nu^{(\beta)}(P_1)h_{AV\tilde{P}}^{\mu\nu}, \quad (7.53)$$

with

$$h_{AV\tilde{P}}^{\mu\nu} = i \{ A_{AV\tilde{P}} g^{\mu\nu} + B_{AV\tilde{P}} [P_1^\mu P_2^\nu + P_2^\mu P_1^\nu - (P_1 \cdot P_2)g^{\mu\nu} - (P \cdot P_2)g^{\mu\nu}] \}, \quad (7.54)$$

where $h_{AV\tilde{P}}^{\mu\nu}$ denotes the $AV\tilde{P}$ vertex.

It will be necessary to determine the modulus square of the scattering amplitude in order to calculate the decay width. We note that the scattering amplitude in Eq. (7.53) depends on the polarization vectors $\varepsilon_\mu^{(\alpha)}(P)$ and $\varepsilon_\nu^{(\beta)}(P_1)$. Therefore, it is necessary to calculate the average of the modulus squared amplitude for all polarization values. Let us denote the masses of the vectors states A and V as m_A and m_V , respectively. Then the averaged modulus squared amplitude $|\overline{-i\mathcal{M}}|^2$ is determined as follows:

$$\begin{aligned} |\overline{-i\mathcal{M}_{A \rightarrow V^0 \tilde{P}^0}}|^2 &= \frac{1}{3} \sum_{\alpha, \beta=1}^3 \left| -i\mathcal{M}_{A \rightarrow V^0 \tilde{P}^0}^{(\alpha, \beta)} \right|^2 \\ &= \frac{1}{3} \sum_{\alpha, \beta=1}^3 \varepsilon_\mu^{(\alpha)}(P) \varepsilon_\nu^{(\beta)}(P_1) h_{AVP}^{\mu\nu} \varepsilon_\kappa^{(\alpha)}(P) \varepsilon_\lambda^{(\beta)}(P_1) h_{AV\tilde{P}}^{*\kappa\lambda}. \end{aligned} \quad (7.55)$$

Given that

$$\sum_{\alpha=1}^3 \varepsilon_\mu^{(\alpha)}(P) \varepsilon_\kappa^{(\alpha)}(P) = -g_{\mu\kappa} + \frac{P_\mu P_\kappa}{m_A^2}, \quad (7.56)$$

[an analogous equation holds for $\varepsilon^{(\beta)}$], we obtain from Eq. (7.55):

$$\begin{aligned} |\overline{-i\mathcal{M}_{A \rightarrow V^0 \tilde{P}^0}}|^2 &= \frac{1}{3} \left(-g_{\mu\kappa} + \frac{P_\mu P_\kappa}{m_A^2} \right) \left(-g_{\nu\lambda} + \frac{P_{1\nu} P_{1\lambda}}{m_V^2} \right) h_{AV\tilde{P}}^{\mu\nu} h_{AV\tilde{P}}^{*\kappa\lambda} \\ &= \frac{1}{3} \left[h_{\mu\nu AV\tilde{P}} h_{AV\tilde{P}}^{*\mu\nu} - \frac{h_{AV\tilde{P}}^{\mu\nu} P_\mu h_{AV\tilde{P}}^{*\nu\kappa} P_\kappa}{m_A^2} - \frac{h_{AV\tilde{P}}^{\mu\nu} P_{1\nu} h_{AV\tilde{P}}^{*\lambda\mu} P_{1\lambda}}{m_V^2} \right. \\ &\quad \left. + \frac{h_{AV\tilde{P}}^{\mu\nu} P_\mu P_{1\nu} h_{AV\tilde{P}}^{*\lambda\kappa} P_\kappa P_{1\lambda}}{m_V^2 m_A^2} \right] \\ &= \frac{1}{3} \left[\left| h_{AV\tilde{P}}^{\mu\nu} \right|^2 - \frac{\left| h_{AV\tilde{P}}^{\mu\nu} P_\mu \right|^2}{m_A^2} - \frac{\left| h_{AV\tilde{P}}^{\mu\nu} P_{1\nu} \right|^2}{m_V^2} + \frac{\left| h_{AV\tilde{P}}^{\mu\nu} P_\mu P_{1\nu} \right|^2}{m_V^2 m_A^2} \right], \end{aligned} \quad (7.57)$$

which contains the metric tensor $g_{\mu\nu} = \text{diag}(1, -1, -1, -1)$. The decay width for the process $A \rightarrow V^0 \tilde{P}^0$ then reads

$$\Gamma_{A \rightarrow V^0 \tilde{P}^0} = \frac{k(m_A, m_V, m_{\tilde{P}})}{8\pi m_A^2} |\overline{-i\mathcal{M}_{A \rightarrow V^0 \tilde{P}^0}}|^2. \quad (7.58)$$

Note that a non-singlet axial-vector field will in general also possess charged decay channels. Therefore, in addition to the decay process considered in Eq. (7.58), we must consider the contribution of the charged modes from the process $A \rightarrow V^\pm \tilde{P}^\mp$ to the full decay width. Then the full decay width is obtained as

$$\Gamma_{A \rightarrow V\tilde{P}} = \Gamma_{A \rightarrow V^0 \tilde{P}^0} + \Gamma_{A \rightarrow V^\pm \tilde{P}^\mp} \equiv I \Gamma_{A \rightarrow V^0 \tilde{P}^0}.$$

Using Eq.(7.57) we obtain the two-body decay width of vector meson, Eq.(7.58), as follows:

$$\Gamma_{A \rightarrow V \tilde{P}} = \frac{K(m_A, m_V, m_{\tilde{P}})}{12\pi m_A^2} \left[\left| h_{AV\tilde{P}}^{\mu\nu} \right|^2 - \frac{\left| h_{AV\tilde{P}}^{\mu\nu} P_\mu \right|^2}{m_A^2} - \frac{\left| h_{AV\tilde{P}}^{\mu\nu} P_{1\nu} \right|^2}{m_V^2} + \frac{\left| h_{AV\tilde{P}}^{\mu\nu} P_\mu P_{1\nu} \right|^2}{m_V^2 m_A^2} \right], \quad (7.59)$$

where the quantities $P^\mu = (m_A, \mathbf{0})$, $P_1^\mu = (E_V, \mathbf{k})$, and $P_2^\mu = (E_{\tilde{P}}, -\mathbf{k})$ are the four-momenta of A , V , and \tilde{P} in the rest frame of A , respectively. The following kinematic relations hold:

$$\begin{aligned} P_V \cdot P_{\tilde{P}} &= \frac{m_A^2 - m_V^2 - m_{\tilde{P}}^2}{2}, \\ P_A \cdot P_V &= m_A E_V = \frac{m_A^2 + m_V - m_{\tilde{P}}^2}{2}, \\ P_A \cdot P_{\tilde{P}} &= m_A E_{\tilde{P}} = \frac{m_A^2 - m_V + m_{\tilde{P}}^2}{2}. \end{aligned}$$

The terms entering in Eq. (7.59) are given by

$$\begin{aligned} \left| h_{AV\tilde{P}}^{\mu\nu} \right|^2 &= 4A_{AV\tilde{P}}^2 + B_{AV\tilde{P}}^2 \left[m_V^2 m_{\tilde{P}}^2 + m_A^2 m_{\tilde{P}}^2 + 2(P_1 \cdot P_2)^2 + 2(P \cdot P_2)^2 + 6(P_1 \cdot P_2)(P \cdot P_2) \right] \\ &\quad - 6A_{AV\tilde{P}} B_{AV\tilde{P}} (P_1 \cdot P_2 + P \cdot P_2), \end{aligned} \quad (7.60)$$

$$\begin{aligned} \left| h_{AV\tilde{P}}^{\mu\nu} P_\mu \right|^2 &= A_{AV\tilde{P}}^2 m_A^2 + B_{AV\tilde{P}}^2 \left[(P \cdot P_1)^2 m_{\tilde{P}}^2 + (P_1 \cdot P_2)^2 m_A^2 - 2(P \cdot P_1)(P \cdot P_2)(P_1 \cdot P_2) \right] \\ &\quad + 2A_{AV\tilde{P}} B_{AV\tilde{P}} \left[(P \cdot P_1)(P \cdot P_2) - (P_1 \cdot P_2) m_A^2 \right], \end{aligned} \quad (7.61)$$

$$\begin{aligned} \left| h_{AV\tilde{P}}^{\mu\nu} P_{1,\nu} \right|^2 &= A_{AV\tilde{P}}^2 m_V^2 + B_{AV\tilde{P}}^2 \left[(P \cdot P_1)^2 m_{\tilde{P}}^2 + (P \cdot P_2)^2 m_V^2 - 2(P \cdot P_1)(P \cdot P_2)(P_1 \cdot P_2) \right] \\ &\quad + 2A_{AV\tilde{P}} B_{AV\tilde{P}} \left[(P \cdot P_1)(P_1 \cdot P_2) - (P \cdot P_2) m_V^2 \right], \end{aligned} \quad (7.62)$$

$$\left| h_{AV\tilde{P}}^{\mu\nu} P_\mu P_{1,\nu} \right|^2 = [A_{AV\tilde{P}} (P \cdot P_1)]^2$$

with $E_V = \sqrt{K^2(m_A, m_V, m_{\tilde{P}}) + m_V^2}$ and $E_{\tilde{P}} = \sqrt{K^2(m_A, m_V, m_{\tilde{P}}) + m_{\tilde{P}}^2}$.

7.4.1. Two-body decay of D_1

We present the relevant interaction Lagrangian for the nonstrange axial-vector meson D_1 which is a light-heavy quark $Q\bar{q}$ and is assigned to $D_1(2420)^{0,\pm}$. This Lagrangian describes only the two-body decays of this state, and is given as:

$$\begin{aligned}
\mathcal{L}_{D_1 D^* \pi} = & A_{D_1 D^* \pi} D_1^{\mu 0} \left(\bar{D}_\mu^{*0} \pi^0 + \sqrt{2} D_\mu^{*+} \pi^- \right) \\
& + B_{D_1 D^* \pi} \left\{ D_1^{\mu 0} \left[(\partial_\nu \bar{D}_\mu^{*0} - \partial_\mu \bar{D}_\nu^{*0}) \partial^\nu \pi^0 + \sqrt{2} (\partial_\nu D_\mu^{*+} - \partial_\mu D_\nu^{*+}) \partial^\nu \pi^- \right] \right. \\
& + \partial^\nu D_1^{\mu 0} \left[(\bar{D}_\nu^{*0} \partial_\mu \pi^0 - \bar{D}_\mu^{*0} \partial_\nu \pi^0) + \sqrt{2} (D_\nu^{*+} \partial_\mu \pi^- - D_\mu^{*+} \partial_\nu \pi^-) \right] \left. \right\} \\
& + A_{D_1 D^* \pi}^* \bar{D}_1^{\mu 0} \left(D_\mu^{*0} \pi^0 + \sqrt{2} D_\mu^{*-} \pi^+ \right) \\
& + B_{D_1 D^* \pi}^* \left\{ \bar{D}_1^{\mu 0} \left[(\partial_\nu D_\mu^{*0} - \partial_\mu \bar{D}_\nu^{*0}) \partial^\nu \pi^0 + \sqrt{2} (\partial_\nu D_\mu^{*-} - \partial_\mu D_\nu^{*-}) \partial^\nu \pi^+ \right] \right. \\
& + \partial^\nu \bar{D}_1^{\mu 0} \left[(D_\nu^{*0} \partial_\mu \pi^0 - D_\mu^{*0} \partial_\nu \pi^0) + \sqrt{2} (D_\nu^{*-} \partial_\mu \pi^+ - D_\mu^{*-} \partial_\nu \pi^+) \right] \left. \right\} \\
& + A_{D_1 D^* \pi} D_1^{\mu +} \left(D_\mu^{*-} \pi^0 - \sqrt{2} D_\mu^{*0} \pi^- \right) \\
& + B_{D_1 D^* \pi} \left\{ D_1^{\mu +} \left[(\partial_\nu D_\mu^{*-} - \partial_\mu D_\nu^{*-}) \partial^\nu \pi^0 - \sqrt{2} (\partial_\nu D_\mu^{*0} - \partial_\mu D_\nu^{*0}) \partial^\nu \pi^- \right] \right. \\
& + \partial^\nu D_1^{\mu +} \left[(D_\nu^{*-} \partial_\mu \pi^0 - D_\mu^{*-} \partial_\nu \pi^0) - \sqrt{2} (D_\nu^{*0} \partial_\mu \pi^- - D_\mu^{*0} \partial_\nu \pi^-) \right] \left. \right\} \\
& + A_{D_1 D^* \pi}^* D_1^{\mu -} \left(D_\mu^{*+} \pi^0 - \sqrt{2} \bar{D}_\mu^{*0} \pi^+ \right) \\
& + B_{D_1 D^* \pi}^* \left\{ D_1^{\mu -} \left[(\partial_\nu D_\mu^{*+} - \partial_\mu D_\nu^{*+}) \partial^\nu \pi^0 - \sqrt{2} (\partial_\nu \bar{D}_\mu^{*0} - \partial_\mu \bar{D}_\nu^{*0}) \partial^\nu \pi^+ \right] \right. \\
& + \partial^\nu D_1^{\mu -} \left[(D_\nu^{*+} \partial_\mu \pi^0 - D_\mu^{*+} \partial_\nu \pi^0) - \sqrt{2} (\bar{D}_\nu^{*0} \partial_\mu \pi^+ - \bar{D}_\mu^{*0} \partial_\nu \pi^+) \right] \left. \right\} , \quad (7.63)
\end{aligned}$$

with the following coefficients

$$A_{D_1 D^* \pi} = \frac{i}{\sqrt{2}} Z_\pi (g_1^2 - h_3) \phi_C , \quad (7.64)$$

$$B_{D_1 D^* \pi} = \frac{i}{2} Z_\pi g_2 w_{a_1} . \quad (7.65)$$

From the interaction Lagrangian (7.63) we obtain that the neutral state of D_1 decays into $D^{*0} \pi^0$, $D^{*+} \pi^-$ and that the positively charged state decays into $D^{*+} \pi^0$, $D^{*0} \pi^+$ (see below). The interesting point is that the decays $D_1^0 \rightarrow D^+ \pi^-$ and $D_1^+ \rightarrow D^0 \pi^+$ (although kinematically allowed) do not occur in our model; because there is no respective tree-level coupling. This is in agreement with the small experimental upper bound. Improvements in the decay channels of $D_1(2420)$ could be made by taking into account also the multiplet of pseudovector quark-antiquark states. In this way, one will be able to evaluate the mixing of these configurations and describe at the same time the resonances $D_1(2420)$ and $D_1(2430)$.

Decay Width $D_1^0 \rightarrow D^* \pi$

The decay width of D_1^0 into $D^{*0} \pi^0$ is given by Eq. (7.59) upon substituting the fields A , V^0 , and \tilde{P}^0 with D_1^0 , D^{*0} , and π^0 respectively. One may do likewise for the decay width of D_1^0 into $D^{*+} \pi^-$, but in this case it is necessary to multiply the expression by an isospin factor 2. Given that all parameters entering Eqs. (7.59, 7.64, 7.65) are known from Tables 4.1, 4.2, and 4.3, we consequently obtain the following value of the decay width of D_1^0 into $D^* \pi$

$$\Gamma_{D_1(2420)^0 \rightarrow D^* \pi} = \Gamma_{D_1(2420)^0 \rightarrow D^{*+} \pi^-} + \Gamma_{D_1(2420)^0 \rightarrow D^{*0} \pi^0} = 65_{-37}^{+51} \text{ MeV} . \quad (7.66)$$

Experimentally the decay width of $D_1(2420)^0$ into $D^{*+}\pi^-$ has been observed.

Decay Width $D_1^+ \rightarrow D^*\pi$

One can proceed in a similar manner for the D_1^+ state, but in this case we set $A \equiv D_1^+$, $V^0 \equiv D^*$, and $\bar{P}^0 \equiv \pi$ in Eq. (7.59). We obtain the following value of the decay width

$$\Gamma_{D_1^+ \rightarrow D^*\pi} = \Gamma_{D_1(2420)^+ \rightarrow D^{*+}\pi^0} + \Gamma_{D_1(2420)^+ \rightarrow D^{*0}\pi^+} = 65_{-36}^{+51} \text{ MeV}. \quad (7.67)$$

7.4.2. Decay Width $D_1 \rightarrow D\pi\pi$

Now we turn to the three-body decays of the open axial-vector nonstrange charmed meson $D_1(2420)^{0,+}$ which decays into three pseudoscalar mesons, $D\pi\pi$. The relevant interaction Lagrangian can be written in a single equation as follows:

$$\begin{aligned} \mathcal{L}_{D_1 D \pi \pi} = & A_{D_1 D \pi \pi} D_1^{\mu 0} \partial_\mu \bar{D}^0 \left(\pi^{0^2} + 2\pi^- \pi^+ \right) \\ & + B_{D_1 D \pi \pi} D_1^{\mu 0} \bar{D}^0 \partial_\mu \pi^0 \pi^0 + C_{D_1 D \pi \pi} D_1^{\mu 0} \bar{D}^0 \partial_\mu \pi^- \pi^+ \\ & + E_{D_1 D \pi \pi} D_1^{\mu 0} \bar{D}^0 \pi^- \partial_\mu \pi^+ + F_{D_1 D \pi \pi} D_1^{\mu 0} D^+ (\pi^0 \partial_\mu \pi^- - \partial_\mu \pi^0 \pi^-) \\ & + A_{D_1 D \pi \pi} \bar{D}_1^{\mu 0} \partial_\mu D^0 \left(\pi^{0^2} + 2\pi^- \pi^+ \right) \\ & + B_{D_1 D \pi \pi} \bar{D}_1^{\mu 0} D^0 \partial_\mu \pi^0 \pi^0 + C_{D_1 D \pi \pi} \bar{D}_1^{\mu 0} D^0 \partial_\mu \pi^+ \pi^- \\ & + E_{D_1 D \pi \pi} \bar{D}_1^{\mu 0} D^0 \pi^+ \partial_\mu \pi^- + F_{D_1 D \pi \pi} \bar{D}_1^{\mu 0} D^- (\pi^0 \partial_\mu \pi^+ - \partial_\mu \pi^0 \pi^+) \\ & + A_{D_1 D \pi \pi} D_1^{\mu +} \partial_\mu D^- \left(\pi^{0^2} + 2\pi^- \pi^+ \right) \\ & + B_{D_1 D \pi \pi} D_1^{\mu +} D^- \partial_\mu \pi^0 \pi^0 + C_{D_1 D \pi \pi} D_1^{\mu +} D^- \partial_\mu \pi^- \pi^+ \\ & + E_{D_1 D \pi \pi} D_1^{\mu +} D^- \pi^- \partial_\mu \pi^+ + F_{D_1 D \pi \pi} D_1^{\mu +} D^0 (\pi^- \partial_\mu \pi^0 - \partial_\mu \pi^- \pi^0) \\ & + A_{D_1 D \pi \pi} D_1^{\mu -} \partial_\mu D^+ \left(\pi^{0^2} + 2\pi^- \pi^+ \right) \\ & + B_{D_1 D \pi \pi} D_1^{\mu -} D^+ \partial_\mu \pi^0 \pi^0 + C_{D_1 D \pi \pi} D_1^{\mu -} D^+ \partial_\mu \pi^+ \pi^- \\ & + E_{D_1 D \pi \pi} D_1^{\mu -} D^+ \pi^+ \partial_\mu \pi^- + F_{D_1 D \pi \pi} D_1^{\mu -} \bar{D}^0 (\pi^+ \partial_\mu \pi^0 - \partial_\mu \pi^+ \pi^0), \end{aligned} \quad (7.68)$$

with the coefficients

$$A_{D_1 D \pi \pi} = \frac{1}{4} Z_\pi^2 Z_D w_{D_1} (g_1^2 + 2h_1 + h_2), \quad (7.69)$$

$$B_{D_1 D \pi \pi} = \frac{1}{4} Z_\pi^2 Z_D w_{a_1} (3g_1^2 + h_2 - 2h_3), \quad (7.70)$$

$$C_{D_1 D \pi \pi} = \frac{1}{2} Z_\pi^2 Z_D w_{a_1} (g_1^2 + h_2), \quad (7.71)$$

$$E_{D_1 D \pi \pi} = Z_\pi^2 Z_D w_{a_1} (g_1^2 - h_3), \quad (7.72)$$

$$F_{D_1 D \pi \pi} = \frac{\sqrt{2}}{4} Z_\pi^2 Z_D w_{a_1} (g_1^2 - h_2 - 2h_3). \quad (7.73)$$

$$(7.74)$$

As seen in the Lagrangian (7.68) there are three relevant channels for the neutral state D_1^0 which are $D_1^0 \rightarrow D^0\pi^0\pi^0$, $D_1^0 \rightarrow D^0\pi^+\pi^-$, and $D_1^0 \rightarrow D^+\pi^-\pi^0$. The positive state also has three relevant channels due to $D_1^+ \rightarrow D^+\pi^+\pi^-$, $D_1^+ \rightarrow D^+\pi^0\pi^0$, and $D_1^+ \rightarrow D^0\pi^0\pi^+$.

Decay Width $D_1^{0,+} \rightarrow D^{0,+}\pi\pi$

The Lagrangian (7.68) allows us to calculate the decay width for the process $D_1 \rightarrow D\pi\pi$. Firstly let us focus on the three body-decay of the neutral state D_1^0 into $D^0\pi^0\pi^0$. We denote the momenta of D_1^0 , D^0 , π^0 and π^0 as P , P_1 , P_2 , and P_3 . A vector state D_1 is involved in this decay process. We then consider the corresponding polarization vector $\varepsilon_\mu^{(\alpha)}(P)$ for D_1 , and substitute $\partial^\mu \rightarrow -iP^\mu$ for the decaying particle and $\partial^\mu \rightarrow iP_{1,2,3}^\mu$ for the decay products. We straightforwardly obtain the following $D_1^0 D^0 \pi^0 \pi^0$ scattering amplitude $-iM_{D_1^0 \rightarrow D^0 \pi^0 \pi^0}^{(\alpha)}$ from the Lagrangian (7.68):

$$-iM_{D_1^0 \rightarrow D^0 \pi^0 \pi^0}^{(\alpha)} = \varepsilon_\mu^{(\alpha)}(P) h_{D_1 D \pi \pi}^\mu, \quad (7.75)$$

where $h_{D_1 D \pi \pi}^\mu$ is the vertex following from the relevant part of the Lagrangian,

$$h_{D_1 D \pi \pi}^\mu = -[A_{D_1 D \pi \pi} P_1^\mu + B_{D_1 D \pi \pi} P_2^\mu]. \quad (7.76)$$

In order to calculate the decay width of D_1^0 we need to calculate the averaged modulus squared decay amplitude $|\overline{-iM_{D_1^0 \rightarrow D^0 \pi^0 \pi^0}}|^2$ from Eq.(7.75):

$$\begin{aligned} |\overline{-iM_{D_1^0 \rightarrow D^0 \pi^0 \pi^0}}|^2 &= \frac{1}{3} \sum_{\alpha=1}^3 | -iM_{D_1^0 \rightarrow D^0 \pi^0 \pi^0}^{(\alpha)} |^2 \\ &= \frac{1}{3} \sum_{\alpha=1}^3 \varepsilon_\mu^{(\alpha)}(P) \varepsilon_\nu^{(\alpha)}(P) h_{D_1 D \pi \pi}^\mu h_{D_1 D \pi \pi}^{*\nu} \\ &= \frac{1}{3} \left(-g_{\mu\nu} + \frac{P_\mu P_\nu}{M^2} \right) h_{D_1 D \pi \pi}^\mu h_{D_1 D \pi \pi}^{*\nu} \\ &= \frac{1}{3} \left[-|h_{D_1 D \pi \pi}^\mu|^2 + \frac{|P_\mu h_{D_1 D \pi \pi}^\mu|^2}{M^2} \right], \end{aligned} \quad (7.77)$$

where

$$|h_{D_1 D \pi \pi}^\mu|^2 = A_{D_1 D \pi \pi}^2 P_1^2 + 2A_{D_1 D \pi \pi} B_{D_1 D \pi \pi} (P_1 \cdot P_2) + B_{D_1 D \pi \pi}^2 P_2^2, \quad (7.78)$$

$$|P_\mu h_{D_1 D \pi \pi}^\mu|^2 = | -[A_{D_1 D \pi \pi} (P \cdot P_1) + B_{D_1 D \pi \pi} (P \cdot P_2)] |^2, \quad (7.79)$$

where $P^\mu = (M, \mathbf{0})$, $P_1^\mu = (E_{P_1}, \mathbf{p})$, $P_2^\mu = (E_{P_2}, -\mathbf{p})$, and $P_3^\mu = (E_{P_3}, -\mathbf{p})$ are the four-momenta of D_1^0 , D^0 , π^0 , and π^0 in the rest frame of D_1^0 , respectively. In this frame,

$$\begin{aligned} P_1 \cdot P_2 &= \frac{m_{12}^2 - m_1^2 - m_2^2}{2}, \\ P \cdot P_1 &= m_1^2 + \frac{m_{12}^2 - m_1^2 - m_2^2}{2} + \frac{m_{13}^2 - m_1^2 - m_3^2}{2}, \\ P \cdot P_2 &= m_2^2 + \frac{m_{12}^2 - m_1^2 - m_2^2}{2} + \frac{m_{23}^2 - m_2^2 - m_3^2}{2}. \end{aligned}$$

The quantities M , m_1 , m_2 , m_3 refer to the mass of D_1^0 , D^0 , π^0 , π^0 , respectively. Using Eq.(6.19) the decay width for the process $D_1^0 \rightarrow D^0\pi^0\pi^0$ can be obtained as

$$\Gamma_{A \rightarrow P_1 P_2 P_3} = \frac{2}{96 (2\pi)^3 M^3} \int_{(m_1+m_2)^2}^{(M-m_3)^2} \int_{(m_{23}^2)_{\min}}^{(m_{23}^2)_{\max}} \times \left[- \left| h_{D_1 D \pi \pi}^\mu \right|^2 + \frac{\left| h_{D_1 D \pi \pi}^\mu P_\mu \right|^2}{M^2} \right] dm_{23}^2 dm_{12}^2 . \quad (7.80)$$

The decay of the neutral states for the processes $D_1^0 \rightarrow D^0\pi^+\pi^-$ and $D_1^0 \rightarrow D^+\pi^-\pi^0$ has the same formula as in Eq. (7.80), only in this case it is multiplied by an isospin factor 2 as given by the Lagrangian (7.68). We then get

$$\Gamma_{D_1^0 \rightarrow D^0 \pi \pi} = \Gamma_{D_1(2420)^0 \rightarrow D^0 \pi^0 \pi^0} + \Gamma_{D_1(2420)^0 \rightarrow D^0 \pi^+ \pi^-} = (0.59 \pm 0.02) \text{ MeV}. \quad (7.81)$$

For the positive state $D_1(2420)^+$ the decay process $D_1^+ \rightarrow D^+\pi^0\pi^0$ has an analogous analytic expression as for the process $D_1^0 \rightarrow D^0\pi^0\pi^0$ (as presented in Eq. (7.80)), while $D_1^+ \rightarrow D^+\pi^+\pi^-$ has the same formula, multiplied by an isospin factor 2 as given from the Lagrangian (7.68).

$$\Gamma_{D_1^0 \rightarrow D^+ \pi \pi} = \Gamma_{D_1(2420)^+ \rightarrow D^+ \pi^0 \pi^0} + \Gamma_{D_1(2420)^+ \rightarrow D^+ \pi^+ \pi^-} = (0.56 \pm 0.02) \text{ MeV}. \quad (7.82)$$

This has been observed experimentally.

Decay Width $D_1^{0,+} \rightarrow D\pi^+\pi^0$

The scattering amplitudes for the processes $D_1^0 \rightarrow D^-\pi^+\pi^0$ and $D_1^+ \rightarrow D^0\pi^+\pi^0$ differ markedly from the previous processes for the three-body decay of $D_1^{0,+}$, as can be seen from the interaction Lagrangian (7.68). Thus, we study the decay widths for these channels differently. Let us firstly focus on the decay width of the neutral state D_1^0 into $D^-\pi^+\pi^0$, which has the same expression as for the decay process $D_1^+ \rightarrow D^0\pi^+\pi^0$. To write the scattering amplitude for $D_1^0 \rightarrow D^-\pi^+\pi^0$ we denote the momenta of D_1^0 , D^- , π^+ , and π^0 as P , P_1 , P_2 , and P_3 . For the meson D_1^0 , we consider the polarization vector $\varepsilon_\mu^{(\alpha)}(P)$ and substitute $\partial^\mu \rightarrow -iP^\mu$ for the decaying particle and $\partial^\mu \rightarrow iP_{1,2,3}^\mu$ for the outgoing particles. We then obtain the following decay amplitude from the Lagrangian (7.68):

$$-iM_{D_1^0 \rightarrow D^0 - \pi^+ \pi^0}^{(\alpha)} = \varepsilon_\mu^{(\alpha)}(P) X_{D_1 D \pi \pi}^\mu , \quad (7.83)$$

where the vertex $X_{D_1 D \pi \pi}^\mu$ is

$$X_{D_1 D \pi \pi}^\mu = -F_{D_1 D \pi \pi} (P_2^\mu - P_3^\mu) . \quad (7.84)$$

The averaged modulus squared amplitude $|\overline{-iM_{D_1^0 \rightarrow D^0 - \pi^+ \pi^0}}|^2$ has the same general formula as in Eq.(7.77), with substituting the vertices $h_{D_1 D \pi \pi}^\mu \rightarrow X_{D_1 D \pi \pi}^\mu$,

$$\begin{aligned}
|\overline{-iM_{D_1^0 \rightarrow D^0 - \pi^+ \pi^0}}|^2 &= \frac{1}{3} \left[-|X_{D_1 D \pi \pi}^\mu|^2 + \frac{|P_\mu X_{D_1 D \pi \pi}^\mu|^2}{M^2} \right] \\
&= \frac{F_{D_1 D \pi \pi}^2}{3} \left[\frac{1}{M^2} (P \cdot P_2 - P \cdot P_3)^2 - (m_2^2 + m_3^2 + 2 P_2 \cdot P_3) \right]. \quad (7.85)
\end{aligned}$$

The decay width $D_1^0 \rightarrow D^+ \pi^- \pi^0$ reads

$$\begin{aligned}
\Gamma_{A \rightarrow P_1 P_2 P_3} &= \frac{F_{D_1 D \pi \pi}^2}{3 \times 32 (2\pi)^3 M^3} \int_{(m_1+m_2)^2}^{(M-m_3)^2} \int_{(m_{23}^2)_{\min}}^{(m_{23}^2)_{\max}} dm_{23}^2 dm_{12}^2 \\
&\quad \times \left[\frac{1}{M^2} (P \cdot P_2 - P \cdot P_3)^2 - (m_2^2 + m_3^2 + 2 P_2 \cdot P_3) \right], \quad (7.86)
\end{aligned}$$

where the quantities M , m_1 , m_2 , and m_3 refer to the masses for the fields D_1^0 , D^+ , π^- , and π^0 , respectively, and the kinematic relations

$$\begin{aligned}
P_2 \cdot P_3 &= \frac{m_{23}^2 - m_2^2 - m_3^2}{2}, \\
P \cdot P_3 &= m_3^2 + \frac{m_{13}^2 - m_1^2 - m_3^2}{2} + \frac{m_{23}^2 - m_2^2 - m_3^2}{2}.
\end{aligned}$$

All the parameters entering Eq.(7.86) are fixed and listed in the Tables 4.1 and 4.3. Consequently we obtain the decay width of $D_1(2420)^0$ into $D^+ \pi^- \pi^0$:

$$\Gamma_{D_1(2420)^0 \rightarrow D^+ \pi^- \pi^0} = 0.21_{-0.015}^{+0.01} \text{ MeV}. \quad (7.87)$$

The decay of the charged state D_1^+ into $D^0 \pi^0 \pi^+$ has an analogous expression and is

$$\Gamma_{D_1(2420)^+ \rightarrow D^0 \pi^0 \pi^+} = (0.22 \pm 0.01) \text{ MeV}. \quad (7.88)$$

This decay is observed experimentally.

7.4.3. Decay Width $D_{S_1} \rightarrow D^* K$

As a last step we turn to the strange-charmed axial-vector state $D_{S_1}^+$ which is assigned to $D_{S_1}(2536)$. This resonance decays into $D^*(2010)^+ K^0$ and $D^*(2007)^0 K^+$ in the model (2.145), whereas kinematically the decay to DK is not allowed. This is in agreement with experimental data in which the decays $D_{S_1}(2536)^+ \rightarrow D^+ K^0$ and $D_{S_1}(2536)^+ \rightarrow D^0 K^+$ are not seen (as stated by the PDG [51]). The $D_{S_1} D^* K$ interaction Lagrangian from Eq. (2.145) reads

$$\begin{aligned}
\mathcal{L}_{D_{S_1} D^* K} &= A_{D_{S_1} D^* K} D_{S_1}^{\mu+} (D_\mu^{\star-} \bar{K}^0 + D_\mu^{\star 0} K^-) \\
&\quad + B_{D_{S_1} D^* K} \{ D_{S_1}^{\mu+} [(\partial_\nu D_\mu^{\star-} - \partial_\mu D_\nu^{\star-}) \partial^\nu \bar{K}^0 + (\partial_\nu D_\mu^{\star 0} - \partial_\mu D_\nu^{\star 0}) \partial^\nu K^-] \\
&\quad + \partial^\nu D_{S_1}^{\mu+} [D_\nu^{\star-} \partial_\mu \bar{K}^0 - D_\mu^{\star-} \partial_\nu \bar{K}^0 + D_\nu^{\star 0} \partial_\mu K^- - D_\mu^{\star 0} \partial_\nu K^-] \} \\
&\quad + A_{D_{S_1} D^* K}^* D_{S_1}^{\mu-} (D_\mu^{\star+} K^0 + \bar{D}_\mu^{\star 0} K^+) \\
&\quad + B_{D_{S_1} D^* K}^* \{ D_{S_1}^{\mu-} [(\partial_\nu D_\mu^{\star+} - \partial_\mu D_\nu^{\star+}) \partial^\nu K^0 + (\partial_\nu \bar{D}_\mu^{\star 0} - \partial_\mu \bar{D}_\nu^{\star 0}) \partial^\nu K^+] \\
&\quad + \partial^\nu D_{S_1}^{\mu-} [D_\nu^{\star+} \partial_\mu K^0 - D_\mu^{\star+} \partial_\nu K^0 + \bar{D}_\nu^{\star 0} \partial_\mu K^+ - \bar{D}_\mu^{\star 0} \partial_\nu K^+] \}, \quad (7.89)
\end{aligned}$$

with the following coefficients

$$A_{D_{S_1}D^*K} = \frac{i}{4}Z_K \left[g_1^2(\sqrt{2}\phi_N - 2\phi_S - 4\phi_C) + h_2(\sqrt{2}\phi_N - 2\phi_S) + 4h_3\phi_C \right], \quad (7.90)$$

$$B_{D_{S_1}D^*K} = -\frac{i}{\sqrt{2}}Z_K g_2 w_{K_1}. \quad (7.91)$$

According to the interaction Lagrangian, D_{S_1} decays into the channels $D^{*+}K^0$ and $D^{*0}K^+$. The formula for the decay widths $\Gamma_{D_{S_1}^+ \rightarrow D^{*+}K^0}$ and $\Gamma_{D_{S_1}^+ \rightarrow D^{*0}K^+}$ is as in Eq. (7.59), when setting $A \equiv D_{S_1}$, $V \equiv D^*$, $\bar{P} \equiv K$ and replacing the vertex $h_{AV\bar{P}}^{\mu\nu}$ by the following vertex $h_{D_{S_1}D^*K}^{\mu\nu}$:

$$h_{D_{S_1}D^*K}^{\mu\nu} = i \{ A_{D_{S_1}D^*K} g^{\mu\nu} + B_{D_{S_1}D^*K} [P_1^\mu P_2^\nu + P_2^\mu P_1^\nu - (P \cdot P_2)g^{\mu\nu} - (P_1 \cdot P_2)g^{\mu\nu}] \}, \quad (7.92)$$

The parameters are fixed and presented in Tables 4.1, 4.2, and 4.3. We then obtain the decay width into D^*K as

$$\begin{aligned} \Gamma_{D_{S_1}(2536)^+ \rightarrow D^*K} &= \Gamma_{D_{S_1}^+ \rightarrow D^{*0}K^+} + \Gamma_{D_{S_1}^+ \rightarrow D^{*+}K^0} \\ &= 25_{-15}^{+22} \text{ MeV}. \end{aligned} \quad (7.93)$$

whereas $\Gamma_{D_{S_1}(2536)^+ \rightarrow D^*K}^{\text{exp}} = (0.92 \pm 0.03 \pm 0.04) \text{ MeV}$.

7.5. Weak decay constants of Charmed mesons

In this subsection we evaluate the weak decay constants of the pseudoscalar mesons D , D_S , and η_C . Their analytic expressions read [see Appendix A and also Ref. [118, 119, 122]]

$$f_D = \frac{\phi_N + \sqrt{2}\phi_C}{\sqrt{2}Z_D}, \quad (7.94)$$

$$f_{D_S} = \frac{\phi_S + \phi_C}{Z_{D_S}}, \quad (7.95)$$

$$f_{\eta_C} = \frac{2\phi_C}{Z_{\eta_C}}. \quad (7.96)$$

Using the parameters of the fit we obtain

$$f_D = (254 \pm 17) \text{ MeV}, \quad (7.97)$$

$$f_{D_S} = (261 \pm 17) \text{ MeV}, \quad (7.98)$$

$$f_{\eta_C} = (314 \pm 39) \text{ MeV}. \quad (7.99)$$

The experimental values $f_D = (206.7 \pm 8.9) \text{ MeV}$ and $f_{D_s} = (260.5 \pm 5.4) \text{ MeV}$ [51] show a good agreement for f_{D_s} and a slightly too large theoretical result for f_D . The quantity f_{η_C} is in fair agreement with the experimental value $f_{\eta_C} = (335 \pm 75) \text{ MeV}$ [232] as well as with the theoretical result $f_{\eta_C} = (300 \pm 50) \text{ MeV}$ obtained in Ref. [233]. These results show that our determination of the condensate ϕ_C is reliable (even if the theoretical uncertainty is still large).

7.6. Summary

We summarize the results of the (OZI-dominant) strong decay widths of the resonances D_0 , D^* , D_1 , and D_{S1} , in Table 7.1. For the calculation of the decay widths we have used the physical masses listed by the PDG [51]. This is necessary in order to have the correct phase space. With the exception of $D_{S1}(2536)^+ \rightarrow D^*K$, all values are in reasonable agreement with the mean experimental values and upper bounds. Although the theoretical uncertainties are still large and the experimental results are not yet well known, the qualitative agreement is anyhow interesting if one considers that the decay amplitudes depend on the parameters of the three-flavour version of the model determined in Ref. [110]. Note that the theoretical errors have been calculated by taking into account the uncertainty in the charm condensate $\phi_C = (176 \pm 28)$ MeV. The lower theoretical value corresponds to $\phi_C = (176 - 28)$ MeV, while the upper one to $\phi_C = (176 + 28)$ MeV. The explicit expressions for the decay widths are reported in the previous.

Here we do not study the decay of other (hidden and open) charmed states because we restrict ourselves to OZI-dominant processes. The study of OZI-suppressed decays which involve the large- N_c suppressed parameters λ_1 and h_1 is left for the next chapter. There, also the decays of the well-known charmonium states (such as χ_{c0} and η_c) will be investigated.

Decay Channel	Theoretical result [MeV]	Experimental result [MeV]
$D_0^*(2400)^0 \rightarrow D\pi$	139_{-114}^{+243}	$D^+\pi^-$ seen; full width $\Gamma = 267 \pm 40$
$D_0^*(2400)^+ \rightarrow D\pi$	51_{-51}^{+182}	$D^+\pi^0$ seen; full width: $\Gamma = 283 \pm 24 \pm 34$
$D^*(2007)^0 \rightarrow D^0\pi^0$	0.025 ± 0.003	seen; < 1.3
$D^*(2007)^0 \rightarrow D^+\pi^-$	0	not seen
$D^*(2010)^+ \rightarrow D^+\pi^0$	$0.018_{-0.003}^{+0.002}$	0.029 ± 0.008
$D^*(2010)^+ \rightarrow D^0\pi^+$	$0.038_{-0.004}^{+0.005}$	0.065 ± 0.017
$D_1(2420)^0 \rightarrow D^*\pi$	65_{-37}^{+51}	$D^{*+}\pi^-$ seen; full width: $\Gamma = 27.4 \pm 2.5$
$D_1(2420)^0 \rightarrow D^0\pi\pi$	0.59 ± 0.02	seen
$D_1(2420)^0 \rightarrow D^+\pi^-\pi^0$	$0.21_{-0.015}^{+0.01}$	seen
$D_1(2420)^0 \rightarrow D^+\pi^-$	0	not seen; $\Gamma(D^+\pi^-)/\Gamma(D^{*+}\pi^-) < 0.24$
$D_1(2420)^+ \rightarrow D^*\pi$	65_{-36}^{+51}	$D^{*0}\pi^+$ seen; full width: $\Gamma = 25 \pm 6$
$D_1(2420)^+ \rightarrow D^+\pi\pi$	0.56 ± 0.02	seen
$D_1(2420)^+ \rightarrow D^0\pi^0\pi^+$	0.22 ± 0.01	seen
$D_1(2420)^+ \rightarrow D^0\pi^+$	0	not seen; $\Gamma(D^0\pi^+)/\Gamma(D^{*0}\pi^+) < 0.18$
$D_{S1}(2536)^+ \rightarrow D^*K$	25_{-15}^{+22}	seen; full width $\Gamma = 0.92 \pm 0.03 \pm 0.04$
$D_{S1}(2536)^+ \rightarrow D^+K^0$	0	not seen
$D_{S1}(2536)^+ \rightarrow D^0K^+$	0	not seen

Table 7.1: Decay widths of charmed mesons.

The following comments are in order:

(i) The decay of $D_0^*(2400)^0$ into $D\pi$ has a very large theoretical error due to the imprecise determination of ϕ_C . A qualitative statement is, however, possible: the decay channel $D_0^*(2400)^0 \rightarrow D\pi$ is large and is the only OZI-dominant decay predicted by our model. This decay channel is also the only one seen in experiment (although the branching ratio is not yet known). A similar discussion holds for the charged counterpart $D_0^*(2400)^+$.

(ii) The decay widths of the vector charmed states $D^*(2007)^0$ and $D^*(2010)^+$ are slightly smaller than the experimental results, but close to the lower bounds of the latter.

(iii) The results for the axial-vector charmed states $D_1(2420)^0$ and $D_1(2420)^+$ are compatible with experiment. Note that the decay into $D^*\pi$ is the only one which is experimentally seen. Moreover, the decays $D_1(2420)^0 \rightarrow D^+\pi^-$ and $D_1(2420)^+ \rightarrow D^0\pi^+$, although kinematically allowed, do not occur in our model because there is no respective tree-level coupling; this is in agreement with the small experimental upper bound. Improvements in the decay channels of $D_1(2420)$ are possible by taking into account also the multiplet of pseudovector quark-antiquark states. In this way, one will be able to evaluate the mixing of these configurations and describe at the same time the resonances $D_1(2420)$ and $D_1(2430)$.

(iv) It is interesting that the decays of the vector states $D^*(2007)^0$ and $D^*(2010)^\pm$ and of the axial-vector states $D_1(2420)^0$ and $D_1(2420)^+$ can be simultaneously described with the same set of (low-energy) parameters. Namely, in the low-energy language these states are chiral partners and the results (even if the experimental knowledge is not yet conclusive and the theoretical uncertainties are still large) show that chiral symmetry is still important in the energy range relevant for charmed mesons.

(v) The decay of the axial-vector strange-charmed $D_{S1}(2536)^+ \rightarrow D^*K$ is too large in our model when compared to the experimental data of about 1 MeV. This result is robust upon variation of the parameters, as the error shows. We thus conclude that the resonance $D_{S1}(2536)^\pm$ is not favored to be (predominantly) a member of the axial-vector multiplet (it can be, however, a member of the pseudovector multiplet). Then, we discuss two possible solutions to the problem of identifying the axial-vector strange-charmed quarkonium:

Solution 1: There is a ‘seed’ quark-antiquark axial-vector state D_{S1} above the D^*K threshold, which is, however, very broad and for this reason has *not yet* been detected. Quantum corrections generate the state $D_{S1}(2460)^\pm$ through pole doubling [223, 225, 226]. In this scenario, $D_{S1}(2460)$ is dynamically generated but is still related to a broad quark-antiquark seed state. In this way, the low mass of $D_{S1}(2460)$ in comparison to the quark-model prediction [47, 48] is due to quantum corrections [179, 200, 201, 202, 234, 235]. Then, the state $D_{S1}(2460)$, being below threshold, has a very small decay width.

Solution 2: Also in this case, there is still a broad and not yet detected quark-antiquark field above threshold, but solution 1 is assumed not to apply (loops are not sufficient to generate $D_{S1}(2460)$). The resonance $D_{S1}(2460)^\pm$ is not a quark-antiquark field, but a tetraquark or a loosely bound molecular state and its existence is not related to the quark-antiquark state of the axial-vector multiplet.

(vi) For the state $D_{S0}^*(2317)$ similar arguments apply. If the mass of this state is above the DK threshold, we predict a very large ($\gtrsim 1$ GeV) decay width into DK (for example: $\Gamma_{D_{S0}^* \rightarrow DK} \simeq 3$ GeV for a D_{S0}^* mass of 2467 MeV as determined in Table 4.5). Then, the two solutions mentioned above are applicable also here:

Solution 1: A quark-antiquark state with a mass above the DK threshold exists, but it is too broad to be seen in experiment. The state $D_{S0}(2317)$ arises through the pole-doubling mechanism.

Solution 2: Loops are not sufficient to dynamically generate $D_{S0}^*(2317)$. The latter is not a quarkonium but either a tetraquark or a molecular state.

In conclusion, a detailed study of loops in the axial-vector and scalar strange-charm sector needs to be performed. In the axial-vector strange-charm sector mixing with a pseudovector quark-antiquark state should also be included. These tasks go beyond the tree-level analysis

of our work but are an interesting subject for the future.

8. Decay of hidden charmed mesons

8.1. Introduction

Charmonia exhibit a spectrum of resonances and play the same role for understanding hadronic dynamics as the hydrogen atom [236]. The properties of charmonia are determined by the strong interaction which is undoubtedly one of the most challenging tasks. Since the discovery of the charmonium state (J/ψ) with quantum numbers $J^{PC} = 1^{--}$ in November 1974 at BNL [42] and at SLAC [41], a significant experimental progress has been achieved in charmonium spectroscopy. As an example of this, the hadronic and electromagnetic transitions between charmonium states and their decays have been measured with high precision with the BESIII spectrometer at the electron-positron collider at IHEP Beijing. Moreover, unconventional narrow charmonium-rich states have been recently discovered in an energy regime above the open-charm threshold by Belle [237, 238, 239, 240] and BaBar [241], which potentially initiates a new area in charmonium spectroscopy. The upcoming PANDA experiment at the research facility FAIR will exploit the annihilation of cooled anti-protons with protons to perform charmonium spectroscopy with an incredible precision.

Recent theoretical developments such as nonrelativistic QCD [242, 243, 244] and heavy-quark effective theory [245], potential models [164, 163], lattice gauge theory [246, 247, 248], and light front quantization have shown the direct connection of charmonium properties with QCD. More details of the experimental and theoretical situation is given in the Ref. [59]. Therefore, we highlight the study of the decays of charmonium states and their mixing with glueballs in the eLSM. The charm quark has been included in the eLSM by its extension from the case $N_f = 3$ [110] to the case $N_f = 4$ [119]. The eLSM has four charmonium states, which are the (pseudo-)scalar ground states $\eta_c(1S)$ and $\chi_{c0}(1P)$ with quantum numbers $J^{PC} = 0^{-+}$ and $J^{PC} = 0^{++}$ as well as the ground-state (axial-)vector $J/\psi(1S)$ and $\chi_{c1}(1P)$ with quantum numbers $J^{PC} = 1^{-+}$ and $J^{PC} = 1^{++}$ [118, 119], respectively. It also includes two glueballs: a scalar glueball (denoted as G) and a pseudoscalar glueball (denoted as \tilde{G}), composed of two gluons. There are two candidates for the scalar glueball which are the resonance $f_0(1500)$ (which shows a flavour-blind decay pattern) and the resonance $f_0(1710)$, because its mass is very close to lattice-QCD predictions, and because it is produced in the gluon-rich decay of the J/ψ , as seen in Refs. [72, 73, 74, 75, 76, 77, 78, 79, 80, 81, 82, 217]. The latter is a mixing between three bare fields: the nonstrange $\sigma_N \equiv (\bar{u}u + \bar{d}d)/\sqrt{2}$, the hidden-strange $\sigma_S \equiv s\bar{s}$, and the scalar glueball $G \equiv gg$. This three-body mixing in the scalar-isoscalar channel was solved in Ref.[83] and generated the physical resonances $f_0(1370)$, $f_0(1500)$, and $f_0(1710)$. The last field that was introduced in the eLSM is a pseudoscalar glueball via a term describing the interaction between the pseudoscalar glueball with scalar and pseudoscalar mesons; as seen in chapter 6. The decay channels of the pseudoscalar glueball into scalar and pseudoscalar mesons [124, 125, 126, 127] could potentially be measured in the upcoming PANDA experiment at the FAIR facility [218], which is based

on proton-antiproton scattering and has the ability to produce the pseudoscalar glueball in an intermediate state with mass above 2.5 GeV. The mass of a pseudoscalar glueball predicted by lattice QCD (in the quenched approximation) is about 2.6 GeV [65, 66, 67, 71].

In the present chapter we study the decay properties of the charmonium states χ_{c0} and η_c within the eLSM. The charmonia region is a good one to look for exotics [249, 250]. As seen in Ref. [251, 252, 253], lattice QCD predicts the existence of various glueball states in the charmonium mass region, some of them with exotic quantum numbers which are not possible in a $q\bar{q}$ state. We then obtain the scalar glueball (due to the decay of χ_{c0}) and the pseudoscalar glueball (due to the decay of η_c). We calculate the decay width of the charmonium state η_c into a pseudoscalar glueball (this decay is allowed in the channel $\eta_c \rightarrow \pi\pi\tilde{G}$), with a mass of 2.6 GeV predicted by lattice QCD and repeat it with a mass of 2.37 GeV, as observed in the BESIII experiment where pseudoscalar resonances have been investigated in J/ψ decays [219, 220, 221]. Particularly, we consider the $X(2370)$ resonance, since its mass lies just below the lattice-QCD prediction. Mixing phenomena, although believed to be smaller than in the light mesonic sector, can occur also between charmonia and glueballs with the same quantum numbers [254, 255]. The parameters have been used in the strange-nonstrange investigation [110] (which are discussed in chapter 3), whereas the three parameters related to the charm sector have been fixed in chapter 4 through a fit including the masses of charmed mesons. There are two parameters, λ_1 , h_1 , which had zero values in the previous case ($N_f = 4$), but in the present chapter this should be re-evaluated, as the decay widths of χ_{c0} depend on their values. For instance, there is a mixing between a scalar glueball G with the charmonium state χ_{c0} , but we neglect it in our evaluation because it is expected to be small. We compute instead the mixing angle between the pseudoscalar glueball (with a mass of 2.6 GeV) with η_c .

8.2. Decay of the scalar charmonium state χ_{c0}

In this section we study the decay properties of the scalar ground-state charmonium $\chi_{c0}(1P)$ in the eLSM, via computing the decay width of this charmonium state into (axial-)vector and (pseudo)scalar mesons and a scalar glueball as well. As a result of the study discussed in Ref.[83], the resonance $f_0(1710)$ is predominantly a scalar glueball.

The terms in the eLSM relevant for the decay of χ_{c0} are

$$\begin{aligned} \mathcal{L}_{\chi_{c0}} = & \mathcal{L}_{dil} - m_0^2 \left(\frac{G}{G_0} \right)^2 \text{Tr}(\Phi^\dagger \Phi) + \text{Tr} \left[\left(\left(\frac{G}{G_0} \right)^2 \frac{m_1^2}{2} + \Delta \right) (L^{\mu 2} + R^{\mu 2}) \right] \\ & - \lambda_1 [\text{Tr}(\Phi^\dagger \Phi)]^2 + \frac{h_1}{2} \text{Tr}(\Phi^\dagger \Phi) \text{Tr}[(L^\mu)^2 + (R^\mu)^2] + c(\det \Phi - \det \Phi^\dagger)^2, \dots \end{aligned} \quad (8.1)$$

These terms contain the decay channels of the charmonium state χ_{c0} into (pseudo)scalar and (axial-)vector mesons as well as a scalar glueball G . The full Lagrangian (2.145) is presented in chapter 2. The term denoted as \mathcal{L}_{dil} is the dilaton Lagrangian which describes the scalar dilaton field which is represented by a scalar glueball $G \equiv |gg\rangle$ with quantum numbers $J^{PC} = 0^{++}$, and emulates the trace anomaly of the pure Yang-Mills sector of QCD

[110, 111, 112, 113, 151, 114, 115]:

$$\mathcal{L}_{dil} = \frac{1}{2}(\partial_\mu G)^2 - \frac{1}{4} \frac{m_G^2}{\Lambda^2} \left(G^4 \ln \left| \frac{G}{\Lambda} \right| - \frac{G^4}{4} \right). \quad (8.2)$$

The energy scale of low-energy QCD is described by the dimensionful parameter Λ which is identical to the minimum G_0 of the dilaton potential, ($G_0 = \Lambda$). The scalar glueball mass m_G has been evaluated by lattice QCD which gives a mass of about (1.5-1.7) GeV [65, 66, 67, 71, 256]. The dilatation symmetry or scale invariance, $x^\mu \rightarrow \lambda^{-1}x^\mu$, is realized at the classical level of the Yang-Mills sector of QCD and explicitly broken due to the logarithmic term of the potential in Eq. (8.2). This breaking leads to a non-vanishing divergence of the corresponding current:

$$\partial_\mu J_{dil}^\mu = T_{dil, \mu}^\mu = -\frac{1}{4} m_G^2 \Lambda^2. \quad (8.3)$$

The importance of including the scalar glueball in the eLSM is to incorporate dilatation invariance meson mass terms. Note that the scalar glueball state was frozen in the previous discussion but here it is elevated to be a dynamical degree of freedom. The details of the terms and the field assignments are presented and discussed for the eLSM in the case $N_f = 4$ in chapter 4.

In our framework, Φ represents the 4×4 (pseudo)scalar multiplets, as seen in Sec.(4.2), as follows:

$$\Phi = (S^a + iP^a)t^a = \frac{1}{\sqrt{2}} \begin{pmatrix} \frac{(\sigma_N + a_0^0) + i(\eta_N + \pi^0)}{\sqrt{2}} & a_0^+ + i\pi^+ & K_0^{*+} + iK^+ & D_0^{*0} + iD^0 \\ a_0^- + i\pi^- & \frac{(\sigma_N - a_0^0) + i(\eta_N - \pi^0)}{\sqrt{2}} & K_0^{*0} + iK^0 & D_0^{*-} + iD^- \\ K_0^{*-} + iK^- & \bar{K}_0^{*0} + i\bar{K}^0 & \sigma_S + i\eta_S & D_{S0}^{*-} + iD_S^- \\ \bar{D}_0^{*0} + i\bar{D}^0 & D_0^{*+} + iD^+ & D_{S0}^{*+} + iD_S^+ & \chi_{C0} + i\eta_C \end{pmatrix}, \quad (8.4)$$

where t^a are the generators of the group $U(N_f)$. The multiplet Φ transforms as $\Phi \rightarrow U_L \Phi U_R^\dagger$ under $U_L(4) \times U_R(4)$ chiral transformations, where $U_{L(R)} = e^{-i\theta_{L(R)}^a t^a}$ is an element of $U(4)_{R(L)}$. Under parity $\Phi(t, \vec{x}) \rightarrow \Phi^\dagger(t, -\vec{x})$, and under charge conjugation $\Phi \rightarrow \Phi^\dagger$. The determinant of Φ is invariant under $SU(4)_L \times SU(4)_R$, but not under $U(1)_A$ because $\det \Phi \rightarrow \det U_A \Phi U_A = e^{-i\theta_A^0 \sqrt{2N_f}} \det \Phi \neq \det \Phi$. Note that Eq. (6.1) is not invariant under $U_A(1)$ which is in agreement with the so-called axial anomaly.

Now we present the left-handed and right-handed matrices containing the vector, V_μ^a , and axial-vector, A_μ^a , degrees of freedom [119]:

$$L^\mu = (V^a + A^a)^\mu t^a = \frac{1}{\sqrt{2}} \begin{pmatrix} \frac{\omega_N + \rho^0}{\sqrt{2}} + \frac{f_{1N} + a_1^0}{\sqrt{2}} & \rho^+ + a_1^+ & K^{*+} + K_1^+ & D^{*0} + D_1^0 \\ \rho^- + a_1^- & \frac{\omega_N - \rho^0}{\sqrt{2}} + \frac{f_{1N} - a_1^0}{\sqrt{2}} & K^{*0} + K_1^0 & D^{*-} + D_1^- \\ K^{*-} + K_1^- & \bar{K}^{*0} + \bar{K}_1^0 & \omega_S + f_{1S} & D_S^{*-} + D_{S1}^- \\ \bar{D}^{*0} + \bar{D}_1^0 & D^{*+} + D_1^+ & D_S^{*+} + D_{S1}^+ & J/\psi + \chi_{C1} \end{pmatrix}^\mu, \quad (8.5)$$

$$R^\mu = (V^a - A^a)^\mu t^a = \frac{1}{\sqrt{2}} \begin{pmatrix} \frac{\omega_N + \rho^0}{\sqrt{2}} - \frac{f_{1N} + a_1^0}{\sqrt{2}} & \rho^+ - a_1^+ & K^{*+} - K_1^+ & D^{*0} - D_1^0 \\ \rho^- - a_1^- & \frac{\omega_N - \rho^0}{\sqrt{2}} - \frac{f_{1N} - a_1^0}{\sqrt{2}} & K^{*0} - K_1^0 & D^{*-} - D_1^- \\ K^{*-} - K_1^- & \bar{K}^{*0} - \bar{K}_1^0 & \omega_S - f_{1S} & D_S^{*-} - D_{S1}^- \\ \bar{D}^{*0} - \bar{D}_1^0 & D^{*+} - D_1^+ & D_S^{*+} - D_{S1}^+ & J/\psi - \chi_{C1} \end{pmatrix}^\mu, \quad (8.6)$$

which transform as $L^\mu \rightarrow U_L L^\mu U_L^\dagger$ and $R^\mu \rightarrow U_R L^\mu U_R^\dagger$ under chiral transformations. These transformation properties of Φ , L^μ , and R^μ have been used to build the chirally invariant Lagrangian (8.1). The matrix Δ is defined as

$$\Delta = \begin{pmatrix} 0 & 0 & 0 & 0 \\ 0 & 0 & 0 & 0 \\ 0 & 0 & \delta_S & 0 \\ 0 & 0 & 0 & \delta_C \end{pmatrix}, \quad (8.7)$$

where $\delta_S \sim m_S^2$ and $\delta_C \sim m_C^2$.

If $m_0^2 < 0$, the Lagrangian (8.1) features spontaneous symmetry breaking. To implement this breaking we have to shift the scalar-isoscalar fields G , σ_N , σ_S , and χ_{C0} by their vacuum expectation values G_0 , ϕ_N , ϕ_S , and ϕ_C [78, 119]

$$\begin{aligned} G &\rightarrow G + G_0, \\ \sigma_N &\rightarrow \sigma_N + \phi_N, \\ \sigma_S &\rightarrow \sigma_S + \phi_S, \\ \chi_{C0} &\rightarrow \chi_{C0} + \phi_C. \end{aligned} \quad (8.8)$$

The identification of the scalar glueball G is still uncertain, the two most likely candidates are $f_0(1500)$ and $f_0(1710)$ and/or admixtures of them. We assign the scalar glueball (G), σ_N , and σ_S from the following mixing matrix which is constructed in Ref. [83]:

$$\begin{pmatrix} f_0(1370) \\ f_0(1500) \\ f_0(1710) \end{pmatrix} = \begin{pmatrix} 0.94 & -0.17 & 0.29 \\ 0.21 & 0.97 & -0.12 \\ -0.26 & 0.18 & 0.95 \end{pmatrix} \begin{pmatrix} \sigma_N \equiv (\bar{u}u + \bar{d}d)/\sqrt{2} \\ \sigma_S \equiv \bar{s}s \\ G \equiv gg \end{pmatrix}. \quad (8.9)$$

Note that we used different mixing matrices in the study of the decay of the pseudoscalar glueball into scalar mesons as seen in chapter 5. From Eq.(8.9), one obtains

$$G = 0.29 f_0(1370) - 0.12 f_0(1500) + 0.95 f_0(1710), \quad (8.10)$$

$$\sigma_N = 0.94 f_0(1370) + 0.21 f_0(1500) - 0.26 f_0(1710), \quad (8.11)$$

$$\sigma_S = -0.17 f_0(1370) + 0.97 f_0(1500) + 0.18 f_0(1710). \quad (8.12)$$

These relations are used in the calculation of the decay widths of χ_{c0} .

8.2.1. Parameters and results

All the parameters in the Lagrangian (8.1) have been fixed in the case of $N_f = 3$, see Ref. [110] for more details, and the three additional parameters related to the charm sector

(ε_C , δ_C , and ϕ_C), in the case of $N_f = 4$, have been determined in chapter 4. The values of the parameters and the wave-function renormalization constants are summarized in the following Table 8.1:

parameter	value	renormalization factor	value
m_1^2	$0.413 \times 10^6 \text{ MeV}^2$	$Z_\pi = Z_{\eta_N}$	1.70927
m_0^2	$-0.918 \times 10^6 \text{ MeV}^2$	Z_K	1.60406
δ_S	$0.151 \times 10^6 \text{ MeV}^2$	Z_{η_C}	1.11892
δ_C	$3.91 \times 10^6 \text{ MeV}^2$	Z_{D_S}	1.15716
ε_C	$2.23 \times 10^6 \text{ MeV}^2$	$Z_{D_0^*} = Z_{D_0^{*0}}$	1.00649
g_1	5.84	Z_{η_S}	1.53854
h_2	9.88	Z_{K_S}	1.00105
λ_2	68.3	Z_D	1.15256
h_3	3.87	$Z_{D_{S0}^*}$	1.00437

Table 8.1.: Parameters and wave-function renormalization constants.

The wave-function renormalization constants for π and η_N are equal because of isospin symmetry, and for D_0^* and D^{*0} as well. The gluon condensate G_0 is equal to $\Lambda \approx 3.3 \text{ GeV}$ [83] in pure YM theory, which is used in the present discussion.

Furthermore, we set the values of the parameters λ_1 and h_1 to zero in eLSM in all cases studied in this framework (as seen also in the previous chapters, in the case of $N_f = 2$ [108, 78, 78], $N_f = 3$ [110], and $N_f = 4$ for the masses of charmed mesons and the (OZI-dominant) strong decays of open charmed mesons [118, 119, 120, 121, 122]), because they are expected to be small, which is in agreement with large- N_c expectations. However, in the OZI-suppressed decays of the charmonium state χ_{c0} , non-zero values of λ_1 and h_1 will become important. To understand the reason for this let us explain in more detail.

Indeed, the decay of the charmonium state χ_{c0} into hadrons is mediated by gluon annihilation. This annihilation must proceed through a three-gluon exchange for the following two reasons:

- (i) Gluons carry colour, but mesons in the final state are colour singlets (colourless). This leads to the fact that the annihilation must be mediated by more than one gluon.
- (ii) The combination of gluons involved in the decay must be such that it conserves all strong-interaction quantum numbers. Consequently, vector particles, with charge-conjugation quantum number -1, cannot decay into two vectors through two-gluon exchange. The charge conjugation quantum number for a two-gluon state is +1, but for a three-gluon state it is -1. Therefore, vector mesons decays only through three-gluon annihilation.

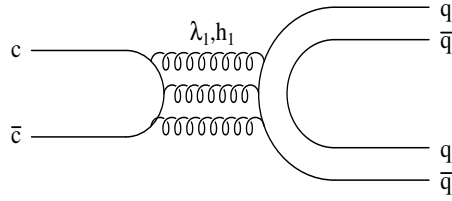


Figure 8.1.: Decay of charmonium state into two mesons. q refers to the up (u), down (d), and strange (s) quark flavours.

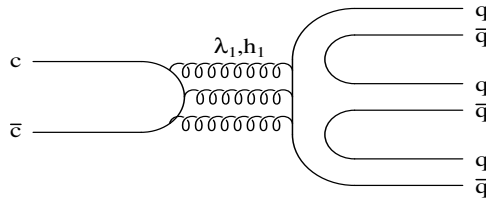


Figure 8.2.: Decay of charmonium state into three mesons.

In our case, gluons carry all the energy. Therefore, the interaction is relatively weak due to asymptotic freedom, which leads to OZI-suppression. As a consequence, the decay of the charmonium state χ_{C0} into (axial-)vector and (pseudo)scalar mesons and a scalar glueball is dynamically suppressed due to annihilation into three ‘hard’ gluons (see Fig. 8.1 and Fig. 8.2). In the eLSM, this is incorporated by small non-zero values of the large- N_c suppressed parameters λ_1 and h_1 , as seen in Fig. 8.1 and Fig. 8.2. If we set them to zero, all the decay channels of χ_{C0} which have been found in the eLSM (8.1) are zero, which is an unacceptable result. This is important evidence for these parameters being nonzero in the OZI-suppressed case. For this reason we determine them using the experimental decay widths of χ_{C0} listed by the PDG [51] via a χ^2 fit,

$$\chi^2(\lambda_1, h_1) \equiv \sum_i^6 \left(\frac{\Gamma_i^{th} - \Gamma_i^{exp}}{\xi \Gamma_i^{exp}} \right)^2, \quad (8.13)$$

where ξ is a constant. We choose $\xi = 1$ which leads to $\chi^2/d.o.f = 0.7$. We then obtain

$$\lambda_1 = -0.16, \quad (8.14)$$

and

$$h_1 = 0.046. \quad (8.15)$$

These values of the parameters λ_1 and h_1 are indeed very small, as mentioned before. So a posteriori we justify the results of Refs. [119, 122]. The partial decay widths of various decay channels which we used in the fit (8.13) are summarized in the Table 8.2

Decay Channel	theoretical result [MeV]	Experimental result [MeV]
$\Gamma_{\chi_{c0} \rightarrow \bar{K}_0^{*0} K_0^{*0}}$	0.01	0.01 ± 0.0047
$\Gamma_{\chi_{c0} \rightarrow K^- K^+}$	0.059	0.061 ± 0.007
$\Gamma_{\chi_{c0} \rightarrow \pi\pi}$	0.089	0.088 ± 0.0092
$\Gamma_{\chi_{c0} \rightarrow \bar{K}^{*0} K^{*0}}$	0.014	0.017 ± 0.0072
$\Gamma_{\chi_{c0} \rightarrow w w}$	0.01	0.0099 ± 0.0017
$\Gamma_{\chi_{c0} \rightarrow \phi\phi}$	0.004	0.0081 ± 0.0013

Table 8.2.: The partial decay widths of χ_{c0} .

Furthermore, we have to change the value of the parameter c , which is the coefficient of the axial anomaly term, to fit the results of the decay widths of χ_{c0} . Therefore, for the determination of c , we use the decay widths of χ_{c0} into $\eta\eta$ and $\eta'\eta'$, which are [51].

$$\Gamma_{\chi_{c0} \rightarrow \eta\eta}^{exp} = (0.031 \pm 0.0039)\text{MeV},$$

and

$$\Gamma_{\chi_{c0} \rightarrow \eta'\eta'}^{exp} = (0.02 \pm 0.0035)\text{MeV}.$$

We then perform a fit by minimizing the χ^2 -function,

$$\chi^2(c) \equiv \left(\frac{\Gamma_{\chi_{c0} \rightarrow \eta\eta}^{th}(c) - \Gamma_{\chi_{c0} \rightarrow \eta\eta}^{exp}}{\xi \Gamma_{\chi_{c0} \rightarrow \eta\eta}^{exp}} \right)^2 + \left(\frac{\Gamma_{\chi_{c0} \rightarrow \eta'\eta'}^{th}(c) - \Gamma_{\chi_{c0} \rightarrow \eta'\eta'}^{exp}}{\xi \Gamma_{\chi_{c0} \rightarrow \eta'\eta'}^{exp}} \right)^2, \quad (8.16)$$

which gives $c = 7.178 \times 10^{-10} \text{ MeV}^{-4}$ with $\chi^2/\text{d.o.f} = 0.18$ where $\xi = 1$.

The mixing between the hidden-charmed scalar meson χ_{c0} and the scalar glueball G is neglected because it is small.

The two- and three-body decays of the hidden-charmed meson χ_{c0} into scalar glueballs and scalar mesons are reported in Table 8.3.

Decay Channel	theoretical result [MeV]	Experimental result [MeV]
$\Gamma_{\chi_{c0} \rightarrow f_0(1370)f_0(1370)}$	$5 \cdot 10^{-3}$	$< 3 \cdot 10^{-3}$
$\Gamma_{\chi_{c0} \rightarrow f_0(1500)f_0(1500)}$	$4 \cdot 10^{-3}$	$< 5 \cdot 10^{-4}$
$\Gamma_{\chi_{c0} \rightarrow f_0(1370)f_0(1500)}$	$2 \cdot 10^{-6}$	$< 1 \cdot 10^{-3}$
$\Gamma_{\chi_{c0} \rightarrow f_0(1370)f_0(1710)}$	$1 \cdot 10^{-4}$	0.0069 ± 0.004
$\Gamma_{\chi_{c0} \rightarrow f_0(1500)f_0(1710)}$	$2 \cdot 10^{-5}$	$< 7 \cdot 10^{-4}$
$\Gamma_{\chi_{c0} \rightarrow f_0(1370)\eta\eta}$	$4 \cdot 10^{-4}$	-
$\Gamma_{\chi_{c0} \rightarrow f_0(1500)\eta\eta}$	$3 \cdot 10^{-3}$	-
$\Gamma_{\chi_{c0} \rightarrow f_0(1370)\eta'\eta'}$	$27 \cdot 10^{-4}$	-
$\Gamma_{\chi_{c0} \rightarrow f_0(1370)\eta\eta'}$	$89 \cdot 10^{-6}$	-
$\Gamma_{\chi_{c0} \rightarrow f_0(1500)\eta\eta'}$	$11 \cdot 10^{-3}$	-
$\Gamma_{\chi_{c0} \rightarrow f_0(1710)\eta\eta}$	$8 \cdot 10^{-5}$	-
$\Gamma_{\chi_{c0} \rightarrow f_0(1710)\eta\eta'}$	$3 \cdot 10^{-5}$	-

Table 8.3.: The partial decay widths of χ_{c0} .

Additionally, the two- and three-body decays of the hidden-charmed meson χ_{c0} into (axial-)vector and (pseudo)scalar mesons are reported in Table 8.4.

Decay Channel	theoretical result [MeV]	Experimental result [MeV]
$\Gamma_{\chi_{c0} \rightarrow a_0 a_0}$	0.004	-
$\Gamma_{\chi_{c0} \rightarrow K_1 \bar{K}_1}$	0.005	-
$\Gamma_{\chi_{c0} \rightarrow K_1^+ K^-}$	0.005	0.063 ± 0.0233
$\Gamma_{\chi_{c0} \rightarrow \eta \eta}$	0.022	0.031 ± 0.0039
$\Gamma_{\chi_{c0} \rightarrow \eta' \eta'}$	0.02	0.02 ± 0.0035
$\Gamma_{\chi_{c0} \rightarrow \eta \eta'}$	0.004	< 0.0024
$\Gamma_{\chi_{c0} \rightarrow K^* K_0^*}$	0.00007	-
$\Gamma_{\chi_{c0} \rightarrow \rho \rho}$	0.01	-
$\Gamma_{\chi_{c0} \rightarrow K_0^* K \eta}$	0.008	-
$\Gamma_{\chi_{c0} \rightarrow K_0^* K \eta'}$	0.004	-

Table 8.4.: The partial decay widths of χ_{c0} .

The results are in good agreement with experimental data [51]. All the relevant expressions for the two- and three-body decay processes of χ_{c0} are presented in the Appendix along with computational details.

8.3. Decay of the pseudoscalar charmonium state η_C

In this section we compute and discuss the decay widths of the pseudoscalar charmonium state $\eta_C(1P)$ into (pseudo)scalar mesons and a pseudoscalar glueball ($\eta_c \rightarrow \pi \pi \tilde{G}$) in the eLSM.

Two terms in the eLSM are relevant for the decay of the pseudoscalar hidden-charmed meson η_C into (pseudo-)scalar mesons and a pseudoscalar glueball \tilde{G} . The first has the form $c(\det\Phi - \det\Phi^\dagger)^2$, which describes the axial anomaly and represents a further breaking of dilatation and chiral symmetry and is additionally responsible for the mass and decays of the η 's. The other term (see Eq. (6.1)) describes the interactions of the pseudoscalar glueball $\tilde{G} \equiv |gg\rangle$, with quantum numbers $J^{PC} = 0^{-+}$, with scalar and pseudoscalar mesons.

8.3.1. Decay of η_C into a pseudoscalar glueball

The effective Lagrangian which describes the interaction of the pseudoscalar glueball \tilde{G} with the (pseudo)scalar mesons (which is described in detail for the case of $N_f = 3$ (6.1) in chapter 6) reads

$$\mathcal{L}_{\tilde{G}}^{int} = ic_{\tilde{G}\Phi} \tilde{G} (\det\Phi - \det\Phi^\dagger) , \quad (8.17)$$

where $c_{\tilde{G}\Phi}$ is a dimensionless coupling constant. The pseudoscalar glueball \tilde{G} is invariant under $U(4)_L \times U(4)_R$ chiral transformations, while under parity, $\tilde{G}(t, \vec{x}) \rightarrow -\tilde{G}(t, -\vec{x})$, and under charge conjugation $\tilde{G} \rightarrow \tilde{G}$. These considerations lead to the interaction Lagrangian $\mathcal{L}_{\tilde{G}}^{int}$ of Eq. (6.1) which is invariant under $SU(4)_L \times SU(4)_R$, parity, and charge conjugation.

To determine the value of the coupling constant $c_{\tilde{G}\phi}$, one can relate it to its counterpart in the three-flavour case $c_{\tilde{G}\Phi(N_f=3)}$, which was computed in the study of the decay of a pseudoscalar glueball \tilde{G} into scalar and pseudoscalar mesons (as seen in chapter 6), with the result $c_{\tilde{G}\Phi(N_f=3)} = 4.48 \pm 0.46$ [124].

The Lagrangian which describes the coupling of the pseudoscalar glueball and (pseudo)scalar mesons was given in Eq. (6.1) for the three-flavour case

$$\mathcal{L}_{\tilde{G}(N_f=3)}^{int} = ic_{\tilde{G}\Phi(N_f=3)} \tilde{G} \left(\det\Phi_{(N_f=3)} - \det\Phi_{(N_f=3)}^\dagger \right). \quad (8.18)$$

By using the relation of the multiplet matrix of (pseudo)scalar mesons (Φ) for the four-flavour case and for the three-flavour case (which is presented in Eq. (4.123)), we can transform the interaction Lagrangian $\mathcal{L}_{\tilde{G}}^{int}$, for the case of $N_f = 4$ (8.17), to be as

$$\mathcal{L}_{\tilde{G}}^{int} = i \frac{\sqrt{2}}{\phi_C} c_{\tilde{G}\Phi(N_f=3)} \tilde{G} \left(\det\Phi - \det\Phi^\dagger \right), \quad (8.19)$$

Comparing Eq.(8.17) with Eq.(8.19), we get

$$c_{\tilde{G}\Phi} = \frac{\sqrt{2} c_{\tilde{G}\Phi(N_f=3)}}{\phi_C}. \quad (8.20)$$

We then get $c_{\tilde{G}\Phi} = 0.036$ in the present case ($N_f = 4$).

The interaction Lagrangian (8.17) contains only one decay process which describes the decay of the pseudoscalar charmonium η_c into a pseudoscalar glueball \tilde{G} through the channel $\eta_C \rightarrow \tilde{G}\pi\pi$. The tree-level vertices of this process have the form

$$\mathcal{L}_{\eta_C \tilde{G}\pi\pi} = -\frac{1}{4} c_{\tilde{G}\Phi} \phi_S Z_{\eta_C} Z_\pi^2 \eta_C \tilde{G} \pi^0{}^2 - \frac{1}{2} c_{\tilde{G}\Phi} \phi_S Z_{\eta_C} Z_\pi^2 \eta_C \tilde{G} \pi^- \pi^+. \quad (8.21)$$

One can compute the full decay width $\Gamma_{\eta_C \rightarrow \tilde{G}\pi\pi}$ from

$$\begin{aligned} \Gamma_{\eta_C \rightarrow \tilde{G}\pi\pi} &= \Gamma_{\eta_C \rightarrow \tilde{G}\pi^0\pi^0} + \Gamma_{\eta_C \rightarrow \tilde{G}\pi^-\pi^+} \\ &= \Gamma_{\eta_C \rightarrow \tilde{G}\pi^0\pi^0} + 2\Gamma_{\eta_C \rightarrow \tilde{G}\pi^0\pi^0} \\ &= 3\Gamma_{\eta_C \rightarrow \tilde{G}\pi^0\pi^0}. \end{aligned} \quad (8.22)$$

The decay amplitude is

$$-iM = \frac{-i}{4} c_{\tilde{G}\Phi} \phi_S Z_{\eta_C} Z_\pi^2. \quad (8.23)$$

one also uses the corresponding decay width for the three-body case, Eq. (5.61). The decay width of the pseudoscalar charmonium state η_c into a pseudoscalar glueball with a mass of 2.6 GeV (as predicted by lattice QCD in the quenched approximation [65, 66, 67, 71, 256]) is

$$\Gamma_{\eta_C \rightarrow \pi\pi\tilde{G}(2600)} = 0.124 \text{ MeV}, \quad (8.24)$$

and for a mass of the charmonium state η_c which is about of 2.37 GeV (corresponding to the mass of the resonance $X(2370)$ measured in the BESIII experiment [219, 220, 221])

$$\Gamma_{\eta_C \rightarrow \pi\pi\tilde{G}(2370)} = 0.16 \text{ MeV}. \quad (8.25)$$

These results could be tested in the PANDA experiment at the upcoming FAIR facility.

8.3.2. Decay of η_C into (pseudo)scalar mesons

The chiral Lagrangian contains the tree-level vertices for the decay processes of the pseudoscalar η_C into (pseudo)scalar mesons, through the chiral anomaly term

$$\mathcal{L}_{U(1)_A} = c(\det\Phi - \det\Phi^\dagger)^2, \quad (8.26)$$

where c is a dimensionful constant and has been determined in Sec. 8.2. After the field transformations Eqs. (4.19 - 4.32) have been performed in Sec. 4.3, the terms in the Lagrangian (8.26) which correspond to decay processes of η_C read

$$\begin{aligned} \mathcal{L}_{\eta_C} = & \frac{c}{8}\phi_N^2\phi_C Z_{\eta_C}\eta_C\{\sqrt{2}\phi_S\phi_N Z_K Z_{K_0^*}(K_0^{*0}\bar{K}^0 + \bar{K}_0^{*0}K^0 + K_0^{*-}K^+ + K_0^{*+}K^-) \\ & + 2Z_\pi\phi_S^2(a_0^0\pi^0 + a_0^+\pi^- + a_0^-\pi^+) - 4\phi_N\phi_S(Z_{\eta_S}\eta_S\sigma_N + Z_{\eta_N}\eta_N\sigma_S) \\ & - 6\phi_S^2 Z_{\eta_N}\eta_N\sigma_N - \phi_N^2\eta_S\sigma_S Z_{\eta_S} + 2\phi_N Z_{\eta_S}^2 Z_{\eta_N}\eta_N^2\eta_N + 6\phi_S Z_{\eta_S} Z_{\eta_N}^2\eta_N^2\eta_S \\ & - \sqrt{2}\phi_N Z_{\eta_S} Z_K^2(\bar{K}^0K^0 + K^-K^+)\eta_S - 3\sqrt{2}\phi_S Z_{\eta_N} Z_K^2(\bar{K}^0K^0 + K^-K^+)\eta_N \\ & + \sqrt{2}\phi_S Z_\pi Z_K^2\left[\sqrt{2}(\bar{K}^0K^+\pi^- + K^0K^-\pi^+) - (K^0\bar{K}^0 - K^-K^+)\pi^0\right] \\ & - 2\phi_S\eta_S Z_{\eta_S} Z_\pi^2(\pi^{02} + 2\pi^-\pi^+)\}. \end{aligned} \quad (8.27)$$

The decay widths of the pseudoscalar hidden charmed meson η_C into scalar and pseudoscalar charmed mesons are presented in Table 8.5. The relevant expressions for these decay processes are presented in the Appendix.

Decay Channel	theoretical result [MeV]	Experimental result [MeV]
$\Gamma_{\eta_c \rightarrow \bar{K}_0^* K}$	0.01	-
$\Gamma_{\eta_c \rightarrow a_0 \pi}$	0.01	-
$\Gamma_{\eta_c \rightarrow f_0(1370)\eta}$	0.00018	-
$\Gamma_{\eta_c \rightarrow f_0(1500)\eta}$	0.006	-
$\Gamma_{\eta_c \rightarrow f_0(1710)\eta}$	0.000032	-
$\Gamma_{\eta_c \rightarrow f_0(1370)\eta'}$	0.027	-
$\Gamma_{\eta_c \rightarrow f_0(1500)\eta'}$	0.024	-
$\Gamma_{\eta_c \rightarrow f_0(1710)\eta'}$	0.0006	-
$\Gamma_{\eta_c \rightarrow \eta\eta\eta}$	0.052	-
$\Gamma_{\eta_c \rightarrow \eta'\eta'\eta'}$	0.0023	-
$\Gamma_{\eta_c \rightarrow \eta'\eta\eta}$	0.44	-
$\Gamma_{\eta_c \rightarrow \eta'\eta'\eta}$	0.0034	-
$\Gamma_{\eta_c \rightarrow \eta K \bar{K}}$	0.15	0.32 ± 0.17
$\Gamma_{\eta_c \rightarrow \eta' K K}$	0.41	-
$\Gamma_{\eta_c \rightarrow \eta \pi \pi}$	0.12	0.54 ± 0.18
$\Gamma_{\eta_c \rightarrow \eta' \pi \pi}$	0.08	1.3 ± 0.6
$\Gamma_{\eta_c \rightarrow K K \pi}$	0.095	-

Table 8.5.: The partial decay widths of η_c .

There are experimental data for these decays firm by the PDG with which we can compare. The three measured decay widths are in reasonably good agreement with experimental data.

8.3.3. Mixing of a pseudoscalar glueball and η_C

The mixing between the pseudoscalar glueball \tilde{G} with the pseudoscalar charm-anticharm meson η_c is described by the non-interacting Lagrangian as follows:

$$\mathcal{L}_{\tilde{G}, \eta_C} = \frac{1}{2}(\partial_\mu \tilde{G})^2 + \frac{1}{2}(\partial_\mu \eta_C)^2 - \frac{1}{2}m_{\tilde{G}}^2 \tilde{G}^2 - \frac{1}{2}m_{\eta_c}^2 \eta_c^2 + Z_{\tilde{G}\eta_C} \tilde{G} \eta_C, \quad (8.28)$$

where

$$Z_{\tilde{G}\eta_C} = \frac{-1}{4} c_{\tilde{G}\Phi} Z_{\eta_C} \phi_N^2 \phi_S. \quad (8.29)$$

The physical fields η_C and \tilde{G} can be obtained through an $SO(2)$ rotation

$$\begin{pmatrix} \tilde{G}' \\ \eta_C' \end{pmatrix} = \begin{pmatrix} \cos \phi & \sin \phi \\ -\sin \phi & \cos \phi \end{pmatrix} = \begin{pmatrix} \tilde{G} \\ \eta_C \end{pmatrix}, \quad (8.30)$$

with

$$m_{\eta_C'}^2 = m_{\tilde{G}}^2 \sin^2 \phi + m_{\eta_C}^2 \cos^2 \phi + Z_{\tilde{G}\eta_C} \sin(2\phi), \quad (8.31)$$

$$m_{\tilde{G}'}^2 = m_{\tilde{G}}^2 \cos^2 \phi + m_{\eta_C}^2 \sin^2 \phi - Z_{\tilde{G}\eta_C} \sin(2\phi), \quad (8.32)$$

where the mixing angle ϕ reads

$$\phi = \frac{1}{2} \arctan \left[\frac{-c_{\tilde{G}\Phi} Z_{\eta_C} \phi_N^2 \phi_S}{2(m_{\eta_C}^2 - m_{\tilde{G}}^2)} \right], \quad (8.33)$$

where $c_{\tilde{G}\Phi}$ is a dimensionless coupling constant between $\tilde{G}\Phi$ which was determined in Eq.(8.20). We then obtain the mixing angle of the pseudoscalar glueball \tilde{G} and the pseudoscalar charm-anticharm meson η_c to be -1° , for a mass of the pseudoscalar glueball which is 2.6 GeV, as predicted by lattice-QCD simulations [65, 66, 71, 67, 256].

9. Conclusions and Outlook

In this work, we have developed a four-flavour extended linear sigma model with vector and axial-vector degrees of freedom. Within this model, we have calculated masses and decay widths of charmed mesons.

For the coupling constants of the model, we have used the values determined in the low-energy study of mesons in Ref. [110] and listed in Table 4.1. The three remaining parameters related to the current charm quark mass were determined in a fit to twelve masses of hidden and open charmed mesons. The results are shown in Table 4.5: the open charmed mesons agree within theoretical errors with the experimental values, while the masses of charmonia are (with the exception of J/ψ) underestimated by about 10%. The precision of our approach cannot compete with methods based on heavy-quark symmetry, but it admits a perspective on charmed states from a low-energy approach based on chiral symmetry and dilatation invariance. The level of agreement with experimental data proves that these symmetries are, at least to some degree, still relevant for the charm sector. In this respect, our approach is a useful tool to investigate the assignment of some charmed states (see below) and to obtain an independent determination of quantities such as the chiral condensate of charm-anticharm quarks. The latter turns out to be sizable, showing that the charm quark, although heavy, is indeed still connected to nontrivial vacuum dynamics.

We have also presented a chirally invariant effective Lagrangian describing the interaction of a pseudoscalar glueball with scalar and pseudoscalar mesons for the three-flavour case $N_f = 3$. We have studied the decays of the pseudoscalar glueball into three pseudoscalar and into a scalar and pseudoscalar quark-antiquark fields.

The branching ratios are parameter-free once the mass of the glueball has been fixed. To this end, we have considered two possibilities: (i) in agreement with lattice QCD, we have chosen $m_{\tilde{G}} = 2.6$ GeV. The existence and the decay properties of such a hypothetical pseudoscalar resonance can be tested in the upcoming PANDA experiment [218]. (ii) We assumed that the resonance $X(2370)$, measured in the experiment BESIII, is (predominantly) a pseudoscalar glueball state, and thus we have also used a mass of 2.37 GeV [219, 220, 221]. The results for both possibilities have been summarized in Tables 6.2 and 6.3: we predict that $KK\pi$ is the dominant decay channel, followed by (almost equally large) $\eta\pi\pi$ and $\eta'\pi\pi$ decay channels. In the case of BESIII, with a measurement of the branching ratio for other decay channels than the measured $\eta'\pi\pi$ one could ascertain if $X(2370)$ is (predominantly) a pseudoscalar glueball. In the case of PANDA, our results may represent a useful guideline for the search of the pseudoscalar glueball.

Then, we have calculated the weak-decay constants of the pseudoscalar states D , D_S , and η_c , which are in fair agreement with the experimental values and, as a last step, we have evaluated the OZI-dominant decays of charmed mesons (Table 7.1). The result for $D_0^*(2400)^0$, $D_0^*(2400)^+$, $D^*(2007)^0$, $D^*(2010)^+$, $D_1(2420)^0$, and $D_1(2420)^+$ are compatible with the results and the upper bounds listed by the PDG [51], although the theoretical errors are still quite large. Nevertheless, we could simultaneously describe the decays of

open-charmed vector and axial-vector states which are chiral partners within our theoretical treatment.

Concerning the assignment of the scalar and axial-vector strange-charmed quarkonium states D_{S0} and D_{S1} , we obtain the following: If the masses of these quarkonia are above the respective thresholds, we find that their decay widths are too large, which probably means that these states, even if they exist, have escaped detection. In this case, the resonances $D_{S0}^*(2317)$ and $D_{S1}(2460)$ can emerge as dynamically generated companion poles (alternatively, they can be tetraquark or molecular states). Our results imply also that the interpretation of the resonance $D_{S1}(2536)$ as a member of the axial-vector multiplet is not favored because the experimental width is too narrow when compared to the theoretical width of a quarkonium state with the same mass. An investigation of these resonances necessitates the calculation of quantum fluctuations.

In summary, the fact that a (although at this stage only rough) qualitative description is obtained by using a chiral model and, more remarkably, by using the parameters determined by a study of $N_f = 3$ mesons, means that a remnant of chiral symmetry is present also in the sector of charmed mesons. Chiral symmetry is (to a large extent) still valid because the parameters of the eLSM do not vary too much as a function of the energy at which they are probed. Besides mass terms which describe the large contribution of the current charm quark mass, all interaction terms are the same as in the low-energy effective model of Refs. [108, 78, 110] which was built under the requirements of chiral symmetry and dilatation invariance. As a by-product of our work we also evaluate the charm condensate which is of the same order as the nonstrange and strange quark condensates. This is also in accord with chiral dynamics enlarged to the group $U(4)_R \times U(4)_L$.

In the present work we have also represented a chirally invariant linear sigma model with (axial-)vector mesons in the four-flavour case, $N_f = 4$, by including a dilaton field and a scalar glueball field, and describing the interaction of the pseudoscalar glueball with (pseudoscalar) mesons. We have calculated the decay widths of the hidden-charmed meson χ_{c0} into two and three strange and nonstrange mesons (Tables 8.2 and 8.4) as well as into a scalar glueball G , which is an admixture of two resonances $f_0(1370)$ and $f_0(1500)$ (Table 8.3). Note here that the decay of charmonium states to open-charmed mesons is forbidden in the eLSM, as discussed also in Ref.[257]. We have also computed the decay widths of the pseudoscalar charmonium state η_C into light mesons (Table 8.5) and into a pseudoscalar glueball \tilde{G} , through the channel $\eta_C \rightarrow \pi\pi\tilde{G}$. The latter is obtained from the interaction term of the pseudoscalar glueball. We have also evaluated the mixing angle between the pseudoscalar glueball and η_c , which is very small and equal to -1° . We have additionally found that the extended linear sigma model (2.145) offers no decay channels for the (axial-)vector charmonium states where $\Gamma_{J/\psi} = 0$ and $\Gamma_{\chi_{c1}} = 0$. The results of the decay widths of χ_{c0} are in good agreement with experimental data [51] and of η_c are in reasonably good agreement with experiment [51], which indicates to what extent the eLSM is a successful and appropriate model to study the phenomenology of hidden-charmed mesons and open-charmed mesons (chapter 7).

The parameters were determined in the case of $N_f = 4$ (see chapter 4). However, there are four parameters that we need to fix: (i) λ_1 and h_1 ; which are assume to have zero values in all the previous investigation for $N_f = 3$ case, (see chapter 3), and $N_f = 4$ case, (see chapter 4), because their values are numerically small and do not affect the previous results.

However, the decay widths of charmonium states χ_{c0} and η_C depend on both, and for this reason we determined them by a χ^2 fit to the decay widths of χ_{c0} , see Table 8.2. (ii) The c parameter; which is in the axial anomaly term. This parameter was determined by the fit (8.16). (iii) $c_{\tilde{G}\Phi}$; which was fixed by the relation $c_{\tilde{G}\Phi(N_f=3)}$ [124].

Note that the decay widths for the (axial-)vector charmonium states J/ψ and χ_{c1} are zero for kinematical reasons.

The restoration of chiral symmetry at nonzero temperature and density is one of the fundamental questions of modern hadronic physics [258, 259, 260, 261]. The two-flavour version of the eLSM has been successful in a study at nonzero density [153]. This leads us to consider the restoration of chiral symmetry at nonzero temperature and density for $N_f = 3$ and $N_f = 4$ with the eLSM, which offers many challenges for future work.

Appendices

A. Determination of the weak decay constants

We compute the decay constants of pion, kaon, the pseudoscalar open-charmed mesons D and D_S , and the pseudoscalar hidden-charmed meson η_C , which are denoted as f_π , f_D , f_{D_S} , and f_{η_C} , by using the formula (5.15),

$$P \rightarrow P + \theta_a(t_a S + S t_a), \quad (\text{A.1})$$

which is discussed in chapter 5 in details. In the case $N_f = 4$, the pseudoscalar mesons are ordered in a 4×4 matrix as follows:

$$P = \frac{1}{\sqrt{2}} \begin{pmatrix} \frac{1}{\sqrt{2}}(\eta_N + \pi^0) & \pi^+ & K^+ & D^0 \\ \pi^- & \frac{1}{\sqrt{2}}(\eta_N - \pi^0) & K^0 & D^- \\ K^- & \bar{K}^0 & \eta_S & D_S^- \\ \bar{D}^0 & D^+ & D_S^+ & \eta_c \end{pmatrix}, \quad (\text{A.2})$$

where

$$\pi^- = \frac{\pi^1 + i\pi^2}{\sqrt{2}}, \quad \pi^+ = \frac{\pi^1 - i\pi^2}{\sqrt{2}}, \quad (\text{A.3})$$

$$K^- = \frac{K^1 + iK^2}{\sqrt{2}}, \quad K^+ = \frac{K^1 - iK^2}{\sqrt{2}}, \quad (\text{A.4})$$

$$\bar{D}^0 = \frac{D^1 + iD^2}{\sqrt{2}}, \quad D^0 = \frac{D^1 - iD^2}{\sqrt{2}}. \quad (\text{A.5})$$

$$D_S^+ = \frac{D_S^1 + iD_S^2}{\sqrt{2}}, \quad D_S^- = \frac{D_S^1 - iD_S^2}{\sqrt{2}}. \quad (\text{A.6})$$

The vacuum expectation values ϕ_N , ϕ_S , and ϕ_C are contained in the following diagonal matrix:

$$\langle \Phi \rangle = \begin{pmatrix} \frac{\phi_N}{\sqrt{2}} & 0 & 0 & 0 \\ 0 & \frac{\phi_N}{\sqrt{2}} & 0 & 0 \\ 0 & 0 & \phi_S & 0 \\ 0 & 0 & 0 & \phi_C \end{pmatrix}. \quad (\text{A.7})$$

In Eq.(A.1), $t_a = \frac{\lambda_a}{2}$ are the generators with $a = 0, 1, \dots, N_f^2 - 1$, where λ_a are the Gell-Mann matrices and chosen to satisfy $\text{Tr}(\lambda_a \lambda_b) = 2\delta_{ab}$. In the case $N_f = 4$, the Gell-Mann matrices are rank-4 tensors and there are 16 generators ($a = 0, \dots, 15$). For $a = 0$, λ_0 is a special unitary $SU(4)$ matrix but it corresponds to a unitary $U(1)$ matrix,

$$t_0 = \frac{1}{2\sqrt{2}} \begin{pmatrix} 1 & 0 & 0 & 0 \\ 0 & 1 & 0 & 0 \\ 0 & 0 & 1 & 0 \\ 0 & 0 & 0 & 1 \end{pmatrix}. \quad (\text{A.8})$$

The canonical form of the 4×4 Gell-Mann matrices is

$$\begin{aligned}
\lambda_1 &= \begin{pmatrix} 0 & 1 & 0 & 0 \\ 1 & 0 & 0 & 0 \\ 0 & 0 & 0 & 0 \\ 0 & 0 & 0 & 0 \end{pmatrix}, \quad \lambda_2 = \begin{pmatrix} 0 & -i & 0 & 0 \\ i & 0 & 0 & 0 \\ 0 & 0 & 0 & 0 \\ 0 & 0 & 0 & 0 \end{pmatrix}, \quad \lambda_3 = \begin{pmatrix} 1 & 0 & 0 & 0 \\ 0 & -1 & 0 & 0 \\ 0 & 0 & 0 & 0 \\ 0 & 0 & 0 & 0 \end{pmatrix}, \\
\lambda_4 &= \begin{pmatrix} 0 & 0 & 1 & 0 \\ 0 & 0 & 0 & 0 \\ 1 & 0 & 0 & 0 \\ 0 & 0 & 0 & 0 \end{pmatrix}, \quad \lambda_5 = \begin{pmatrix} 0 & 0 & -i & 0 \\ 0 & 0 & 0 & 0 \\ i & 0 & 0 & 0 \\ 0 & 0 & 0 & 0 \end{pmatrix}, \quad \lambda_6 = \begin{pmatrix} 0 & 0 & 0 & 0 \\ 0 & 0 & 1 & 0 \\ 0 & 1 & 0 & 0 \\ 0 & 0 & 0 & 0 \end{pmatrix}, \\
\lambda_7 &= \begin{pmatrix} 0 & 0 & 0 & 0 \\ 0 & 0 & -i & 0 \\ 0 & i & 0 & 0 \\ 0 & 0 & 0 & 0 \end{pmatrix}, \quad \lambda_8 = \begin{pmatrix} 1 & 0 & 0 & 0 \\ 0 & 1 & 0 & 0 \\ 0 & 0 & -2 & 0 \\ 0 & 0 & 0 & 0 \end{pmatrix}, \quad \lambda_9 = \begin{pmatrix} 0 & 0 & 0 & 1 \\ 0 & 0 & 0 & 0 \\ 0 & 0 & 0 & 0 \\ 1 & 0 & 0 & 0 \end{pmatrix}, \\
\lambda_{10} &= \begin{pmatrix} 0 & 0 & 0 & -i \\ 0 & 0 & 0 & 0 \\ 0 & 0 & 0 & 0 \\ i & 0 & 0 & 0 \end{pmatrix}, \quad \lambda_{11} = \begin{pmatrix} 0 & 0 & 0 & 0 \\ 0 & 0 & 0 & 1 \\ 0 & 0 & 0 & 0 \\ 0 & 1 & 0 & 0 \end{pmatrix}, \quad \lambda_{12} = \begin{pmatrix} 0 & 0 & 0 & 0 \\ 0 & 0 & 0 & -i \\ 0 & 0 & 0 & 0 \\ 0 & i & 0 & 0 \end{pmatrix}, \quad (\text{A.9}) \\
\lambda_{13} &= \begin{pmatrix} 0 & 0 & 0 & 0 \\ 0 & 0 & 0 & 0 \\ 0 & 0 & 0 & 1 \\ 0 & 0 & 1 & 0 \end{pmatrix}, \quad \lambda_{14} = \begin{pmatrix} 0 & 0 & 0 & 0 \\ 0 & 0 & 0 & 0 \\ 0 & 0 & 0 & -i \\ 0 & 0 & i & 0 \end{pmatrix}, \quad \lambda_{15} = \frac{1}{\sqrt{6}} \begin{pmatrix} 1 & 0 & 0 & 0 \\ 0 & 1 & 0 & 0 \\ 0 & 0 & 1 & 0 \\ 0 & 0 & 0 & -3 \end{pmatrix}.
\end{aligned}$$

Note that the rank-3 Gell-Mann matrices of the $SU(3)$ group are described by the first eight matrices [262], whereas transitions between $SU(3)$ and $SU(4)$ elements are generated by the matrices $\lambda_9 - \lambda_{15}$ [263]. We now use Eq.(A.1) to determine the decay constants.

A.1. Pion decay constant

In order to determine the pion decay constant, it suffices to take the corresponding direction in a-space, for instance $a = 1$.

Firstly, for $a = 1$, the generator $t_1 = \frac{1}{2} \begin{pmatrix} 0 & 1 & 0 & 0 \\ 1 & 0 & 0 & 0 \\ 0 & 0 & 0 & 0 \\ 0 & 0 & 0 & 0 \end{pmatrix}$, and Eq.(A.1) takes the following form

$$P \rightarrow P + \theta_1(t_1 \langle S \rangle + \langle S \rangle t_1). \quad (\text{A.10})$$

Explicitly,

$$\begin{aligned}
\frac{1}{2} \begin{pmatrix} 0 & \pi^1 & 0 & 0 \\ \pi^1 & 0 & 0 & 0 \\ 0 & 0 & 0 & 0 \\ 0 & 0 & 0 & 0 \end{pmatrix} &\mapsto \frac{1}{2} \begin{pmatrix} 0 & \pi^1 & 0 & 0 \\ \pi^1 & 0 & 0 & 0 \\ 0 & 0 & 0 & 0 \\ 0 & 0 & 0 & 0 \end{pmatrix} \\
&+ \frac{1}{2} \theta_1 \left[\begin{pmatrix} 0 & 1 & 0 & 0 \\ 1 & 0 & 0 & 0 \\ 0 & 0 & 0 & 0 \\ 0 & 0 & 0 & 0 \end{pmatrix} \begin{pmatrix} \frac{\phi_N}{\sqrt{2}} & 0 & 0 & 0 \\ 0 & \frac{\phi_N}{\sqrt{2}} & 0 & 0 \\ 0 & 0 & \phi_S & 0 \\ 0 & 0 & 0 & \phi_C \end{pmatrix} \right. \\
&+ \left. \begin{pmatrix} \frac{\phi_N}{\sqrt{2}} & 0 & 0 & 0 \\ 0 & \frac{\phi_N}{\sqrt{2}} & 0 & 0 \\ 0 & 0 & \phi_S & 0 \\ 0 & 0 & 0 & \phi_C \end{pmatrix} \begin{pmatrix} 0 & 1 & 0 & 0 \\ 1 & 0 & 0 & 0 \\ 0 & 0 & 0 & 0 \\ 0 & 0 & 0 & 0 \end{pmatrix} \right], \\
\frac{1}{2} \begin{pmatrix} 0 & \pi^1 & 0 & 0 \\ \pi^1 & 0 & 0 & 0 \\ 0 & 0 & 0 & 0 \\ 0 & 0 & 0 & 0 \end{pmatrix} &\mapsto \frac{1}{2} \begin{pmatrix} 0 & \pi^1 & 0 & 0 \\ \pi^1 & 0 & 0 & 0 \\ 0 & 0 & 0 & 0 \\ 0 & 0 & 0 & 0 \end{pmatrix} + \theta_1 \begin{pmatrix} 0 & \frac{\phi_N}{\sqrt{2}} & 0 & 0 \\ \frac{\phi_N}{\sqrt{2}} & 0 & 0 & 0 \\ 0 & 0 & 0 & 0 \\ 0 & 0 & 0 & 0 \end{pmatrix}. \tag{A.11}
\end{aligned}$$

We obtain

$$\pi^1 \mapsto \pi^1 + \sqrt{2} \phi_N \theta_1. \tag{A.12}$$

Similarly, for $a = 2, 3$, we obtain

$$\pi^2 \mapsto \pi^2 + \sqrt{2} \phi_N \theta_2, \tag{A.13}$$

$$\pi^0 \mapsto \pi^0 + \sqrt{2} \phi_N \theta_3. \tag{A.14}$$

After introducing the wave-function renormalization for the pion, we get

$$Z_\pi \pi^0 \mapsto Z_\pi \pi^0 + \sqrt{2} \phi_N \theta_3, \tag{A.15}$$

$$Z_\pi \pi^1 \mapsto Z_\pi \pi^1 + \sqrt{2} \phi_N \theta_1, \tag{A.16}$$

$$Z_\pi \pi^2 \mapsto Z_\pi \pi^2 + \sqrt{2} \phi_N \theta_2, \tag{A.17}$$

which can be written

$$\pi^0 \mapsto \pi^0 + \frac{\sqrt{2} \phi_N}{Z_\pi} \theta_3, \tag{A.18}$$

$$\pi^1 \mapsto \pi^1 + \frac{\sqrt{2} \phi_N}{Z_\pi} \theta_1, \tag{A.19}$$

$$\pi^2 \mapsto \pi^2 + \frac{\sqrt{2} \phi_N}{Z_\pi} \theta_2. \tag{A.20}$$

This gives the decay constant of the pion as

$$f_\pi = \frac{\sqrt{2} \phi_N}{Z_\pi}. \tag{A.21}$$

A.2. Kaon decay constant

Let us determine the decay constant f_K of the kaon.

In the case of $a = 4$, the generator $t_4 = \frac{1}{2} \begin{pmatrix} 0 & 0 & 1 & 0 \\ 0 & 0 & 0 & 0 \\ 1 & 0 & 0 & 0 \\ 0 & 0 & 0 & 0 \end{pmatrix}$, then Eq.(A.1) takes the following form

$$P \rightarrow P + \theta_4(t_4 \langle S \rangle + \langle S \rangle t_4). \quad (\text{A.22})$$

$$\begin{aligned} \frac{1}{\sqrt{2}} \begin{pmatrix} 0 & 0 & \frac{K^1}{\sqrt{2}} & 0 \\ 0 & 0 & 0 & 0 \\ \frac{K^1}{\sqrt{2}} & 0 & 0 & 0 \\ 0 & 0 & 0 & 0 \end{pmatrix} &\mapsto \frac{1}{\sqrt{2}} \begin{pmatrix} 0 & 0 & \frac{K^1}{\sqrt{2}} & 0 \\ 0 & 0 & 0 & 0 \\ \frac{K^1}{\sqrt{2}} & 0 & 0 & 0 \\ 0 & 0 & 0 & 0 \end{pmatrix} \\ &+ \frac{1}{2} \theta_4 \left[\begin{pmatrix} 0 & 0 & 1 & 0 \\ 0 & 0 & 0 & 0 \\ 1 & 0 & 0 & 0 \\ 0 & 0 & 0 & 0 \end{pmatrix} \begin{pmatrix} \frac{\phi_N}{\sqrt{2}} & 0 & 0 & 0 \\ 0 & \frac{\phi_N}{\sqrt{2}} & 0 & 0 \\ 0 & 0 & \phi_S & 0 \\ 0 & 0 & 0 & \phi_C \end{pmatrix} \right. \\ &\left. + \begin{pmatrix} \frac{\phi_N}{\sqrt{2}} & 0 & 0 & 0 \\ 0 & \frac{\phi_N}{\sqrt{2}} & 0 & 0 \\ 0 & 0 & \phi_S & 0 \\ 0 & 0 & 0 & \phi_C \end{pmatrix} \begin{pmatrix} 0 & 0 & 1 & 0 \\ 0 & 0 & 0 & 0 \\ 1 & 0 & 0 & 0 \\ 0 & 0 & 0 & 0 \end{pmatrix} \right], \\ \frac{1}{\sqrt{2}} \begin{pmatrix} 0 & 0 & \frac{K^1}{\sqrt{2}} & 0 \\ 0 & 0 & 0 & 0 \\ \frac{K^1}{\sqrt{2}} & 0 & 0 & 0 \\ 0 & 0 & 0 & 0 \end{pmatrix} &\mapsto \frac{1}{\sqrt{2}} \begin{pmatrix} 0 & 0 & \frac{K^1}{\sqrt{2}} & 0 \\ 0 & 0 & 0 & 0 \\ \frac{K^1}{\sqrt{2}} & 0 & 0 & 0 \\ 0 & 0 & 0 & 0 \end{pmatrix} + \frac{1}{2} \theta_4 \begin{pmatrix} 0 & 0 & \phi_S + \frac{\phi_N}{\sqrt{2}} & 0 \\ 0 & 0 & 0 & 0 \\ \phi_S + \frac{\phi_N}{\sqrt{2}} & 0 & 0 & 0 \\ 0 & 0 & 0 & 0 \end{pmatrix}, \end{aligned} \quad (\text{A.23})$$

$$\frac{1}{2} K^1 \mapsto \frac{1}{2} K^1 + \frac{1}{2} (\phi_S + \frac{\phi_N}{\sqrt{2}}) \theta_4, \quad (\text{A.24})$$

$$K^1 \mapsto K^1 + \frac{\sqrt{2} \phi_S + \phi_N}{\sqrt{2}} \theta_4. \quad (\text{A.25})$$

After introducing the wave-function renormalization of the kaons,

$$\begin{aligned} Z_K K^1 &\mapsto Z_K K^1 + \frac{(\sqrt{2} \phi_S + \phi_N)}{\sqrt{2}} \theta_4 \\ \Rightarrow K^1 &\mapsto K^1 + \frac{(\sqrt{2} \phi_S + \phi_N)}{\sqrt{2} Z_K} \theta_4. \end{aligned} \quad (\text{A.26})$$

Similarly for $a = 5, 6, 7, 8$, which can be written in general as

$$K \mapsto K + \frac{\sqrt{2}\phi_S + \phi_N}{\sqrt{2}Z_K} \theta_{4,5,6,8}, \quad (\text{A.27})$$

Then we can obtain the kaon decay constant as

$$f_K = \frac{\sqrt{2}\phi_S + \phi_N}{\sqrt{2}Z_K}. \quad (\text{A.28})$$

Note that, in the case $N_f = 3$, we used the formulas for the weak decay constants of pion and kaon divided by $\sqrt{2}$ as follows:

$$f_\pi = \frac{\phi_N}{Z_\pi}, \quad (\text{A.29})$$

and

$$f_K = \frac{\sqrt{2}\phi_S + \phi_N}{2Z_K}, \quad (\text{A.30})$$

because these theoretical formulas of the weak decay constants have been used in the fit [110], which are compared to the experimental data as listed by the PDG [51], where they are divided by $\sqrt{2}$.

A.3. Decay constant of D and D_S

Now let us turn to determine the weak decay constants of the open charmed mesons D and D_S :

For $a = 9$, the generator $t_9 = \frac{1}{2} \begin{pmatrix} 0 & 0 & 0 & 1 \\ 0 & 0 & 0 & 0 \\ 0 & 0 & 0 & 0 \\ 1 & 0 & 0 & 0 \end{pmatrix}$, and Eq.(5.15) reads

$$P \rightarrow P + \theta_9(t_9 \langle S \rangle + \langle S \rangle t_9). \quad (\text{A.31})$$

Then,

$$\begin{aligned} \frac{1}{2} \begin{pmatrix} 0 & 0 & 0 & D^1 \\ 0 & 0 & 0 & 0 \\ 0 & 0 & 0 & 0 \\ D^1 & 0 & 0 & 0 \end{pmatrix} &\mapsto \frac{1}{2} \begin{pmatrix} 0 & 0 & 0 & D^1 \\ 0 & 0 & 0 & 0 \\ 0 & 0 & 0 & 0 \\ D^1 & 0 & 0 & 0 \end{pmatrix} \\ &+ \frac{1}{2} \theta_9 \left[\begin{pmatrix} 0 & 0 & 0 & 1 \\ 0 & 0 & 0 & 0 \\ 0 & 0 & 0 & 0 \\ 1 & 0 & 0 & 0 \end{pmatrix} \begin{pmatrix} \frac{\phi_N}{\sqrt{2}} & 0 & 0 & 0 \\ 0 & \frac{\phi_N}{\sqrt{2}} & 0 & 0 \\ 0 & 0 & \phi_S & 0 \\ 0 & 0 & 0 & \phi_C \end{pmatrix} \right. \\ &\left. + \begin{pmatrix} \frac{\phi_N}{\sqrt{2}} & 0 & 0 & 0 \\ 0 & \frac{\phi_N}{\sqrt{2}} & 0 & 0 \\ 0 & 0 & \phi_S & 0 \\ 0 & 0 & 0 & \phi_C \end{pmatrix} \begin{pmatrix} 0 & 0 & 0 & 1 \\ 0 & 0 & 0 & 0 \\ 0 & 0 & 0 & 0 \\ 1 & 0 & 0 & 0 \end{pmatrix} \right], \end{aligned}$$

$$\begin{pmatrix} 0 & 0 & 0 & D^1 \\ 0 & 0 & 0 & 0 \\ 0 & 0 & 0 & 0 \\ D^1 & 0 & 0 & 0 \end{pmatrix} \mapsto \begin{pmatrix} 0 & 0 & 0 & D^1 \\ 0 & 0 & 0 & 0 \\ 0 & 0 & 0 & 0 \\ D^1 & 0 & 0 & 0 \end{pmatrix} + \theta_9 \begin{pmatrix} 0 & 0 & 0 & (\frac{\phi_N}{\sqrt{2}} + \phi_C) \\ 0 & 0 & 0 & 0 \\ 0 & 0 & 0 & 0 \\ (\frac{\phi_N}{\sqrt{2}} + \phi_C) & 0 & 0 & 0 \end{pmatrix}, \quad (\text{A.32})$$

$$D^1 \mapsto D^1 + (\frac{\phi_N}{\sqrt{2}} + \phi_C) \theta_9. \quad (\text{A.33})$$

After introducing the wave-function renormalization of the D mesons

$$\begin{aligned} Z_D D^1 &\mapsto Z_D D^1 + (\frac{\phi_N}{\sqrt{2}} + \phi_C) \theta_9, \\ \Rightarrow D^1 &\mapsto D^1 + \frac{\phi_N + \sqrt{2} \phi_C}{\sqrt{2}} \theta_9. \end{aligned} \quad (\text{A.34})$$

Similarly for $a = 10, 11, 12$, which can be written in general as

$$D \mapsto D + \frac{\phi_N + \sqrt{2} \phi_C}{\sqrt{2} Z_D} \theta_{9,10,11,12}. \quad (\text{A.35})$$

Then we can obtain the decay constant of D as

$$f_D = \frac{\phi_N + \sqrt{2} \phi_C}{\sqrt{2} Z_D}. \quad (\text{A.36})$$

For $a = 13$, the generator $t_{13} = \frac{1}{2} \begin{pmatrix} 0 & 0 & 0 & 0 \\ 0 & 0 & 0 & 0 \\ 0 & 0 & 0 & 1 \\ 0 & 0 & 1 & 0 \end{pmatrix}$, and Eq.(5.15) is

$$P \rightarrow P + \theta_{13}(t_{13} \langle S \rangle + \langle S \rangle t_{13}). \quad (\text{A.37})$$

$$\begin{aligned} \frac{1}{2} \begin{pmatrix} 0 & 0 & 0 & 0 \\ 0 & 0 & 0 & 0 \\ 0 & 0 & 0 & D_S^1 \\ 0 & 0 & D_S^1 & 0 \end{pmatrix} &\mapsto \frac{1}{2} \begin{pmatrix} 0 & 0 & 0 & 0 \\ 0 & 0 & 0 & 0 \\ 0 & 0 & 0 & D_S^1 \\ 0 & 0 & D_S^1 & 0 \end{pmatrix} \\ &+ \frac{1}{2} \theta_{13} \left[\begin{pmatrix} 0 & 0 & 0 & 0 \\ 0 & 0 & 0 & 0 \\ 0 & 0 & 0 & 1 \\ 0 & 0 & 1 & 0 \end{pmatrix} \begin{pmatrix} \frac{\phi_N}{\sqrt{2}} & 0 & 0 & 0 \\ 0 & \frac{\phi_N}{\sqrt{2}} & 0 & 0 \\ 0 & 0 & \phi_S & 0 \\ 0 & 0 & 0 & \phi_C \end{pmatrix} \right. \\ &\left. + \begin{pmatrix} \frac{\phi_N}{\sqrt{2}} & 0 & 0 & 0 \\ 0 & \frac{\phi_N}{\sqrt{2}} & 0 & 0 \\ 0 & 0 & \phi_S & 0 \\ 0 & 0 & 0 & \phi_C \end{pmatrix} \begin{pmatrix} 0 & 0 & 0 & 0 \\ 0 & 0 & 0 & 0 \\ 0 & 0 & 0 & 1 \\ 0 & 0 & 1 & 0 \end{pmatrix} \right], \end{aligned} \quad (\text{A.38})$$

$$\begin{pmatrix} 0 & 0 & 0 & 0 \\ 0 & 0 & 0 & 0 \\ 0 & 0 & 0 & D_S^1 \\ 0 & 0 & D_S^1 & 0 \end{pmatrix} \mapsto \begin{pmatrix} 0 & 0 & 0 & 0 \\ 0 & 0 & 0 & 0 \\ 0 & 0 & 0 & D_S^1 \\ 0 & 0 & D_S^1 & 0 \end{pmatrix} + \theta_{13} \begin{pmatrix} 0 & 0 & 0 & 0 \\ 0 & 0 & 0 & 0 \\ 0 & 0 & 0 & \phi_S + \phi_C \\ 0 & 0 & \phi_S + \phi_C & 0 \end{pmatrix}, \quad (\text{A.39})$$

$$D_S^1 \mapsto D_S^1 + (\phi_S + \phi_C) \theta_{13}, \quad (\text{A.40})$$

we get

$$\begin{aligned} Z_{D_S} D_S^1 &\mapsto Z_{D_S} D_S^1 + (\phi_S + \phi_C) \theta_{13} \\ \Rightarrow D_S^1 &\mapsto D_S^1 + \frac{\phi_S + \phi_C}{Z_{D_S}} \theta_{13}. \end{aligned} \quad (\text{A.41})$$

Similarly for $a = 14$, which can be written in general as

$$D_S \mapsto D_S + \frac{\phi_S + \phi_C}{Z_{D_S}} \theta_{13,14}, \quad (\text{A.42})$$

Then we obtain the decay constant of D_S as

$$f_{D_S} = \frac{\phi_N + \phi_C}{Z_{D_S}}, \quad (\text{A.43})$$

A.4. Decay constant of η_C

Finally, the decay constant of the charmonium state η_C can be determined from the combination of two generators, $a = 0$ and $a = 15$, as follows:

For $a = 0$, the generator $t_0 = \frac{\lambda_0}{2} = \frac{1}{2\sqrt{2}} \begin{pmatrix} 1 & 0 & 0 & 0 \\ 0 & 1 & 0 & 0 \\ 0 & 0 & 1 & 0 \\ 0 & 0 & 0 & 1 \end{pmatrix}$, and Eq.(5.15) reads

$$P \rightarrow P + \theta_0(t_0 \langle S \rangle + \langle S \rangle t_0). \quad (\text{A.44})$$

$$\begin{aligned} \frac{1}{\sqrt{2}} \begin{pmatrix} \frac{\eta_N}{\sqrt{2}} & 0 & 0 & 0 \\ 0 & \frac{\eta_N}{\sqrt{2}} & 0 & 0 \\ 0 & 0 & \eta_S & 0 \\ 0 & 0 & 0 & \eta_C \end{pmatrix} &\mapsto \frac{1}{\sqrt{2}} \begin{pmatrix} \frac{\eta_N}{\sqrt{2}} & 0 & 0 & 0 \\ 0 & \frac{\eta_N}{\sqrt{2}} & 0 & 0 \\ 0 & 0 & \eta_S & 0 \\ 0 & 0 & 0 & \eta_C \end{pmatrix} \\ &+ \frac{1}{2\sqrt{2}} \theta_0 \left[\begin{pmatrix} 1 & 0 & 0 & 0 \\ 0 & 1 & 0 & 0 \\ 0 & 0 & 1 & 0 \\ 0 & 0 & 0 & 1 \end{pmatrix} \begin{pmatrix} \frac{\phi_N}{\sqrt{2}} & 0 & 0 & 0 \\ 0 & \frac{\phi_N}{\sqrt{2}} & 0 & 0 \\ 0 & 0 & \phi_S & 0 \\ 0 & 0 & 0 & \phi_C \end{pmatrix} \right. \\ &\left. + \begin{pmatrix} \frac{\phi_N}{\sqrt{2}} & 0 & 0 & 0 \\ 0 & \frac{\phi_N}{\sqrt{2}} & 0 & 0 \\ 0 & 0 & \phi_S & 0 \\ 0 & 0 & 0 & \phi_C \end{pmatrix} \begin{pmatrix} 1 & 0 & 0 & 0 \\ 0 & 1 & 0 & 0 \\ 0 & 0 & 1 & 0 \\ 0 & 0 & 0 & 1 \end{pmatrix} \right], \end{aligned}$$

$$\begin{pmatrix} \frac{\eta_N}{\sqrt{2}} & 0 & 0 & 0 \\ 0 & \frac{\eta_N}{\sqrt{2}} & 0 & 0 \\ 0 & 0 & \eta_S & 0 \\ 0 & 0 & 0 & \eta_C \end{pmatrix} \mapsto \begin{pmatrix} \frac{\eta_N}{\sqrt{2}} & 0 & 0 & 0 \\ 0 & \frac{\eta_N}{\sqrt{2}} & 0 & 0 \\ 0 & 0 & \phi_S & 0 \\ 0 & 0 & 0 & \phi_C \end{pmatrix} + \theta_0 \begin{pmatrix} \frac{\phi_N}{\sqrt{2}} & 0 & 0 & 0 \\ 0 & \frac{\phi_N}{\sqrt{2}} & 0 & 0 \\ 0 & 0 & \phi_S & 0 \\ 0 & 0 & 0 & \phi_C \end{pmatrix}. \quad (\text{A.45})$$

For $a = 15$, the generator $t_{15} = \frac{1}{2\sqrt{6}} \begin{pmatrix} 1 & 0 & 0 & 0 \\ 0 & 1 & 0 & 0 \\ 0 & 0 & 1 & 0 \\ 0 & 0 & 0 & -3 \end{pmatrix}$, and Eq.(A.1) reads

$$P \rightarrow P + \theta_{15}(t_{15} \langle S \rangle + \langle S \rangle t_{15}). \quad (\text{A.46})$$

Then,

$$\begin{aligned}
\frac{1}{\sqrt{2}} \begin{pmatrix} \frac{\eta_N}{\sqrt{2}} & 0 & 0 & 0 \\ 0 & \frac{\eta_N}{\sqrt{2}} & 0 & 0 \\ 0 & 0 & \eta_S & 0 \\ 0 & 0 & 0 & \eta_C \end{pmatrix} &\mapsto \frac{1}{\sqrt{2}} \begin{pmatrix} \frac{\eta_N}{\sqrt{2}} & 0 & 0 & 0 \\ 0 & \frac{\eta_N}{\sqrt{2}} & 0 & 0 \\ 0 & 0 & \eta_S & 0 \\ 0 & 0 & 0 & \eta_C \end{pmatrix} \\
&+ \frac{1}{2\sqrt{6}} \theta_{15} \left[\begin{pmatrix} 1 & 0 & 0 & 0 \\ 0 & 1 & 0 & 0 \\ 0 & 0 & 1 & 0 \\ 0 & 0 & 0 & -3 \end{pmatrix} \begin{pmatrix} \frac{\phi_N}{\sqrt{2}} & 0 & 0 & 0 \\ 0 & \frac{\phi_N}{\sqrt{2}} & 0 & 0 \\ 0 & 0 & \phi_S & 0 \\ 0 & 0 & 0 & \phi_C \end{pmatrix} \right. \\
&\left. + \begin{pmatrix} \frac{\phi_N}{\sqrt{2}} & 0 & 0 & 0 \\ 0 & \frac{\phi_N}{\sqrt{2}} & 0 & 0 \\ 0 & 0 & \phi_S & 0 \\ 0 & 0 & 0 & \phi_C \end{pmatrix} \begin{pmatrix} 1 & 0 & 0 & 0 \\ 0 & 1 & 0 & 0 \\ 0 & 0 & 1 & 0 \\ 0 & 0 & 0 & -3 \end{pmatrix} \right], \\
\begin{pmatrix} \frac{\eta_N}{\sqrt{2}} & 0 & 0 & 0 \\ 0 & \frac{\eta_N}{\sqrt{2}} & 0 & 0 \\ 0 & 0 & \eta_S & 0 \\ 0 & 0 & 0 & \eta_C \end{pmatrix} &\mapsto \begin{pmatrix} \frac{\eta_N}{\sqrt{2}} & 0 & 0 & 0 \\ 0 & \frac{\eta_N}{\sqrt{2}} & 0 & 0 \\ 0 & 0 & \eta_S & 0 \\ 0 & 0 & 0 & \eta_C \end{pmatrix} + \frac{\theta_{15}}{\sqrt{3}} \begin{pmatrix} \frac{\phi_N}{\sqrt{2}} & 0 & 0 & 0 \\ 0 & \frac{\phi_N}{\sqrt{2}} & 0 & 0 \\ 0 & 0 & \phi_S & 0 \\ 0 & 0 & 0 & -3\phi_C \end{pmatrix}. \tag{A.47}
\end{aligned}$$

To find a combination of diagonal Lambdas which has only a nonzero entry in the fourth column and in the fourth row, we consider the relation between the singlet angle of transformation θ_0 and the multiplet angle transformation θ_{15} as follows:

$$\theta_{15} = -\sqrt{3}\theta_0.$$

Therefore, Eq.(A.47), can be written as

$$\begin{pmatrix} \frac{\eta_N}{\sqrt{2}} & 0 & 0 & 0 \\ 0 & \frac{\eta_N}{\sqrt{2}} & 0 & 0 \\ 0 & 0 & \eta_S & 0 \\ 0 & 0 & 0 & \eta_C \end{pmatrix} \mapsto \begin{pmatrix} \frac{\eta_N}{\sqrt{2}} & 0 & 0 & 0 \\ 0 & \frac{\eta_N}{\sqrt{2}} & 0 & 0 \\ 0 & 0 & \eta_S & 0 \\ 0 & 0 & 0 & \eta_C \end{pmatrix} - \theta_0 \begin{pmatrix} \frac{\phi_N}{\sqrt{2}} & 0 & 0 & 0 \\ 0 & \frac{\phi_N}{\sqrt{2}} & 0 & 0 \\ 0 & 0 & \phi_S & 0 \\ 0 & 0 & 0 & -3\phi_C \end{pmatrix}. \tag{A.48}$$

Adding Eq.(A.45) and Eq.(A.48), we obtain

$$2 \begin{pmatrix} \frac{\eta_N}{\sqrt{2}} & 0 & 0 & 0 \\ 0 & \frac{\eta_N}{\sqrt{2}} & 0 & 0 \\ 0 & 0 & \eta_S & 0 \\ 0 & 0 & 0 & \eta_C \end{pmatrix} \mapsto 2 \begin{pmatrix} \frac{\eta_N}{\sqrt{2}} & 0 & 0 & 0 \\ 0 & \frac{\eta_N}{\sqrt{2}} & 0 & 0 \\ 0 & 0 & \eta_S & 0 \\ 0 & 0 & 0 & \eta_C \end{pmatrix} + \theta_0 \begin{pmatrix} 0 & 0 & 0 & 0 \\ 0 & 0 & 0 & 0 \\ 0 & 0 & 0 & 0 \\ 0 & 0 & 0 & 4\phi_C \end{pmatrix}. \tag{A.49}$$

Then,

$$2\eta_C \mapsto 2\eta_C + 4\phi_C\theta_0, \tag{A.50}$$

After introducing the wave-function renormalization of the η_C meson

$$Z_{\eta_C} \eta_C \mapsto Z_{\eta_C} \eta_C + 2\phi_C \theta_0. \quad (\text{A.51})$$

Therefore, the weak decay constant of η_C is

$$f_{\eta_C} = \frac{2\phi_C}{Z_{\eta_C}}. \quad (\text{A.52})$$

B. Decay rates for χ_{c0}

We show the explicit expressions for the two- and three-body decay rates for the scalar hidden-charmed meson χ_{c0} , which are extracted from the Lagrangian (8.1) at tree level. The results are listed in Tables 8.2, 8.3, and Table 8.4 in Sec.8.2.

B.1. Two-body decay rates for χ_{C0}

The explicit expression for the two-body decay rates of χ_{c0} are extracted from the Lagrangian (8.1), and are presented in the following.

Decay channel $\chi_{C0} \rightarrow \bar{K}_0^{*0} K_0^{*0}$

The corresponding interaction Lagrangian from the Lagrangian (8.1) reads

$$\begin{aligned} \mathcal{L}_{\chi_{C0}\bar{K}_0^*K_0^*} = & -2\lambda_1 Z_{K_0^*}^2 \phi_C \chi_{C0} (\bar{K}_0^{*0} K_0^{*0} + K_0^{*-} K_0^{*+}) \\ & - h_1 \phi_C Z_{K_0^*}^2 \omega_{K^*}^2 \chi_{C0} (\partial_\mu K_0^{*0} \partial^\mu \bar{K}_0^{*0} + \partial_\mu K_0^{*-} \partial^\mu K_0^{*+}). \end{aligned} \quad (\text{B.1})$$

Consider only the $\chi_{C0} \rightarrow \bar{K}_0^{*0} K_0^{*0}$ decay channel, the $\chi_{C0} \rightarrow K_0^{*-} K_0^{*+}$ will give the same contribution due to isospin symmetry,

$$\mathcal{L}_{\chi_{C0}\bar{K}_0^{*0}K_0^{*0}} = -2\lambda_1 Z_{K_0^*}^2 \phi_C \chi_{C0} \bar{K}_0^{*0} K_0^{*0} - h_1 \phi_C Z_{K_0^*}^2 \omega_{K^*}^2 \chi_{C0} \partial_\mu K_0^{*0} \partial^\mu \bar{K}_0^{*0}. \quad (\text{B.2})$$

Let us denote the momenta of K_0^{*0} and \bar{K}_0^{*0} as P_1 and P_2 , respectively. The energy-momentum conservation on the vertex implies $P = P_1 + P_2$, where P denotes the momenta of the decaying particle χ_{C0} . Given that our particles are on-shell, we obtain

$$P_1 \cdot P_2 = \frac{P^2 - P_1^2 - P_2^2}{2} = \frac{m_{\chi_{C0}}^2 - 2m_{K_0^{*0}}^2}{2}. \quad (\text{B.3})$$

Upon substituting $\partial_\mu \rightarrow -iP^\mu$ for the decay particle and $\partial_\mu \rightarrow +iP_{1,2}^\mu$ for the outgoing particles, one obtains

$$\mathcal{L}_{\chi_{C0}\bar{K}_0^{*0}K_0^{*0}} = \phi_C Z_{K_0^*}^2 \left[-2\lambda_1 + h_1 \omega_{K^*}^2 \frac{m_{\chi_{c0}}^2 - 2m_{K_0^*}^2}{2} \right] \chi_{C0} K_0^{*0} \bar{K}_0^{*0}. \quad (\text{B.4})$$

Consequently, the decay amplitude is given by

$$-i\mathcal{M}_{\chi_{C0} \rightarrow \bar{K}_0^{*0} K_0^{*0}} = i\phi_C Z_{K_0^*}^2 \left[2\lambda_1 - h_1 \omega_{K^*}^2 \frac{m_{\chi_{c0}}^2 - 2m_{K_0^*}^2}{2} \right]. \quad (\text{B.5})$$

The decay width is obtained as

$$\Gamma_{\chi_{c0} \rightarrow \bar{K}_0^{*0} K_0^{*0}} = \frac{|\vec{k}_1|}{8\pi m_{\chi_{c0}}^2} | -i\mathcal{M}_{\chi_{c0} \rightarrow \bar{K}_0^{*0} K_0^{*0}} |^2. \quad (\text{B.6})$$

where

$$|\vec{k}_1| = \frac{1}{2m_{\chi_{c0}}} \left[m_{\chi_{c0}}^4 + (m_{\bar{K}_0^{*0}}^2 - m_{K_0^{*0}}^2)^2 - 2(m_{\bar{K}_0^{*0}}^2 + m_{K_0^{*0}}^2)m_{\chi_{c0}}^2 \right]^{1/2}. \quad (\text{B.7})$$

Decay channel $\chi_{c0} \rightarrow K^- K^+$

The corresponding interaction Lagrangian from the Lagrangian (8.1) has the following form

$$\begin{aligned} \mathcal{L}_{\chi_{c0}KK} = & -2\lambda_1 Z_K^2 \phi_C \chi_{c0} (\bar{K}^0 K^0 + K^- K^+) \\ & + h_1 \phi_C Z_K^2 \omega_{K_1}^2 \chi_{c0} (\partial_\mu K^0 \partial^\mu \bar{K}^0 + \partial_\mu K^- \partial^\mu K^+). \end{aligned} \quad (\text{B.8})$$

In a similar way as the previous case, one can obtain the decay width for the channel $\chi_{c0} \rightarrow K^- K^+$ as

$$\Gamma_{\chi_{c0} \rightarrow K^- K^+} = \frac{|\vec{k}_1|}{8\pi m_{\chi_{c0}}^2} \phi_C^2 Z_K^4 \left[2\lambda_1 + h_1 \omega_{K_1}^2 \left(\frac{m_{\chi_{c0}}^2 - 2m_K^2}{2} \right) \right]^2, \quad (\text{B.9})$$

where

$$|\vec{k}_1| = \frac{1}{2m_{\chi_{c0}}} \left[m_{\chi_{c0}}^4 - 4m_K^2 m_{\chi_{c0}}^2 \right]^{1/2}. \quad (\text{B.10})$$

Decay channel $\chi_{c0} \rightarrow \pi\pi$

The corresponding interaction Lagrangian is extracted from the Lagrangian (8.1) as

$$\mathcal{L}_{\chi_{c0}\pi\pi} = -\lambda_1 \phi_C Z_\pi^2 \chi_{c0} (\pi^{02} + 2\pi^- \pi^+) + \frac{1}{2} h_1 \phi_C Z_\pi^2 \omega_{a_1}^2 \chi_{c0} [(\partial_\mu \pi^0)^2 + 2\partial_\mu \pi^- \partial^\mu \pi^+]. \quad (\text{B.11})$$

The decay width for the channel $\chi_{c0} \rightarrow \pi\pi$ can be obtained in complete analogous as the previous cases

$$\Gamma_{\chi_{c0} \rightarrow \pi\pi} = \frac{3}{8} \frac{|\vec{k}_1|}{8\pi m_{\chi_{c0}}^2} \phi_C^2 Z_\pi^4 \left[2\lambda_1 + h_1 \omega_{a_1}^2 \left(\frac{m_{\chi_{c0}}^2 - 2m_\pi^2}{2} \right) \right]^2, \quad (\text{B.12})$$

where

$$|\vec{k}_1| = \frac{(m_{\chi_{c0}}^4 - 4m_\pi^2 m_{\chi_{c0}}^2)^{1/2}}{2m_{\chi_{c0}}}. \quad (\text{B.13})$$

Decay channel $\chi_{C0} \rightarrow \bar{K}^{*0} K^{*0}$

The corresponding interaction Lagrangian is extracted as

$$\mathcal{L}_{\chi_{C0}\bar{K}^{*0}K^{*0}} = h_1 \phi_C \chi_{C0} (K_\mu^{*-} K^{*+\mu} + K_\mu^{*0} \bar{K}^{*0\mu}). \quad (\text{B.14})$$

Consider only the $K_\mu^{*0} \bar{K}^{*0\mu}$ decay channel, then

$$\mathcal{L}_{\chi_{C0}\bar{K}^{*0}K^{*0}} = h_1 \phi_C \chi_{C0} K_\mu^{*0} \bar{K}^{*0\mu}. \quad (\text{B.15})$$

Put

$$A_{\chi_{C0}\bar{K}^{*0}K^{*0}} = h_1 \phi_C. \quad (\text{B.16})$$

Let us denote the momenta of χ_{C0} , \bar{K}^{*0} , and K^{*0} as P , P_1 , and P_2 , respectively, while the polarisation vectors are denoted as $\varepsilon_\mu^{(\alpha)}(P_1)$ and $\varepsilon_\nu^{(\beta)}(P_2)$. Then, upon substituting $\partial^\mu \rightarrow iP_{1,2}^\mu$ for the outgoing particles, we obtain the following Lorentz-invariant $\chi_{C0}\bar{K}^{*0}K^{*0}$ scattering amplitude $-i\mathcal{M}_{\chi_{C0}\rightarrow\bar{K}^{*0}K^{*0}}^{(\alpha,\beta)}$:

$$-i\mathcal{M}_{\chi_{C0}\rightarrow\bar{K}^{*0}K^{*0}}^{(\alpha,\beta)} = \varepsilon_\mu^{(\alpha)}(P_1)\varepsilon_\nu^{(\beta)}(P_2)h_{\chi_{C0}\bar{K}^{*0}K^{*0}}^{\mu\nu}, \quad (\text{B.17})$$

with

$$h_{\chi_{C0}\bar{K}^{*0}K^{*0}}^{\mu\nu} = iA_{\chi_{C0}\bar{K}^{*0}K^{*0}}g^{\mu\nu}, \quad (\text{B.18})$$

where $h_{\chi_{C0}\bar{K}^{*0}K^{*0}}^{\mu\nu}$ denotes the $\chi_{C0}\bar{K}^{*0}K^{*0}$ vertex.

The averaged squared amplitude $|\overline{-i\mathcal{M}}|^2$ is determined as follows:

$$\begin{aligned} |\overline{-i\mathcal{M}_{\chi_{C0}\rightarrow\bar{K}^{*0}K^{*0}}}|^2 &= \frac{1}{3} \sum_{\alpha,\beta=1}^3 \left| -i\mathcal{M}_{\chi_{C0}\rightarrow\bar{K}^{*0}K^{*0}}^{(\alpha,\beta)} \right|^2 \\ &= \frac{1}{3} \sum_{\alpha,\beta=1}^3 \varepsilon_\mu^{(\alpha)}(P_1)\varepsilon_\nu^{(\beta)}(P_2)h_{\chi_{C0}\bar{K}^{*0}K^{*0}}^{\mu\nu}\varepsilon_\kappa^{(\alpha)}(P_1) \\ &\quad \times \varepsilon_\lambda^{(\beta)}(P_2)h_{\chi_{C0}\bar{K}^{*0}K^{*0}}^{*\kappa\lambda}. \end{aligned} \quad (\text{B.19})$$

Equation (B.19) then yields the same expression as the one presented in Eq. (7.57):

$$\begin{aligned} |\overline{-i\mathcal{M}_{\chi_{C0}\rightarrow\bar{K}^{*0}K^{*0}}}|^2 &= \frac{1}{3} \left[\left| h_{\chi_{C0}\bar{K}^{*0}K^{*0}}^{\mu\nu} \right|^2 - \frac{\left| h_{\chi_{C0}\bar{K}^{*0}K^{*0}}^{\mu\nu} P_{1\mu} \right|^2}{m_{V_1}^2} - \frac{\left| h_{\chi_{C0}\bar{K}^{*0}K^{*0}}^{\mu\nu} P_{2\nu} \right|^2}{m_{V_2}^2} \right. \\ &\quad \left. + \frac{\left| h_{\chi_{C0}\bar{K}^{*0}K^{*0}}^{\mu\nu} P_{1\mu} P_{2\nu} \right|^2}{m_{V_1}^2 m_{V_2}^2} \right]. \end{aligned} \quad (\text{B.20})$$

From Eq. (B.18) we obtain

$$h^{\mu\nu}_{\chi_{C0}\bar{K}^{*0}K^{*0}}P_{1\mu} = iA_{\chi_{C0}\bar{K}^{*0}K^{*0}}P_1^\nu,$$

$$h^{\mu\nu}_{\chi_{C0}\bar{K}^{*0}K^{*0}}P_{2\nu} = iA_{\chi_{C0}\bar{K}^{*0}K^{*0}}P_2^\mu,$$

and

$$h^{\mu\nu}_{\chi_{C0}\bar{K}^{*0}K^{*0}}P_{1\mu}P_{2\nu} = iA_{\chi_{C0}\bar{K}^{*0}K^{*0}}P_1 \cdot P_2,$$

and consequently

$$|\overline{-i\mathcal{M}_{\chi_{C0}\rightarrow\bar{K}^{*0}K^{*0}}}|^2 = \frac{1}{3} \left[4 - \frac{P_1^2}{m_{K^{*0}}^2} - \frac{P_2^2}{m_{\bar{K}^{*0}}^2} + \frac{(P_1 \cdot P_2)^2}{m_{K^{*0}}^2 m_{\bar{K}^{*0}}^2} \right] A_{\chi_{C0}\bar{K}^{*0}K^{*0}}^2. \quad (\text{B.21})$$

For on-shell states, $P_{1,2}^2 = m_{K^{*0},\bar{K}^{*0}}^2$ and Eq. (B.21) reduces to

$$\begin{aligned} |\overline{-i\mathcal{M}_{\chi_{C0}\rightarrow\bar{K}^{*0}K^{*0}}}|^2 &= \frac{1}{3} \left[2 + \frac{(P_1 \cdot P_2)^2}{m_{K^{*0}}^2 m_{\bar{K}^{*0}}^2} \right] A_{\chi_{C0}\bar{K}^{*0}K^{*0}}^2 \\ &= \frac{1}{3} \left[2 + \frac{(m_{\chi_{C0}}^2 - m_{\bar{K}^{*0}}^2 - m_{K^{*0}}^2)^2}{4m_{K^{*0}}^2 m_{\bar{K}^{*0}}^2} \right] A_{\chi_{C0}\bar{K}^{*0}K^{*0}}^2. \end{aligned} \quad (\text{B.22})$$

Consequently, the decay width is

$$\Gamma_{\chi_{C0}\rightarrow\bar{K}^{*0}K^{*0}} = \frac{|\vec{k}_1|}{8\pi m_{\chi_{C0}}^2} |\overline{-i\mathcal{M}_{\chi_{C0}\rightarrow\bar{K}^{*0}K^{*0}}}|^2, \quad (\text{B.23})$$

where

$$|\vec{k}_1| = \frac{1}{2m_{\chi_{C0}}} [m_{\chi_{C0}}^4 + (m_{K^{*0}}^2 - m_{\bar{K}^{*0}}^2)^2 - 2(m_{K^{*0}}^2 + m_{\bar{K}^{*0}}^2)m_{\chi_{C0}}^2]^{1/2}. \quad (\text{B.24})$$

Decay channel $\chi_{C0} \rightarrow K_1 \bar{K}_1$

The corresponding interaction Lagrangian is extracted as

$$\mathcal{L}_{\chi_{C0}\bar{K}_1 K_1} = h_1 \phi_C \chi_{C0} (K_1^{+\mu} K_{1\mu}^- + K_1^{0\mu} \bar{K}_{1\mu}^0). \quad (\text{B.25})$$

Consider only the $\chi_{C0} \rightarrow K_1^0 \bar{K}_1^0$ decay channel, which gives the same contribution as the $\chi_{C0} \rightarrow K_1^{+\mu} K_{1\mu}^-$ decay channel due to the isospin symmetry

$$\mathcal{L}_{\chi_{C0}K_1^0 \bar{K}_1^0} = h_1 \phi_C \chi_{C0} K_1^{0\mu} \bar{K}_{1\mu}^0, \quad (\text{B.26})$$

which has the same form of the interaction Lagrangian $\mathcal{L}_{\chi_{C0}\bar{K}^{*0}K^{*0}}$. Therefore, in a similar way as was discussed in the previous case for the decay width of χ_{C0} into $\bar{K}^{*0}K^{*0}$, one can obviously obtain the decay width of the channel $\chi_{C0} \rightarrow K_1^0\bar{K}_1^0$ as

$$\Gamma_{\chi_{C0} \rightarrow K_1^0\bar{K}_1^0} = \frac{|\vec{k}_1|}{8\pi m_{\chi_{C0}}^2} \frac{1}{3} h_1^2 \phi_C^2 \left[2 + \frac{(m_{\chi_{C0}}^2 - m_{K_1^0}^2 - m_{\bar{K}_1^0}^2)^2}{4m_{K_1^0}^2 m_{\bar{K}_1^0}^2} \right], \quad (\text{B.27})$$

where

$$|\vec{k}_1| = \frac{1}{2m_{\chi_{C0}}} [m_{\chi_{C0}}^4 + (m_{K_1^0}^2 - m_{\bar{K}_1^0}^2)^2 - 2(m_{K_1^0}^2 + m_{\bar{K}_1^0}^2)m_{\chi_{C0}}^2]^{1/2}. \quad (\text{B.28})$$

Decay channel $\chi_{C0} \rightarrow \omega\omega$

The corresponding interaction Lagrangian is extracted as

$$\mathcal{L}_{\chi_{C0}\omega\omega} = \frac{1}{2} h_1 \phi_C \chi_{C0} \omega_N^\mu \omega_{N\mu}, \quad (\text{B.29})$$

which also has the same form as the interaction Lagrangian $\mathcal{L}_{\chi_{C0}\bar{K}^{*0}K^{*0}}$. Thus one can obtain the decay width of $\chi_{C0} \rightarrow \omega\omega$ as

$$\Gamma_{\chi_{C0} \rightarrow \omega\omega} = 2 \frac{[m_{\chi_{C0}}^4 - 4m_\omega^2 m_{\chi_{C0}}^2]^{1/2}}{16\pi m_{\chi_{C0}}^3} \frac{1}{12} h_1^2 \phi_C^2 \left[2 + \frac{(m_{\chi_{C0}}^2 - 2m_\omega^2)^2}{4m_\omega^4} \right]. \quad (\text{B.30})$$

Decay channel $\chi_{C0} \rightarrow \phi\phi$

The corresponding interaction Lagrangian is extracted as

$$\mathcal{L}_{\chi_{C0}\phi\phi} = \frac{1}{2} h_1 \phi_C \chi_{C0} \omega_S^\mu \omega_{S\mu}. \quad (\text{B.31})$$

Similar to the decay width for $\chi_{C0} \rightarrow \omega\omega$, the decay width for $\chi_{C0} \rightarrow \phi\phi$ is

$$\Gamma_{\chi_{C0} \rightarrow \phi\phi} = 2 \frac{[m_{\chi_{C0}}^4 - 4m_\phi^2 m_{\chi_{C0}}^2]^{1/2}}{16\pi m_{\chi_{C0}}^3} \frac{1}{12} h_1^2 \phi_C^2 \left[2 + \frac{(m_{\chi_{C0}}^2 - 2m_\phi^2)^2}{4m_\phi^4} \right]. \quad (\text{B.32})$$

Decay channel $\chi_{C0} \rightarrow \rho\rho$

The corresponding interaction Lagrangian is extracted as

$$\mathcal{L}_{\chi_{C0}\rho\rho} = \frac{1}{2} h_1 \phi_C \chi_{C0} (\rho^{0\mu} \rho_\mu^0 + 2\rho^{-\mu} \rho_\mu^+), \quad (\text{B.33})$$

which also has the same form as $\mathcal{L}_{\chi_{C0}\omega\omega}$. We thus obtain the decay width as

$$\begin{aligned}\Gamma_{\chi_{C0}\rightarrow\rho\rho} &= 3\Gamma_{\chi_{C0}\rightarrow\rho^0\rho^0} \\ &= 3\frac{[m_{\chi_{C0}}^4 - 4m_{\rho^0}^2 m_{\chi_{C0}}^2]^{1/2}}{16\pi m_{\chi_{C0}}^3} \times \frac{1}{12} h_1^2 \phi_C^2 \left[2 + \frac{(m_{\chi_{C0}}^2 - 2m_{\rho^0}^2)^2}{4m_{\rho^0}^4} \right].\end{aligned}\quad (\text{B.34})$$

Decay channel $\chi_{C0} \rightarrow a_0 a_0$

The corresponding interaction Lagrangian has the form

$$\mathcal{L}_{\chi_{C0}a_0a_0} = -\lambda_1 \phi_C \chi_{C0} (a_0^{02} + 2a_0^- a_0^+). \quad (\text{B.35})$$

The decay width of χ_{C0} into $a_0 a_0$ can be obtained as

$$\begin{aligned}\Gamma_{\chi_{C0}\rightarrow a_0 a_0} &= 3\Gamma_{\chi_{C0}\rightarrow a_0^0 a_0^0} \\ &= 3\frac{\lambda_1^2 \phi_C^2}{8\pi m_{\chi_{C0}}^2} \frac{[m_{\chi_{C0}}^4 - 4m_{a_0^0}^2 m_{\chi_{C0}}^2]^{1/2}}{2m_{\chi_{C0}}}.\end{aligned}\quad (\text{B.36})$$

Decay channel $\chi_{C0} \rightarrow K_1^+ K^-$

The corresponding interaction Lagrangian from the Lagrangian (8.1) reads

$$\mathcal{L}_{\chi_{C0}K_1K} = Z_K w_{K_1} h_1 \phi_C \chi_{C0} (K_1^{0\mu} \partial_\mu \bar{K}^0 + \partial_\mu K^+ K_1^\mu + K_1^{+\mu} \partial_\mu K^- + \bar{K}_1^{0\mu} \partial_\mu K^0). \quad (\text{B.37})$$

Let us consider only the decay channel $\chi_{C0} \rightarrow K_1^+ K^-$; the decay channels $\chi_{C0} \rightarrow K_1^0 \bar{K}^0$, $\bar{K}_1^0 K^0$, $K_1^- K^+$ will give the same contribution as a result of the isospin symmetry, so consider only

$$\mathcal{L}_{\chi_{C0}K_1^+K^-} = Z_K w_{K_1} h_1 \phi_C \chi_{C0} K_1^{+\mu} \partial_\mu K^-. \quad (\text{B.38})$$

We denote the momenta of K^- and K_1^+ as P_1 and P_2 , respectively. The energy-momentum conservation on the vertex implies $P = P_1 + P_2$, where P denotes the momentum of the decaying particle χ_{C0} . Given that our particles are on-shell, we obtain

$$P_1 \cdot P_2 = \frac{P^2 - P_1^2 - P_2^2}{2} = \frac{m_{\chi_{C0}}^2 - m_{K^-}^2 - m_{K_1^+}^2}{2}. \quad (\text{B.39})$$

Note that the scattering amplitude depends on the polarisation vector $\varepsilon_\mu^{(\alpha)}(P_2)$, Upon substituting $\partial_\mu \rightarrow +iP^\mu$ for the outgoing particles, one obtains

$$-i\mathcal{M}_{\chi_{C0}\rightarrow K_1^+K^-}^{(\alpha)} = iA_{\chi_{C0}K_1K} iP_1^\mu \varepsilon_\mu^{(\alpha)}(P_2), \quad (\text{B.40})$$

The average modulus squared amplitude reads

$$\left| \overline{-i\mathcal{M}_{\chi_{C0}\rightarrow K_1^+K^-}} \right|^2 = \frac{1}{3} A_{\chi_{C0}K_1K}^2 \left[-P_1^2 + \frac{(P_1 \cdot P_2)^2}{m_{K_1^+}^2} \right], \quad (\text{B.41})$$

where

$$A_{\chi_{C0}K_1K} = Z_K w_{K_1} h_1 \phi_C, \quad (\text{B.42})$$

and

$$P_1^2 = m_{K^-}^2.$$

Then, the decay width $\Gamma_{\chi_{C0} \rightarrow K_1^+ K^-}$ is

$$\Gamma_{\chi_{C0} \rightarrow K_1^+ K^-} = \frac{|\vec{k}_1|}{8\pi m_{\chi_{C0}}^2} \left| \overline{-i\mathcal{M}_{\chi_{C0} \rightarrow K_1^+ K^-}} \right|^2, \quad (\text{B.43})$$

where

$$|\vec{k}_1| = \frac{1}{2m_{\chi_{C0}}} \left[m_{\chi_{C0}}^4 + (m_{K^-}^2 - m_{K_1^+}^2)^2 - 2(m_{K^-}^2 + m_{K_1^+}^2)m_{\chi_{C0}}^2 \right]^{1/2}. \quad (\text{B.44})$$

Similarly, one can obtain the decay width of $\chi_{C0} \rightarrow K^* K_0^*$ as follows.

Decay channel $\chi_{C0} \rightarrow K^* \bar{K}_0^*$

From the interaction Lagrangian

$$\mathcal{L}_{\chi_{C0}K^*\bar{K}_0^*} = Z_{K_0^*} w_{K^*} h_1 \phi_C \chi_{C0} \bar{K}_0^{*0\mu} \partial_\mu K_0^{*0}, \quad (\text{B.45})$$

which obtain from the corresponding interaction Lagrangian

$$\mathcal{L}_{\chi_{C0}K^*\bar{K}_0^*} = Z_{K_0^*} w_{K^*} h_1 \phi_C \chi_{C0} (\bar{K}_0^{*0\mu} \partial_\mu K_0^{*0} - \partial_\mu K_0^{*-} K^{*+\mu} + \partial_\mu K_0^{*+} K^{*- \mu} - \partial_\mu \bar{K}_0^{*0\mu} K^{*0\mu}). \quad (\text{B.46})$$

We compute the decay width as

$$\Gamma_{\chi_{C0} \rightarrow K^* \bar{K}_0^*} = \frac{|\vec{k}_1|}{8\pi m_{\chi_{C0}}^2} w_{K^*}^2 Z_{K^*}^2 h_1^2 \phi_C^2 \left| -m_{K^*}^2 + \frac{(m_{\chi_{C0}}^2 - m_{K^*}^2 - m_{\bar{K}_0^*}^2)^2}{4m_{\bar{K}_0^*}^2} \right|, \quad (\text{B.47})$$

where

$$|\vec{k}_1| = \frac{1}{2m_{\chi_{C0}}} \left[m_{\chi_{C0}}^4 + (m_{K^*}^2 - m_{\bar{K}_0^*}^2)^2 - 2(m_{K^*}^2 + m_{\bar{K}_0^*}^2)m_{\chi_{C0}}^2 \right]^{1/2}. \quad (\text{B.48})$$

Note that we considered only the decay channel $\chi_{C0} K^* \bar{K}_0^*$ because the other decay channels contribute the same of isospin symmetry reasons. Thus,

$$\Gamma_{\chi_{C0} \rightarrow K^* \bar{K}_0^*} = \Gamma_{\chi_{C0} \rightarrow K^* \bar{K}_0^*} + \Gamma_{\chi_{C0} \rightarrow K^{*+} K_0^{*-}} + \Gamma_{\chi_{C0} \rightarrow K^{*-} K_0^{*+}} + \Gamma_{\chi_{C0} \rightarrow K_0^{*0} \bar{K}^{*0}}. \quad (\text{B.49})$$

Decay channels $\chi_{C0} \rightarrow \eta, \eta'$

The corresponding interaction Lagrangian of χ_{C0} with the η' and the η resonances reads

$$\begin{aligned}
\mathcal{L}_{\chi_{c0}\eta_N\eta_N,\eta_S\eta_S,\eta_N\eta_S} = & (-\lambda_1 - \frac{1}{2}c\phi_N^2\phi_S^2)Z_{\eta_N}^2\phi_C\chi_{c0}\eta_N^2 + \frac{1}{2}h_1w_{f_{1N}}^2Z_{\eta_N}^2\chi_{c0}\partial_\mu\eta_N\partial^\mu\eta_N \\
& + (-\lambda_1 - \frac{1}{8}c\phi_N^4)Z_{\eta_S}^2\phi_C\chi_{c0}\eta_S^2 + \frac{1}{2}h_1w_{f_{1S}}^2Z_{\eta_S}^2\chi_{c0}\partial_\mu\eta_S\partial^\mu\eta_S \\
& - \frac{1}{2}\phi_N^3\phi_C\phi_S Z_{\eta_N} Z_{\eta_S} \eta_N\eta_S. \tag{B.50}
\end{aligned}$$

Using Eq.(4.101) and Eq.(4.102), the interaction Lagrangian (B.50) will transform to a Lagrangian which describes the interaction of χ_{c0} with η and η' ,

$$\begin{aligned}
\mathcal{L}_{\chi_{c0}\eta^2,\eta'^2,\eta\eta'} = & [-\lambda_1(Z_{\eta_N}^2\cos^2\varphi_\eta + Z_{\eta_S}^2\sin^2\varphi_\eta) - \frac{1}{2}c\phi_N^2(\phi_S^2Z_{\eta_N}^2\cos^2\varphi_\eta \\
& + \frac{1}{4}\phi_N^2Z_{\eta_S}^2\sin^2\varphi_\eta + \phi_N\phi_S Z_{\eta_N}Z_{\eta_S}\sin\varphi_\eta\cos\varphi_\eta)]\phi_C\chi_{c0}\eta^2 \\
& + \left[\frac{1}{2}h_1\phi_C(w_{f_{1N}}^2Z_{\eta_N}^2\cos^2\varphi_\eta + w_{f_{1S}}^2Z_{\eta_S}^2\sin^2\varphi_\eta)\right]\chi_{c0}\partial_\mu\eta\partial^\mu\eta \\
& [-\lambda_1(Z_{\eta_N}^2\sin^2\varphi_\eta + Z_{\eta_S}^2\cos^2\varphi_\eta) - \frac{1}{2}c\phi_N^2(\phi_S^2Z_{\eta_N}^2\sin^2\varphi_\eta \\
& + \frac{1}{4}\phi_N^2Z_{\eta_S}^2\cos^2\varphi_\eta - \phi_N\phi_S Z_{\eta_N}Z_{\eta_S}\sin\varphi_\eta\cos\varphi_\eta)]\phi_C\chi_{c0}\eta'^2 \\
& + \left[\frac{1}{2}h_1\phi_C(w_{f_{1N}}^2Z_{\eta_N}^2\sin^2\varphi_\eta + w_{f_{1S}}^2Z_{\eta_S}^2\cos^2\varphi_\eta)\right]\chi_{c0}\partial_\mu\eta'\partial^\mu\eta' \\
& + [-2\lambda_1(-Z_{\eta_N}^2 + Z_{\eta_S}^2)\sin\varphi_\eta\cos\varphi_\eta] \\
& + \frac{1}{2}c\phi_N^2(2\phi_S^2Z_{\eta_N}^2 - \frac{1}{2}\phi_N^2Z_{\eta_S}^2)\cos\varphi_\eta\sin\varphi_\eta \\
& - \frac{1}{2}c\phi_N^3\phi_S Z_{\eta_N}Z_{\eta_S}(\cos^2\varphi_\eta - \sin^2\varphi_\eta\cos\varphi_\eta)]\phi_C\chi_{c0}\eta\eta' \\
& + h_1\phi_C\cos\varphi_\eta\sin\varphi_\eta(w_{f_{1S}}^2Z_{\eta_S}^2 - w_{f_{1N}}^2Z_{\eta_N}^2)\chi_{c0}\partial_\mu\eta\partial^\mu\eta', \tag{B.51}
\end{aligned}$$

which contains three different decay channels, $\chi_{c0} \rightarrow \eta\eta$, $\chi_{c0} \rightarrow \eta'\eta'$, and $\chi_{c0} \rightarrow \eta\eta'$, with the following vertices

$$\begin{aligned}
A_{\chi_{c0}\eta\eta} = & -\lambda_1\phi_C(Z_{\eta_N}^2\cos^2\varphi_\eta + Z_{\eta_S}^2\sin^2\varphi_\eta) \\
& - \frac{1}{2}c\phi_N^2\phi_C(\phi_S^2Z_{\eta_N}^2\cos^2\varphi_\eta + \frac{1}{4}\phi_N^2Z_{\eta_S}^2\sin^2\varphi_\eta + \phi_N\phi_S Z_{\eta_N}Z_{\eta_S}\sin\varphi_\eta\cos\varphi_\eta), \tag{B.52}
\end{aligned}$$

$$B_{\chi_{c0}\eta\eta} = \frac{1}{2}h_1\phi_C(w_{f_{1N}}^2Z_{\eta_N}^2\cos^2\varphi_\eta + w_{f_{1S}}^2Z_{\eta_S}^2\sin^2\varphi_\eta), \tag{B.53}$$

$$\begin{aligned}
A_{\chi_{c0}\eta'\eta'} = & -\lambda_1\phi_C(Z_{\eta_N}^2\sin^2\varphi_\eta + Z_{\eta_S}^2\cos^2\varphi_\eta) \\
& - \frac{1}{2}c\phi_N^2\phi_C(\phi_S^2Z_{\eta_N}^2\sin^2\varphi_\eta + \frac{1}{4}\phi_N^2Z_{\eta_S}^2\cos^2\varphi_\eta - \phi_N\phi_S Z_{\eta_N}Z_{\eta_S}\sin\varphi_\eta\cos\varphi_\eta), \tag{B.54}
\end{aligned}$$

$$B_{\chi_{c0}\eta'\eta'} = \frac{1}{2}h_1\phi_C(w_{f_{1N}}^2Z_{\eta_N}^2\sin^2\varphi_\eta + w_{f_{1S}}^2Z_{\eta_S}^2\cos^2\varphi_\eta), \tag{B.55}$$

$$A_{\chi_{C0}\eta\eta'} = -2\lambda_1\phi_C(-Z_{\eta_N}^2 + Z_{\eta_S}^2)\sin\varphi_\eta\cos\varphi_\eta + \frac{1}{2}c\phi_N^2\phi_C(2\phi_S^2Z_{\eta_N}^2 - \frac{1}{2}\phi_N^2Z_{\eta_S}^2)\cos\varphi_\eta\sin\varphi_\eta - \frac{1}{2}c\phi_N^3\phi_S\phi_CZ_{\eta_N}Z_{\eta_S}(\cos^2\varphi_\eta - \sin^2\varphi_\eta\cos\varphi_\eta), \quad (\text{B.56})$$

$$B_{\chi_{C0}\eta\eta'} = h_1\phi_C\cos\varphi_\eta\sin\varphi_\eta(w_{f_{1S}}^2Z_{\eta_S}^2 - w_{f_{1N}}^2Z_{\eta_N}^2). \quad (\text{B.57})$$

Let us firstly consider the channel $\chi_{C0} \rightarrow \eta\eta$. We denote the momenta of the two outgoing η particles as P_1 and P_2 , and P denotes the momentum of the decaying χ_{C0} particle. Given that our particles are on shell, we obtain

$$P_1 \cdot P_2 = \frac{P^2 - P_1^2 - P_2^2}{2} = \frac{m_{\chi_{C0}}^2 - 2m_\eta^2}{2}. \quad (\text{B.58})$$

After replacing $\partial_\mu \rightarrow +iP^\mu$ for the outgoing particles, one obtains the decay amplitude as

$$-iM_{\chi_{C0} \rightarrow \eta\eta} = i \left[A_{\chi_{C0}\eta\eta} - B_{\chi_{C0}\eta\eta} \frac{m_{\chi_{C0}}^2 - 2m_\eta^2}{2} \right]. \quad (\text{B.59})$$

Then the decay width is

$$\Gamma_{\chi_{C0} \rightarrow \eta\eta} = 2 \frac{|\vec{k}_1|}{8\pi m_{\chi_{C0}}^2} \left| -iM_{\chi_{C0} \rightarrow \eta\eta} \right|^2, \quad (\text{B.60})$$

where

$$|\vec{k}_1| = \frac{1}{2m_{\chi_{C0}}} \left[m_{\chi_{C0}}^4 - 4m_\eta^2 m_{\chi_{C0}}^2 \right]^{1/2}. \quad (\text{B.61})$$

Similarly, the decay width of χ_{C0} into $\eta'\eta'$ is obtained as

$$\Gamma_{\chi_{C0} \rightarrow \eta'\eta'} = 2 \frac{|\vec{k}_1|}{8\pi m_{\chi_{C0}}^2} \left| A_{\chi_{C0}\eta'\eta'} - B_{\chi_{C0}\eta'\eta'} \frac{m_{\chi_{C0}}^2 - 2m_{\eta'}^2}{2} \right|^2, \quad (\text{B.62})$$

where

$$|\vec{k}_1| = \frac{1}{2m_{\chi_{C0}}} \left[m_{\chi_{C0}}^4 - 4m_{\eta'}^2 m_{\chi_{C0}}^2 \right]^{1/2}. \quad (\text{B.63})$$

In a similar way, the decay width of χ_{C0} into $\eta\eta'$ can be obtained as

$$\Gamma_{\chi_{C0} \rightarrow \eta\eta'} = \frac{|\vec{k}_1|}{8\pi m_{\chi_{C0}}^2} \left| A_{\chi_{C0}\eta\eta'} - B_{\chi_{C0}\eta\eta'} \frac{m_{\chi_{C0}}^2 - m_\eta^2 - m_{\eta'}^2}{2} \right|^2, \quad (\text{B.64})$$

where

$$|\vec{k}_1| = \frac{1}{2m_{\chi_{C0}}} \left[m_{\chi_{C0}}^4 + (m_\eta^2 + m_{\eta'}^2)^2 - 2(m_\eta^2 + m_{\eta'}^2)m_{\chi_{C0}}^2 \right]^{1/2}. \quad (\text{B.65})$$

Decay channels $\chi_{C0} \rightarrow f_0 f_0$

The corresponding interaction Lagrangian is extracted from the Lagrangian (8.1)

$$\mathcal{L}_{\chi_{c0}f'_0} = -\lambda_1 \phi_C \chi_{c0} (\sigma_N^2 + \sigma_S^2) - \frac{m_0^2}{G_0^2} \phi_C \chi_{c0} G^2. \quad (\text{B.66})$$

Using the mixing matrix (8.9), the interaction Lagrangian becomes

$$\begin{aligned} \mathcal{L}_{\chi_{c0}f_0f_0} = & - \left[0.9125\lambda_1 + 0.0841 \frac{m_0^2}{G_0^2} \right] \phi_C \chi_{c0} f_0(1370)^2 \\ & - \left[0.985\lambda_1 + 0.0144 \frac{m_0^2}{G_0^2} \right] \phi_C \chi_{c0} f_0(1500)^2 \\ & - \left[0.065\lambda_1 - 0.0696 \frac{m_0^2}{G_0^2} \right] \phi_C \chi_{c0} f_0(1370) f_0(1500) \\ & - \left[0.55\lambda_1 - 0.551 \frac{m_0^2}{G_0^2} \right] \phi_C \chi_{c0} f_0(1370) f_0(1710) \\ & - \left[0.24\lambda_1 - 0.228 \frac{m_0^2}{G_0^2} \right] \phi_C \chi_{c0} f_0(1500) f_0(1710). \end{aligned} \quad (\text{B.67})$$

Therefore, we obtain the decay widths for all channels represented in the interaction Lagrangian (B.67) as follows:

Decay channels $\chi_{c0} \rightarrow f_0(1370) f_0(1370)$

$$\Gamma_{\chi_{c0} \rightarrow f_0(1370)^2} = 2 \frac{[m_{\chi_{c0}}^2 - 4m_{f_0(1370)}^2 m_{\chi_{c0}}^2]^{1/2}}{2 \times 8\pi m_{\chi_{c0}}^3} \left| -0.9125\lambda_1 \phi_C - 0.0841 \frac{m_0^2}{G_0^2} \phi_C \right|^2, \quad (\text{B.68})$$

Decay channels $\chi_{c0} \rightarrow f_0(1500) f_0(1500)$

$$\Gamma_{\chi_{c0} \rightarrow f_0(1500)^2} = 2 \frac{[m_{\chi_{c0}}^2 - 4m_{f_0(1500)}^2 m_{\chi_{c0}}^2]^{1/2}}{2 \times 8\pi m_{\chi_{c0}}^3} \left| -0.985\lambda_1 \phi_C - 0.0144 \frac{m_0^2}{G_0^2} \phi_C \right|^2, \quad (\text{B.69})$$

Decay channels $\chi_{c0} \rightarrow f_0(1370) f_0(1500)$

$$\begin{aligned} \Gamma_{\chi_{c0} \rightarrow f_0(1370) f_0(1500)} = & \frac{1}{8\pi m_{\chi_{c0}}^2} \left| -0.065\lambda_1 \phi_C + 0.0696 \frac{m_0^2}{G_0^2} \phi_C \right|^2 \\ & \times \frac{[m_{\chi_{c0}}^2 + (m_{f_0(1370)}^2 - m_{f_0(1500)}^2)^2 - 2(m_{f_0(1370)}^2 + m_{f_0(1500)}^2) m_{\chi_{c0}}^2]^{1/2}}{2m_{\chi_{c0}}}, \end{aligned} \quad (\text{B.70})$$

Decay channels $\chi_{C0} \rightarrow f_0(1370)f_0(1710)$

$$\Gamma_{\chi_{C0} \rightarrow f_0(1370)f_0(1710)} = \frac{1}{8\pi m_{\chi_{C0}}^2} \left| -0.55\lambda_1\phi_C + 0.551 \frac{m_0^2}{G_0^2}\phi_C \right|^2 \times \frac{[m_{\chi_{C0}}^2 + (m_{f_0(1370)}^2 - m_{f_0(1710)}^2)^2 - 2(m_{f_0(1370)}^2 + m_{f_0(1710)}^2)m_{\chi_{C0}}^2]^{1/2}}{2m_{\chi_{C0}}}, \quad (\text{B.71})$$

Decay channels $\chi_{C0} \rightarrow f_0(1500)f_0(1710)$

$$\Gamma_{\chi_{C0} \rightarrow f_0(1500)f_0(1710)} = \frac{1}{8\pi m_{\chi_{C0}}^2} \left| -0.228\lambda_1\phi_C - 0.24 \frac{m_0^2}{G_0^2}\phi_C \right|^2 \times \frac{[m_{\chi_{C0}}^2 + (m_{f_0(1500)}^2 - m_{f_0(1710)}^2)^2 - 2(m_{f_0(1500)}^2 + m_{f_0(1710)}^2)m_{\chi_{C0}}^2]^{1/2}}{2m_{\chi_{C0}}}. \quad (\text{B.72})$$

B.2. Three-body decay rates for χ_{C0}

The general formula for the three-body decay width for χ_{C0} , which is proved in chapter 5, takes the following form

$$\Gamma_{\chi_{C0} \rightarrow B_1 B_2 B_3} = \frac{S}{32(2\pi)^3 m_{\chi_{C0}}^3} \int_{(m_1+m_2)^2}^{(m_{\chi_{C0}}-m_3)^2} | -i\mathcal{M}_{A \rightarrow B_1 B_2 B_3} |^2 dm_{12}^2 \sqrt{\frac{(-m_1 + m_{12} - m_2)(m_1 + m_{12} - m_2)(-m_1 + m_{12} + m_2)(m_1 + m_{12} + m_2)}{m_{12}^2}} \sqrt{\frac{(-m_{\eta_C} + m_{12} - m_3)(m_{\chi_{C0}} + m_{12} - m_3)(-m_{\chi_{C0}} + m_{12} + m_3)(m_{\chi_{C0}} + m_{12} + m_3)}{m_{12}^2}}, \quad (\text{B.73})$$

The quantities m_1, m_2, m_3 refer to the masses of the three outgoing particles (P_1, P_2 , and P_3), which are (pseudo)scalar mesons in the present case, $\mathcal{M}_{\eta_C \rightarrow P_1 P_2 P_3}$ is the corresponding tree-level decay amplitude, and S is a symmetrization factor (it equals 1 if all P_1, P_2 , and P_3 are different, it equals 2 for two identical particles in the final state, and it equals 6 for three identical particles in the final state)

Now let us list the corresponding tree-level decay amplitudes for χ_{C0} which are presented in Tables 8.3 and 8.4 as follows:

Decay channel $\chi_{C0} \rightarrow K_0^* K \eta, \eta'$

The corresponding interaction Lagrangian can be obtained from the Lagrangian (8.1) as

$$\begin{aligned} \mathcal{L}_{\chi_{C0} K_0^* K \eta_N, \eta_S} &= \frac{1}{\sqrt{2}} c Z_K Z_{K_0^*} Z_{\eta_N} \phi_N^2 \phi_S \phi_C \chi_{C0} \eta_N (K_0^{*0} \bar{K}^0 + \bar{K}_0^{*0} K^0 + K_0^{*-} K^+ + K_0^{*+} K^-) \\ &\quad + \frac{\sqrt{2}}{4} c Z_K Z_{K_0^*} Z_{\eta_S} \phi_N^3 \phi_C \chi_{C0} \eta_S (K_0^{*0} \bar{K}^0 + \bar{K}_0^{*0} K^0 + K_0^{*-} K^+ + K_0^{*+} K^-). \end{aligned} \quad (\text{B.74})$$

Using Eqs. (4.101, 4.102), the interaction Lagrangian (B.74) can be written as

$$\begin{aligned} \mathcal{L}_{\chi_{C0} K_0^* K \eta, \eta'} &= \frac{1}{\sqrt{2}} c \phi_C \phi_N^2 Z_K Z_{K_0^*} \chi_{C0} \left[(\phi_S Z_{\eta_N} \cos \varphi_\eta + \frac{1}{2} \phi_N Z_{\eta_S} \sin \varphi_\eta) \eta \right. \\ &\quad \left. - (\phi_S Z_{\eta_N} \sin \varphi_\eta - \frac{1}{2} \phi_N Z_{\eta_S} \cos \varphi_\eta) \eta' \right] \\ &\quad \times [K_0^{*0} \bar{K}^0 + \bar{K}_0^{*0} K^0 + K_0^{*-} K^+ + K_0^{*+} K^-]. \end{aligned} \quad (\text{B.75})$$

Consequently, the amplitude decay for the decay channels $\chi_{C0} \rightarrow K_0^* K \eta$ and $\chi_{C0} \rightarrow K_0^* K \eta'$ can be obtain as

$$-i \mathcal{M}_{\chi_{C0} \rightarrow K_0^* K \eta} = -i \frac{1}{\sqrt{2}} c \phi_C \phi_N^2 Z_K Z_{K_0^*} (\phi_S Z_{\eta_N} \cos \varphi_\eta + \frac{1}{2} \phi_N Z_{\eta_S} \sin \varphi_\eta), \quad (\text{B.76})$$

and

$$-i \mathcal{M}_{\chi_{C0} \rightarrow K_0^* K \eta'} = \frac{1}{\sqrt{2}} c \phi_C \phi_N^2 Z_K Z_{K_0^*} (-\phi_S Z_{\eta_N} \sin \varphi_\eta + \frac{1}{2} \phi_N Z_{\eta_S} \cos \varphi_\eta), \quad (\text{B.77})$$

which are used to compute $\Gamma_{\chi_{C0} \rightarrow K_0^* K \eta}$ and $\Gamma_{\chi_{C0} \rightarrow K_0^* K \eta'}$ by Eq.(B.73).

Decay channel $\chi_{C0} \rightarrow f_0 \eta, \eta'$

The corresponding interaction Lagrangian is extracted from the Lagrangian (8.1) and given by

$$\begin{aligned} \mathcal{L}_{\chi_{C0} \sigma_N, S \eta_N S} &= -\frac{3}{2} c Z_{\eta_N} Z_{\eta_S} \phi_N^2 \phi_S \phi_C \chi_{C0} \sigma_N \eta_N \eta_S - c Z_{\eta_N}^2 \phi_N^2 \phi_S \phi_C \chi_{C0} \sigma_S \eta_N^2 \\ &\quad - c Z_{\eta_N}^2 \phi_N^2 \phi_S^2 \phi_C \chi_{C0} \sigma_N \eta_N^2 - \frac{1}{2} c Z_{\eta_S}^2 \phi_N^3 \phi_C \chi_{C0} \sigma_N \eta_S^2 \\ &\quad - \frac{1}{2} c Z_{\eta_N}, Z_{\eta_S} \phi_N^3 \phi_C \chi_{C0} \sigma_S \eta_S \eta_N. \end{aligned} \quad (\text{B.78})$$

Substituting Eqs.(4.101, 4.102, 4.113, 4.114) and the relations (8.11) and (8.12), we get the decay amplitudes for several channels, which are used in Eq.(B.73) to compute the decay widths, as follows:

Decay channel $\chi_{C0} \rightarrow f_0(1370)\eta\eta$

$$\begin{aligned} \mathcal{L}_{\chi_{C0}f_0(1370)\eta\eta} = & c\phi_N\phi_C [(0.085\phi_N - 1.41\phi_S) \cos\varphi_\eta \sin\varphi_\eta Z_{\eta_N} Z_{\eta_S} \phi_N \\ & - 0.47 \sin^2\varphi_\eta Z_{\eta_S}^2 \phi_N^2 + (0.17\phi_N - 0.94\phi_S)\phi_S \cos^2\varphi_\eta Z_{\eta_N}^2] \chi_{C0} \eta^2 f_0(1370). \end{aligned} \quad (\text{B.79})$$

Thus, the decay amplitude for the decay width $\Gamma_{\chi_{C0} \rightarrow f_0(1370)\eta\eta}$ reads

$$\begin{aligned} -i\mathcal{M}_{\chi_{C0} \rightarrow f_0(1370)\eta\eta} = & c\phi_N\phi_C [(0.085\phi_N - 1.41\phi_S) \cos\varphi_\eta \sin\varphi_\eta Z_{\eta_N} Z_{\eta_S} \phi_N \\ & - 0.47 \sin^2\varphi_\eta Z_{\eta_S}^2 \phi_N^2 + (0.17\phi_N - 0.94\phi_S)\phi_S \cos^2\varphi_\eta Z_{\eta_N}^2]. \end{aligned} \quad (\text{B.80})$$

Decay channel $\chi_{C0} \rightarrow f_0(1370)\eta'\eta'$

$$\begin{aligned} \mathcal{L}_{\chi_{C0}f_0(1370)\eta'\eta'} = & c\phi_N\phi_C [(-0.085\phi_N + 1.41\phi_S) \cos\varphi_\eta \sin\varphi_\eta Z_{\eta_N} Z_{\eta_S} \phi_N \\ & - 0.47 \cos^2\varphi_\eta Z_{\eta_S}^2 \phi_N^2 + (0.17\phi_N - 0.94\phi_S)\phi_S \sin^2\varphi_\eta Z_{\eta_N}^2] \chi_{C0} \eta'^2 f_0(1370). \end{aligned} \quad (\text{B.81})$$

Thus, the decay amplitude for the decay width $\Gamma_{\chi_{C0} \rightarrow f_0(1370)\eta'\eta'}$ reads

$$\begin{aligned} -i\mathcal{M}_{\chi_{C0} \rightarrow f_0(1370)\eta'\eta'} = & c\phi_N\phi_C [(-0.085\phi_N + 1.41\phi_S) \cos\varphi_\eta \sin\varphi_\eta Z_{\eta_N} Z_{\eta_S} \phi_N \\ & - 0.47 \cos^2\varphi_\eta Z_{\eta_S}^2 \phi_N^2 + (0.17\phi_N - 0.94\phi_S)\phi_S \sin^2\varphi_\eta Z_{\eta_N}^2]. \end{aligned} \quad (\text{B.82})$$

Decay channel $\chi_{C0} \rightarrow f_0(1370)\eta\eta'$

$$\begin{aligned} \mathcal{L}_{\chi_{C0}f_0(1370)\eta\eta'} = & c\phi_N\phi_C [(0.085\phi_N - 1.41\phi_S) \cos^2\varphi_\eta Z_{\eta_N} Z_{\eta_S} \phi_N \\ & + (-0.085\phi_N + 1.41\phi_S) \sin^2\varphi_\eta Z_{\eta_N} Z_{\eta_S} \phi_N \\ & + -0.94 Z_{\eta_S}^2 \phi_N^2 + (-0.34\phi_N + 1.88\phi_S)\phi_S Z_{\eta_N}^2 \sin\varphi_\eta \cos\varphi_\eta] \chi_{C0} \eta \eta' f_0(1370). \end{aligned} \quad (\text{B.83})$$

Thus, the decay amplitude for the decay width $\Gamma_{\chi_{C0} \rightarrow f_0(1370)\eta\eta'}$ reads

$$\begin{aligned} -i\mathcal{M}_{\chi_{C0} \rightarrow f_0(1370)\eta\eta'} = & c\phi_N\phi_C [(0.085\phi_N - 1.41\phi_S) \cos^2\varphi_\eta Z_{\eta_N} Z_{\eta_S} \phi_N \\ & + (-0.085\phi_N + 1.41\phi_S) \sin^2\varphi_\eta Z_{\eta_N} Z_{\eta_S} \phi_N \\ & + -0.94 Z_{\eta_S}^2 \phi_N^2 + (-0.34\phi_N + 1.88\phi_S)\phi_S Z_{\eta_N}^2 \sin\varphi_\eta \cos\varphi_\eta]. \end{aligned} \quad (\text{B.84})$$

Decay channel $\chi_{c0} \rightarrow f_0(1500)\eta\eta$

$$\begin{aligned} \mathcal{L}_{\chi_{c0}f_0(1500)\eta\eta} = & c\phi_N\phi_C [(-0.485\phi_N - 0.3151\phi_S) \cos\varphi_\eta \sin\varphi_\eta Z_{\eta_N} Z_{\eta_S} \phi_N \\ & - 0.105 \sin^2\varphi_\eta Z_{\eta_S}^2 \phi_N^2 + (-0.97\phi_N - 0.21\phi_S)\phi_S \cos^2\varphi_\eta Z_{\eta_N}^2] \chi_{c0}\eta^2 f_0(1500). \end{aligned} \quad (\text{B.85})$$

Thus, the decay amplitude for the decay width $\Gamma_{\chi_{c0} \rightarrow f_0(1500)\eta\eta}$ reads

$$\begin{aligned} -i\mathcal{M}_{\chi_{c0} \rightarrow f_0(1500)\eta\eta} = & c\phi_N\phi_C [(-0.485\phi_N - 0.3151\phi_S) \cos\varphi_\eta \sin\varphi_\eta Z_{\eta_N} Z_{\eta_S} \phi_N \\ & - 0.105 \sin^2\varphi_\eta Z_{\eta_S}^2 \phi_N^2 + (-0.97\phi_N - 0.21\phi_S)\phi_S \cos^2\varphi_\eta Z_{\eta_N}^2]. \end{aligned} \quad (\text{B.86})$$

Decay channel $\chi_{c0} \rightarrow f_0(1500)\eta\eta'$

$$\begin{aligned} \mathcal{L}_{\chi_{c0}f_0(1500)\eta\eta'} = & c\phi_N\phi_C [(-0.485\phi_N - 0.3151\phi_S) \cos^2\varphi_\eta Z_{\eta_N} Z_{\eta_S} \phi_N \\ & + (0.48\phi_N + 0.315\phi_S) \sin^2\varphi_\eta Z_{\eta_N} Z_{\eta_S} \phi_N \\ & + -0.21 Z_{\eta_S}^2 \phi_N^2 + (1.94\phi_N + 0.42\phi_S)\phi_S Z_{\eta_N}^2 \sin\varphi_\eta \cos\varphi_\eta] \chi_{c0}\eta\eta' f_0(1500). \end{aligned} \quad (\text{B.87})$$

Thus, the decay amplitude for the decay width $\Gamma_{\chi_{c0} \rightarrow f_0(1500)\eta\eta'}$ reads

$$\begin{aligned} -i\mathcal{M}_{\chi_{c0} \rightarrow f_0(1500)\eta\eta'} = & c\phi_N\phi_C [(-0.485\phi_N - 0.3151\phi_S) \cos^2\varphi_\eta Z_{\eta_N} Z_{\eta_S} \phi_N \\ & + (0.48\phi_N + 0.315\phi_S) \sin^2\varphi_\eta Z_{\eta_N} Z_{\eta_S} \phi_N \\ & + -0.21 Z_{\eta_S}^2 \phi_N^2 + (1.94\phi_N + 0.42\phi_S)\phi_S Z_{\eta_N}^2 \sin\varphi_\eta \cos\varphi_\eta]. \end{aligned} \quad (\text{B.88})$$

Decay channel $\chi_{c0} \rightarrow f_0(1710)\eta\eta$

$$\begin{aligned} \mathcal{L}_{\chi_{c0}f_0(1710)\eta\eta} = & c\phi_N\phi_C [(-0.09\phi_N - 0.39\phi_S) \cos\varphi_\eta \sin\varphi_\eta Z_{\eta_N} Z_{\eta_S} \phi_N \\ & + 0.13 \sin^2\varphi_\eta Z_{\eta_S}^2 \phi_N^2 + (-0.18\phi_N + 0.26\phi_S)\phi_S \cos^2\varphi_\eta Z_{\eta_N}^2] \chi_{c0}\eta^2 f_0(1710). \end{aligned} \quad (\text{B.89})$$

Thus, the decay amplitude for the decay width $\Gamma_{\chi_{c0} \rightarrow f_0(1710)\eta\eta}$ reads

$$\begin{aligned} -i\mathcal{M}_{\chi_{c0} \rightarrow f_0(1710)\eta\eta} = & c\phi_N\phi_C [(-0.09\phi_N - 0.39\phi_S) \cos\varphi_\eta \sin\varphi_\eta Z_{\eta_N} Z_{\eta_S} \phi_N \\ & + 0.13 \sin^2\varphi_\eta Z_{\eta_S}^2 \phi_N^2 + (-0.18\phi_N + 0.26\phi_S)\phi_S \cos^2\varphi_\eta Z_{\eta_N}^2]. \end{aligned} \quad (\text{B.90})$$

Decay channel $\chi_{C0} \rightarrow f_0(1710)\eta\eta'$

$$\begin{aligned} \mathcal{L}_{\chi_{C0}f_0(1710)\eta\eta'} = & c\phi_N\phi_C [(-0.09\phi_N - 0.39\phi_S) \sin^2 \varphi_\eta Z_{\eta_N} Z_{\eta_S} \phi_N \\ & + (-0.09\phi_N + 0.39\phi_S) \cos^2 \varphi_\eta Z_{\eta_N} Z_{\eta_S} \phi_N \\ & + -0.26Z_{\eta_S}^2 \phi_N^2 + (0.36\phi_N - 0.52\phi_S)\phi_S Z_{\eta_N}^2 \sin \varphi_\eta \cos \varphi_\eta] \chi_{C0}\eta\eta' f_0(1710). \end{aligned} \quad (\text{B.91})$$

Thus, the decay amplitude for the decay width $\Gamma_{\chi_{C0} \rightarrow f_0(1710)\eta\eta'}$ reads

$$\begin{aligned} -i\mathcal{M}_{\chi_{C0} \rightarrow f_0(1710)\eta\eta'} = & c\phi_N\phi_C c\phi_N\phi_C [(-0.09\phi_N - 0.39\phi_S) \sin^2 \varphi_\eta Z_{\eta_N} Z_{\eta_S} \phi_N \\ & + (-0.09\phi_N + 0.39\phi_S) \cos^2 \varphi_\eta Z_{\eta_N} Z_{\eta_S} \phi_N \\ & + -0.26Z_{\eta_S}^2 \phi_N^2 + (0.36\phi_N - 0.52\phi_S)\phi_S Z_{\eta_N}^2 \sin \varphi_\eta \cos \varphi_\eta]. \end{aligned} \quad (\text{B.92})$$

C. Decay rates for η_C

We present the explicit expressions for the two- and three-body decay rates for the pseudoscalar hidden-charmed meson η_C , which are listed in Table 8.5 in Sec.8.3.

C.1. Two-body decay expressions for η_C

The explicit expressions for the two-body decay widths of η_C are given by

Decay channel $\eta_C \rightarrow \bar{K}_0^* K$

The corresponding interaction Lagrangian can be obtained from the Lagrangian (8.27) as

$$\mathcal{L}_{\eta_C} = \frac{c\sqrt{2}}{8} \phi_N^3 \phi_S \phi_C Z_K Z_{K_0^*} Z_{\eta_C} \eta_C (K_0^{*0} \bar{K}^0 + \bar{K}_0^{*0} K^0 + K_0^{*-} K^+ + K_0^{*+} K^-). \quad (\text{C.1})$$

The decay width is obtained as

$$\Gamma_{\eta_C \rightarrow \bar{K}_0^* K} = \frac{|\vec{k}_1|}{68\pi m_{\eta_C}^2} c^2 \phi_N^6 \phi_S^2 \phi_C^2 Z_K^2 Z_{K_0^*}^2 Z_{\eta_C}^2, \quad (\text{C.2})$$

with

$$|\vec{k}_1| = \frac{1}{2m_{\eta_C}} \left[m_{\eta_C}^4 + (m_K^2 - m_{K_0^*}^2)^2 - 2(m_{K_0^*}^2 + m_K^2)m_{\eta_C}^2 \right]^{1/2}. \quad (\text{C.3})$$

Decay channel $\eta_C \rightarrow a_0 \pi$

The corresponding interaction Lagrangian is extracted as

$$\mathcal{L}_{\eta_C} = \frac{c}{4} \phi_N^2 \phi_S^2 \phi_C Z_\pi Z_{\eta_C} \eta_C (a_0^0 \pi^0 + a_0^+ \pi^- + a_0^- \pi^+). \quad (\text{C.4})$$

The decay width is obtained as

$$\Gamma_{\eta_C \rightarrow a_0 \pi} = 3 \frac{|\vec{k}_1|}{128\pi m_{\eta_C}^2} c^2 \phi_N^4 \phi_S^4 \phi_C^2 Z_\pi^2 Z_{\eta_C}^2, \quad (\text{C.5})$$

with

$$|\vec{k}_1| = \frac{1}{2m_{\eta_C}} \left[m_{\eta_C}^4 + (m_\pi^2 - m_{a_0}^2)^2 - 2(m_\pi^2 + m_{a_0}^2)m_{\eta_C}^2 \right]^{1/2}. \quad (\text{C.6})$$

Decay channel $\eta_C \rightarrow f_0\eta, \eta'$

The corresponding interaction Lagrangian can be obtained from the Lagrangian (8.27) as

$$\begin{aligned} \mathcal{L}_{\eta_C\eta\sigma} = \frac{c}{8}\phi_N^2\phi_C Z_{\eta_C}\eta_C\{ & -4\phi_N\phi_S(Z_{\eta_S}\eta_S\sigma_N + Z_{\eta_N}\eta_N\sigma_S) \\ & - 6\phi_S^2 Z_{\eta_N}\eta_N \sigma_N - \phi_N^2\eta_S\sigma_S Z_{\eta_S}\}. \end{aligned} \quad (\text{C.7})$$

Substituting Eqs.(4.102, 4.103) and the relations (8.11) and (8.12), the interaction Lagrangian (C.7) can be written as

$$\begin{aligned} \mathcal{L}_{\eta_C f_0\eta, \eta'} = \frac{c}{8}\phi_N^2\phi_C Z_{\eta_C} \left[\right. & \{(3.76\phi_S - 0.17\phi_N)\phi_N Z_{\eta_S} \sin \varphi_\eta \\ & + (5.64\phi_S - 0.68\phi_N)\phi_S Z_{\eta_N} \cos \varphi_\eta\}\eta_C f_0(1370)\eta \\ & + \{(0.84\phi_S + 0.97\phi_N)\phi_N Z_{\eta_S} \sin \varphi_\eta \\ & + (1.26\phi_S + 3.88\phi_N)\phi_S Z_{\eta_N} \cos \varphi_\eta\}\eta_C f_0(1500)\eta \\ & + \{(0.18\phi_N - 1.04\phi_S)\phi_N Z_{\eta_S} \sin \varphi_\eta \\ & + (0.72\phi_N - 1.56\phi_S)\phi_S Z_{\eta_N} \cos \varphi_\eta\}\eta_C f_0(1710)\eta \\ & + \{(3.76\phi_S - 0.17\phi_N)\phi_N Z_{\eta_S} \cos \varphi_\eta \\ & - (5.64\phi_S + 0.68\phi_N)\phi_S Z_{\eta_N} \sin \varphi_\eta\}\eta_C f_0(1370)\eta' \\ & + \{(0.84\phi_S + 0.97\phi_N)\phi_N Z_{\eta_S} \cos \varphi_\eta \\ & - (1.26\phi_S + 3.88\phi_N)\phi_S Z_{\eta_N} \sin \varphi_\eta\}\eta_C f_0(1500)\eta' \\ & + \{(0.18\phi_N - 1.04\phi_S)\phi_N Z_{\eta_S} \cos \varphi_\eta \\ & \left. - (1.56\phi_S - 0.72\phi_N)\phi_S Z_{\eta_N} \sin \varphi_\eta\}\eta_C f_0(1710)\eta' \right]. \end{aligned} \quad (\text{C.8})$$

We then obtain the following decay amplitudes:

Decay channel $\eta_C \rightarrow f_0(1370)\eta$

$$\begin{aligned} \Gamma_{\eta_C \rightarrow f_0(1370)\eta} = \frac{|\vec{k}_1|}{512\pi m_{\eta_C}^2} c^2 \phi_N^4 \phi_C^2 Z_{\eta_C}^2 \left[\right. & (3.76\phi_S - 0.17\phi_N)\phi_N Z_{\eta_S} \sin \varphi_\eta \\ & \left. + (5.64\phi_S - 0.68\phi_N)\phi_S Z_{\eta_N} \cos \varphi_\eta \right]^2, \end{aligned} \quad (\text{C.9})$$

with

$$|\vec{k}_1| = \frac{1}{2m_{\eta_C}} \left[m_{\eta_C}^4 + (m_{f_0(1370)}^2 - m_\eta^2)^2 - 2(m_{f_0(1370)}^2 + m_\eta^2)m_{\eta_C}^2 \right]^{1/2}. \quad (\text{C.10})$$

Decay channel $\eta_C \rightarrow f_0(1500)\eta$

$$\Gamma_{\eta_C \rightarrow f_0(1500)\eta} = \frac{|\vec{k}_1|}{512\pi m_{\eta_C}^2} c^2 \phi_N^4 \phi_C^2 Z_{\eta_C}^2 \left[(0.84\phi_S + 0.97\phi_N)\phi_N Z_{\eta_S} \sin \varphi_\eta + (1.26\phi_S + 3.88\phi_N)\phi_S Z_{\eta_N} \cos \varphi_\eta \right]^2, \quad (\text{C.11})$$

with

$$|\vec{k}_1| = \frac{1}{2m_{\eta_C}} \left[m_{\eta_C}^4 + (m_{f_0(1500)}^2 - m_\eta^2)^2 - 2(m_{f_0(1500)}^2 + m_\eta^2)m_{\eta_C}^2 \right]^{1/2}. \quad (\text{C.12})$$

Decay channel $\eta_C \rightarrow f_0(1710)\eta$

$$\Gamma_{\eta_C \rightarrow f_0(1710)\eta} = \frac{|\vec{k}_1|}{512\pi m_{\eta_C}^2} c^2 \phi_N^4 \phi_C^2 Z_{\eta_C}^2 \left[(0.18\phi_N - 1.04\phi_S)\phi_N Z_{\eta_S} \sin \varphi_\eta + (0.72\phi_N - 1.56\phi_S)\phi_S Z_{\eta_N} \cos \varphi_\eta \right]^2, \quad (\text{C.13})$$

with

$$|\vec{k}_1| = \frac{1}{2m_{\eta_C}} \left[m_{\eta_C}^4 + (m_{f_0(1710)}^2 - m_\eta^2)^2 - 2(m_{f_0(1710)}^2 + m_\eta^2)m_{\eta_C}^2 \right]^{1/2}. \quad (\text{C.14})$$

Decay channel $\eta_C \rightarrow f_0(1370)\eta'$

$$\Gamma_{\eta_C \rightarrow f_0(1370)\eta'} = \frac{|\vec{k}_1|}{512\pi m_{\eta_C}^2} c^2 \phi_N^4 \phi_C^2 Z_{\eta_C}^2 \left[(3.76\phi_S - 0.17\phi_N)\phi_N Z_{\eta_S} \cos \varphi_\eta - (5.64\phi_S + 0.68\phi_N)\phi_S Z_{\eta_N} \sin \varphi_\eta \right]^2, \quad (\text{C.15})$$

with

$$|\vec{k}_1| = \frac{1}{2m_{\eta_C}} \left[m_{\eta_C}^4 + (m_{f_0(1370)}^2 - m_{\eta'}^2)^2 - 2(m_{f_0(1370)}^2 + m_{\eta'}^2)m_{\eta_C}^2 \right]^{1/2}. \quad (\text{C.16})$$

Decay channel $\eta_C \rightarrow f_0(1500)\eta'$

$$\Gamma_{\eta_C \rightarrow f_0(1500)\eta'} = \frac{|\vec{k}_1|}{512\pi m_{\eta_C}^2} c^2 \phi_N^4 \phi_C^2 Z_{\eta_C}^2 \left[(0.84\phi_S + 0.97\phi_N)\phi_N Z_{\eta_S} \cos \varphi_\eta - (1.26\phi_S + 3.88\phi_N)\phi_S Z_{\eta_N} \sin \varphi_\eta \right]^2, \quad (\text{C.17})$$

with

$$|\vec{k}_1| = \frac{1}{2m_{\eta_C}} \left[m_{\eta_C}^4 + (m_{f_0(1500)}^2 - m_{\eta'}^2)^2 - 2(m_{f_0(1500)}^2 + m_{\eta'}^2)m_{\eta_C}^2 \right]^{1/2}. \quad (\text{C.18})$$

Decay channel $\eta_C \rightarrow f_0(1710)\eta'$

$$\Gamma_{\eta_C \rightarrow f_0(1710)\eta'} = \frac{|\vec{k}_1|}{512\pi m_{\eta_C}^2} c^2 \phi_N^4 \phi_C^2 Z_{\eta_C}^2 \left[(0.18\phi_N - 1.04\phi_S)\phi_N Z_{\eta_S} \cos \varphi_\eta - (1.56\phi_S - 0.72\phi_N)\phi_S Z_{\eta_N} \sin \varphi_\eta \right]^2, \quad (\text{C.19})$$

with

$$|\vec{k}_1| = \frac{1}{2m_{\eta_C}} \left[m_{\eta_C}^4 + (m_{f_0(1710)}^2 - m_{\eta'}^2)^2 - 2(m_{f_0(1710)}^2 + m_{\eta'}^2)m_{\eta_C}^2 \right]^{1/2}. \quad (\text{C.20})$$

C.2. Three-body decay expressions for η_C

The corresponding interaction Lagrangian, contains the three-body decay rates for the η_C meson, is extracted as

$$\begin{aligned} \mathcal{L}_{\eta_C} = & \frac{c}{8} \phi_N^2 \phi_C Z_{\eta_C} \eta_C \{ 2\phi_N Z_{\eta_S}^2 Z_{\eta_N} \eta_S^2 \eta_N + 6\phi_S Z_{\eta_S} Z_{\eta_N}^2 \eta_N^2 \eta_S \\ & - \sqrt{2}\phi_N Z_{\eta_S} Z_K^2 (\bar{K}^0 K^0 + K^- K^+) \eta_S - 3\sqrt{2}\phi_S Z_{\eta_N} Z_K^2 (\bar{K}^0 K^0 + K^- K^+) \eta_N \\ & + \sqrt{2}\phi_S Z_\pi Z_K^2 [\sqrt{2}(\bar{K}^0 K^+ \pi^- + K^0 K^- \pi^+) - (K^0 \bar{K}^0 - K^- K^+) \pi^0] \\ & - 2\phi_S \eta_S Z_{\eta_S} Z_\pi^2 (\pi^{0^2} + 2\pi^- \pi^+) \}. \end{aligned} \quad (\text{C.21})$$

The general formula for the three-body decay width for η_C , which is proved in chapter 5, takes the following form

$$\begin{aligned} \Gamma_{A \rightarrow B_1 B_2 B_3} = & \frac{S}{32(2\pi)^3 m_{\eta_C}^3} \int_{(m_1+m_2)^2}^{(m_{\eta_C}-m_3)^2} | -i\mathcal{M}_{A \rightarrow B_1 B_2 B_3} |^2 \\ & \sqrt{\frac{(-m_1 + m_{12} - m_2)(m_1 + m_{12} - m_2)(-m_1 + m_{12} + m_2)(m_1 + m_{12} + m_2)}{m_{12}^2}} \\ & \sqrt{\frac{(-m_{\eta_C} + m_{12} - m_3)(m_{\eta_C} + m_{12} - m_3)(-m_{\eta_C} + m_{12} + m_3)(m_{\eta_C} + m_{12} + m_3)}{m_{12}^2}} dm_{12}^2. \end{aligned}$$

Now let us list the corresponding tree-level decay amplitudes for η_C which are obtained from the Lagrangian (C.21) and are presented in Table 8.5 as follows:

Decay channel $\eta_C \rightarrow \eta^3$: $m_1 = m_2 = m_3 = m_\eta$ and $S = 6$

$$|\overline{-iM_{\eta_C \rightarrow \eta^3}}|^2 = \left[\frac{1}{4} c \phi_N^2 \phi_C \sin \varphi_\eta \cos \varphi_\eta (Z_{\eta_S} \phi_N \sin \varphi_\eta + 3Z_{\eta_N} \phi_S \cos \varphi_\eta) Z_{\eta_C} Z_{\eta_N} Z_{\eta_S} \right]^2. \quad (\text{C.22})$$

Decay channel $\eta_C \rightarrow \eta'^3$: $m_1 = m_2 = m_3 = m_{\eta'}$ and $S = 6$

$$|\overline{-iM_{\eta_C \rightarrow \eta'^3}}|^2 = \left[\frac{1}{4} c \phi_N^2 \phi_C \sin \varphi_\eta \cos \varphi_\eta (Z_{\eta_S} \phi_N \cos \varphi_\eta - 3Z_{\eta_N} \phi_S \sin \varphi_\eta) Z_{\eta_C} Z_{\eta_N} Z_{\eta_S} \right]^2. \quad (\text{C.23})$$

Decay channel $\eta_C \rightarrow \eta' \eta^2$: $m_1 = m_{\eta'}$, $m_2 = m_3 = m_\eta$ and $S = 2$

$$|\overline{-iM_{\eta_C \rightarrow \eta' \eta^2}}|^2 = \frac{1}{16} c^2 \phi_N^4 \phi_C^2 \left[\phi_N Z_{\eta_S} \sin \varphi_\eta (2 \cos^2 \varphi_\eta - \sin^2 \varphi_\eta) + 3Z_{\eta_N} \phi_S \cos \varphi_\eta (\cos^2 \varphi_\eta - 2 \sin^2 \varphi_\eta) \right]^2. \quad (\text{C.24})$$

Decay channel $\eta_C \rightarrow \eta'^2 \eta$: $m_1 = m_2 = m_{\eta'}$, $m_3 = m_\eta$ and $S = 2$

$$|\overline{-iM_{\eta_C \rightarrow \eta'^2 \eta}}|^2 = \frac{1}{16} c^2 \phi_N^4 \phi_C^2 Z_{\eta_C}^2 Z_{\eta_N}^2 Z_{\eta_S}^2 \left[Z_{\eta_S} \phi_N \cos \varphi_\eta (\cos^2 \varphi_\eta - 2 \sin^2 \varphi_\eta) + 3Z_{\eta_N} \phi_S \sin \varphi_\eta (\cos^2 \varphi_\eta - 2 \cos^2 \varphi_\eta) \right]^2. \quad (\text{C.25})$$

Decay channel $\eta_C \rightarrow \eta K \bar{K}$: $m_1 = K^0$, $m_2 = m_{\bar{K}^0}$, $m_3 = m_\eta$

$$\begin{aligned} \Gamma_{\eta_C \rightarrow \eta K \bar{K}} &= \Gamma_{\eta_C \rightarrow \eta K^+ K^-} + \Gamma_{\eta_C \rightarrow \eta K^0 \bar{K}^0} \\ &= 2\Gamma_{\eta_C \rightarrow \eta K^0 \bar{K}^0}. \end{aligned} \quad (\text{C.26})$$

with the average modulus squared decay amplitude

$$|\overline{-iM_{\eta_C \rightarrow \eta K \bar{K}}}|^2 = \frac{1}{32} c^2 \phi_N^4 \phi_C^2 Z_{\eta_C}^2 Z_K^4 (\phi_N Z_{\eta_S} \sin \varphi_\eta + 3\phi_S Z_{\eta_N} \cos \varphi_\eta)^2. \quad (\text{C.27})$$

Decay channel $\eta_C \rightarrow \eta' K \bar{K}$: $m_1 = K^0$, $m_2 = m_{\bar{K}^0}$, $m_3 = m_{\eta'}$

$$\Gamma_{\eta_C \rightarrow \eta' K \bar{K}} = 2\Gamma_{\eta_C \rightarrow \eta' K^0 \bar{K}^0}. \quad (\text{C.28})$$

The average modulus squared decay amplitude for this process reads

$$|\overline{-iM_{\eta_C \rightarrow \eta' K \bar{K}}}|^2 = \frac{1}{32} c^2 \phi_N^4 \phi_C^2 Z_{\eta_C}^2 Z_K^4 (\phi_N Z_{\eta_S} \cos \varphi_\eta - 3\phi_S Z_{\eta_N} \sin \varphi_\eta)^2. \quad (\text{C.29})$$

Decay channel $\eta_C \rightarrow \eta\pi\pi$: $m_1 = \eta$, $m_2 = m_3 = m_{\pi^0}$ and $S = 2$

$$\Gamma_{\eta_C \rightarrow \eta\pi\pi} = 3\Gamma_{\eta_C \rightarrow \eta\pi^0\pi^0}, \quad (\text{C.30})$$

where the average modulus squared decay amplitude for this process is obtained from the Lagrangian (C.21) as

$$|\overline{-iM_{\eta_C \rightarrow \eta\pi\pi}}|^2 = \frac{1}{16}c^2\phi_N^4\phi_S^2\phi_C^2Z_{\eta_C}^2Z_{\eta_S}^2Z_\pi^4\sin^2\varphi_\eta. \quad (\text{C.31})$$

Decay channel $\eta_C \rightarrow \eta'\pi\pi$: $m_1 = \eta'$, $m_2 = m_3 = m_{\pi^0}$ and $S = 2$

$$\Gamma_{\eta_C \rightarrow \eta'\pi\pi} = 3\Gamma_{\eta_C \rightarrow \eta'\pi^0\pi^0}, \quad (\text{C.32})$$

where the average modulus squared decay amplitude for this process is

$$|\overline{-iM_{\eta_C \rightarrow \eta'\pi\pi}}|^2 = \frac{1}{16}c^2\phi_N^4\phi_S^2\phi_C^2Z_{\eta_C}^2Z_{\eta_S}^2Z_\pi^4\cos^2\varphi_\eta. \quad (\text{C.33})$$

Decay channel $\eta_C \rightarrow KK\pi$: $m_1 = K^+$, $m_2 = K^-$, $m_3 = m_{\pi^0}$ and $S = 2$

$$\begin{aligned} \Gamma_{\eta_C \rightarrow KK\pi} &= \Gamma_{\eta_C \rightarrow K^+K^-\pi^0} + \Gamma_{\eta_C \rightarrow K^0\bar{K}^0\pi^0} + \Gamma_{\eta_C \rightarrow \bar{K}^0K^+\pi^-} + \Gamma_{\eta_C \rightarrow K^0K^-\pi^+} \\ &= 4\Gamma_{\eta_C \rightarrow K^+K^-\pi^0}. \end{aligned} \quad (\text{C.34})$$

with the average modulus squared decay amplitude

$$|\overline{-iM_{\eta_C \rightarrow K^+K^-\pi^0}}|^2 = \frac{1}{32}c^2\phi_N^4\phi_S^2\phi_C^2Z_{\eta_C}^2Z_{\eta_K}^4Z_\pi^2. \quad (\text{C.35})$$

Bibliography

- [1] B. Povh, K. Rith, C. Scholz, and F. Zetsche. Particles and nuclei: An introduction to the physical concepts. 2008.
- [2] J. Clerk Maxwell. A dynamical theory of the electromagnetic field. *Phil. Trans. Roy. Soc. Lond.*, 155:459–512, 1865.
- [3] G. Aad et al. Observation of a new particle in the search for the Standard Model Higgs boson with the ATLAS detector at the LHC. *Phys.Lett.*, B716:1–29, 2012.
- [4] S. Chatrchyan et al. Observation of a new boson at a mass of 125 GeV with the CMS experiment at the LHC. *Phys.Lett.*, B716:30–61, 2012.
- [5] S. M. Bilenky and J. Hosek. Glashow-Weinberg-Salam theory of electroweak interactions and the neutral currents. *Phys.Rept.*, 90:73–157, 1982.
- [6] W. J. Marciano and H. Pagels. Quantum chromodynamics: A review. *Phys.Rept.*, 36:137, 1978.
- [7] T. Muta. Foundation of quantum chromodynamics: An introduction to perturbative methods in gauge theories. 1998.
- [8] K. Hagiwara, K. Harada, M. Haruyama, K. Kato, T. Kubota, et al. Quantum chromodynamics at short distances. *Prog.Theor.Phys.Suppl.*, 77:1–334, 1983.
- [9] C. Amsler and N.A. Tornqvist. Mesons beyond the naive quark model. *Phys.Rept.*, 389:61–117, 2004.
- [10] E. Klempt and A. Zaitsev. Glueballs, Hybrids, Multiquarks. Experimental facts versus QCD inspired concepts. *Phys.Rept.*, 454:1–202, 2007.
- [11] S. Gasiorowicz and D.A. Geffen. Effective Lagrangians and field algebras with chiral symmetry. *Rev.Mod.Phys.*, 41:531–573, 1969.
- [12] U. G. Meissner. Low-Energy hadron physics from effective chiral Lagrangians with vector mesons. *Phys.Rept.*, 161:213, 1988.
- [13] C. Vafa and E. Witten. Restrictions on symmetry breaking in vector-like gauge theories. *Nucl.Phys.*, B234:173, 1984.
- [14] L. Giusti and S. Necco. Spontaneous chiral symmetry breaking in QCD: A Finite-size scaling study on the lattice. *JHEP*, 0704:090, 2007.
- [15] R. D. Pisarski and F. Wilczek. Remarks on the chiral phase transition in chromodynamics. *Phys.Rev.*, D29:338–341, 1984.

-
- [16] G. 't Hooft. Computation of the quantum effects due to a four-dimensional pseudoparticle. *Phys.Rev.*, D14:3432–3450, 1976.
- [17] G. 't Hooft. Symmetry breaking through Bell-Jackiw anomalies. *Phys.Rev.Lett.*, 37:8–11, 1976.
- [18] G. 't Hooft. How instantons solve the U(1) Problem. *Phys.Rept.*, 142:357–387, 1986.
- [19] D. J. Gross and F. Wilczek. Ultraviolet Behavior of Nonabelian Gauge Theories. *Phys.Rev.Lett.*, 30:1343–1346, 1973.
- [20] H. D. Politzer. Reliable perturbative results for strong interactions? *Phys.Rev.Lett.*, 30:1346–1349, 1973.
- [21] J. I. Kapusta. Quantum chromodynamics at high temperature. *Nucl.Phys.*, B148:461–498, 1979.
- [22] I.J.R. Aitchison and A.J.G. Hey. Gauge Theories in particle physics. A practical introduction. 1982.
- [23] K. Nakamura et al. Review of particle physics. *J.Phys.*, G37:075021, 2010.
- [24] D.J. Gross and Frank Wilczek. Asymptotically free gauge theories. 1. *Phys.Rev.*, D8:3633–3652, 1973.
- [25] H. D. Politzer. Setting the scale for predictions of asymptotic freedom. *Phys.Rev.*, D9:2174–2175, 1974.
- [26] H. D. Politzer. Asymptotic freedom: An approach to strong interactions. *Phys.Rept.*, 14:129–180, 1974.
- [27] Stephan Hartmann. Models and Stories in Hadron Physics. *Morgan and Morrison*, pages 326–346, 1999.
- [28] L. Wilets, S. Hartmann, and P. Tang. The chromodielectric soliton model: Quark selfenergy and hadron bags. *Phys.Rev.*, C55:2067–2077, 1997.
- [29] R. D. Pisarski. Applications of chiral symmetry. 1994.
- [30] A. Pich. The Standard model of electroweak interactions. pages 1–48, 2005.
- [31] S. Eidelman et al. Review of particle physics. Particle Data Group. *Phys.Lett.*, B592:1–1109, 2004.
- [32] M. Veltman. Theoretical aspects of high energy neutrino interactions. *Proc. Roy. Soc.*, A301:107–112, 1967.
- [33] S. L. Adler. Axial vector vertex in spinor electrodynamics. *Phys.Rev.*, 177:2426–2438, 1969.
- [34] J.S. Bell and R. Jackiw. A PCAC puzzle: $\pi^0 \rightarrow \gamma \gamma$ in the sigma model. *Nuovo Cim.*, A60:47–61, 1969.

-
- [35] L. D. Roper. Evidence for a P-11 pion-nucleon resonance at 556 MeV. *Phys.Rev.Lett.*, 12:340–342, 1964.
- [36] M.G. Olsson and G.B. Yodh. Analysis of single-pion production reactions $\pi+N \rightarrow \pi_1+\pi_2+N$ -prime below 1 BeV. *Phys.Rev.*, 145:1309–1326, 1966.
- [37] W. Pauli. The connection between spin and statistics. *Phys.Rev.*, 58:716–722, 1940.
- [38] C.M.G. Lattes, H. Muirhead, G.P.S. Occhialini, and C.F. Powell. Processes involving charged involving charged mesons. *Nature*, 159:694–697, 1947.
- [39] C.M.G. Lattes, G.P.S. Occhialini, and C.F. Powell. Observations on the tracks of slow mesons in photographic emulsions. 1. *Nature*, 160:453–456, 1947.
- [40] C.M.G. Lattes, G.P.S. Occhialini, and C.F. Powell. Observations on the tracks of slow mesons in photographic emulsions. 2. *Nature*, 160:486–492, 1947.
- [41] J.E. Augustin et al. Discovery of a narrow resonance in $e^+ e^-$ annihilation. *Phys.Rev.Lett.*, 33:1406–1408, 1974.
- [42] J.J. Aubert et al. Experimental observation of a heavy particle J. *Phys.Rev.Lett.*, 33:1404–1406, 1974.
- [43] H.B. Li. Recent results on charm physics at BESIII. *Nucl.Phys.Proc.Suppl.*, 233:185–191, 2012.
- [44] H. Albrecht et al. A Partial wave analysis of the decay $D^0 \rightarrow K^0(s) \pi^+ \pi^-$. *Phys.Lett.*, B308:435–443, 1993.
- [45] A. Anastassov et al. First measurement of $\Gamma(D^{*+})$ and precision measurement of $m(D^{*+}) - m(D^0)$. *Phys.Rev.*, D65:032003, 2002.
- [46] J. E. Bartelt and S. Shukla. Charmed meson spectroscopy. *Ann.Rev.Nucl.Part.Sci.*, 45:133–161, 1995.
- [47] S. Godfrey and N. Isgur. Mesons in a relativized quark model with chromodynamics. *Phys.Rev.*, D32:189–231, 1985.
- [48] S. Godfrey and R. Kokoski. The properties of p wave mesons with one heavy quark. *Phys.Rev.*, D43:1679–1687, 1991.
- [49] S. Capstick and N. Isgur. Baryons in a relativized quark model with chromodynamics. *Phys.Rev.*, D34:2809, 1986.
- [50] M. Neubert. Heavy quark symmetry. *Phys.Rept.*, 245:259–396, 1994.
- [51] J. Beringer et al. Review of particle physics (RPP). *Phys.Rev.*, D86:010001, 2012.
- [52] F.K. Guo, C. Hanhart, and U.G. Meissner. Implications of heavy quark spin symmetry on heavy meson hadronic molecules. *Phys.Rev.Lett.*, 102:242004, 2009.

-
- [53] L. Liu, K. Orginos, F.K. Guo, C. Hanhart, and U.G. Meissner. Interactions of charmed mesons with light pseudoscalar mesons from lattice QCD and implications on the nature of the $D_{s_0}^*$ (2317). *Phys.Rev.*, D87:014508, 2013.
- [54] T. Gutsche and V. E. Lyubovitskij. Heavy flavor hadron molecules. *AIP Conf.Proc.*, 1322:289–297, 2010.
- [55] T. Gutsche and V. E. Lyubovitskij. Heavy hadron molecules. *AIP Conf.Proc.*, 1257:385–389, 2010.
- [56] F.K. Guo, P.N. Shen, and H.C. Chiang. Dynamically generated $1+$ heavy mesons. *Phys.Lett.*, B647:133–139, 2007.
- [57] M. Cleven, F.K. Guo, C. Hanhart, and U.G. Meissner. Light meson mass dependence of the positive parity heavy-strange mesons. *Eur.Phys.J.*, A47:19, 2011.
- [58] F.K. Guo, C. Hanhart, and U.G. Meissner. Interactions between heavy mesons and Goldstone bosons from chiral dynamics. *Eur.Phys.J.*, A40:171–179, 2009.
- [59] N. Brambilla, S. Eidelman, B.K. Heltsley, R. Vogt, G.T. Bodwin, et al. Heavy quarkonium: progress, puzzles, and opportunities. *Eur.Phys.J.*, C71:1534, 2011.
- [60] R.L. Jaffe and K. Johnson. Unconventional States of Confined Quarks and Gluons. *Phys.Lett.*, B60:201, 1976.
- [61] R. Konoplich and M. Shchepkin. Glueballs' Masses in the Bag Model. *Nuovo Cim.*, A67:211, 1982.
- [62] M. Jezabek and J. Szwed. Glueballs in the bag models. *Acta Phys.Polon.*, B14:599, 1983.
- [63] M. Strohmeier-Presicek, T. Gutsche, R. V. Mau, and A. Faessler. Glueball quarkonia content and decay of scalar - isoscalar mesons. *Phys.Rev.*, D60:054010, 1999.
- [64] R.L. Jaffe, K. Johnson, and Z. Ryzak. Qualitative features of the glueball spectrum. *Annals Phys.*, 168:344, 1986.
- [65] C. J. Morningstar and M. J. Peardon. The Glueball spectrum from an anisotropic lattice study. *Phys.Rev.*, D60:034509, 1999.
- [66] M. Loan, X.Q. Luo, and Z.H. Luo. Monte Carlo study of glueball masses in the Hamiltonian limit of SU(3) lattice gauge theory. *Int.J.Mod.Phys.*, A21:2905–2936, 2006.
- [67] Y. Chen, A. Alexandru, S.J. Dong, Terrence Draper, I. Horvath, et al. Glueball spectrum and matrix elements on anisotropic lattices. *Phys.Rev.*, D73:014516, 2006.
- [68] F.E. Close. Gluonic hadrons. *Rept.Prog.Phys.*, 51:833, 1988.
- [69] S. Godfrey and J. Napolitano. Light meson spectroscopy. *Rev.Mod.Phys.*, 71:1411–1462, 1999.

-
- [70] F. Giacosa. Dynamical generation and dynamical reconstruction. *Phys.Rev.*, D80:074028, 2009.
- [71] E. Gregory, A. Irving, B. Lucini, C. McNeile, A. Rago, et al. Towards the glueball spectrum from unquenched lattice QCD. *JHEP*, 1210:170, 2012.
- [72] C. Amsler and F. E. Close. Is $f_0(1500)$ a scalar glueball? *Phys.Rev.*, D53:295–311, 1996.
- [73] W.J. Lee and D. Weingarten. Scalar quarkonium masses and mixing with the lightest scalar glueball. *Phys.Rev.*, D61:014015, 2000.
- [74] F. E. Close and A. Kirk. Scalar glueball q anti- q mixing above 1-GeV and implications for lattice QCD. *Eur.Phys.J.*, C21:531–543, 2001.
- [75] F. Giacosa, Th. Gutsche, V.E. Lyubovitskij, and A. Faessler. Scalar meson and glueball decays within a effective chiral approach. *Phys.Lett.*, B622:277–285, 2005.
- [76] F. Giacosa, Th. Gutsche, and A. Faessler. A Covariant constituent quark / gluon model for the glueball-quarkonia content of scalar - isoscalar mesons. *Phys.Rev.*, C71:025202, 2005.
- [77] V. Mathieu, N. Kochelev, and V. Vento. The physics of glueballs. *Int.J.Mod.Phys.*, E18:1–49, 2009.
- [78] S. Janowski, D. Parganlija, F. Giacosa, and D. H. Rischke. The glueball in a chiral linear sigma model with vector mesons. *Phys.Rev.*, D84:054007, 2011.
- [79] F. Giacosa, Th. Gutsche, V.E. Lyubovitskij, and A. Faessler. Scalar nonet quarkonia and the scalar glueball: Mixing and decays in an effective chiral approach. *Phys.Rev.*, D72:094006, 2005.
- [80] H.Y. Cheng, C.K. Chua, and K.F. Liu. Scalar glueball, scalar quarkonia, and their mixing. *Phys.Rev.*, D74:094005, 2006.
- [81] P. Chatzis, A. Faessler, Th. Gutsche, and V. E. Lyubovitskij. Hadronic and radiative three-body decays of J/ψ involving the scalars $f_0(1370)$, $f_0(1500)$ and $f_0(1710)$. *Phys.Rev.*, D84:034027, 2011.
- [82] Th. Gutsche. Exotic mesons. *Prog.Part.Nucl.Phys.*, 67:380–389, 2012.
- [83] S. Janowski, F. Giacosa, and D. H. Rischke. Is $f_0(1710)$ a glueball? *Phys.Rev.*, D90(11):114005, 2014.
- [84] F. Giacosa, Th. Gutsche, V.E. Lyubovitskij, and A. Faessler. Decays of tensor mesons and the tensor glueball in an effective field approach. *Phys.Rev.*, D72:114021, 2005.
- [85] L. Burakovsky and J. Terrance Goldman. Towards resolution of the enigmas of P wave meson spectroscopy. *Phys.Rev.*, D57:2879–2888, 1998.
- [86] A. Masoni, C. Cicalo, and G.L. Usai. The case of the pseudoscalar glueball. *J.Phys.*, G32:R293–R335, 2006.

-
- [87] Th. Gutsche, V. E. Lyubovitskij, and M. C. Tichy. $\eta(1405)$ in a chiral approach based on mixing of the pseudoscalar glueball with the first radial excitations of η and η' . *Phys.Rev.*, D80:014014, 2009.
- [88] H.Y. Cheng, H.n. Li, and K.F. Liu. Pseudoscalar glueball mass from $\eta - \eta' - G$ mixing. *Phys.Rev.*, D79:014024, 2009.
- [89] V. Mathieu and V. Vento. Pseudoscalar glueball and $\eta - \eta'$ mixing. *Phys.Rev.*, D81:034004, 2010.
- [90] C. Di Donato, G. Ricciardi, and I. Bigi. $\eta - \eta'$ Mixing - From electromagnetic transitions to weak decays of charm and beauty hadrons. *Phys.Rev.*, D85:013016, 2012.
- [91] B. A. Li. Chiral field theory of 0^-+ glueball. *Phys.Rev.*, D81:114002, 2010.
- [92] F. Ambrosino, A. Antonelli, M. Antonelli, F. Archilli, P. Beltrame, et al. A Global fit to determine the pseudoscalar mixing angle and the gluonium content of the η' meson. *JHEP*, 0907:105, 2009.
- [93] R. Escribano and J. Nadal. On the gluon content of the η and η' mesons. *JHEP*, 0705:006, 2007.
- [94] S. Gasiorowicz and D.A. Geffen. Effective Lagrangians and field algebras with chiral symmetry. *Rev.Mod.Phys.*, 41:531–573, 1969.
- [95] J. S. Schwinger. A theory of the fundamental interactions. *Annals Phys.*, 2:407–434, 1957.
- [96] M. Gell-Mann and M Levy. The axial vector current in beta decay. *Nuovo Cim.*, 16:705, 1960.
- [97] S. Weinberg. Dynamical approach to current algebra. *Phys.Rev.Lett.*, 18:188–191, 1967.
- [98] J. Gasser and H. Leutwyler. Chiral Perturbation Theory to One Loop. *Annals Phys.*, 158:142, 1984.
- [99] S. Scherer. Introduction to chiral perturbation theory. *Adv.Nucl.Phys.*, 27:277, 2003.
- [100] M. Bando, T. Kugo, and K. Yamawaki. Nonlinear Realization and Hidden Local Symmetries. *Phys.Rept.*, 164:217–314, 1988.
- [101] G. Ecker, J. Gasser, A. Pich, and E. de Rafael. The role of resonances in chiral perturbation theory. *Nucl.Phys.*, B321:311, 1989.
- [102] E. E. Jenkins, A. V. Manohar, and M. B. Wise. Chiral perturbation theory for vector mesons. *Phys.Rev.Lett.*, 75:2272–2275, 1995.
- [103] C. Terschlusen and S. Leupold. Electromagnetic transition form factors of mesons. *Prog.Part.Nucl.Phys.*, 67:401–405, 2012.
- [104] J. S. Schwinger. Chiral dynamics. *Phys.Lett.*, B24:473–476, 1967.

-
- [105] S. Weinberg. Nonlinear realizations of chiral symmetry. *Phys.Rev.*, 166:1568–1577, 1968.
- [106] P. Ko and S. Rudaz. Phenomenology of scalar and vector mesons in the linear sigma model. *Phys.Rev.*, D50:6877–6894, 1994.
- [107] M. Urban, M. Buballa, and J. Wambach. Vector and axial vector correlators in a chirally symmetric model. *Nucl.Phys.*, A697:338–371, 2002.
- [108] D. Parganlija, F. Giacosa, and D. H. Rischke. Vacuum properties of mesons in a linear sigma model with vector mesons and global chiral invariance. *Phys.Rev.*, D82:054024, 2010.
- [109] S. Gallas, F. Giacosa, and D. H. Rischke. Vacuum phenomenology of the chiral partner of the nucleon in a linear sigma model with vector mesons. *Phys.Rev.*, D82:014004, 2010.
- [110] D. Parganlija, P. Kovacs, G. Wolf, F. Giacosa, and D. H. Rischke. Meson vacuum phenomenology in a three-flavor linear sigma model with (axial-)vector mesons. *Phys.Rev.*, D87(1):014011, 2013.
- [111] C. Rosenzweig, A. Salomone, and J. Schechter. A pseudoscalar glueball, the Axial anomaly and the mixing problem for pseudoscalar mesons. *Phys.Rev.*, D24:2545–2548, 1981.
- [112] A. Salomone, J. Schechter, and T. Tudron. Properties of scalar gluonium. *Phys.Rev.*, D23:1143, 1981.
- [113] C. Rosenzweig, A. Salomone, and J. Schechter. How does a pseudoscalar glueball come unglued? *Nucl.Phys.*, B206:12, 1982.
- [114] H. Gomm and J. Schechter. Goldstone bosons and scalar gluonium. *Phys.Lett.*, B158:449, 1985.
- [115] R. Gomm, P. Jain, R. Johnson, and J. Schechter. Scale anomaly and the scalars. *Phys.Rev.*, D33:801, 1986.
- [116] D. Parganlija. Quarkonium Phenomenology in Vacuum. 2012.
- [117] J. T. Lenaghan, D. H. Rischke, and J. Schaffner-Bielich. Chiral symmetry restoration at nonzero temperature in the $SU(3)_r \times SU(3)_l$ linear sigma model. *Phys.Rev.*, D62:085008, 2000.
- [118] W. I. Eshraim. Masses of light and heavy mesons in a $U(4)_r \times U(4)_l$ linear sigma model. *PoS*, QCD-TNT-III:049, 2013.
- [119] Walaa I. Eshraim, Francesco Giacosa, and Dirk H. Rischke. Phenomenology of charmed mesons in the extended Linear Sigma Model. *Eur. Phys. J.*, A51(9):112, 2015.
- [120] W. I. Eshraim and F. Giacosa. Decays of open charmed mesons in the extended Linear Sigma Model. *EPJ Web Conf.*, 81:05009, 2014.

-
- [121] Walaa I. Eshraim. A pseudoscalar glueball and charmed mesons in the extended Linear Sigma Model. *EPJ Web Conf.*, 95:04018, 2015.
- [122] Walaa I. Eshraim. Vacuum properties of open charmed mesons in a chiral symmetric model. *J. Phys. Conf. Ser.*, 599(1):012009, 2015.
- [123] S. Gallas and F. Giacosa. Mirror versus naive assignment in chiral models for the nucleon. *Int.J.Mod.Phys.*, A29(17):1450098, 2014.
- [124] W. I. Eshraim, S. Janowski, F. Giacosa, and D. H. Rischke. Decay of the pseudoscalar glueball into scalar and pseudoscalar mesons. *Phys.Rev.*, D87(5):054036, 2013.
- [125] W. I. Eshraim and S. Janowski. Phenomenology of the pseudoscalar glueball with a mass of 2.6 GeV. *J.Phys.Conf.Ser.*, 426:012018, 2013.
- [126] W. I. Eshraim, S. Janowski, A. Peters, K. Neuschwander, and F. Giacosa. Interaction of the pseudoscalar glueball with (pseudo)scalar mesons and nucleons. *Acta Phys.Polon.Supp.*, 5:1101–1108, 2012.
- [127] W. I. Eshraim and S. Janowski. Branching ratios of the pseudoscalar glueball with a mass of 2.6 GeV. *PoS, ConfinementX*:118, 2012.
- [128] F. Giacosa. Mixing of scalar tetraquark and quarkonia states in a chiral approach. *Phys.Rev.*, D75:054007, 2007.
- [129] P. Kovacs and Zs. Szepl. The critical surface of the SU(3)(L) x SU(3)(R) chiral quark model at non-zero baryon density. *Phys.Rev.*, D75:025015, 2007.
- [130] P. Kovacs and Zs. Szepl. Influence of the isospin and hypercharge chemical potentials on the location of the CEP in the mu(B) - T phase diagram of the SU(3)(L) x SU(3)(R) chiral quark model. *Phys.Rev.*, D77:065016, 2008.
- [131] A. Heinz, S. Struber, F. Giacosa, and D. H. Rischke. Role of the tetraquark in the chiral phase transition. *Phys.Rev.*, D79:037502, 2009.
- [132] M.Y. Han and Y. Nambu. Three triplet model with double SU(3) symmetry. *Phys.Rev.*, 139:B1006–B1010, 1965.
- [133] Chen-Ning Yang and Robert L. Mills. Conservation of Isotopic Spin and Isotopic Gauge Invariance. *Phys.Rev.*, 96:191–195, 1954.
- [134] V. Koch. Aspects of chiral symmetry. *Int.J.Mod.Phys.*, E6:203–250, 1997.
- [135] F. Halzen and Martin A. D. Quarks and Leptons: an introductory course in modern particle physics.
- [136] C.M. Hung and E. V. Shuryak. Hydrodynamics near the QCD phase transition: Looking for the longest lived fireball. *Phys.Rev.Lett.*, 75:4003–4006, 1995.
- [137] M. E. Peskin and D. V. Schroeder. An Introduction to quantum field theory. 1995.
- [138] E. Noether. Invariant variation problems. *Gott.Nachr.*, 1918:235–257, 1918.

-
- [139] V. Koch. Introduction to chiral symmetry. 1995.
- [140] T. Muta. Foundations of quantum chromodynamics. Second edition. *World Sci.Lect.Notes Phys.*, 57:1–409, 1998.
- [141] J. Goldstone. Field theories with superconductor solutions. *Nuovo Cim.*, 19:154–164, 1961.
- [142] F. Giacosa. Ein effektives chirales Modell der QCD mit Vektormesonen, Dilaton und Tetraquarks: Physik im Vakuum und bei nichtverschwindender Dichte und Temperatur. 2012.
- [143] J. Boguta. A saturating chiral field theory of nuclear matter. *Phys.Lett.*, B120:34–38, 1983.
- [144] O. Kaymakçalan and J. Schechter. Chiral lagrangian of pseudoscalars and vectors. *Phys.Rev.*, D31:1109, 1985.
- [145] S. Janowski. Phänomenologie des Dilatons in einem chiralen Modell mit (Axial-) Vektormesonen. *Diploma, Thesis, Faculty of Physics at Johann Wolfgang Goethe-Universität Frankfurt am Main*, 2010.
- [146] R. F. Lebed. Phenomenology of large $N(c)$ QCD. *Czech.J.Phys.*, 49:1273–1306, 1999.
- [147] G. 't Hooft. A planar diagram theory for strong interactions. *Nucl.Phys.*, B72:461, 1974.
- [148] E. Witten. Baryons in the $1/n$ expansion. *Nucl.Phys.*, B160:57, 1979.
- [149] E.I. Lashin. CP conserved nonleptonic $K \rightarrow \pi \pi \pi$ decays in the chiral quark model. *Int.J.Mod.Phys.*, A21:3699–3726, 2006.
- [150] M. A. Shifman, A.I. Vainshtein, and V. I. Zakharov. Resonance properties in quantum chromodynamics. *Phys.Rev.Lett.*, 42:297, 1979.
- [151] A. A. Migdal and M. A. Shifman. Dilaton effective Lagrangian in gluodynamics. *Phys.Lett.*, B114:445, 1982.
- [152] A. Di Giacomo, H. G. Dosch, V.I. Shevchenko, and Yu.A. Simonov. Field correlators in QCD: Theory and applications. *Phys.Rept.*, 372:319–368, 2002.
- [153] S. Struber and D. H. Rischke. Vector and axialvector mesons at nonzero temperature within a gauged linear sigma model. *Phys.Rev.*, D77:085004, 2008.
- [154] D. Jido, Y. Nemoto, M. Oka, and A. Hosaka. Chiral symmetry for positive and negative parity nucleons. *Nucl.Phys.*, A671:471–480, 2000.
- [155] D. Zschesche, L. Tolos, J. Schaffner-Bielich, and R. D. Pisarski. Cold, dense nuclear matter in a $SU(2)$ parity doublet model. *Phys.Rev.*, C75:055202, 2007.
- [156] C. E. Detar and T. Kunihiro. Linear σ Model with parity doubling. *Phys.Rev.*, D39:2805, 1989.

- [157] B.W. Lee. Chiral dynamics. *Gordon and breach*, New York:1972.
- [158] S. Gallas, F. Giacosa, and G. Pagliara. Nuclear matter within a dilatation-invariant parity doublet model: the role of the tetraquark at nonzero density. *Nucl.Phys.*, A872:13–24, 2011.
- [159] F. Giacosa. Two-photon decay of light scalars: A Comparison of tetraquark and quarkonium assignments. 2007.
- [160] N. Isgur and M. B. Wise. Spectroscopy with heavy quark symmetry. *Phys.Rev.Lett.*, 66:1130–1133, 1991.
- [161] E. J. Eichten, C. T. Hill, and C. Quigg. Properties of orbitally excited heavy - light mesons. *Phys.Rev.Lett.*, 71:4116–4119, 1993.
- [162] Z. Maki and I. Umemura. Masses and decay constants of charmed mesons. *Prog.Theor.Phys.*, 59:507, 1978.
- [163] J. Segovia, D.R. Entem, and F. Fernandez. Strong charmonium decays in a microscopic model. *Nucl.Phys.*, A915:125–141, 2013.
- [164] L. Cao, Y.-C. Yang, and H. Chen. Charmonium states in QCD-inspired quark potential model using Gaussian expansion method. *Few Body Syst.*, 53:327–342, 2012.
- [165] G. S. Bali. Charmonia from lattice QCD. *Int.J.Mod.Phys.*, A21:5610–5617, 2006.
- [166] G.C. Donald, C.T.H. Davies, R.J. Dowdall, E. Follana, K. Hornbostel, et al. Precision tests of the J/ψ from full lattice QCD: mass, leptonic width and radiative decay rate to η_c . *Phys.Rev.*, D86:094501, 2012.
- [167] M. Kalinowski and M. Wagner. Strange and charm meson masses from twisted mass lattice QCD. *PoS, ConfinementX*:303, 2012.
- [168] R. Casalbuoni, A. Deandrea, N. Di Bartolomeo, R. Gatto, F. Feruglio, et al. Phenomenology of heavy meson chiral Lagrangians. *Phys.Rept.*, 281:145–238, 1997.
- [169] H. Georgi. An Effective field theory for heavy quarks at low-energies. *Phys.Lett.*, B240:447–450, 1990.
- [170] H. Georgi. Heavy quark effective field theory. 1991.
- [171] F. De Fazio. Weak decays of heavy quarks. 2000.
- [172] M. B. Wise. Chiral perturbation theory for hadrons containing a heavy quark. *Phys.Rev.*, D45:2188–2191, 1992.
- [173] E.E. Kolomeitsev and M.F.M. Lutz. On Heavy light meson resonances and chiral symmetry. *Phys.Lett.*, B582:39–48, 2004.
- [174] W. A. Bardeen and C. T. Hill. Chiral dynamics and heavy quark symmetry in a solvable toy field theoretic model. *Phys.Rev.*, D49:409–425, 1994.

-
- [175] W. A. Bardeen, E. J. Eichten, and C. T. Hill. Chiral multiplets of heavy - light mesons. *Phys.Rev.*, D68:054024, 2003.
- [176] M. A. Nowak, M. Rho, and I. Zahed. Chiral effective action with heavy quark symmetry. *Phys.Rev.*, D48:4370–4374, 1993.
- [177] M. A. Nowak, M. Rho, and I. Zahed. Chiral doubling of heavy light hadrons: BABAR 2317-MeV/c^{**2} and CLEO 2463-MeV/c^{**2} discoveries. *Acta Phys.Polon.*, B35:2377–2392, 2004.
- [178] C. Sasaki. Fate of charmed mesons near chiral symmetry restoration in hot matter. *Phys.Rev.*, D90(11):114007, 2014.
- [179] M. F.M. Lutz and M. Soyeur. Radiative and isospin-violating decays of D(s)-mesons in the hadrogenesis conjecture. *Nucl.Phys.*, A813:14–95, 2008.
- [180] I. Caprini, G. Colangelo, and H. Leutwyler. Mass and width of the lowest resonance in QCD. *Phys.Rev.Lett.*, 96:132001, 2006.
- [181] F.J. Yndurain, R. Garcia-Martin, and J.R. Pelaez. Experimental status of the pi pi isoscalar S wave at low energy: f(0)(600) pole and scattering length. *Phys.Rev.*, D76:074034, 2007.
- [182] R. Garcia-Martin, R. Kaminski, J.R. Pelaez, and J. Ruiz de Elvira. Precise determination of the f0(600) and f0(980) pole parameters from a dispersive data analysis. *Phys.Rev.Lett.*, 107:072001, 2011.
- [183] D.V. Bugg. A Study in Depth of f0(1370). *Eur.Phys.J.*, C52:55–74, 2007.
- [184] D. Black, A. H. Fariborz, and J. Schechter. Chiral Lagrangian treatment of pi eta scattering. *Phys.Rev.*, D61:074030, 2000.
- [185] A. H. Fariborz, R. Jora, and J. Schechter. Two chiral nonet model with massless quarks. *Phys.Rev.*, D77:034006, 2008.
- [186] A. H. Fariborz, R. Jora, and J. Schechter. Global aspects of the scalar meson puzzle. *Phys.Rev.*, D79:074014, 2009.
- [187] A. H. Fariborz, R. Jora, J. Schechter, and M. N. Shahid. Chiral nonet mixing in pi pi scattering. *Phys.Rev.*, D84:113004, 2011.
- [188] T. K. Mukherjee, M. Huang, and Q.S. Yan. Low-lying scalars in an extended Linear σ Model. *Phys.Rev.*, D86:114022, 2012.
- [189] D. Mohler and R.M. Woloshyn. D and D_s meson spectroscopy. *Phys.Rev.*, D84:054505, 2011.
- [190] G. Moir, M. Peardon, S. M. Ryan, C. E. Thomas, and L. Liu. Excited spectroscopy of charmed mesons from lattice QCD. *JHEP*, 1305:021, 2013.
- [191] D. Ebert, R.N. Faustov, and V.O. Galkin. Heavy-light meson spectroscopy and Regge trajectories in the relativistic quark model. *Eur.Phys.J.*, C66:197–206, 2010.

- [192] E. Klempt. Glueballs, hybrids, pentaquarks: Introduction to hadron spectroscopy and review of selected topics. 2004.
- [193] F. Divotgey, L. Olbrich, and F. Giacosa. Phenomenology of axial-vector and pseudovector mesons: decays and mixing in the kaonic sector. *Eur.Phys.J.*, A49:135, 2013.
- [194] H.Y. Cheng. Hadronic charmed meson decays involving axial vector mesons. *Phys.Rev.*, D67:094007, 2003.
- [195] H. Hatanaka and K.C. Yang. $K(1)(1270)$ - $K(1)(1400)$ mixing angle and new-physics effects in $B \rightarrow K(1) l^+ l^-$ decays. *Phys.Rev.*, D78:074007, 2008.
- [196] A. Ahmed, I. Ahmed, M. Ali Paracha, and A. Rehman. $K_1(1270) - K_1(1400)$ mixing and the fourth generation SM effects in $B \rightarrow K_1 \ell^+ \ell^-$ decays. *Phys.Rev.*, D84:033010, 2011.
- [197] X. Liu, Z.T. Zou, and Z.J. Xiao. Penguin-dominated $B \rightarrow \text{Phi} K_1(1270)$ and $\text{Phi} K_1(1400)$ decays in the perturbative QCD approach. *Phys.Rev.*, D90(9):094019, 2014.
- [198] Th. Gutsche, T. Branz, A. Faessler, I. W. Lee, and V. E. Lyubovitskij. Hadron molecules. 2010.
- [199] M. Gell-Mann, R.J. Oakes, and B. Renner. Behavior of current divergences under $SU(3) \times SU(3)$. *Phys.Rev.*, 175:2195–2199, 1968.
- [200] N.N. Achasov and A.V. Kiselev. Propagators of light scalar mesons. *Phys.Rev.*, D70:111901, 2004.
- [201] F. Giacosa and G. Pagliara. On the spectral functions of scalar mesons. *Phys.Rev.*, C76:065204, 2007.
- [202] F. Giacosa and Th. Wolkanowski. Propagator poles and an emergent stable state below threshold: general discussion and the $E(38)$ state. *Mod.Phys.Lett.*, A27:1250229, 2012.
- [203] A. Mishra, E. L. Bratkovskaya, J. Schaffner-Bielich, S. Schramm, and Horst Stoecker. Mass modification of D meson in hot hadronic matter. *Phys. Rev.*, C69:015202, 2004.
- [204] F. O. Gottfried and S. P. Klevansky. Thermodynamics of open and hidden charmed mesons within the NJL model. *Phys. Lett.*, B286:221–224, 1992.
- [205] S. Okubo. Phi meson and unitary symmetry model. *Phys.Lett.*, 5:165–168, 1963.
- [206] G. Zweig. An $SU(3)$ model for strong interaction symmetry and its breaking. Version 2. pages 22–101, 1964.
- [207] J. Iizuka. Systematics and phenomenology of meson family. *Prog.Theor.Phys.Suppl.*, 37:21–34, 1966.
- [208] F. Giacosa. Glueball phenomenology within a nonlocal approach. *PhD, Thesis, Faculty of Physics at Eberhard Karls University Tübingen*, 2005.
- [209] O. Nachtmann. Elementary particle physics: concepts and phenomena.

-
- [210] C. Rosenzweig, J. Schechter, and C.G. Trahern. Is the Effective Lagrangian for QCD a Sigma Model? *Phys.Rev.*, D21:3388, 1980.
- [211] K. Kawarabayashi and N. Ohta. The problem of η in the large N limit: Effective Lagrangian approach. *Nucl.Phys.*, B175:477, 1980.
- [212] L. Maiani, F. Piccinini, A.D. Polosa, and V. Riquer. A New look at scalar mesons. *Phys.Rev.Lett.*, 93:212002, 2004.
- [213] F. Giacosa. Strong and electromagnetic decays of the light scalar mesons interpreted as tetraquark states. *Phys.Rev.*, D74:014028, 2006.
- [214] A. H. Fariborz, R. Jora, and J. Schechter. Toy model for two chiral nonets. *Phys.Rev.*, D72:034001, 2005.
- [215] A. H. Fariborz. Isosinglet scalar mesons below 2-GeV and the scalar glueball mass. *Int.J.Mod.Phys.*, A19:2095–2112, 2004.
- [216] M. Napsuciale and S. Rodriguez. A Chiral model for anti-q q and anti-qq qq mesons. *Phys.Rev.*, D70:094043, 2004.
- [217] F. Giacosa and G. Pagliara. Decay of light scalar mesons into vector-photon and into pseudoscalar mesons. *Nucl.Phys.*, A833:138–155, 2010.
- [218] M.F.M. Lutz et al. Physics performance report for PANDA: Strong interaction studies with antiprotons. 2009.
- [219] M. Ablikim et al. Observation of a resonance X(1835) in $J/\psi \rightarrow \gamma \pi^+ \pi^- \eta'$. *Phys.Rev.Lett.*, 95:262001, 2005.
- [220] N. Kochelev and D.-P. Min. X(1835) as the lowest mass pseudoscalar glueball and proton spin problem. *Phys.Lett.*, B633:283–288, 2006.
- [221] M. Ablikim et al. Confirmation of the X(1835) and observation of the resonances X(2120) and X(2370) in $J/\psi \rightarrow \gamma \pi^+ \pi^- \eta'$. *Phys.Rev.Lett.*, 106:072002, 2011.
- [222] R. L. Jaffe. Multi-quark hadrons. 1. the phenomenology of (2 quark 2 anti-quark) mesons. *Phys.Rev.*, D15:267, 1977.
- [223] E. van Beveren, T.A. Rijken, K. Metzger, C. Dullemond, G. Rupp, et al. A Low lying scalar meson nonet in a unitarized meson model. *Z.Phys.*, C30:615–620, 1986.
- [224] N. A. Tornqvist. Understanding the scalar meson q anti-q nonet. *Z.Phys.*, C68:647–660, 1995.
- [225] M. Boglione and M.R. Pennington. Dynamical generation of scalar mesons. *Phys.Rev.*, D65:114010, 2002.
- [226] E. van Beveren, D.V. Bugg, F. Kleefeld, and G. Rupp. The Nature of sigma, kappa, $a(0)(980)$ and $f(0)(980)$. *Phys.Lett.*, B641:265–271, 2006.

- [227] J.R. Pelaez. On the nature of light scalar mesons from their large $N(c)$ behavior. *Phys.Rev.Lett.*, 92:102001, 2004.
- [228] J.A. Oller and E. Oset. Chiral symmetry amplitudes in the S wave isoscalar and isovector channels and the sigma, $f_0(980)$, $a_0(980)$ scalar mesons. *Nucl.Phys.*, A620:438–456, 1997.
- [229] D.V. Bugg. An alternative interpretation of Belle data on $\gamma\text{-}\gamma \rightarrow \eta' - \pi^\pm \pi^-$. *Phys.Rev.*, D86:114006, 2012.
- [230] A. Peters. Baryonische Zweikörper zerfälle im erweiterten Linearen Sigma-Modell. *Bachelor, Thesis, Faculty of Physics at Johann Wolfgang Goethe-Universität Frankfurt am Main*, 2012.
- [231] N. Brambilla, A. Pineda, J. Soto, and A. Vairo. Effective field theories for heavy quarkonium. *Rev.Mod.Phys.*, 77:1423, 2005.
- [232] K.W. Edwards et al. Study of B decays to charmonium states $B \rightarrow \eta(c) K$ and $B \rightarrow \chi(c_0) K$. *Phys.Rev.Lett.*, 86:30–34, 2001.
- [233] N.G. Deshpande and J. Trampetic. Exclusive and semiinclusive B decays based on $b \rightarrow s \eta(c)$ transition. *Phys.Lett.*, B339:270–274, 1994.
- [234] S. Coito, G. Rupp, and E. van Beveren. Quasi-bound states in the continuum: a dynamical coupled-channel calculation of axial-vector charmed mesons. *Phys.Rev.*, D84:094020, 2011.
- [235] G. Rupp, S. Coito, and E. van Beveren. Meson spectroscopy: too much excitement and too few excitations. *Acta Phys.Polon.Supp.*, 5:1007–1014, 2012.
- [236] V.A. Novikov, L.B. Okun, Mikhail A. Shifman, A.I. Vainshtein, M.B. Voloshin, et al. Charmonium and gluons: Basic experimental facts and theoretical introduction. *Phys.Rept.*, 41:1–133, 1978.
- [237] S.K. Choi et al. Observation of the $\eta(c)(2S)$ in exclusive $B \rightarrow K K(S) K - \pi^+$ decays. *Phys.Rev.Lett.*, 89:102001, 2002.
- [238] A. Vinokurova et al. Study of $B^{+-} \rightarrow K^{+-}(KS K \pi)^0$ decay and determination of $\eta(c)$ and $\eta(c)(2S)$ parameters. *Phys.Lett.*, B706:139–149, 2011.
- [239] S. Uehara et al. Study of charmonia in four-meson final states produced in two-photon collisions. *Eur.Phys.J.*, C53:1–14, 2008.
- [240] D. Liventsev. Exotic/charmonium hadron spectroscopy at Belle and BaBar. 2011.
- [241] J.P. Lees et al. Measurement of the $\gamma\gamma^* \rightarrow \eta(c)$ transition form factor. *Phys.Rev.*, D81:052010, 2010.
- [242] L.P. Sun, H. Han, and K.T. Chao. Impact of J/ψ pair production at the LHC and predictions in nonrelativistic QCD. 2014.

-
- [243] M. S. Khan. J/ψ Production within the framework of nonrelativistic QCD.
- [244] B. Kniehl. Testing nonrelativistic-QCD factorization in charmonium production at next-to-leading order. *PoS*, LL2012:009, 2012.
- [245] T. Mannel. Heavy quark effective field theory. *Rept.Prog.Phys.*, 60:1113–1172, 1997.
- [246] T. Kawanai and S. Sasaki. Charmonium potential from full lattice QCD. *Phys.Rev.*, D85:091503, 2012.
- [247] C. DeTar. Charmonium spectroscopy from Lattice QCD. *Int.J.Mod.Phys.Conf.Ser.*, 02:31–35, 2011.
- [248] L. Liu et al. Excited and exotic charmonium spectroscopy from lattice QCD. *JHEP*, 1207:126, 2012.
- [249] K. Peters. Charmonium and exotic hadrons at PANDA. *Int.J.Mod.Phys.*, E16:919–924, 2007.
- [250] F. E. Close and P. R. Page. Gluonic charmonium resonances at BaBar and BELLE? *Phys.Lett.*, B628:215–222, 2005.
- [251] G.S. Bali et al. A Comprehensive lattice study of SU(3) glueballs. *Phys.Lett.*, B309:378–384, 1993.
- [252] G. S. Bali et al. Static potentials and glueball masses from QCD simulations with Wilson sea quarks. *Phys.Rev.*, D62:054503, 2000.
- [253] C. Morningstar and M. J. Peardon. Simulating the scalar glueball on the lattice. *AIP Conf.Proc.*, 688:220–230, 2004.
- [254] M. Suzuki. Elusive vector glueball. *Phys.Rev.*, D65:097507, 2002.
- [255] C.T. Chan and W.S. Hou. On the mixing amplitude of J/ψ and vector glueball O . *Nucl.Phys.*, A675:367C–370C, 2000.
- [256] E. B. Gregory, A. C. Irving, C. C. McNeile, S. Miller, and Z. Sroczynski. Scalar glueball and meson spectroscopy in unquenched lattice QCD with improved staggered quarks. *PoS*, LAT2005:027, 2006.
- [257] D. Bettoni and R. Calabrese. Charmonium spectroscopy. *Prog.Part.Nucl.Phys.*, 54:615–651, 2005.
- [258] D.M. Asner et al. Hadronic structure in the decay $\tau^- \rightarrow \tau^- \nu_\tau \pi^- \pi^0 \pi^0$ and the sign of the tau-neutrino helicity. *Phys.Rev.*, D61:012002, 2000.
- [259] C. Bromberg, J. Dickey, G. Fox, R. Gomez, W. Kropac, et al. Observations of the D and E mesons and possible three kaon enhancements in $\pi^- p \rightarrow K^0 K^\pm \pi^\mp X$, $K^0 K^+ K^- X$ at 50-GeV/ c and 100-GeV/ c . *Phys.Rev.*, D22:1513, 1980.
- [260] C. Dionisi et al. Observation and quantum numbers determination of the E(1420) meson in $\pi^- p$ interactions at 3.95-GeV/ c . *Nucl.Phys.*, B169:1, 1980.

- [261] M. Harada and K. Yamawaki. Hidden local symmetry at loop: A New perspective of composite gauge boson and chiral phase transition. *Phys.Rept.*, 381:1–233, 2003.
- [262] T. E. Tilma, M. Byrd, and G. Sudarshan. A parametrization of bipartite systems based on $SU(4)$ Euler angles. *J.Phys.*, A35:10445–10465, 2002.
- [263] W. Greiner and Müller B. Quantum mechanics - symmetries. *Springer Verlag*, 2nd. ed, 1994.

Acknowledgments

First of all, I would like to express my gratitude to my God who guided and aided me to bring this thesis to light.

I am deeply thankful to my supervisor Prof. Dr. Dirk H. Rischke for giving me the opportunity to be one of his students, for his meticulous supervision as well as his contagious enthusiasm, continual encouragement, and suggestions throughout my research work, and for carefully correcting my thesis.

I am very grateful to Dr. Francesco Giacosa for useful discussions and cooperation.

I am also most grateful to Prof. Schramm for useful discussions about the extension of the eLSM to four flavors, and Dr. Peter Kovacs and Dr. Gyuri Wolf for discussions about the fit in the three-flavor case.

I am also grateful to Dr. Denis Parganlija for very helpful discussions and for answering my questions about “the $U(3)_R \times U(3)_L$ Linear Sigma Model” although he was busy writing his PhD thesis.

I thank Stanislaus Janowski for useful cooperation in the phenomenology of the pseudoscalar glueball in the extended Linear Sigma Model.

I am also very grateful to my mother and my father for their encouragement and financial support and for their standing beside me all my life and for giving me my freedom by allowing me to live as I want and do what I like as well as for supporting me and pushing me to keep going to my aim for my future. Special thanks to my sisters (Marwa, Hanan, Norhan, Alaa, and Ruba) and my brothers (Mohamed and Hussam).

I thank also my colleagues for exchanges and discussions: Barbara Betz, Francesca Cuteri, Mara Grahl, Antje Peters, Elina Seel, Jürgen Eser, Achim Heinz, Timotheus Kozłowski, Klaus Neuschwander, Christopher Pinke, Dr. Joachim Reinhardt, Khaled Teilab, Thomas Wolkanowski, Dr. Miklos Zetenyi.

I thank the Deutsche Akademischer Austausch Dienst (DAAD) for their financial support. Without their support this thesis would not have been possible.

My gratefulness goes to my friends for the beautiful times that we spent together and for their help: Kholud Abuschaar, Katharine Henninger, Nabila Ibrahim, Stephanie Merker, and Carina Popovici.

Curriculum vitae

Personal Information

Name: Ms. Walaa I. Eshraim

Languages: English (very good), German (good), Arabic (native)

Web page: <http://th.physik.uni-frankfurt.de/weshraim/>

Academic Qualifications

1- Master of Science (M. Sc. in Physics), the Islamic University of Gaza (IUG), Gaza, Gaza Strip, 18 Feb., 2007.

2- Bachelor of Science (B.Sc. in Physics), the Islamic University of Gaza (IUG), Gaza, Gaza Strip, 2003.

3- Diploma of Education, Al-Quds Open University, Gaza, Gaza Strip 2008.

Awards and Honors

1- Special Prize for the Best Poster, at the 13th Workshop on Mesons Production, Properties and Interaction MESON2014, Cracow, Poland, June 2, 2014.

2- DAAD (Deutscher Akademischer Austausch Dienst-German Academic Exchange Service) PhD scholarship, Germany, 2010.

3- Majorana Prize for the best research published in the Electronic Journal of Theoretical Physics in 2008, Italy.

4- The Islamic University Prize for the best scientific research in Science Faculty at the Islamic University of Gaza in 2007.

Books

1. "Hamilton-Jacobi Treatment of Fields with Constraints", LAP Lambert Academic Publishing, Germany, 2012.

Professional Experience

04.2015 - 07.2015 Tutorial for Quantum Mechanics II, J. W. Goethe University, Frankfurt am Main, Germany.

10.2012 - 03.2013 Tutorial for Electrodynamics, J. W. Goethe University, Frankfurt am Main, Germany.

09.2009 - 02.2010 Teacher for Medical Physics in Dental Medicine College, University of Palestine, Gaza, Gaza strip.

09.2006 – 06.2010 Teacher for Physics for the Abettor, High School, Gaza, Gaza Strip.

Technical and Skills Courses

Attended and obtained certificates for the following technical courses:

- 1- Training course in Latex-Duration.
- 2- Training course in ICDL –Duration.
- 3- Training course in Mathematica Program.
- 4- Training courses in soft skills program in Helmholtz Graduate School for Hadron and Ion Research for FAIR at Germany:
 - a) ‘Making an Impact as an Effective Researcher’.
 - b) Leading Teams in a Research Environment.
 - c) Leadership and Career Development.

Activities

1. Participant of the HGS-HIRE Lecture Week on Hadron Physics, presentation of “Tracking techniques for high energy physics experiments”, Ebsdorfergrund, Germany, 15-20 July, 2012.

2. Participant of the 52nd Winter School on Theoretical Physics in Schladming, which focussed on “Physics Beyond the Higgs” and presentation of “A $U(4)_r \times U(4)_l$ linear sigma model with (axial-)vector mesons”, Austria, March 1-8, 2014.

Posters

1. Poster entitled “Charmed mesons in the extended Linear Sigma Model”, at the 13th Workshop on Mesons Production, Properties and Interaction MESON2014, Cracow, Poland, June 2, 2014.

Presentations

A. Presentations at Conferences:

1. “Phenomenology of a pseudoscalar glueball and charmed mesons in the extended linear sigma model”, at the 3rd International Conference on New Frontiers in Physics, Chania, Crete, Greece, July 28 -August 6, 2014.
2. “Phenomenology of Charmed Mesons in the extended Linear Sigma Model”, at the 78th Annual Meeting of the DPG (DPG Spring Meeting), Frankfurt am Main, Germany, March 17-21, 2014.
3. “A $U(4)_r \times U(4)_l$ linear sigma model with (axial-)vector mesons”, at the 77th Annual Meeting of the DPG (DPG Spring Meeting), Dresden, March 4 - 8, 2013.
4. “Decay of the pseudoscalar Glueball into scalar and Pseudoscalar mesons”, at the Xth International Conference on Quark Confinement and the Hadron Spectrum, München, Germany, October 11, 2012.

B. Presentations at Workshops:

1. “Phenomenology of a pseudoscalar glueball and charmed mesons in a chiral symmetric model”, at Bound states in QCD and beyond workshop, Schlosshotel Rheinfels, St. Goar, Germany, March 24-27, 2015.
2. “Phenomenology of (open and hidden) charmed mesons in a chiral symmetric model”, at FAIRNESS workshop, Vietri sul Mare, Italy, September 22-27, 2014.
3. “Phenomenology of charmed mesons in a chiral symmetric model”, at the HICforFAIR workshop: Heavy flavor physics with CBM, FIAS, Frankfurt/Main, Germany, May 26-28, 2014.
4. “A $U(4)_r \times U(4)_l$ linear sigma model with (axial-)vector mesons”, at ‘QCD-TNT-III, From quarks and gluons to hadronic matter: A bridge too far?’ workshop ECT* Trento, Italy, Sep. 2-6, 2013.
5. “Decay of the pseudoscalar Glueball into scalar and Pseudoscalar mesons”, at the FAIRNESS workshop, Hersonissos, Greece, September 3-8, 2012.
6. “Decay of the pseudoscalar Glueball into scalar and Pseudoscalar mesons”, at the ‘Excited QCD 2012’ workshop, Peniche, Portugal, May 6-12, 2012.

C. Presentations in Seminars:

1. “Phenomenology of (open and hidden) charmed mesons in Chiral Symmetric Model”, in the institute seminar at JW Goethe University, Frankfurt am Main, Germany, May 5, 2014.
2. “A $U(4)_r \times U(4)_l$ linear sigma model with vector and axial-vector mesons”, in the institute seminar at JW Goethe University, Frankfurt am Main, Germany, June 3, 2013.
3. “Decay of the pseudoscalar glueball into scalar and pseudoscalar mesons”, in the institute seminar at JW Goethe University, Frankfurt am Main, Germany, October 25, 2012.
4. “A Chiral Lagrangian for the Pseudoscalar Glueball”, in the chiral group seminar at JW Goethe University, Frankfurt am Main, Germany, June 25, 2012.
5. “Including the charm quark into the Linear Sigma Model”, in chiral group seminar at JW Goethe University, Frankfurt am Main, Germany, December 19, 2011.

Publications

A. Publications in Journals

1. W. I. Eshraim and D. H. Rischke, “Decays of charmonium states in the extended Linear Sigma Model”, in preparation.
2. W. I. Eshraim, F. Giacosa, and D. H. Rischke, “Phenomenology of charmed mesons in the extended Linear Sigma Model”, *Eur. Phys. J. A* 51, no. 9, 112 (2015) [arXiv:1405.5861 [hep-ph]].
3. W. I. Eshraim, S. Janowski, F. Giacosa and D. H. Rischke, “Decay of the pseudoscalar glueball into scalar and pseudoscalar mesons”, *Phys. Rev. D* 87, 054036 (2013) [arXiv:1208.6474 [hep-ph]].
4. W. I. Eshraim, “Path Integral Quantization of Landau-Ginzburg Theory”, *Islamic University Journal*, 18, 42 (2010) [arXiv: 1301.2478 [physics.gen-ph]].
5. W. I. Eshraim, and N. I. Farahat, “Path Integral Quantization of The Electromagnetic Field Coupled to A Spinor”, *Electronic Journal of Theoretical Physics*, 22, (2009) 189.
6. W. I. Eshraim, and N. I. Farahat, “Hamilton-Jacobi formulation of a non-abelian Yang-Mills theories”, *Electronic Journal of theoretical Physics*, 17, (2008) 69.
7. W. I. Eshraim, and N. I. Farahat, “Hamilton-Jacobi treatment of Lagrangian with fermionic and scalar field”, *Romanian Journal of Physics*, 53, (2008).
8. W. I. Eshraim, and N. I. Farahat, “Hamilton-Jacobi formulation of the scalar field coupled to two flavours Fermionic through Yukawa couplings”, *Islamic University Journal*, 15, (2007), 151.
9. W. I. Eshraim, and N. I. Farahat, “Quantization of the scalar field coupled minimally to the vector potential” *Electronic Journal of Theoretical Physics*, 14, (2007), 61.
10. W. I. Eshraim, and N. I. Farahat, “Hamilton-Jacobi Approach to the Relativistic Local Free Field with Linear velocity of Dimension D” *Hadronic Journal*, 29, (2006), 553.

B. Conference Proceedings

1. W. I. Eshraim “Vacuum properties of open charmed mesons in a chiral symmetric model”, *J. Phys. Conf. Ser.* 599, no. 1, 012009 (2015) [arXiv:1411.4749 [hep-ph]].

2. W. I. Eshraim “A pseudoscalar glueball and charmed mesons in the extended linear sigma model”, EPJ Web Conf. 95, 04018 (2015) [arXiv:1411.2218 [hep-ph]].
3. W. I. Eshraim and F. Giacosa “Decay of open charmed mesons in the extended linear sigma model”, EPJ Web Conf. 81, 05009 (2014) [arXiv:1409.5082 [hep-ph]].
4. W. I. Eshraim, “Masses of light and heavy mesons in a $U(4)_R \times U(4)_L$ linear sigma model”, PoS QCD-TNT-III 049 (2014) [arXiv:1401.3260 [hep-ph]].
5. W. I. Eshraim and S. Janowski, “Phenomenology of the pseudoscalar glueball with a mass of 2.6 GeV”, J. Phys. Conf. Ser. 426, 012018 (2013) [arXiv:1211.7323 [hep-ph]].
6. W. I. Eshraim and S. Janowski, “Branching ratios of the pseudoscalar glueball with a mass of 2.6 GeV”, PoS ConfinementX, 118 (2012) [arXiv:1301.3345 [hep-ph]].
7. W. I. Eshraim, S. Janowski, A. Peters, K. Neuschwander and F. Giacosa, “Interaction of the pseudoscalar glueball with (pseudo)scalar mesons and nucleons”, Acta Phys. Polon. Supp. 5, 1101(2012) [arXiv:1209.3976 [hep-ph]].
8. W. I. Eshraim, “On the Lagrangian Formalism of Landau-Ginzburg Theory”. The Third International Conference for Science and Development, The Islamic University of Gaza (IUG), Faculty of Science, Gaza, Palestine, March 7-8, 2009.
9. W. I. Eshraim and N. I. Farahat, “Quantization of the Relativistic Local Free Field with Linear Velocity of Dimension D”. The Third International Conference for Science and Development, The Islamic University of Gaza (IUG), Faculty of Science, Gaza, Palestine, March 7-8, 2009.
10. W. I. Eshraim and N. I. Farahat, “Hamilton-Jacobi formulation of the scalar field coupled to two flavours Fermionic through Yukawa couplings”. The Second International Conference for Science and Development, The Islamic University of Gaza (IUG), Faculty of Science, Gaza, Palestine, March 6-7, 2007.